CHEMICAL REVIEWS

pubs.acs.org/CR

Review

Tailoring Crosslinks through Time—A Paradigm for Tough Hydrogels

Published as part of Chemical Reviews special issue "Tough Gels".

Hana Tabit, Aiden Saul, Kennalee Orme, Timea Kolozsvary, Zachary A. Bernheimer, Hongyi Cai, Manto Lam, Si Chen, Rebecca Tobias, Manh Khang Trang, Ryan Doherty, Meredith Silberstein,* and Benjamin R. McDonald*

Cite This: https://doi.org/10.1021/acs.chemrev.5c00466

Read Online

ACCESS | Metrics & More | Article Recommendations | Supporting Information

ABSTRACT: The multidisciplinary applications of hydrogels have motivated a thorough exploration of the relationship between their structural and mechanical properties, *i.e.*, spatial structure−function relationships, with particular regard to strength and toughness. While this approach has driven fundamental advancements in the design of robust hydrogel structures, further complementary perspectives are needed to enable holistic, rational design schemes that integrate considerations such as fabrication and advanced functions like response and adaptation. To these ends, this review focuses on the dynamics of temporal-function relationships and their fundamental bases in order to highlight how the dynamic regulation of polymer interactions programs: 1) polymer assembly and material structure; 2) response to deformation and fracture behavior; 3) dynamic modulation of properties and structural remodeling/self-healing. By exploring this intersection of hydrogel formation, function, and remodeling, this review seeks to shed light on the fundamental relationship between molecular structure, material assembly, and performance in order to connect the emerging area of bioinspired materials processing with tough hydrogel design, and further provides a lasting inspiration and impetus for future hydrogel development that enables valuable scientific and technological advancements.

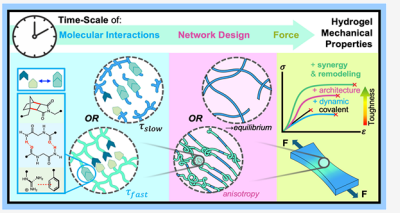

CONTENTS

Received: June 17, 2025
Revised: January 8, 2026
Accepted: January 12, 2026

1. INTRODUCTION

The soft, viscoelastic nature of hydrogels leads to numerous applications across a broad range of fields. The selection of specific hydrogels for medical applications such as contact lenses,[1] tissue engineering scaffolds,[2] medical implants,[3] wound dressings,[4] drug delivery,[5] soft robotics[6] as well as industrial applications, including soil conditioners in agriculture,[7] functional coatings,[8] wearable electronic devices,[9] sensors, energy capture and energy storage,[10] is often driven by their mechanical properties. Parameters such as strength, toughness, and fatigue resistance are critical determinants of gel performance and longevity, particularly in applications requiring large or repeated loading conditions.[11] Specifically, toughness, the property of resisting defect growth by storing and/or dissipating energy under deformation,[12] plays a central role in defining hydrogel application space.

Defined by their soft yet solid-like nature, gels consist of polymer networks swollen with ionic, organic, or aqueous solvent,[13−16] and can thus be broadly classified as ionogels, organogels, and hydrogels, respectively.[17−19] Hydrogels have advantageous properties such as compliant elasticity, high water content and facile diffusion, as well as other similarities to human tissues.[20−25] However, many traditional hydrogel systems with permanent chemical crosslinks struggle to meet standards for self-healing, shape memory, material circularity, processability, and tunable viscoelasticity, as set by their biological analogues and demanded by adjacent fields of materials science and biotechnology. For example, biological materials such as load bearing tissues present fracture energies between 10,000 and 30,000 J/m^2, whereas unmodified permanent covalent synthetic hydrogels only reach fracture energies <10 J/m^2, due to their high-water content, nonuniformity, and static crosslinkers.[12] To address these limitations, dynamic, *i.e.*, reversible and modulable, interactions are introduced into gels as a means of dissipating mechanical energy.[12] These interactions can break and reform either autonomously[26] or when modulated by external stimuli like mechanical deformation, heat,[27,28] pH,[29,30] or light.[31−34]

Notably, a classic focus in tough gel design is tailoring dynamic structures, from molecular scale to micro/macro structure, to achieve desirable mechanical properties.[12] For example, in the emerging pursuit of improving the toughness of hydrogels while maintaining their softness, strategies such as introducing energy dissipation structures on multiple length scales have been widely explored.[35,36] From the simplest chemical perspective, dynamic covalent (DCB) and/or physical crosslinks have been incorporated into hydrogels as sacrificial energy dissipation mechanisms, enabled by bond energies lower than covalent. Progressing in length scales, network structures themselves have been tuned to function as higher order energy distributing and dissipating mechanisms. Established network architectures include single networks, interpenetrating networks (IPNs) and composite hydrogels with nanoparticle fillers or additives, where the composition of molecular interactions within these architectures determine multiscale structures and interactions.[12,37,38] Additionally, stimuli-triggered assembly and disassembly, and even "remodeling", *i.e.*, the revision of structure and properties after fabrication, are emerging strategies in biofabrication-inspired tissue-like materials.[39−42] These dynamic interactions have enabled significant improvements in toughness, with some state of the art materials capable of achieving near biomimetic fracture energies (measured: 1−20 kJ/m^2).[12]

Interestingly, the time-dependence of certain mechanical properties (*e.g.*, viscoelasticity and poroelasticity) are critical to their design and fabrication, but are not a central focus of reviews on hydrogel mechanical properties[35,43,44] (Figure 1).

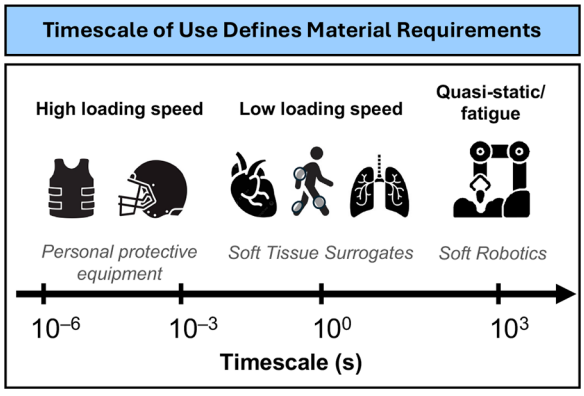

Figure 1. Loading timescales of relevant hydrogel applications.

https://doi.org/10.1021/acs.chemrev.5c00466
Chem. Rev. XXXX, XXX, XXX−XXX

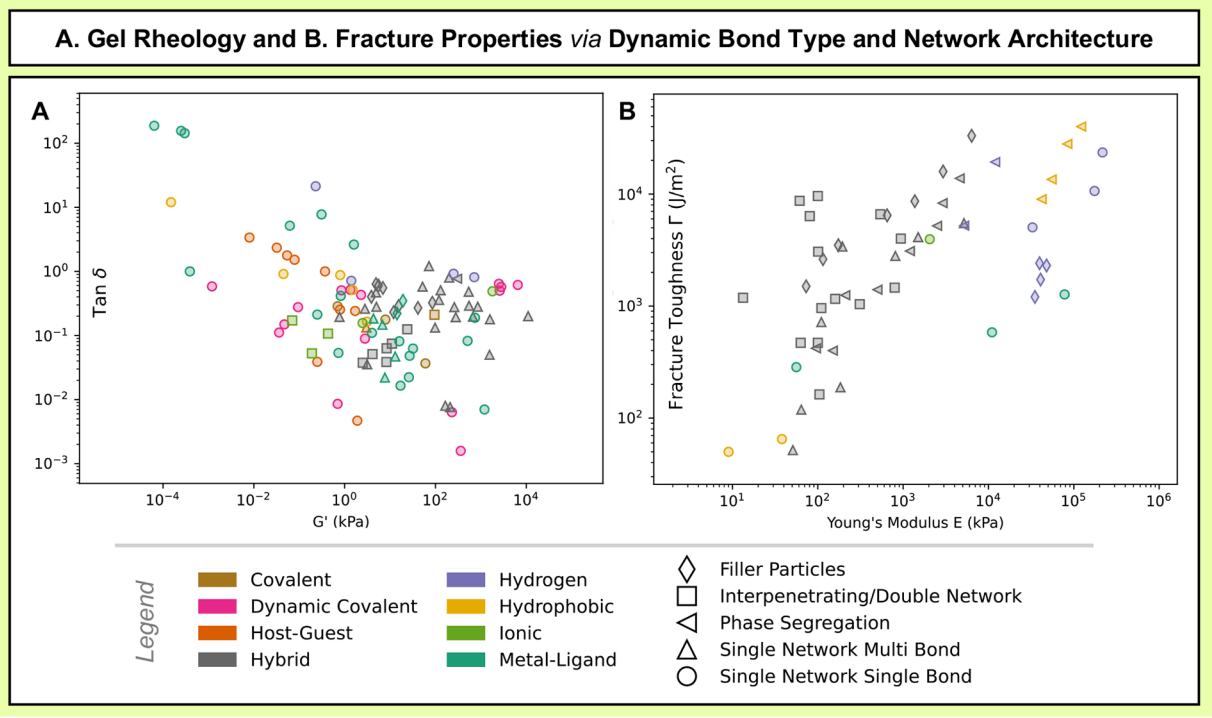

Figure 2. Ashby pots. A) Tan delta vs storage modulus near a frequency of 1 Hz at room temperature. B) Fracture toughness vs quasi-static elastic modulus. See SI for data point identities and sources.

As deformation responses depend on the rate of deformation and reformation relative to the applied strain rate,[45] the temporal mechanics of gels must be considered to ensure appropriate stiffness over relevant timescales or operating frequencies.[46] In tissue engineering scaffolds, for example, while hydrogel stiffness is known to be a crucial performance parameter, the relaxation timescale of the gel has additionally been identified as a driver of cell key cellular behaviors such as differentiation and even the etiology of cancers.[47,48]

Approaching synthetic hydrogel systems from a molecular engineering perspective, *i.e.*, linking constituent molecular structures with the formation of multiscale structure and resulting system scale properties, it becomes clear that the timescale of dynamic bond exchange is the key to achieving different gel properties. Since each dynamic bond has a characteristic kinetic profile and thermodynamic equilibrium, timescales of these motifs can range from fractions of a second to months,[49] depending on the type of bond and/or applied stimuli. Sufficiently tough hydrogels dissipate energy through the breaking of dynamic motifs (crosslinking, structural motifs) which exchange on short timescales,[50,51] while variable timescales (long in ambient, but short under stimuli) are needed for material processability.[34,52] Gel elasticity, the ability to withstand stress through deformation and return to its original dimensions after stress is removed, *i.e.*, the storage of mechanical energy, can also be modulated through the length and timescale of dynamic bonds within the gel. Thus, selecting the appropriate timescale, or rather, *molecular design parameter* to engender said timescale, is crucial to building gels with target material properties, such as viscoelasticity, extensibility, and toughness suitable for biological compatibility or other applications.

The interconnected chemical and mechanical attributes of hydrogels along with their broad compositional space has enabled systems with increasing sophistication and diverse application. As such, perspectives on tough hydrogels are diverse and somewhat disconnected, spanning chemistry, soft matter physics, as well as material and biomedical engineering. It is therefore the intention of this review to bridge principles of molecular, macromolecular, and materials engineering as they pertain to tough hydrogels; explicating a molecular scale driven perspective to reconcile perceptions of these inherently time dependent systems, and providing insight into the fundamental drivers of gel behavior accessible to all practitioners and users. The following sections will build a fundamental understanding of how desired characteristics of a tough hydrogel are quantified (Section 2), the molecular design and timescales of dynamic energy dissipation motifs and their implications on material properties (Section 3), the strategic manipulation of dynamic bond energy landscapes to program assembly and higher order toughening structures (Section 4), as well as dynamic remodeling of hydrogel toughness (Section 5), specifically illuminating how the multiscale thermodynamic landscape can be sculpted to achieve target material performance and functionality with particular regards to tough hydrogels.

2. ESTABLISHING A CONCEPTUAL FRAMEWORK FOR MEASURING TIME DEPENDENT MECHANICAL PROPERTIES

The mechanical properties of gels, including toughness, depend on the composition of both polymer and solvent, the assembly dictated nano- to micro- structure, as well as the strength and dynamics of the bonds within those structures.[38] The Ashby plots in Figure 2 show how gel rheological (Figure 2, **A**) and fracture properties (Figure 2, **B**) vary with both bond type and network architecture. Foremost, it is apparent that a core range of rheological properties can be accessed by many different chemical motifs; including hydrogen bonding, metal–

https://doi.org/10.1021/acs.chemrev.5c00466
Chem. Rev. XXXX, XXX, XXX−XXX

ligand coordination, and DCBs. Enabled by dynamic bonds, these properties are striking when compared to early synthetic single-network covalent hydrogels, which were fragile, not mechanically robust, and primarily limited to the small strain regime. Within the Ashby plots (Figure 2) it can be observed that a combination of dynamic bond types and assembly processes result in gels with a diverse array of time dependent mechanical properties.

As bonding schemes and architectures grew in sophistication, gels progressed to be studied through larger deformation under either uniaxial compression or shear, and then later under uniaxial tension and pure shear fracture.[38,53,54] These chemical approaches have been applied within many different architectures, including single networks, IPNs, and composite networks with nanoparticle fillers or additives. Single network metal ligand gels stand out for their huge degree of tunability in terms of storage modulus (G', in phase response to mechanical loading at small strain) with proportional change in tan delta (energy dissipation ratio at small strain). Gels with DCBs and more than one bond type (hybrid) tend to have low dissipation relative to their storage modulus at small strains.

Likewise, a wide range of tunability with an overall positive correlation of fracture toughness with Young's modulus is observed (Figure 2, **B**). There are relatively few single bond and single network gels on this plot compared to the rheological plot because these networks tend to be too brittle for straightforward measurement of the fracture toughness. The data from these networks that does exist, however, shows relatively low fracture toughness to Young's modulus ratio (occupying the lower-right edge of the populated area). As these networks are susceptible to localized failure, load is not redistributed once either covalent of dynamic bond damage initiates. In contrast, networks with nano- and microstructural hierarchies can obtain relatively high fracture toughness over a broad range of Young's moduli. Multiple bond types incorporated within a single network create an additional means for tuning fracture toughness and, to a lesser extent, Young's modulus.

As many uses for hydrogels require specific levels of stiffness and must exceed a threshold toughness, a framework that can utilize unique dynamic crosslinks cooperatively to achieve the desired mechanical properties would yield a new taxonomy of strong, tough and useful materials.[55−58] However, toughness then becomes a function of dynamic bond composition and arrangement, requiring that differences in underlying bond thermodynamics and kinetics be appropriately characterized and considered within any framework for the development of tough hydrogels. In the following section, a model for single-network gels is defined with the intention to highlight relevant mechanical properties that characterize local crosslink and macroscopic response to deformation. As deformation response is relative to applied strain, small strain, large deformation, and fracture behavior are specifically examined. By beginning with covalently crosslinked single-network gels, a baseline conceptual framework is established which can be further transformed for networks containing dynamic bonds.

2.1. Single Gel Networks with Covalent Cross-Links as a Reference Point for Dynamically Cross-Linked Gels

Covalent crosslinks have long been used to tune mechanical properties of elastomers and hydrogels.[13] The loss modulus of these materials (G", out of phase response to mechanical loading at small strain) is typically orders of magnitude lower than their storage modulus, as they contain few dissipation mechanisms.[59] Covalently crosslinked gels typically have a storage modulus on the order of 1 kPa that is relatively invariant with changes in frequency.[14,60] It has been shown that increasing the crosslinking density can enhance the storage modulus of hydrogels,[61,62] sometimes by orders of magnitude,[62] but the effect on loss modulus is minimal as the tan delta of these materials is often quite small.[61] Similar to the trend in observed storage modulus change, quasi-static stiffness also increases when more covalent crosslinks are introduced in the hydrogel.[62−64] Richbourg et al.[65] derives the relationship between number-average molecular weight between crosslinks and shear modulus based on rubberlike elasticity theory,[66] equilibrium swelling theory,[67] and mesh size theory:[68]

$$G = RT\left(1 - \frac{2}{f}\right)(1 - \gamma)\frac{\rho_d}{\overline{M_c}}\varphi_r^{2/3}\varphi_s^{1/3} \tag{1}$$

where G is the shear modulus, R is the ideal gas constant, T is the absolute temperature, f is the junction functionality in a polymer network, γ is the frequency of chain-end defects, ρ_d is the dry density of the polymer network, $\overline{M_c}$ is the number-average molecular weight between cross-links in a polymer network, φ_r is the polymer volume fraction in the relaxed state, and φ_s is the polymer volume fraction in the swollen equilibrium state.

When a covalently crosslinked elastomer or gel is deformed beyond the linear elastic regime it will typically follow a hyperelastic behavior (*e.g.*, Neo-Hookean, Arruda-Boyce, displaying stiffening with increasing strain),[69] begin to experience damage via covalent bond scission, or some combination of the two. Elasticity will occur due to orientation and decreased entropic configurational space of the polymer chains.[70] For single network covalent gels, however, damage usually starts to occur relatively early in the chain alignment process. For instance, shear rheology strain sweeps exhibit the deviation from linear viscoelasticity as a drop in storage modulus toward zero and a transient increase and then decrease in loss modulus corresponding to the dissipation from damage. Compression tests performed on hyperelastic gels display an upturn in strain before stress drops dramatically, indicating brittle fracture.[71]

Damage resistance in covalent gels can be systematically understood through fracture behavior. The fracture energy of hydrogels consists of two parts:[35] 1) the intrinsic fracture energy, which is the energy per unit area needed to rupture polymer chains lying across the crack plane by stretching every covalent bond in the chain until it is at the breaking threshold,[72] and 2) energy due to mechanical dissipation. According to the Lake-Thomas theory, which explains fracture energy in elastomers, the intrinsic fracture energy is

$$\Gamma_0 = U_f m \tag{2}$$

where U_f is the energy needed to break a polymer chain and m is the number of chains per unit area.[72] To be applicable to hydrogels, this equation can be further modified to consider the volume concentration of polymers φ_s:[35,73]

$$m = m_{\text{dry}}\varphi_s \tag{3}$$

The intrinsic fracture energy for covalent single network elastomers is on the order of 100 J m^{-2}.[72] By comparison, for a covalent single network hydrogel with 90% water, this number

https://doi.org/10.1021/acs.chemrev.5c00466
Chem. Rev. XXXX, XXX, XXX−XXX

is estimated to be on the order of 10 J m^{-2},[35] with Bai et. al showing experimental results of 8.4 J m^{-2} while the model gave 8.5 J m^{-2} as the intrinsic fracture energy of a purely covalent gel network.[74] This number is small compared to the overall facture energy of that network (71 J m^{-2}), indicating that even in conventional covalent gels, most of the energy absorbed during fracture comes from mechanical dissipation.[74] While covalent crosslinks provide structural integrity, their irreversibility inherently limits energy dissipation and adaptability of the gel. In contrast, dynamic crosslinks that can break and reform in response to mechanical loads have therefore been extensively studied to tune gel viscoelasticity, toughness, and adaptability.[75−77]

2.2. Deformation Regimes for Dynamic Networks

As alluded to throughout the previous sections, toughness and viscoelasticity are highly dependent on the timescale and deformation regime in which they are measured.[60,78−82] Valuable information is gleaned from seemingly apparent relationships: Dynamic structures which withstand the force and timescale of deformation do not effectively dissipate energy, while dynamic structures that do adapt within the critical force and timescales can enhance toughness. Additionally, larger strain regimes are typically correspond to larger scale structural deformation, which can, in some cases, lead to mechanically induced toughening. In the following sections, the characteristic hydrogel responses within small (Section 2.2.1.) and large (Section 2.2.2.) deformation regimes are described and the extraction of information on toughness and other time dependent properties from mechanical testing further discussed. Single network gels, consisting of covalent bonds and/or the addition of dynamic crosslinks, are used as the primary focus of these discussions to establish a basic model of interpretation. While different experimental methods may be employed to measure toughness, each possess their own caveats and difficulty in standardization with other forms of analysis. Given this variability, this section additionally highlights where various experimental methods may disagree, or present opportunities to achieve a consensus across methods when relevant.

2.2.1. Small Strain—Linear Viscoelasticity. The deformation response of hydrogels within the small strain regime, *i.e.*, the linear viscoelastic limit (strain $\lesssim$1−5%),[83,84] is critical to their performance and application. Most commonly, this regime is experimentally characterized using shear rheology, which elucidates a hydrogel's complex moduli and its constituent moduli.[85] The storage (G') and loss (G") moduli indicate the elastic-like and fluid-like nature of the gel (respectively), as elastic solids respond in phase (G') and fluids respond perfectly out of phase (G").[86,87] As mentioned in Section 2.1, ideal covalently crosslinked gels will have a frequency independent response with the storage modulus well above the loss modulus. Conversely, the loss modulus of a viscous fluid will always be greater than its storage modulus, and both moduli will increase with frequency. The variation of the dynamic moduli with frequency is a critical signature of dynamic gels (Figure 3).[86,88] The ratio changes of these two moduli (tan delta) with frequency and/or temperature can also be an informative signature, as this parameter indicates the fraction of energy dissipation at a given loading condition.[14,60] In particular, the breadth of a tan delta peak indicates the breadth of timescales or temperatures over which the dissipation/relaxation occurs.[60,89] If the gel is in the linear viscoelastic regime, equivalent information can also be obtained from stress relaxation (constant strain) and creep (constant stress) experiments by using the principle of linear superposition.[87]

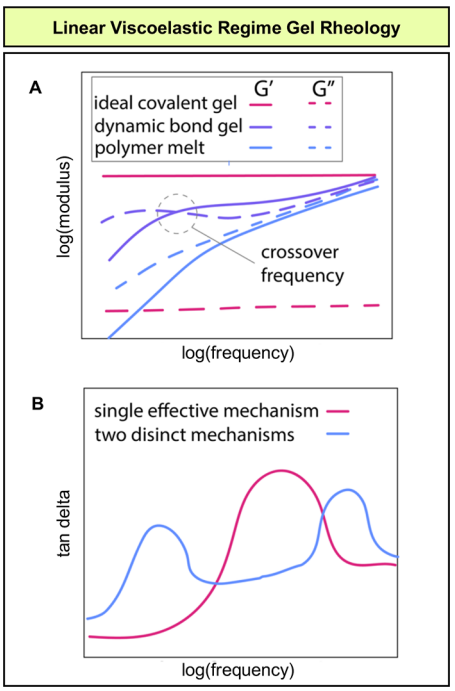

Figure 3. Typical shear rheology characterizing the linear viscoelastic regime of gels. A) Schematic of typical gel G' and G" vs frequency for an ideal covalent gel, dynamically bonded gel, and unentangled polymer melt. B) Schematic of typical tan delta vs frequency for a gel with one effective dissipation mechanism and with two distinct dissipation mechanisms (exaggerated vs common gels). Dissipation mechanisms need to be sufficiently separated in their timescales to appear as distinct peaks.

A wide range of single network dynamically bonded gels have been characterized in the small strain regime. In this range, dynamic bonds are minimally mechanically disrupted, and the structure of the gel remains near its equilibrium configuration. As expected, the storage moduli, loss moduli, and tan delta are all typically frequency dependent for these gels.[90] The crossover of the storage and loss modulus (*i.e.*, the peak(s) of the tan delta) seen in dynamically crosslinked gels is a *critical timescale*[91] set by both the dynamic bond timescale and the network architecture. For the most part, these materials have a single tan delta peak (key timescale) because a single bond dynamic dominates energy dissipation. However, the presence of more than one peak indicates multiple structures with distinct relaxation timescales.

Dimensionless parameters such as the Deborah (De) and Weissenberg (Wi) numbers can be extracted from the linear viscoelastic rheology regime to further contextualize a material's time dependent response.[92,93] Although these terms are often used interchangeably, they require a necessary and relevant distinction. The Weissenberg number represents a ratio of elastic to viscous forces, and is often related to recoverable shear.[94] The Deborah number represents the ratio of a hydrogel's relaxation (τ_R) to its observation (τ_{bs}, deformation) timescales (De = τ_R/τ_{obs}), and is used to describe a material's viscoelastic state within a defined timescale.[92,95] With regards to toughness and application, De

https://doi.org/10.1021/acs.chemrev.5c00466
Chem. Rev. XXXX, XXX, XXX−XXX

can frame a network's propensity to dissipate energy or rearrange on short (De < 1, 0.1s ≤ τ_R ≤ 100s), intermediate (De ∼ 1, 10s < τ_R ≤ 1,000s), or long and often thermally malleable timescales (De ≫ 1, τ_R ≥ 1,000s).[92] While these dimensionless values provide an interesting framing of time-dependent mechanics, they are not often referenced in literature with regards to toughness. Perhaps future studies may use De and Wi to homogenize inconsistencies between testing methods, but this remains to be seen.

When developing models for dynamic noncovalent bonds, the sticky-Rouse model, originally developed for ionomers, is the most often referenced theoretical basis for understanding the linear viscoelastic behavior of single network, unentangled, dynamically crosslinked gels.[96] As implied by its name, this model builds dynamic bond effects (stickers) into the 1953 Rouse model on linear viscoelasticity of dilute polymer solutions, which is effectively a physics grounded Maxwell model.[97] The key idea of the sticky-Rouse model compared to the Rouse model, is that dynamic bonds between polymer chains delay terminal relaxation of the bulk network according to the activation energy required for a dynamic bond to dissociate, following an Arrhenius type dependence. The timescale delay is a function of both crosslink dynamics and crosslink density within the network.

2.2.2. Large Deformation—Hyperelasticity and Nonlinear Viscoelasticity. Increasingly, gels are utilized beyond the small strain regime, leading to a much broader set of function-relevant mechanical properties.[98] Historically, large deformation behavior was studied via compression tests to avoid fracture during gripping, but as gel strength improved, tension testing became more feasible. Shear rheology is also used to characterize the limit of the linear viscoelastic region, but not usually the properties beyond this point.[99,100] Using a monotonic uniaxial or pure shear test to failure, experimental purview extends beyond the elastic modulus to the exhibited nonlinear response, which is commonly hyperelastic and/or nonlinear viscoelastic (Figure 4, **A**). We note here that the terminology "hyperelasticity" and "nonlinear viscoelasticity" in gels is relatively arbitrary. Therefore, we use these terms to indicate a conventional shape of the stress−strain curve rather than to imply these phenomena are mutually exclusive or to imply true "elasticity" for which all deformation is expected to recover on a reasonable timescale when the load is removed.

For a hyperelastic response, the initial linear stress−strain regime under monotonic loading is followed by nonlinear stiffening that eventually results in failure, *i.e.*, a drop in the force to zero as the specimen breaks.[101,102] Especially for gels with dynamic bonds, it is common for this nominally hyperelastic response to be strain-rate dependent. Some dynamically bonded gels may even show strain-stiffening at reference strain rates and then flow in a more fluid-like manner at slower strain rates. For gels exhibiting nonlinear viscoelastic behavior, the linear elastic regime is followed by a pseudoyield strength, and then possible strain softening and or strain hardening until failure occurs. This response is expected to be strain-rate dependent, with the yield stress increasing with strain rate as the testing rate is faster relative to any critical gel timescales.[102,78,79] In both cases, the area under the curves characterizes the toughness. These nonlinear, time dependent, behaviors are governed by the interplay of the dynamic bond dissociation/reassociation kinetics, polymer network deformation (orientation and stretching) and the deformation rate. Both the magnitude and shape of a stress−strain curve are

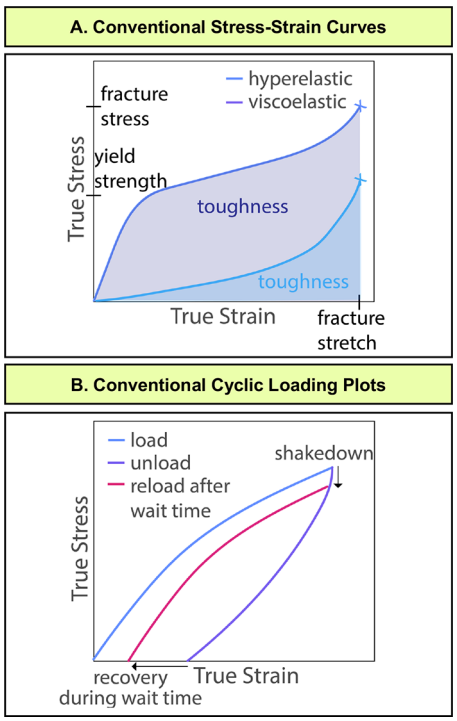

Figure 4. A) Features in a monotonic to failure compression or tension true stress-true strain curve showing both a typical hyperelastic behavior and a typical viscoelastic behavior. B) Features in a representative cyclic loading plot with a wait time prior to reloading.

important for applications, it not only sets the inelastic limit, but also toughness, and susceptibility to deformation localization.

Additional insight into gel mechanical behavior can be gained through cyclic testing in which the specimen is unloaded prior to failure at a constant strain rate and then reloaded either immediately or after a wait time (Figure 4, **B**).[103,104] The key signatures in this type of experiment are the strain at 0 force upon unloading, how much strain recovers before reloading, and the reduction in peak stress upon reloading (also termed 'shakedown'). This recovery (or lack thereof) typically reflects both gel network rearrangement, and possibly restoration of dynamic bonds.[105] Many different cyclic loading histories are applied with no standard convention, so while common and incredibly useful for understanding gel network dynamics, this data is, unfortunately, difficult to compare across experimental studies. The authors recommend selecting cyclic testing conditions that adequately convey the mechanical behaviors of a system with respect to hydrogel composition and intended applications for better comparative analysis.

Creep—gradual elongation over time—and stress relaxation in this large deformation regime can also provide information about gel mechanics, further distinguishing dynamic gels from ideal covalent gels.[103] Creep testing has also been used to reveal information related to structural elements within polymer melts[106] and hydrogel networks.[59] A key signature is whether, at a given stress level, creep proceeds indefinitely until the specimen breaks and/or whether, at a given strain level, the stress relaxes all the way down to zero. Creep is characteristic of the loss of network memory in dynamic hydrogels, caused by continuous bond dissociation and

https://doi.org/10.1021/acs.chemrev.5c00466
Chem. Rev. XXXX, XXX, XXX−XXX

reassociation under sustained loads or strains.[107] The bond rearrangement enables polymer chains to slide past each other and reorganize. Conversely, under fixed strain conditions, gels exhibit significant stress relaxation, where internal stresses decline as dynamic bonds break and reform in lower-energy configurations.[108] Critically, in contrast to the linear viscoelastic regime, the information gained from different magnitudes of stress or strain is not directly transferable to other magnitudes.

2.2.3. Fracture of Dynamic Networks. Fracture toughness is a critical property for practical utilization of hydrogels, as it characterizes their ability to resist failure in the presence of a defect and/or localized concentration of stress. To obtain an accurate measure of fracture toughness, a test on a specimen with a known defect location and size is needed, ideally a pure shear fracture. This specimen has a large width to height ratio and a sharp horizontal notch on one side that sets a stress concentration for initiation of fracture. The work to propagate the crack results in a fracture toughness characteristic of the material and strain rate—this property is considered reliable for comparisons across studies, whereas toughness from homogeneous material testing is less so.[109] Though less common, trouser tear tests provide similar information if properly executed.[110]

Systematic studies and extensive reviews on fracture through single network, dynamically crosslinked gels have been conducted over the past 20 years. Because dynamic bonds have the ability to repeatedly break and reform, hydrogels with dynamic bonds can display higher fracture energy and resistance to catastrophic crack growth when compared to single network covalent gels; however, this is not always the case. Relatively few studies on single networks with single bond types report fracture toughness, suggesting these values are not impressive. Fracture in these gels are time- and rate-dependent, with crack initiation and propagation influenced by loading rate and deformation history.[81,82] Two main mechanisms contribute to this behavior; viscoelasticity, as discussed above, and poroelasticity,[109] wherein deformation induces flow of solvent and distribution of mechanical force, resulting in an apparent elastic response, which can additionally alter the stress field near a crack tip and dissipate energy, resulting in poroelastic toughening.[111] A path-independent modified J integral has been developed to quantify the energy release rate, accounting for the energy dissipated through solvent diffusion.[112]

Defining criteria for crack initiation and growth remains challenging due to discrepancies between intrinsic fracture energy (the energy driving local crack propagation) and the externally applied energy, due to viscoelastic dissipation.[113] Experimental approaches have been developed to isolate dissipation effects. For example, Chen and Ravi-Chandar used full-field measurements with Schapery's Jv-integral to exclude bulk viscoelastic dissipation,[114] while Qi et al. captured the full dissipation history using a combination of full-field deformation measurements and nonlinear viscoelastic model.[115] Foundational fracture theories in linear viscoelastic materials have been developed by Knauss[116−118] Schapery,[119−121] Persson, and Brener.[122] However, near the crack tip, nonlinear viscoelastic effects become significant due to large deformation, which inhibits crack propagation and increases fracture toughness.[123]

Another characteristic relevant to the discussion of network deformation and damage, is self-healing. This refers to a gel's ability to recover mechanical properties when damaged, including internal damages or fractures related to mechanical stress.[44] While beyond the focus of this review, self-healing can be used as a partner approach to toughness, providing a pathway for long-term durability via recovery between loading phases.[44] Nondynamic, covalently crosslinked networks are generally unable to undergo self-healing processes due to the irreversible nature of bond rupture when fracture occurs, and require externally activated crosslinking mechanisms to undergo network repair.[124] Dynamically bonded networks, however, tend to show excellent self-healing from scratch tests, cut and rejoin tests, or shear past yield and recovery rheology tests because of their intrinsic reversibility. Fast healing rates and high degree of healing can be achieved depending on network mobility, crosslinker identity, and environmental sensitivity.[44,125]

2.3. Summary

The comparison of mechanical behaviors for single covalent network hydrogels versus dynamic networks reveals stark differences in mechanisms of energy dissipation and relaxation. While comparative analysis across the entire range of hydrogels is challenging due to inconsistencies in experimental conditions and testing, broader trends in analogous hydrogel systems can be elucidated that point to specific behaviors in the small and large strain regimes, static regimes, and behaviors during and after fracture. Covalently bonded networks tend to be brittle, with low fracture energy and high fracture propagation due to limited modes of energy dissipation along the network. Conversely, the reversible nature of dynamic bonds leads to a temporal component within dynamic networks that is visible in rate- and frequency-dependent testing, creating opportunities for new modes of energy dissipation and relaxation that are particularly consequential in the apparent toughness of hydrogels containing dynamic bonds. This toughness is largely determined by the thermodynamic and kinetic properties of dynamic bonds; as such, a deep understanding of how molecular design dictates dynamic crosslinking is critical in the development of tough hydrogels, with key insights and opportunities for such designs being reviewed in Section 3.

3. OPPORTUNITIES FOR TEMPORAL MODULATION OF MATERIAL DYNAMICS

Given the central role that timescale plays in the mechanical properties of hydrogels, the ability to tailor and modulate the constituent interactions determining material timescales is therefore correspondingly critical. A diverse host of dynamic bonding motifs varying in thermodynamic bases, *i.e.*, intermolecular interactions with enthalpic or entropic driving forces, and sensitivities to environmental parameters have been developed. These provide a broad palette with which to tune crosslink energies and timescales, and ultimately program the assembly, structure, and function of hydrogels. These dynamic bonds consist of two main groupings: DCBs (*e.g.*, disulfide, borate-diol, imines, and urethanes), and dynamic noncovalent bonds (*e.g.*, dipole−dipole, ion−dipole, cation−pi, ionic bonds, metal−ligand coordination, and hydrogen bonding). The integration of these bonds, either as the primary crosslinking agents or as a secondary, dynamic crosslinks within a covalently crosslinked network have been shown to greatly improve toughness, increasing the fracture energy by multiple orders of magnitude in some cases.[12] All dynamic bonds exist

https://doi.org/10.1021/acs.chemrev.5c00466
Chem. Rev. XXXX, XXX, XXX−XXX

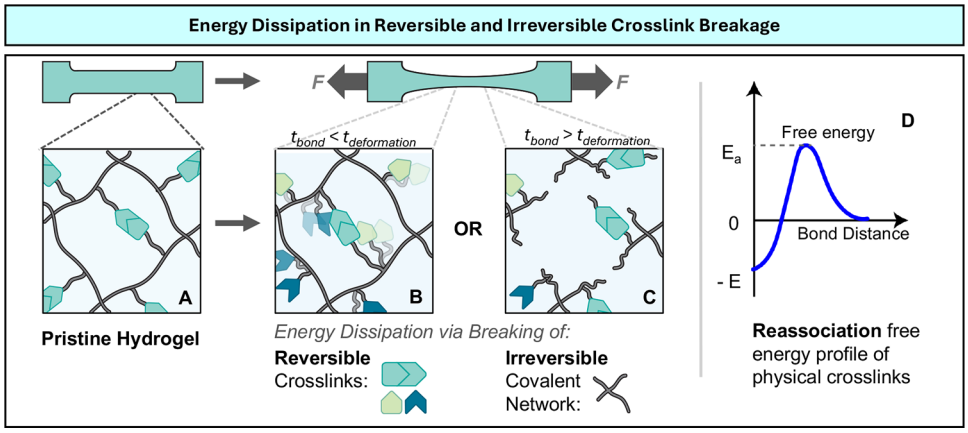

Figure 5. A) The state of physical and chemical bonds in a pristine hydrogel before undergoing mechanical deformation on B) a timescale longer than the lifetime of physical bonds, allowing them to dissipate energy, and C) a timescale shorter than the lifetime of some physical bonds, such that they cannot dissipate energy and irreversible damage to the covalent network occurs. D) is a plot of the free energy of association for dissociated stickers as a function of their separation distance, where E_a is the energy of activation of association and E is the energy gain for pair formation. Adapted with permission from Zhao et al., 2025 (ref 133, Copyright 2025 Springer Nature).

within a range of tunable timescales and are subject to secondary interactions with solvent, ions, pH, temperature, and other external stimuli, which provides the opportunity to dynamically alter the strength and dynamics of the crosslinking interactions, *i.e.*, the energetic landscape of dynamic bonds. These cumulatively provide a substantial set of opportunities for triggered self-assembly to create toughening structures, as seen in biofabrication, and to dynamically modulate the properties/structure (remodeling) and recovery from deformation or failure (self-healing).[126] The relationship between molecular structure and dynamic bond properties along with their spatial organization will be discussed in detail in the following subsections to contextualize hydrogel toughness. First, by building an understanding of the fundamental energetic bases connecting dynamic bonds to material timescale, and then extending this foundation to higher order structures as temporally tunable toughing mechanisms.

3.1. The Central Role of Dynamic Bond Thermodynamics and Kinetics in Defining Material Time Scale

The timescale of dynamic bond exchange and rate of deformation are deeply entwined with toughness as well as stiffness and strength. If dynamic bonds can be broken at a similar timescale to deformation, they convert mechanical energy to thermal energy, thus dissipating stress and preserving the structural integrity of the network.[127] Should the lifetime of dynamic bonds surpass the timescale of deformation, dynamic bonds act as static crosslinkers, resulting in distribution of mechanical energy and ultimately irreversible damage to the primary network via covalent bond scission, *i.e.*, fracture. More specifically, for dynamic bonds to enhance gel mechanical properties, the timescale of deformation and bond lifetime must complement each other such that the bond is stable enough to provide initial resistance to deformation, enabling distribution and improved dissipation of mechanical energy throughout the network,[128] but is also weak enough to break (and even reform) as deformation progresses to maximize energy dissipation (Figure 5, **A-C**). Most dynamic bonds are "slip bonds", in that their kinetic equilibrium shifts toward unbound state as the force effectively performs mechanical work to reduce the energy barrier for dissociation and decrease the characteristic timescale of bond breaking.[128−130]

More broadly, it can be helpful to think about these bond dynamics in terms of critical timescales. As suggested above, one such critical timescale for dynamic bonds in polymer networks is the bond dissociation time (τ_d)—the average time from when a bond forms to when it breaks. The bond dissociation time is related to the bond energy (E_d) relative to available thermal energy (k_BT) as expressed in eq 4,

$$\tau_d \propto \exp(E_d/k_BT) \tag{4}$$

where k_B is the Boltzmann's constant. Notably, both the scaling of timescale and free energy with temperature must be considered, as will discussed later in this section. Furthermore, this dissociation timescale on its own does not necessarily lead to gel relaxation or reconfiguration, as the original bond pair may simply reform.[131] Stukalin et al. introduced the idea of a renormalized bond lifetime when working on *intrinsic* elastomer self-healing, *i.e.*, the restoration of material cohesion after damage.[132] This timescale incorporates the bond dissociation, Rouse diffusion (thermal polymer segment motion), and the spatial density of other potential binding partners, stickers. "Sticker" density can therefore influence the rate dependent mechanical properties in two competing ways: (1) a high density of bonds leads to greater resistance to stress-driven network reconfiguration (which can manifest macroscopically as increased stiffness or strength, decreased failure strain, increased stress relaxation and creep timescales); (2) this greater bond density leads to more bond exchange and therefore locks in changes in the relative polymer chain configuration, slowing recovery after deformation. Additionally, the separation distance between two stickers has an impact on their free energy of association and resultant timescale of exchange, and so, increased density of physical crosslinking sites can minimize energy barriers otherwise enhanced by distance (Figure 5, **D**).[133] Correspondingly, configurational entropy penalties are minimized when dynamic bonds form proximally to covalent crosslinks. Therefore, those which form further away must have significantly favorable bond enthalpies or exist in high enough concentrations to compensate for the entropic restrictions they place on the network.[134]

In addition to these considerations, the timescale of dynamic bond exchange is primarily defined by the fundamental molecular structure and properties of the bonds themselves.

https://doi.org/10.1021/acs.chemrev.5c00466
Chem. Rev. XXXX, XXX, XXX−XXX

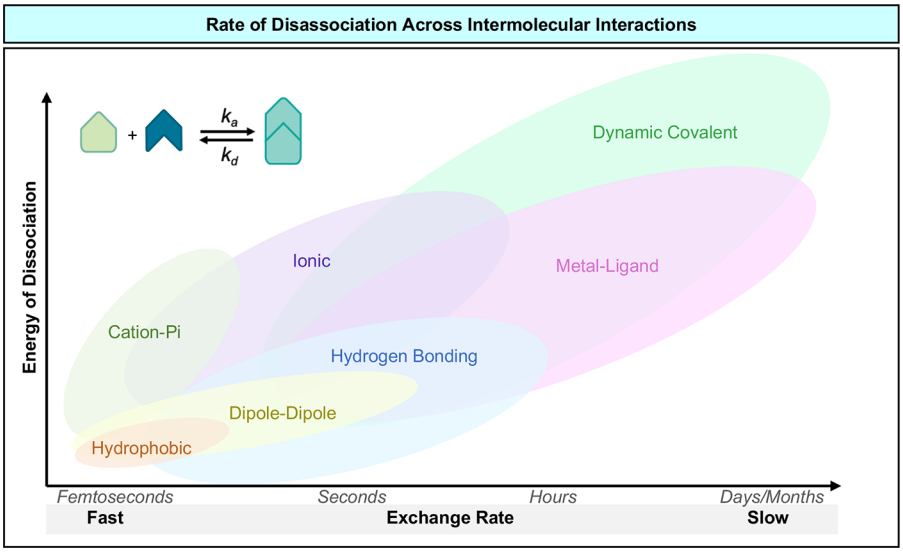

Figure 6. A schematic of the relative E_d and lifetime of the classes of dynamic bonds discussed in this review, compiled from Zhao et al., 2021 (ref 38), Zhao et al., 2025 (ref 133), Wanasinghe et al., 2022 (ref 49), and Zhang et al., 2018 (ref 139).

Likewise, the average dynamic bond lifetime determines macroscopic mechanical behavior and responsiveness,[92,135−137] and so it is vital to understand the exchange rates these motifs from a fundamental perspective. The kinetic equilibrium (K_{eq}, eq 5) between the association (k_a) and disassociation (k_d) rate constants of a dynamic bond can be related via the Eyring theory (eq 6), which can be rewritten to represent an Arrhenius relationship with temperature and activation energy (eq 7), and constituent entropic and enthalpic terms (eq 8).[92,135−137] Note that pairs of eqs 6−8 exist for both the association and disassociation kinetic pathways, k_a and k_d, as described by eq 5. In the following equations, h is Planck's constant, R is the ideal gas constant, and "‡" denotes that the property corresponds to a transition state.[135,137] For context, the thermal energy of dynamic bonds (typically a few to tens of k_BT) is much lower than that of covalent bonds (>100 k_BT).[138,139] In the context of temperatures traditionally associated with hydrogels, it is also important to note that referring to noncovalent bonds as dynamic could be seen as redundant given the relatively low bond enthalpy of many of these motifs. However, within the broader context of toughness, it is critical that this implicit assumption of temperature, or an average kinetic energy in a system be acknowledged, given its direct relationship to interaction timescale.[140]

$$K_{eq} = \frac{k_a}{k_d} \tag{5}$$

$$k = \frac{k_B T}{h} \exp\left(-\frac{\Delta G^{\ddagger}}{RT}\right) \tag{6}$$

$$k = A \exp\left(-\frac{E_a}{RT}\right) \tag{7}$$

$$k = \frac{k_B T}{h} \exp\left(-\frac{\Delta S^{\ddagger}}{R}\right) \exp\left(-\frac{\Delta H^{\ddagger}}{RT}\right) \tag{8}$$

The mechanism of dynamic bond exchange during deformation can occur through one of several pathways depending on their interaction energy and can be categorized as dissociative or associative exchange.[126] Dissociative exchange occurs via the complete dissociation of a reversible bond pair. Dynamic bonds that undergo this exchange mechanism are characterized by closely matched activation energies of association (E_a) and dissociation (E_d) such that the difference $E_d - E_a$ is small (several k_BT per mole) and a moderate bond energy, *i.e.*, modest energy difference between bound and unbound states. Conversely, in the associative exchange mechanism, a dynamic bond encounters a new bonding partner and forms an associated complex, that subsequently undergoes dissociation to form a new bonding pair. In these systems, the activation energy of association is typically higher than the energy of activation for dissociation from the associated complex. As such, the availability of unbound bonding motifs increases the apparent bond exchange rate. Importantly, both associative and disassociate exchange pathways have generally been found to obey an Arrhenius-like scaling relationship between temperature and viscosity.[141] It is additionally worth noting that most dynamic noncovalent bonds have low energies of formation (relative to k_BT per mole) and rapid exchange kinetics, making the distinction of these mechanistic pathways challenging. The specific mechanistic pathways of dissociative and associative exchange become relevant to higher energy dynamic bonds such as DCBs and some metal−ligand coordination bonds.[126]

Although it is usually the case that dynamic covalent bonds have a lower exchange rate and higher E_d than their dynamic noncovalent counterparts,[126] it is difficult to make general statements about all dynamic bonds due to their unique energies and timescales (Figure 6). To understand the true complexity of these dynamic systems, we must consider specific molecular scale contributions to their association and exchange, the timescale of which directly influence the material properties of the network.[38,142] Equilibrium rates of dissociation and reassociation, to either the same or different sites, are governed by molecular parameters such as directionality (*e.g.*, steric hindrance or anisotropy of electron density/molecular orbitals) and bond enthalpy, resulting in a broad range of dynamic bond equilibrium exchange timescales, from femtoseconds to days/months (quasi-static).[143,144] External stimuli

https://doi.org/10.1021/acs.chemrev.5c00466
Chem. Rev. XXXX, XXX, XXX−XXX

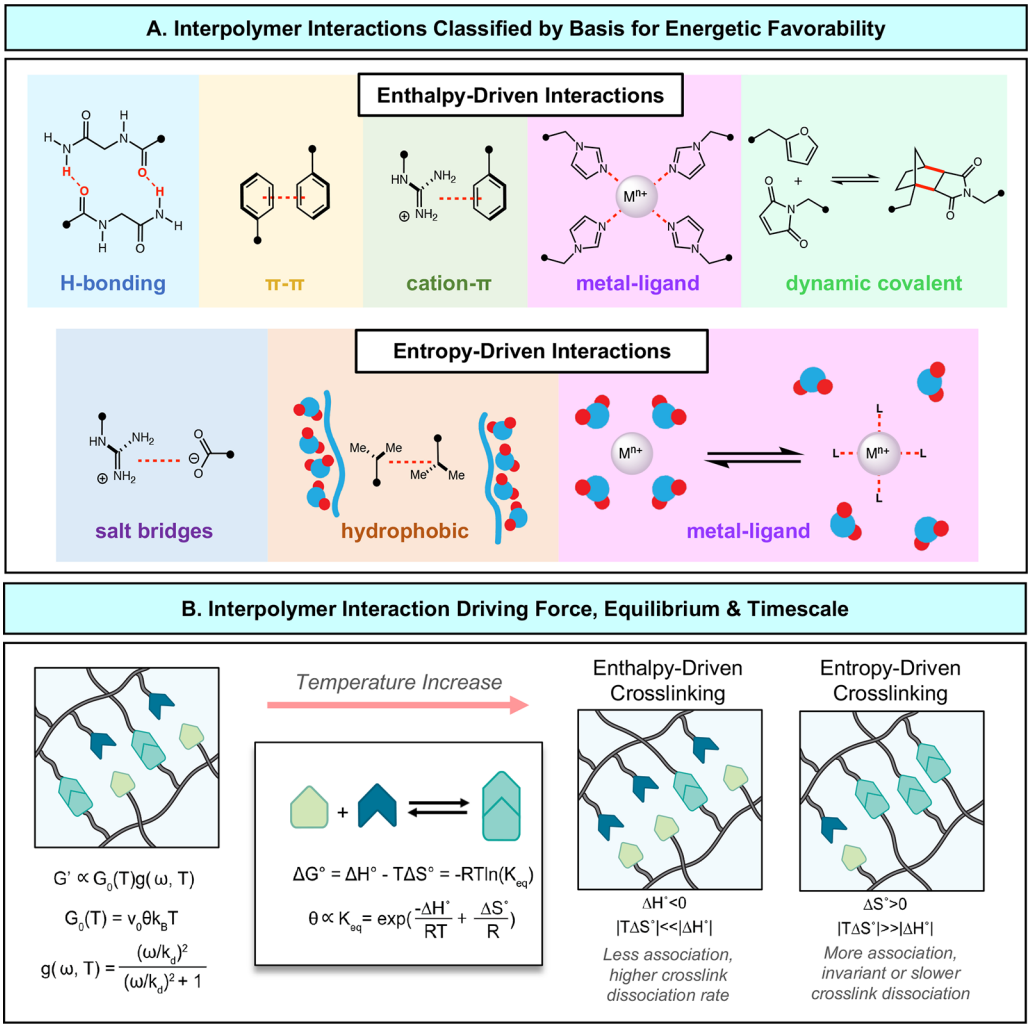

Figure 7. A) Reversible interactions discussed in this review are grouped according to their dominating thermodynamic term. B) Equations necessary to understand the equilibrium reversible bond exchange within a network. A depiction of the difference in temperature effects on enthalpic and entropic interactions, further relating temperature to the storage modulus G', plateau modulus $G_0(T)$, and frequency-dependent single-mode Maxwell term $g(w,T)$. Adapted with permission from Yu et al., 2021 (ref 145, Copyright 2021 Springer Nature).

(pH, temperature, dielectric) also serve as simple tools to shift equilibrium, modifying timescales of exchange at this elementary level.[92] Therefore, molecular structure, both of bonds and environment are critical considerations to developing an informed picture of the energy landscape of dynamic bonds and their role in energy dissipation in hydrogels and soft materials.

3.2. Molecular Structure Defines Dynamic Bond Energy Landscape

The energy landscape of dynamic bonds, *i.e.*, the activation energies defining exchange timescale and Gibbs free energy (ΔG), is defined by the molecular structure of the interacting groups. Broadly categorizing these bonding motifs by the major contributor to their Gibbs free energy, enthalpy or entropy, provides a straightforward and useful conceptual model for conceiving of dynamic bond energy landscapes that evolve as a function of solvation and temperature and is therefore critical to holistically evaluating thermodynamic and kinetic equilibria of dynamic bonds in the context of material environment and application.

Enthalpically driven interactions are characterized by the exothermic formation of dynamic bonds with a defined stoichiometry. The corresponding dissociation rates generally follow an Arrhenius relationship, such that higher temperature results in faster exchange.[145] As such, enthalpically driven interactions result in hydrogels that obey the time−temperature superposition principle (TTS), wherein a material has the same bulk mechanical response on a long timescale at low temperature as it does on a short timescale at high temperature.[146,147] Dynamic bonds can be entropically driven by interactions leading to large increases in translational entropy, such as the release of solvent or mobile counterions. Given the relationship between temperature and entropic contributions to the Gibbs free energy, such systems show slowed dynamic crosslink exchange at elevated temperature and can even be functionally temperature independent[145] (Figure 7, **B**).

It is additionally important to consider the directionality of noncovalent interactions, as this directly relates to the entropic penalty of forming a physical bond, and can impose competition between enthalpic and entropic contributions to the overall free energy (Figure 8, **A**). This is a particularly critical consideration for multivalent noncovalent interactions, which endow hydrogels with robust mechanical properties, but

https://doi.org/10.1021/acs.chemrev.5c00466
Chem. Rev. XXXX, XXX, XXX−XXX

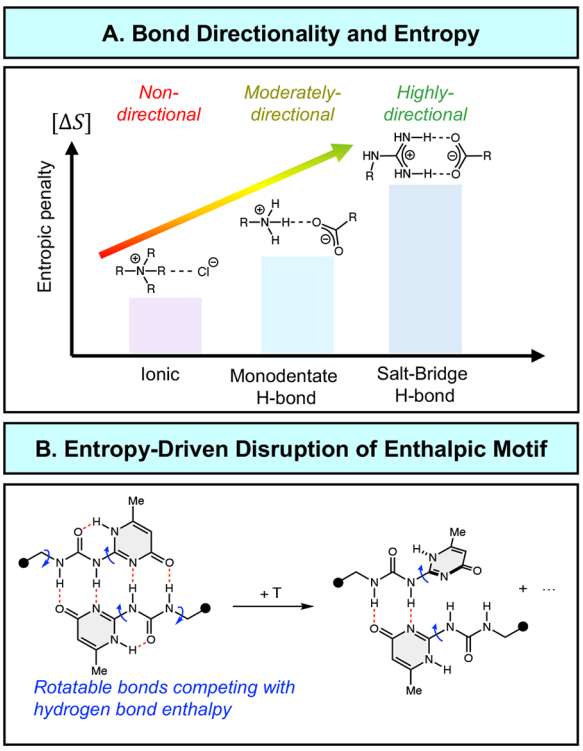

Figure 8. A) A scheme of the entropic penalty vs degree of directionality for select physical bonds. Reproduced with permission from Qiao et al., 2024 (ref 607, Copyright 2024 American Chemical Society). B) Entropic constrictions placed on the enthalpy of hydrogen bonding in UPy motifs, resulting in poorer association with increasing temperature.

can come at a substantial entropic penalty. This enthalpy–entropy trade-off is exemplified by the canonical dimeric hydrogen bonding motif 2-ureido-4[1H]-pyrimidinone (UPy), which consists of a quartet of complementary hydrogen bonds (Figure 8, B). In the UPy motif, urea and pyrimidone (shaded in gray) are locked into a bicyclic structure by a single hydrogen bond. While this structural confinement increases association constants several orders of magnitude,[148] the constrained rotational freedom and commensurate entropic penalty results in a steep decay in association as temperature increases,[149] thus requiring careful consideration of intended application or the incorporation of additional functional groups. Conversely, enthalpy–entropy competition can be constructively utilized to engineer the mechanical properties of materials, as directional interactions can be "activated", *i.e.*, the bonding equilibrium shifted from dissociated to associated, during material deformation. This dynamic change in the equilibrium constant is due to polymer chain extension, which reduces their conformational variability and commensurately reduces the penalty of directional bonding interactions.[150] Thus, a number of latent interactions can be incorporated into a material without undesirably increasing its stiffness/brittleness, effectively serving as a timescale-based catch bond.[75,76] Recently, salt bridges, specifically guanidinium-carboxylate pairs, were highlighted as new chemical motif engendering this behavior. The directionality imposed by the planar structure of both ions was attributed to creating a supramolecular elastomeric material with an incredible impacting stiffening response, evolving from a soft dissipating state (21 kPa, 0.1 Hz) to a glassy state (45.3 MPa, 100 Hz), an approximate ∼2100-fold increase in stiffness. Taken in sum, these examples underscore the necessity of rigorously connecting molecular structure and their relationship with the underlying thermodynamics relationships defining material mechanical properties.

While time–temperature scaling relationships are generally essential for understanding material properties,[147] gels, particularly hydrogels, pose another essential consideration; the nature of solvent–solvent and solvent–solute interactions as well as their impact on the enthalpic and entropic contributions to polymer solvation and polymer–polymer interactions. Polymer solvation can be simply conceptualized with the lattice model of the Flory–Huggins theory,[151] which describes the free energy of mixing, ΔG_{mix}, of polymer solutions as a balance between polymer–polymer, solvent–solvent, and polymer–solvent interactions.[152] The free energy of mixing per lattice site can be described by eq 9,

$$\frac{\Delta G_{mix}}{kT} = \Phi_1 \ln\Phi_1 + \frac{\Phi_2}{N}\ln\Phi_2 + \Phi_1\Phi_2\chi \tag{9}$$

where Φ_1 is the volume fraction of solvent, Φ_2 is the volume fraction of polymer, N is the degree of polymerization, and χ is the dimensionless Flory parameter. Correspondingly, the first two terms of eq 9 describe the entropic contributions toward mixing while the last term describes enthalpic contributions. Generally, solvation is largely entropy driven, as mixing two pure species always provides a configurational incentive. The consequence of confining molecules to a polymeric backbone, however, limits the gain in configurational entropy upon mixing. Thus, favorable solvation of polymer chains requires a greater enthalpic contribution relative to the solvation of small molecules.

The enthalpy of mixing, ΔH_{mix}, describes the difference in enthalpy between polymer–solvent, polymer–polymer, and solvent–solvent interactions. This enthalpic cost is encompassed in χ, where positive values indicate enthalpically unfavorable interactions between the polymer–solvent pair (relative to polymer–polymer interactions) while negative values indicate energetically favorable polymer–solvent interactions. Therefore, molecular structure dictates solvation based on the capability of forming energetically favorable intermolecular interactions between polymer and solvent (*e.g.*, hydrogen bonding and dipolar interactions in the case of hydrogels). Critically, these intermolecular interactions must be balanced, as the organization of interaction sites across a polymer backbone engenders multivalent interactions between polymer chains, which can increase the penalty of solvation if they are of sufficient energy.[153,154] The presence of additional solutes further poses significant implications for polymer solvation, as will be discussed in Section 4. Therefore, careful analysis of potential solute–solvent interactions must be considered if hydrogels are applied in ionic solutions.

Moreover, from a molecular perspective, water is an exceptionally unique small molecule that poses intriguing considerations as a solvent.[155−159] As a polar protic molecule, water can engage in hydrogen bond donation and acceptance, and additionally has a dipole moment of 1.855 D that increases to 2.5 D in the condensed phase.[160] This strong self-interaction allows water to form local tetrahedral structures for which experimental evidence of dynamic, high order structures continues to emerge (Figure 9, **A**).[161] These self-assembly properties therefore create the strong potential for entropic penalties with accommodating guest molecules and give rise to

https://doi.org/10.1021/acs.chemrev.5c00466
Chem. Rev. XXXX, XXX, XXX−XXX

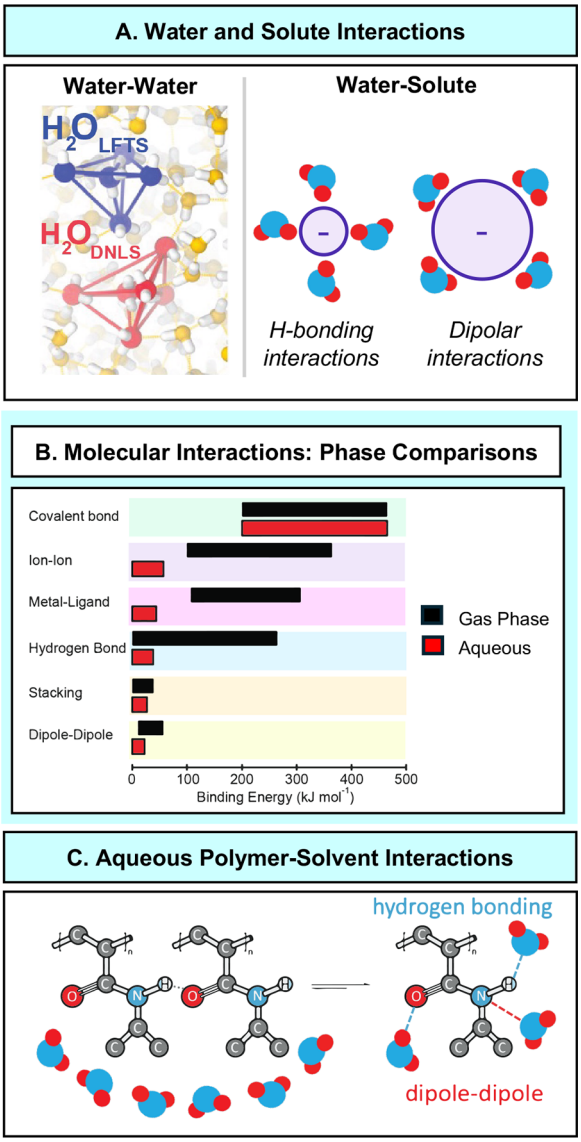

Figure 9. A) Locally favored tetrahedral state (LFTS) has four H-bonded nearest neighbors with tetrahedral coordination, whereas disordered natural liquid state (DNLS) typically has five or more nearest neighbors, (typically three of them being H-bonded) with broken tetrahedral symmetry. The addition of solutes perturbs water structuring, charge dense solute (left) favor directional hydrogen bonding with water inducing ordered structures. Polarizable solutes (right) interact with water via less-directional ion-dipole interactions. B) Qualitative analysis of various covalent and noncovalent interactions in the gas (black) and aqueous (red) phase. As expected, there is no perturbation of covalent interactions between phases as solvation does not compete. Through space interactions are characterized with weakened binding energies in aqueous phase owing to modification of dielectrics and competitive interaction with solvent. C) Polymer mixing requires disruption of interpolymer interactions for formation of favorable polymer−solvent interactions (hydrogen bonding and dipolar interactions shown in blue and red, respectively). Disruption of polymer−solvent interactions induces ordered solvation shells that can be energetically unfavorable. A is reproduced with permission from Shi and Tanaka 2020 (ref 161, Copyright 2020 American Chemical Society). B collected from Zhao et al., 2021 (ref 366), Biedermann and Schneider 2016 (ref 166), Muthukumar 2017 (ref 227), Hobza 2012 (ref 167), Steiner 2002 (ref 168), Markovitch and Agmon 2007 (ref 169). C is adapted with permission from Levin and Cohen 2025 (ref 165, Copyright 2025 American Chemical Society).

responsive phenomena discussed in Section 4.1.4. Further considering solvent−solute interactions, the multimodality of water's intermolecular interactions enables it to broadly engage charged and polar molecules. Thus, water broadly competes with strong polymer−polymer intermolecular interactions, such as ionic, hydrogen bonding, and ion-dipole interactions. Thus, while many polymeric soft material reviews highlight the general enthalpy of intermolecular interactions, it is critical to consider the impact of solvation in water on intermolecular interactions (Figure 9).[162−169] This points to the consideration of solvation energy as a critical and emerging facet in the engineering of intermolecular interactions and by extension the mechanical properties of hydrogels; specifically, how the molecular structure of interacting motifs dictates their solvation and how conjunction with their thermodynamic basis influences interaction strength, equilibrium (fraction of motifs actually interacting), and the exchange timescale as a function of environmental factors such as temperature and cosolute species.

Given the defining role molecular structure plays on a dynamic bond's underlying driving forces and dynamics as well as sensitivity to environmental features, the following sections will examine different classes of dynamic bonds and explore the underlying thermodynamic driving forces behind these interactions and relate these to scaling behavior as a function of environment (energy and timescale of interaction, energy as a function of distance). This detailed examination will provide the basis to understand the application of dynamic bond modulation to programming the assembly and structure of hydrogel networks (Section 4) to tailor mechanical deformation response and toughness, as well as the structural recovery/remodeling of hydrogels that will enable future technological applications (Section 5).

3.2.1. Dynamic Covalent Bonds. Dynamic covalent bonds (DCBs) are reversible, covalent bonds that can equilibrate between thermodynamically favorable species without the production of byproducts and have been employed in a number of hydrogel applications ranging from drug delivery and tissue engineering to biosensors and adhesives.[170,171] DCBs are characterized by intermediates with energies commensurate with the available thermal energy, thus enabling the exchange of crosslinking sites with approximately degenerate energies (Figure 10, A)[172] and endowing them with responsive properties such as shape memory and self-healing while maintaining relatively strain rate independent stiffness and toughness.[49,173,174] This bond exchange has been reported to endow gels with improved toughness, dissipating mechanical energy within the network.[49,175] Dynamic covalent chemistries retain the stimuli-responsive properties of dynamic bonds, but they sustain the mechanical strength of covalently crosslinked networks. DCB exchange can be facilitated by light, heat, pH, or other solution chemistry.[176,177] This enables tuning for the dynamics for a range of applications.

Common DCB motifs in hydrogels include Diels−Alder chemistry, transesterification, disulfide bonds, and imine bonds. Each of these chemistries has unique association energies for bond formation and relaxation times. DCBs typically exhibit activation energies in the range of 10−470 kJ mol^{-1} at room temperature, with solvated bond systems at the lower end of this range[38] (Figure 6). The activation energies and relaxation times can be modulated through steric, electronic, and solvent interactions.[178,179] The concentration of reactants, the presence of a catalyst,[180,181] and phase

https://doi.org/10.1021/acs.chemrev.5c00466
Chem. Rev. XXXX, XXX, XXX−XXX

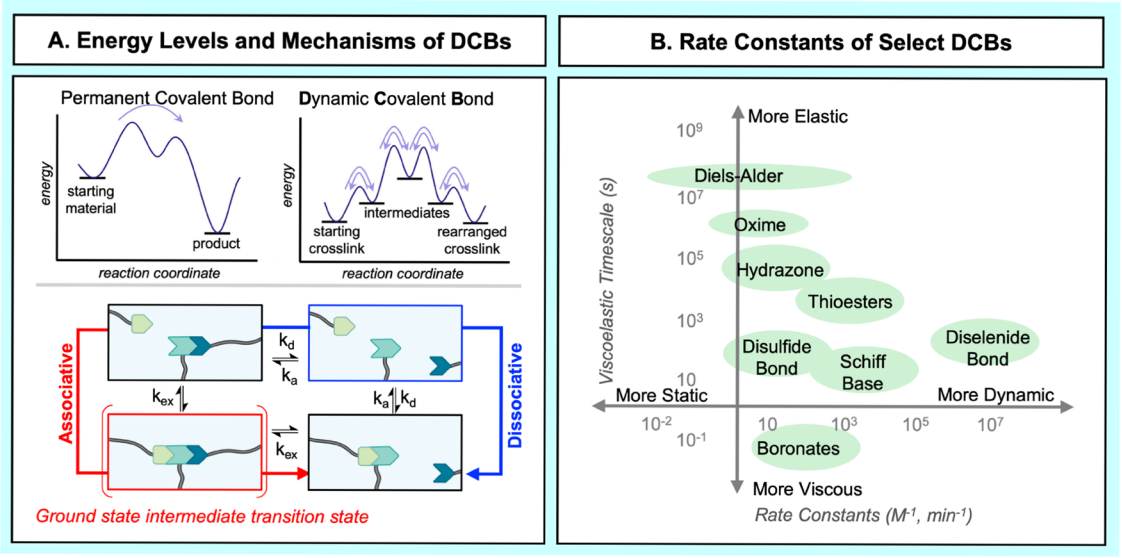

Figure 10. A) Sketches of energy level diagrams for dynamic covalent bonding and permanent covalent bonding in addition to representations of associative and dissociative mechanisms. Adapted with permission from Zhang et al., 2022 (ref 172, Copyright 2022 American Chemical Society). B) Rate constants and viscoelastic timescale for various dynamic covalent chemistries, adapted with permission from Han et al., 2022 (ref 175, Copyright 2022 MDPI).

separation all impact activation energy, offering pathways for further tunability of gels.[182] The array of dynamic bonds and data that illustrate the range of reactivity within dynamic covalent chemistry, have been well tabulated in a number of reviews and perspectives,[183−187] and excellently overviewed by Kalow and co-workers, wherein the quantitative structure−reactivity−property relationships of DCB motifs, *i.e.*, linear free energy relationships, are directly linked to the macroscale time-dependent properties of soft materials (Figure 10, **B**).[172]

The reversibility of DCBs can be tuned via steric or electronic effects to drive either bond formation or bond dissociation, providing diverse opportunities to modulate material properties for a range of applications. DCBs typically exchange more slowly than noncovalent dynamic interactions[49] and typically undergo multiple intermediate exchange mechanisms, offering additional complexity compared to physical bonds. For associative mechanisms, viscoelasticity is determined by the exchange rate, whereas in dissociative mechanisms, it is determined by the rate of dissociation. Stiffness is determined by the crosslinking density in associative systems and the binding constant in dissociative systems.[188] Notably, discrepancies in small-molecule bonding parameters and macroscopic polymer network parameters have been reported in DCB networks, underscoring the complexities of their mechanisms.[172] For example, small molecule and network activation energy often differ due to mechanisms not fully understood, but hypothesized to be related to entropic penalties from rigid chain backbones and matrix hydrophobicity or polarity.[172]

Zhang et al. incorporated dithioalkylidenes within hydrogels, which proceed via an associative mechanism.[188] Modulating the structure of the dithioalkylidenes, they were able to tune the molecular exchange rate and alter the gel's stress relaxation time (τ) in a 1:1 direct relationship. This relationship underscores the importance of molecular design and its connection to the material properties of hydrogels. Gels with DCB have been systematically tailored to investigate how bond dynamics and network architecture set the frequency dependence of the storage and loss moduli.[137,189−191] For example, Lou et al. investigated catalyst-modulated hydrazone bonds in linear polymers with functional side groups, 4-arm polymers, and 8-arm polymers.[189] Hydrazone-bonded linear polymers used stress relaxation experiments to find that increasing catalyst concentration (which increases bond dissociation kinetics) decreases the critical timescale for network relaxation without changing the high frequency modulus. For linear, 4-arm, and 8-arm polymers, both the modulus and critical relaxation timescale increased with crosslink density as would be expected.

Tough gels and polymer networks may be formed through leveraging multiple dynamic covalent interactions, allowing for the tuning of relaxation time over a wide range.[192,193] For example, Cornellà et al. utilized Diels−Alder chemistry, a dissociative mechanism, and associative transesterification chemistry.[49] By changing the composition of polymers in an elastomeric network, the characteristic relaxation time was modulated over 6 orders of magnitude from τ = 0 to 10^6 seconds.[194] The weaker Diels−Alder interactions have faster exchange, whereas transesterification had slower exchange; these dual relaxation modes led to polymer networks that reduced creep while exhibiting shape memory and self-healing.

Studies regarding DCB polymer networks primarily focus on properties such as self-healing, often neglecting explorations of toughness. Nevertheless, DCB networks with high toughness have been reported; for example, as described by Liu et al., a 7-hydroxy-ethoxy-4-methylcoumarin and polyurethane network exhibited a toughness of 55 MJ/m^3. This network undergoes a photo reversible dimerization process, which researchers attributed to endowing the network with enhanced mechanical properties.[195] After the removal of a stimulus, sacrificial bonds within the network can reform, endowing the gel with properties such as shape memory. Notably, the mechanism by which dynamic covalent bonds dissipate energy is often not discussed in detail in current literature; as such, further exploration of how different chemistries dissipate energy is

https://doi.org/10.1021/acs.chemrev.5c00466
Chem. Rev. XXXX, XXX, XXX−XXX

required as well further experimental analysis of toughness in gels with DCBs.

3.2.2. Metal−Ligand Coordination. Metal−ligand coordination refers to a diverse class of Lewis acid/base interactions with molecular character spanning near-covalent to electrostatic binding, thus broadly varying in energy, timescale, and directionality. This range of bond energy and timescale is reflected empirically in values of E_d = 20−300 kJ mol^{-1} and K_a (binding constants) between 10^3−10^{40}.[142,196] When incorporated into a polymer or hydrogel, a metal center either acts as a crosslink by bridging polymers decorated with ligands, or as a structural motif, inducing coils, micelles, or other uniquely ordered structures.[197−199] Metal−ligand coordinated networks are an exemplar for understanding how bond timescales and network morphology influence dynamic moduli in the small strain regime, as the broad array of ligand structures and metal coordination modes provides an exceptional breadth of bond dynamics.

While metal−ligand interactions can be similar to dynamic covalent bonds in their nuanced exchange mechanisms, metal centers are further characterized molecular properties such as charge as well as molecular orbital energy and geometry, both of which modulate coordination energies of ligands based on their structure as well as their approximate stoichiometry. For example, divalent metals show higher binding reversibility than trivalent metals,[200] while divalent metals vary in coordination number and geometry based on their identity. Additionally, higher oxidation states and multidentate ligands share more electrostatic interactions, resulting in greater bond stability and greatly shifting the timescales of association.[200−202] Thus, the coordination geometry associated with a specific metal center lends to its stability in a given ligand system and influences the structure and mechanical properties of a hydrogel accordingly.[127,142]

A classic example of metal−ligand coordination in tough hydrogels is the use of calcium-carboxylate complexes for crosslinking linear polysaccharide alginate. Alginates are copolymers of β-D-mannuronic acid (M) and its C-5 epimer α-L-guluronic acid (G) linked by 1,4 glycosidic bonds. This stereochemical context results in G-G blocks forming cavities with Ca^{2+} affinity, that when crosslinked are referred to as an "egg-box" (Figure 11, **B**).[203−205] This egg-box topology has been hypothesized to result in a distinct toughening mechanism, in which applied stress is localized to unzip alginate-Ca^{2+} units in a small area, thereby dissipating energy. Although individual Ca^{2+}-alginate bonds are 2 orders of magnitude weaker than covalent bonds, when incorporated into an appropriate gel architecture, these motifs work in concert to achieve remarkable toughness (∼16 kJ/m^2) compared to a poly(acrylamide) gel in their absence (100 J/m^2).[206,207] Other metal centers, such as sodium, zinc, and magnesium can be used in place of calcium to modulate gel kinetics and also biological interactions.[200,204,205,208]

As previously noted, the timescale of metal−ligand coordination depends on the identity of both the metal crosslinker and the ligand. The favorability of these interactions can be broadly understood using the hard−soft acid−base (HSAB) theory, which classifies the "hardness" or "softness" of a Lewis acid (metal cation) or base (ligand) by its charge density and polarizability, and further predicts that stronger pairs form on the basis of similarity in hardness/softness.[209−211] Additionally, harder metal ions with larger coordination numbers will be strongly hydrated, resulting in

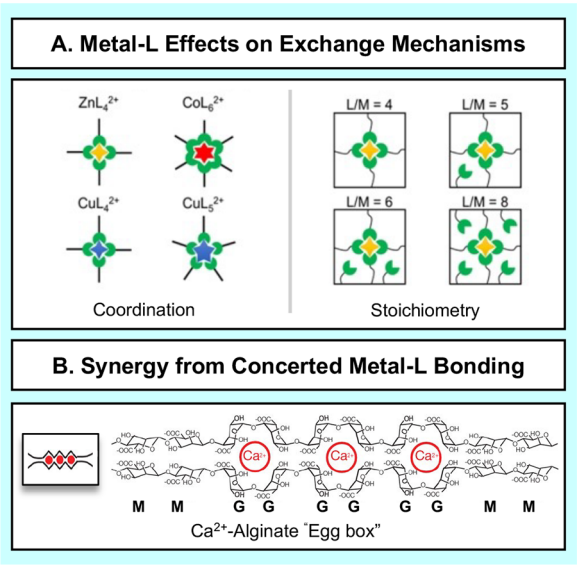

Figure 11. A) Coordination geometries for divalent metals (Zn, Co, Cu) with monodentate imidazole ligands. As coordination geometry shifts from tetrahedral (Zn, Cu), to octahedral (Co), the binding site becomes increasingly crowded resulting in a switch from associative exchange to dissociative ligand exchange. Reproduced with permission from Mozhdehi et al., 2016 (ref 127, Copyright 2016 American Chemical Society). B) the "Egg-box" like cage formed by guluronic acid (G) and mannuronic acid (M) units of alginate with Ca^{2+}. Reproduced with permission from Sun et al., 2012 (ref 206, Copyright 2012 Nature).

longer recovery times after deformation, as the energy of bond reformation is highly dependent on the displacement of coordinated water (outer sphere aqua ligands) from the metal center.[200] This is often the rate-determining step of association and introduces an entropic penalty to bond reformation. The Irving-Williams series is another useful framework to predict the stability of bivalent metal complexes, which are observed to follow the order Zn^{2+} < Cu^{2+} ≫ Ni^{2+} > Co^{2+} > Fe^{2+} > Mn^{2+}[201,202] unless there is significant steric hindrance at higher coordination numbers (*e.g.*, imidazole-Co^{2+}).[127,142] Thus, changing the metal identity results in ligand−metal pairs of unique stabilities and timescales as a result of the metal's Lewis acidity, coordination geometry, and oxidation state (Figure 11, **A**). Local dynamics are reflected in the macroscopic properties of gels, and so, stable binding pairs with longer lifetimes result in longer gel relaxation times.[133]

In 2016 Tang and Olsen showed that for a linear gel with sufficient density of metal-coordinating bifunctional side groups, the bond lifetime closely matches the bond exchange timescale and sets the macroscale relaxation crossover timescale.[212] In 2021, Ahmadi and Seiffert showed that metal centers with different stability effectively shift the dynamic moduli of a tetrafunctional network such than an overall master curve can be constructed.[213] These trends demonstrate that the modulation of linear viscoelasticity in the small strain regime is modular based on dynamic metal bonding methods of crosslinks, including in metal ligand coordination and metal identity. Grindy et al. demonstrated that by regulating the relative quantity of two metal salts, they could control how many crosslinks were active at a given timescale.[91] Specifically, working with a histidine functionalized 4-arm pol(yethylene glycol) (PEG), two separate systems of metal−ligand crosslinks were investigated. Introducing either nickel and zinc or

https://doi.org/10.1021/acs.chemrev.5c00466
Chem. Rev. XXXX, XXX, XXX−XXX

nickel and copper salts resulted in dynamic networks that displayed two distinct relaxation modes respectively, as evidenced by two local maxima in the loss viscoelastic modulus for each system: a slow relaxation that occurs at frequencies of $\sim 10^{-2}-10^{\circ}$ rad s^{-1}, and a fast relaxation at $\sim 10^{1}-10^{2}$ rad s^{-1}. When the ratios of Zn:Ni or Cu:Ni in each respective network were varied, noticeable shifts in relaxation mode were observed. As the concentration of Ni decreased, the prominence of the slow relaxation mode also decreased, whereas increasing the concentration of either Zn or Cu resulted in an increased prominence of the fast relaxation mode. Additionally, the relative contributions of the metal crosslinks to slow or fast relaxation modes were specific to metal ion identity, where the fast relaxation mode showed greater prominence at lower concentrations of Zn, compared to Cu, which required greater concentrations to achieve the same effect. The quantitative relationship between metal−ligand identity and relaxation modes suggests direct control of network relaxation.

Monomer Lewis basicity, as well as concentration, has a profound effect on the material properties of these hydrogels. Naturally, by modulating the ratio of metal ion to chelator, different network connectivity and mobility can be achieved. Zheng et al. in 2016 showed that the tear energy of the iron coordinated poly(acrylamide-*co*-acrylic acid) was around 300−1300 J m^{-2}.[214] As stress is applied, this material transitions from the elastic regime to a nonlinear viscoelastic regime, exhibiting an apparent yield. This regime exhibits moderate and fairly constant strain hardening when plotted as engineering stress−strain. However, it should be noted that this implies a dramatic nonlinear intrinsic material strain hardening, as applied strains reach well over 100%. As is typical for dynamically crosslinked gels, the stress−strain response is rate dependent. For a single formulation, the yield stress increased by three times and the failure strain decreased by three times as the strain rate increased by 100 times. When the molar fraction of acrylic acid is varied from 25% down to 10%, the elastic modulus at a given strain rate decreases from 80 to 5 MPa, the yield stress from 17 to 5 MPa, and the failure strain increased from 160% to 520%. Interestingly, when the molar fraction of acrylic acid was further decreased to 8%, the tensile curve took on an essentially a linear characteristic. Although impossible to tell without unloading data, it is likely that this linear curve indicates a viscous fluid behavior. Then in a follow up study of the same material system in 2020, fracture energy under pure shear fracture was found that monotonically increased from 1000 J m^{-2} to 2200 J m^{-2} as the molar fraction of acrylic acid was varied from 8% to 25%.[80] As expected, these values were found to be moderately rate dependent.[80] A study by Mozhdehi et al. on metallopolymer networks found that increasing either stability or quantity of metal ligand coordination crosslinks increases stiffness and strength, and decreases failure strain.[127] This Mozhdehi et al. study systematically examined formulations with weak overall effective dynamic crosslinking and found a range over which the stress−strain response was independent of exactly how many crosslink sites were utilized.

A simple environmental parameter for the modulation of metal−ligand coordination bonds is pH. As Lewis basic ligands additionally exhibit Brønsted basicity, the protonation state and corresponding electron density of a ligand can be altered to change the energy and/or stoichiometry of metal−ligand complexes. In the case of metal−ligand coordination, pH can be used as a metric to either "shut-off" binding, or it can be used to switch the ligand valency and resultant coordination geometry between high and low binding enthalpies or dissociation rates.[215−217] This field emerged from the seminal work of Holten-Andersen et al. in 2011 on mussel-inspired polymer networks.[218] They found that with pH they could tune a Dopa-Fe^{3+} coordination structure in a PEG network from mono- to di- to trifunctional and thereby tune the gel from viscous fluid to gels with a crossover frequency (where G' crosses G") around 10 Hz to gels with a crossover frequency of well less than 1 Hz. Also inspired by motifs found in the mussel byssus, Lu and co-workers use pH to cleverly shift populations of strong and weak coordination bonds. Adjusting the pH of a dopamine (DA) functionalized 4-arm PEG (4-armed PEG−DA) effectively cycles between the mono- (pH 3−5), bis- (pH 5−9) and tris(pH > 9) catechol-Fe^{3+} complexes, tuning the strength and exchange rate of interactions to nearly that of a covalent bond at higher coordinate forms.[217,218] The aforementioned Fe^{3+}−poly(acrylamide-*co*-acrylic acid) gels designed by Zheng et al. are also tunable by pH (Figure 12).[214] These gels achieved maximum strength when the concentration of $FeCl_3$ salt approximately matched the stoichiometry of available ligands for the formation of trivalent complexes, and when the pH was raised from 1.7 to 5, which enhanced the stability to metal complexes.

Hydrogels that undergo a pH induced sol−gel transition in response to subtle pH changes in relevant physiological sites are of particular interest for drug-delivery.[216] Tang et al. describe the use of Ni^{2+} to crosslink polyhistidine-terminated PEG with iminodiacetic acid functionalized oligochitosan. Acidification (pH 5) induces dissolution of the network by protonating iminodiacetic acid units and therefore disrupting crosslinking.[216]

In hydrogels, metal−ligand bonds are a balance of entropic and enthalpically dominated contributions, as the displacement of water is necessary and rate-limiting in complexation, but the stability of the complex formed determines timescales of disassociation. Ligand bulk[219] and denticity, as well as metal valency and coordination geometry provide efficient handles to tune the thermodynamics of binding from a molecular level. External stimuli such as pH and salt can be used to further shift the equilibrium of bond exchange within these hydrogels, however, neither metal nor ligand counterion effects are typically explored in metal−ligand hydrogels, or they are simply dialyzed away from the ligands during gel equilibration. Although often overlooked, the effect of counterions cannot be underestimated. In an organogel (dimethyl sulfoxide solvent, DMSO) of poly(4-vinylpyridine), Loveless and co-workers find that the counterion, or competing acid, must have sufficiently low affinity for the metal in order for crosslinking and gelation to occur. The counterion must remain uncompetitive against solvent-metal and ligand−metal binding.[220] In elastomers, it has been shown that balancing counterion and metal association strengths, such that some anions remain coordinated, may stabilize complexes formed with ligands and strategically improve energy dissipation.[221] Perhaps future work may contextualize these effects on bond exchange within hydrogels, specifically as a means to modulate the strength and dissociation rate of metal−ligand complexes when a counterion is competitive with the main binding scheme.

3.2.3. Ionic Bonds. Ionic polymers, *e.g.*, polyelectrolytes,[222−224] polyampholytes,[76] and polyzwitterions[225,226] can

https://doi.org/10.1021/acs.chemrev.5c00466
Chem. Rev. XXXX, XXX, XXX−XXX

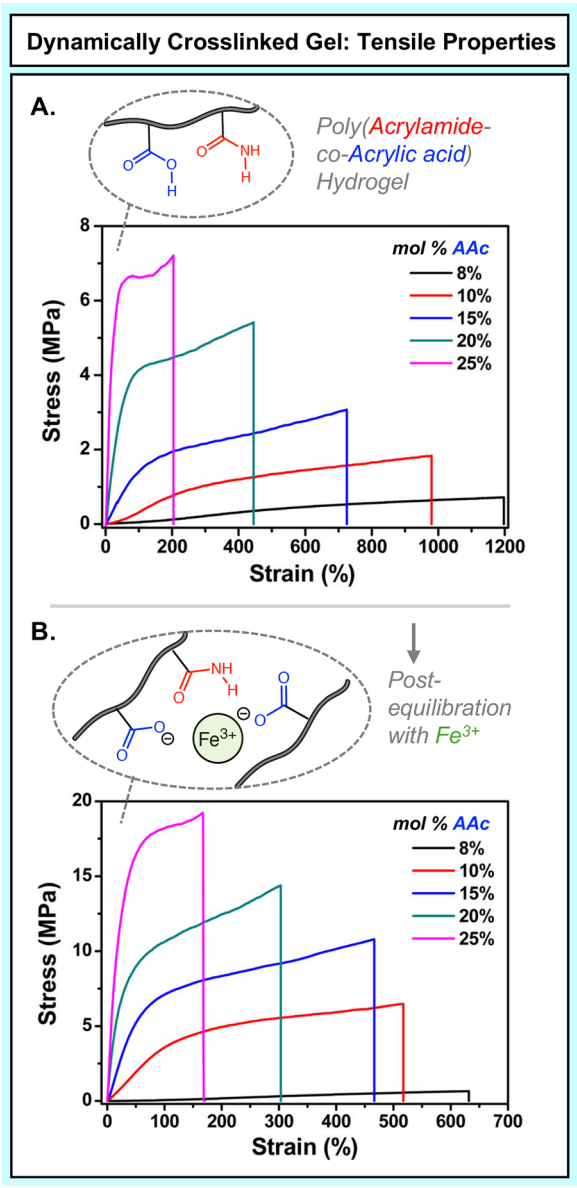

Figure 12. Tensile stress−strain curves of the A) as prepared physical hydrogel poly(acrylamide-*co*-acrylic acid) (P(AM-*co*-AAc)), and B) equilibrated with Fe^{3+} and water. Adapted with permission from Zheng et al., 2016 (ref 214, Copyright 2016 American Chemical Society).

be made of a range of ionic structures (Figure 13)[227] and enable numerous applications as stimuli-responsive actuators, adhesives, ionic conductors/electrical insulators for batteries and fuel cells, deformation sensors, and in information storage/processing.[228−231] Additionally, these structures have played a central and enduring role in the engineering of hydrogel mechanical properties.[12,38] Interactions between ionic moieties are electrostatic and can either consist of an attractive or repulsive force that is typically nondirectional, existing on a range of timescales from milliseconds to decades. The overall lifetime and strength of an ionic bond (E_d = 10−250 kJ mol^{-1}) is influenced by a host of factors, such as ionic strength, counterion radius, and distance, as well as indirect interactions with counterions, neighboring functional groups, and secondary inputs (salt, temperature, pH).[196,232] Therefore, by controlling the strength of ionic interactions, the mechanical behavior of ionic hydrogels can be tuned, allowing access to a broad range of dynamic materials.

Charged polymers can interact with one another and/or cosolutes in a variety of scenarios that depend on their molecular structure. A pair of polyelectrolytes with opposite backbone tethered charges can directly interact with each other to form polyelectrolyte complexes (PECs), driven by the translation entropy gain of liberated mobile counterions.[233] Like-charged polyelectrolytes can be bridged (ionically crosslinked) by multivalent ions or charged nanoparticles. In these contexts, the mechanical properties of ionically bound materials are inherently coupled with the ionic strength, distance between charges, and exchange rates of their constituent ionic motifs.[234] Polyampholytes and polyzwitterions, consisting of both cationic and anionic charges, can undergo self-complexation to form ionically crosslinked networks.[76,235] Along these lines, zwitterionic motifs, literally translated as "hermaphrodite" ions from the German "Zwitterion",[236] can be considered as a covalently tethered ion pair, with dipole strengths that correspond the tether length as well as the chemical structure of the charges themselves.[237−243] Polyampholyte gels offer a distinct opportunity for tuning the stress−strain response. The concentration of monomers during the polymerization process influences the final chemical structure/sequence of anions and cations, which then influences the bulk mechanical properties.[76]

In polyelectrolytes, it is critical to consider that "cationic" or "anionic" is simply referring to the identity of the charged motif covalently tethered to the polymer backbone and that these polymers are effectively charge-neutral, as each ionic motif has a counterion that can either be adsorbed and mobile, such as those in polyelectrolytes, or covalent tethered, as seen in polyzwitterions. Thus, charged motifs of ionic polymers can be consistently viewed as dipoles with dynamics and properties specific to their chemical structure.[227,244,245] Moreover, the effective "charge", or specifically the electrokinetic potential (*i.e.*, zeta potential) depends on the counterion equilibrium distance, which in turn is dependent on the molecular structure of the ionic motif[246,247] as well as environmental conditions such as solvent identity, cosolute concentration, and temperature.[248,249] Thus, it is important to consider the impact of small molecule ionic motifs. For example, in polyampholytes, the removal of excess salt that otherwise shields the inter and intra chain ionic bonds is critical to achieve robust mechanical properties.[76] Alternatively, added salt can serve as a plasticizer that adds toughness to glassy polyelectrolyte complex gels.[250]

The Coulombic energy ($E = e^2/(\varepsilon\varepsilon_0 r)$ (where e is a unit charge, ε is the dielectric constant, ε_0 is the permittivity of vacuum, and r is the average distance between charges) is an adequate description of the relationship between ionic strength and size, demonstrating that they are inversely correlated. E_d grows higher as the distance between charges (and ion size) decreases.[139] Columbic attraction is an enthalpic term, but expulsion of water and counterions are the dominating entropic contributions.[233] The effect of ion size is seen in the positive shift of dissociation time and E_d values of sulfonated poly(styrene) (SPS) units with decreasing counterion size (Figure 14).[139,251,252] Additionally, the availability of unsaturated monomer units is instrumental in lowering the energy of ion pair dissociation, particularly under applied strain, as reflected by a shortened relaxation time at an optimal ratio.[252,253]

https://doi.org/10.1021/acs.chemrev.5c00466
Chem. Rev. XXXX, XXX, XXX−XXX

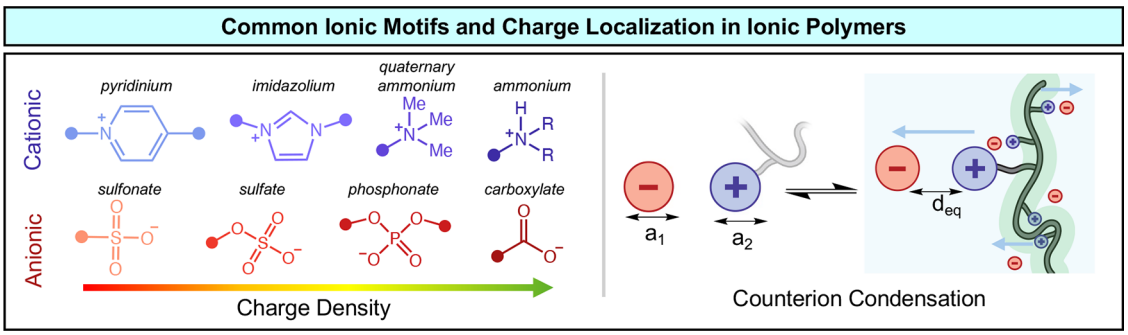

Figure 13. Common cationic and anionic motifs. Charge dense species trend toward darker colors, while charge diffuse species are lighter. Additionally, counterion condensation is depicted, wherein the adsorption of a counterion neutralizes charge and forms a temporary dipole. The likelihood of these ion pairs forming is dependent on their relative size (a_n), and their equilibrium separation distance (r), which is case dependent. Green hue represent areas of relatively lower dielectric constant due to the hydrophobic character of the polymer backbone. Modified from Muthukumar, 2017 (ref 227, Copyright 2017 American Chemical Society).

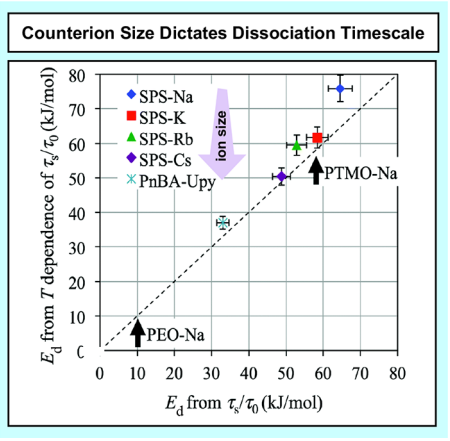

Figure 14. A graph of the activation energy for dissociation of sulfonated polystyrene (SPS) ionomers with different sized counterions, as well as other polymers with variant backbone and hydrogen bonding character. The sticker lifetime also increases with energy. Adapted with permission from Zhang et al., 2018 (ref 139, Copyright 2018 Royal Society of Chemistry).

The character of the primary covalent network also influences the bond interaction strength. As shown by Figure 14, poly(ethylene oxide) (PEO) screens and softens electrostatic association of SPS with Na^+, whereas poly(tetramethylene oxide) (PTMO) only weakly associates with Na^+, compared to the hydrogen bonding system poly(*n*-butyl acrylate)-UPy (PnBA-UPy).[139,251] Ionic groups interact with the PEO backbone, improving dissociation of ion pairs, and lowering activation energy of dissociation from ionic clusters about the covalent crosslinks. Additionally, increasing dielectric constant of the hydrogel environment yields improves ion transport and weakens binding.[96] Likewise, increasing solvent polarity has the same effect, increasing the dielectric constant and decreasing the lifetime of ion pairs.[254] The Bjerrum principle can be used to relate electrostatic attraction to the dielectric of the medium, as well as describe the effect of charge separation in polyelectrolytes.[254]

For weak polyelectrolytes, pH can shift the number of ionic bonds in a gel and therefore its time dependent mechanical properties. Polyampholyte and polyzwitterionic hydrogels with bidirectional pH switching have been used for selective material adsorption, water treatment, shape memory and actuation.[255−257] The isoelectric point (IEP, zeta potential = 0) is a useful framework for conceptualizing the pH induced shift from polyzwitterions to polycations (pH < IEP), or polyanions (pH > IEP). As pH deviates from the IEP, the polymer begins to predominantly experience charge repulsion, screening attractive forces and inducing swelling behavior in water.[258] In some cases, pH can also be used as a method to switch from charged to neutral, hydrophobic interactions.[259] In a polyion complex hydrogel comprised of cationic poly(2-(diethylamino)ethyl methacrylate) and anionic poly(4-styrenesulfonic acid), deprotonation by 1 M NaOH weakens ionic interactions, destroying crosslinking sites within the gel. By adjusting the pH of the hydrogel, a number of states are accessed, from stiff and tough (no NaOH), to brittle and weak (short NaOH immersion time), to soft and tough (long NaOH immersion time). As the immersion time in NaOH, and pH, increases, ionic bonding events transition to hydrophobic aggregates and entanglements that then dominate energy dissipation.[259]

Weak ionic interactions yield high exchange rates where the enthalpy of bond breaking and reforming are comparable, such that stress applied to the polymer network is easily diffused through the breaking of transient ionic bonds, which face a low energy barrier to reforming. Strong ionic interactions require a higher mechanical force to break, which can result instead in breakdown of covalent bonds under mechanical loading.[76,260] Sun et al. describe a hydrogel composed of anionic sodium p-styrenesulfonate (NaPSS) and cationic 3-(methacryloylamino)propyl-trimethylammonium chloride (MPTC) copolymerized to form a polyampholyte. The resulting complexation of individually weak ionic bonds (on the order of k_BT) at high concentrations forms both strong (tens to hundreds of ion pairs) and weak regimes (several to tens of ion pairs) as a result of their random distribution during synthesis. Under mechanical deformation, the weak binding regimes dissociate to dissipate energy, while the strong binding regimes distribute stress (provided the NaCl byproduct of complexation is removed).[76] A sufficient content of strong crosslinks and high concentration of weak crosslinks optimizes the toughness and reassociation time of reversible bonds in such a network. The salt free gel has an elastic behavior followed by yield to significant strain hardening. Above a critical monomer concentration, the stiffness and equilibrium water content stabilize, but the yield stress and failure strain continue to increase. This trend is distinct from the metal coordination systems described previously, for which yield

https://doi.org/10.1021/acs.chemrev.5c00466
Chem. Rev. XXXX, XXX, XXX−XXX

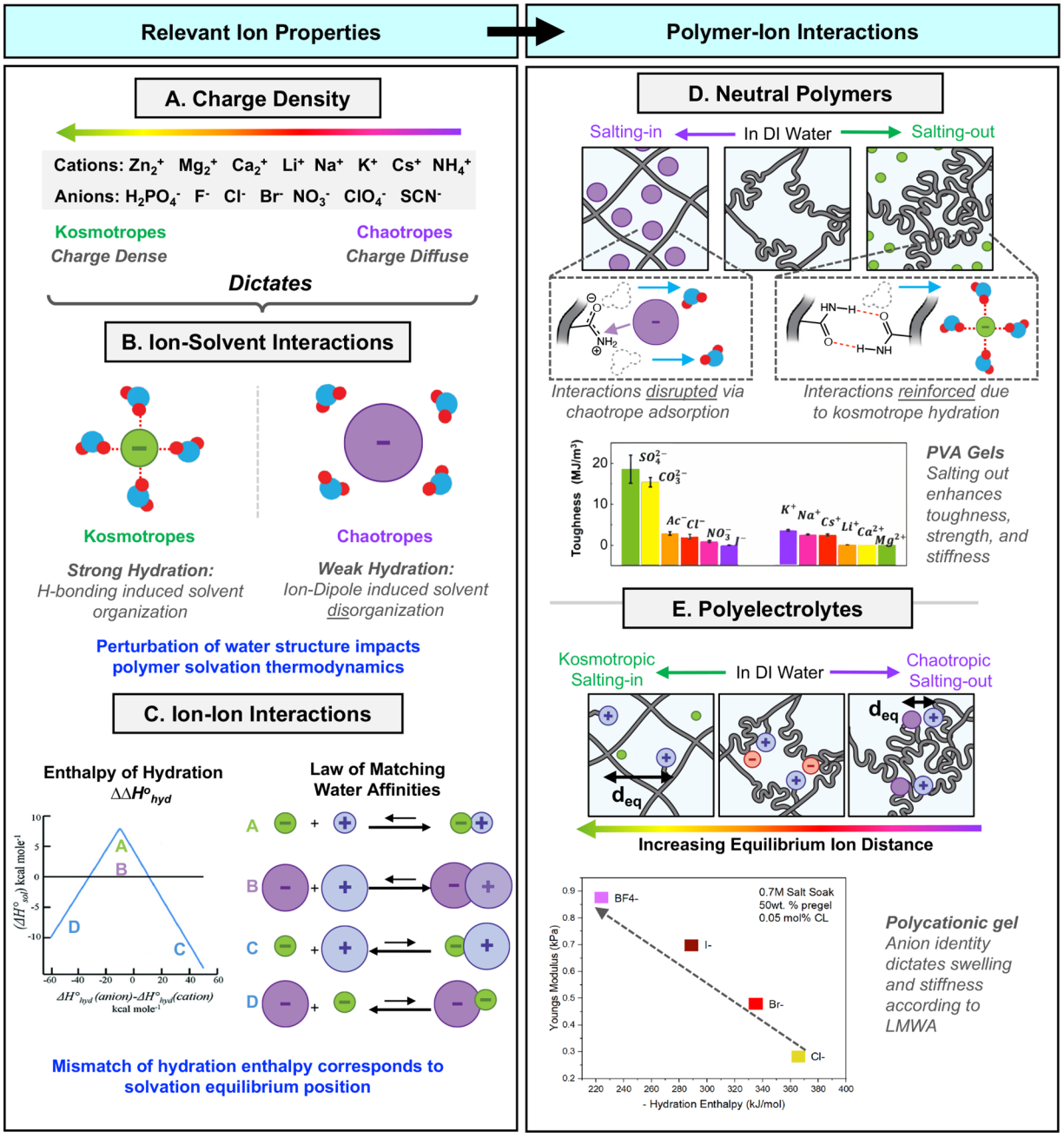

Figure 15. Left) Properties of Ionic interactions which underpin polymer−ion interactions. A) Charge Dense (Kosmotropic) and Charge Diffuse (Chaotropic) trends in a selection of cationic and anionic species. Charge density dictates B) ion−solvent interactions, as well as C) ion−ion interactions. These interactions govern Polymer−Ion Interactions, **Right)** where both D) Neutral Polymer and E) Polyelectrolytes material properties are influenced by salt identity based on specific molecular composition. In the polyelectrolyte example, the cation is depicted as relatively charge-diffuse and factors such as the equilibrium distance of polymer−salt interactions and differences in enthalpy of hydration between charged species, determines their electrostatic interaction ranges and overall polymer solubility. Adapted with permission from He and Ewing 2023 (ref 264, Copyright 2023 John Wiley and Sons), Aubrecht et al., 2024 (ref 265, Copyright 2024 John Wiley and Sons), Gregory et al., 2022. (ref 246, Copyright 2022 Royal Society of Chemistry), and Jin et al., 2024 (ref 266, Copyright 2024 American Chemical Society).

stress and failure strain have opposing trends from each other. This polyampholyte has a yield stress that increases noticeably with strain rate (4 times increase for 100 times strain rate increase) and almost no change in failure strain. The mechanistic picture underlying these behaviors is one of a distribution of ionic interactions with different strengths based on their spatial distribution along the polymer chains that progressively break and reform as stretch is applied. This concept is supported by the gel behaving in a fluid-like manner at much lower stresses and with progressively less strain hardening once mobile salt ions are reintroduced. A follow-up paper by the same group combining mechanical testing with constitutive modeling provided some additional evidence for this mechanistic concept.[261] The polyampholyte system by Sun et al. only recovers 30% after an hour of healing at 50 °C; to achieve near full healing they switch to a weaker ionic bond, which also results in a much less stiff and strong gel.[76] In similar polyampholyte gels, creep will progress to material

https://doi.org/10.1021/acs.chemrev.5c00466
Chem. Rev. XXXX, XXX, XXX−XXX

failure given enough time. Interestingly in those gels, strain from creep at about 1/4 the monotonic loading yield stress is fully recoverable upon unloading when stress is applied for 3 h and only about 70% recoverable when stress is applied for 10 h, indicating loss of memory of the initial material configuration.[262] For instance, alginate gels with only ionic crosslinks show characteristic times of ∼20 s for the stress to relax by 50%, whereas if covalent crosslinks are added, 50% relaxation takes an hour.[263]

The structure of ions dictates their charge density and intermolecular interactions with solvent as well as other ions (Figure 15).[246,264−266] These structure dependent interactions, known as ion-specific effects, are reliably exploitable to modulate polymer and hydrogel properties, with ionic cosolutes capable of tuning ionic and metal−ligand coordination bonds within 25−95% the strength of a covalent bond,[267] as well as manipulating fundamental solvation thermodynamics and therefore mechanical properties (Figure 15, **A**). Generally, the ion-macromolecule interactions can be categorized into two regimes, indirect and direct.[247,268] Indirect interactions are orchestrated by the organizational perturbation of water surrounding the ion (Figure 15, **B**), specifically the primary and potentially secondary solvation shells, and is typically described in terms of solution viscosity.[269] This alteration in water organization therefore impacts the solvation energy of macromolecular cosolutes. It is the traditional conceptualization of the Hofmeister effect, which refers to the phenomenon wherein ionic identity is a parameter to modulate the entropic cost of macromolecule solvation in water.[270] Ion structure dictates the interaction modality with water; charge dense anions, known as kosmotropes, strongly interact with water via hydrogen bonding, inducing order, while charge diffuse anions, known as chaotropes, interact with water molecules via weaker inductive interactions and induce disorder in water.[270] While the computational and experimental elucidation of these ion−water interactions remains under vigorous investigation,[271−281] this conceptual model remains useful to rationalize ion−polymer interactions at high salt concentrations, as indirect impacts are stoichiometric in nature.

The direct interaction regime is characterized by the chemical interaction of ions and polymers via electrostatic, inductive, or dispersive modalities.[246,247] Direct interactions can be further subcategorized based on polymer structure, ion-neutral polymer interactions and ion-polyelectrolyte interactions. In ion-neutral polymer direct interactions, stronger interactions of chaotropic ions with uncharged polymers relative to kosmotropic ions has been documented via NMR and calorimetric experiments(Figure 15, **D**).[282−287] This specificity has been attributed to the polarizability of chaotropes, enabling inductive interactions with motifs such as the dipoles of amides[288,289] and the induced dipoles of vinyl backbones.[247,290,291] Notably, the displacement of the solvation shell has been observed to render these interactions entropically favorable, but is highly dependent on the structure and composition of the polymer.[287] The outcome of these neutral polymer-chaotrope interactions is an increased electrokinetic potential, which results in interpolymer repulsion in analogy to polyelectrolytes and provides a molecular basis for the increased solubility of neutral polymers with chaotropic anions.

The second direct interaction regime, ion-charged polymer interactions, rationalizes the inverse Hofmeister series behavior often observed with polyelectrolytes. This can be conceptualized as an outcome of pairing preferences of ions in solution, *i.e.*, mixtures of solvated ionic complexes will exchange to form the lowest energy structures, with strong pairing of ions making them less soluble, due to the imbalance in the relative energies of ion−solvent and ion−ion interactions.[246] This corresponds with the longstanding observation that the solubility of salts in aqueous solutions corresponds to the mismatch in ion size, with the greater size imbalance corresponding to a greater degree of solubility (Figure 15 , **C**).[292] Thus, the relative favorability of an ion pair can be generally assessed as the relative energetic favorability of interaction through electrostatic, inductive, and dispersive interactions, more broadly referred to as HSAB theory.[246] Thus, differences in pairing affinity of polymer backbone, confined charged motifs, and mobile ions allow the molecular structure of counterions to influence the equilibrium pairing distance, dipole strength, and hydrophilicity of the polymer. This enables the assembly of polyelectrolytes (discussed in Section 3.2) and further the material timescale of polyelectrolyte-derived hydrogels.[265] Additionally, this enables the manipulation of the physicochemical properties of polyzwitterionic species.[226]

In polyampholyte and polyzwitterionic hydrogels, ion specific effects are also observed, wherein the addition of kosmotropic salts screen and weaken electrostatic interactions, increasing their rates of dissociation (Figure 15, D). Time-salt-concentration and time-salt-identity superposition principles have been observed in electrostatic and hydrogen bonding hydrogels; increased salt concentration and short timescales can be equated to mechanical behavior at low salt concentration and long timescales.[26] Emerging work categorizing the time-salt identity superposition for hydrogen bonding poly(methacrylamide) gel finds agreement with the Hofmeister series, wherein chaotropic salts at short timescales induce the same mechanical properties as kosmotropic salts at long timescales. This effect was observed for both cations and anions, with the latter having the most dramatic contributions.[266] For imidazolium-based polyzwitterionic gel poly(3-(1-(4-vinylbenzyl)-1H-imidazol-3-ium-3-yl)propane-1-sulfonate) (pVBIPS) crosslinked by Fe^{3+}, association dynamics of the counteranion with cationic motif follow the antipolyelectrolyte trend (Figure 16). Larger, more chaotropic anions associate with the soft imidazolium motif to an effective degree such that anionic sulfonate groups are free to coordinate with Fe^{3+}. Chaotropic ClO_4^- anions showed a dramatic increase in toughness (fracture energy = 19.55 kJ/m^2) compared to the pristine gel (∼0.465 kJ/m^2) and other counter-anions (∼1−5 kJ/m^2).[226]

The strength and exchange dynamics of ionic bonding motifs are a balance between enthalpic contributions from Coulombic attraction, and entropic contributions from displacement of solvent. The state of the medium is incredibly important to this thermodynamic equation. Altering the dielectric constant, pH, and temperature can greatly screen attraction. While ionic interactions are conventionally regarded as inherently nondirectional, an emerging area is the molecular design of directional ionic bonding schemes, which could render ionic bonds time-dependent catch-bonds. Hutskalov et al. have explored the concept of directional ionic interactions by designing cation−anion pairs comprised of sterically hindered, bulky groups. These systems show strict directionality and even spatial ordering as small molecules (Figure 17).[293] Incorporation of these motifs into hydrogels may introduce further entropic penalties, resulting in high

https://doi.org/10.1021/acs.chemrev.5c00466
Chem. Rev. XXXX, XXX, XXX−XXX

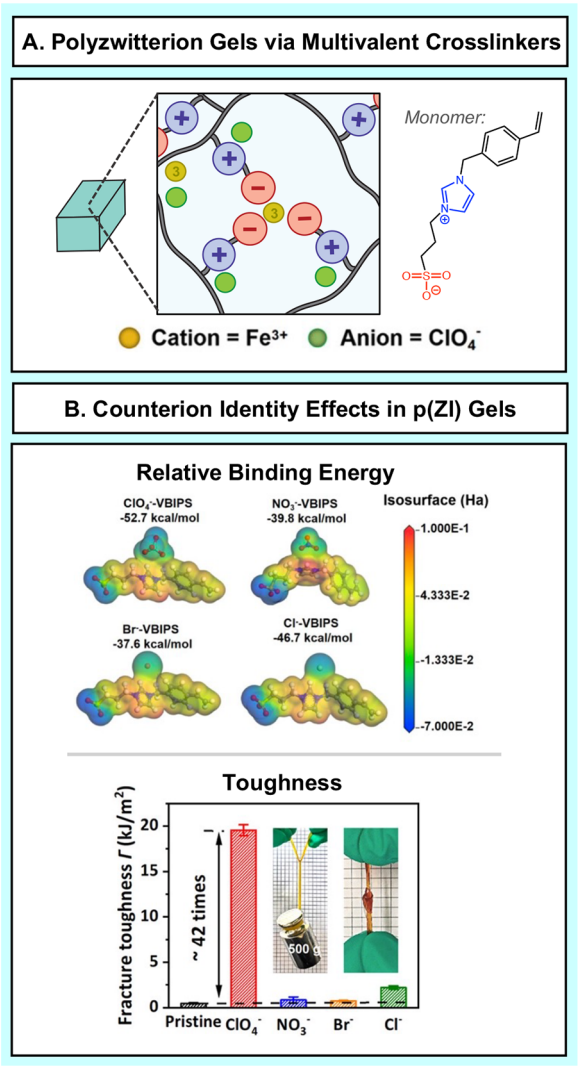

Figure 16. A) The imidazolium-based polyzwitterionic gel (pVBIPS) crosslinked with $Fe(ClO_4)_3$. B) A comparison of fracture toughness of gels crosslinked by various iron salts. The effect of counterion on toughness is greatly exaggerated in the case of ClO_4^-. The relative binding energy of counterions to pVBIPS in the absence of water, as calculated from DFT. Adapted with permission from Deng et al., 2025 (ref 226, Copyright 2025 American Chemical Society).

specificity of binding during deformation, enabling programming of material response to strain.

3.2.4. Cation-Π Interactions. Cation−π interactions, formed between the electrostatic interactions of cationic moieties and the electron rich π clouds of arenyl systems are among the strongest intermolecular forces in water.[294−297] Such interactions underpin the function of many biological systems, such as potassium channels[298] and nicotinic acetylcholine receptors,[299] and give rise to the strong underwater adhesion of marine organisms, such as mussels and barnacles.[300−304] This class of noncovalent interaction has spurred considerable interest in the areas of organic synthesis,[305,306] molecular recognition systems,[301,307] as well as mechanically robust and responsive organic materials.[308−310] The incorporation of cation-π interactions into polymer hydrogels has been well demonstrated to yield responsive, self-healing materials with exceptional adhesive[224,311] and mechanical properties.[312,313] Indeed, the ubiquity and broad

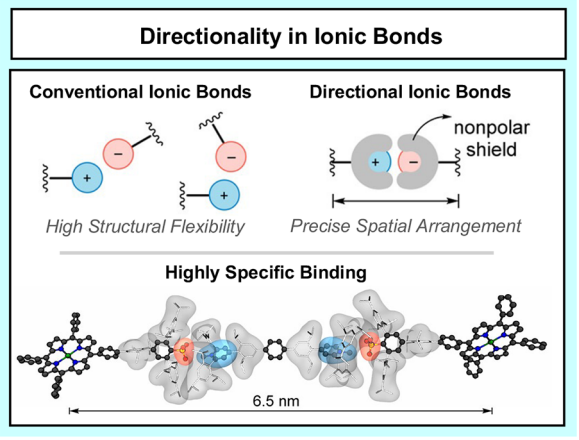

Figure 17. Conventional and nonconventional ionic bonds. Bulk and electric field directing character create directional interactions. The π-systems of anionic *N*-methylpyridinium and cationic arylsulfonates create a nonpolar shield around charges, creating highly specific binding. Adapted from Hutskalov et al., 2023 (ref 293, Copyright 2023 American Chemical Society).

utility of this interaction has seen it extensively reviewed, in contexts of biomimetic adhesion,[310] sensing,[314] metal coordination compounds and networks,[315,316] small molecule catalysis,[305,306] etc. and the fundamentals of these interactions deeply studied.[317]

The enthalpy of cation-π interactions is determined by the arene's quadrupole moment, as well as cation structure, which dictates how strongly water competes with the arene (Figure 18). The planar nature of the quadrupole makes cation-π interaction inherently directional. Additionally, the structure, or degree of planarity of organic cations, such as quaternary ammonium, imidazolium, pyridinium, or other more complex structures adds additional directionality considerations, with the distribution of charge across the arene group and cation determine ideal orientations (face-to-face, edge-to-face).[317] Notably, the directionality of cation-π interactions makes them sensitive to conformational freedom. Elegant studies by Gong[318] and Israelachvili[319] have revealed intriguing dynamics that indicate entropic factors surrounding arene mobility and counterion placement strongly influence the energetic favorability of cation-π interactions (Figure 18). These entropic considerations arise from the spatial confinement of the arene and cationic moieties to polymer chains, making conformational and/or positional freedom a significant driver of macroscopic properties such as cohesion and stiffness. Materials with longer, more flexible ethylene oxide tethered arenes showed weaker cohesion, which was attributed to conformations less favorable to the directionally sensitive cation-arene interaction being in equilibrium with favorable confromations.[318] Israelachvili et al. demonstrated that placement of the accompanying anion within the polymer network is critical, with phenyl rings showing enhanced cohesive energies relative to catechol, which they attributed to the restriction of counterion locations. Environment additionally plays a strong role in determining the favorability of cation-π bond formation. Similar to ionic bonds, the strength of cation-π interactions are inversely proportional to the dielectric constant of the medium.[317] Additionally, there is sensitivity to cationic cosolutes that, depending on their relative desolvation energy, will compete with the desired cation-π interaction. In polymers with a high cation content, such as mussel foot

https://doi.org/10.1021/acs.chemrev.5c00466
Chem. Rev. XXXX, XXX, XXX−XXX

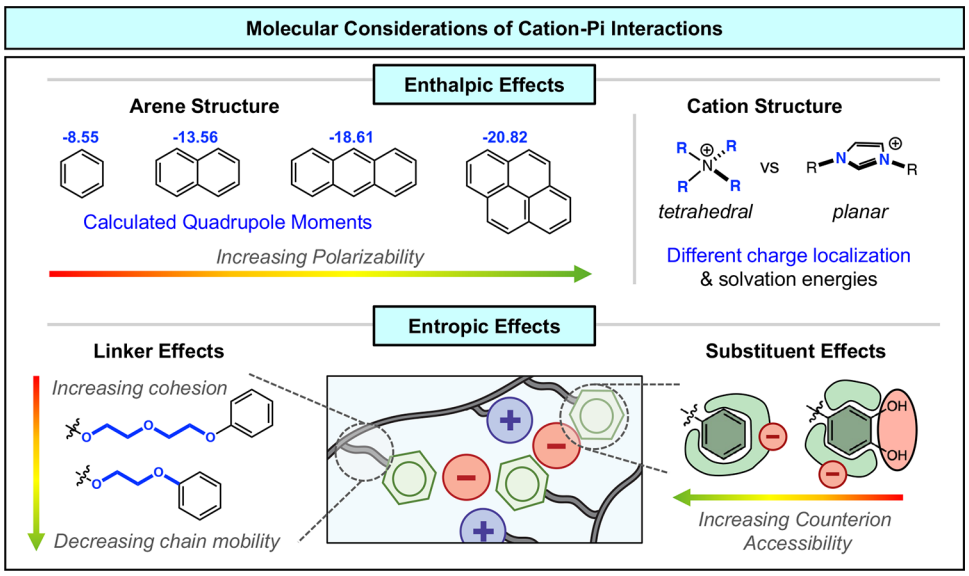

Figure 18. Molecular considerations of cation-π interactions. Top) arene and cation structure drive the overall enthalpic favorability. Bottom) Bonding motif flexibility and counterion placement have also emerged as important considerations driving entropy favorability.

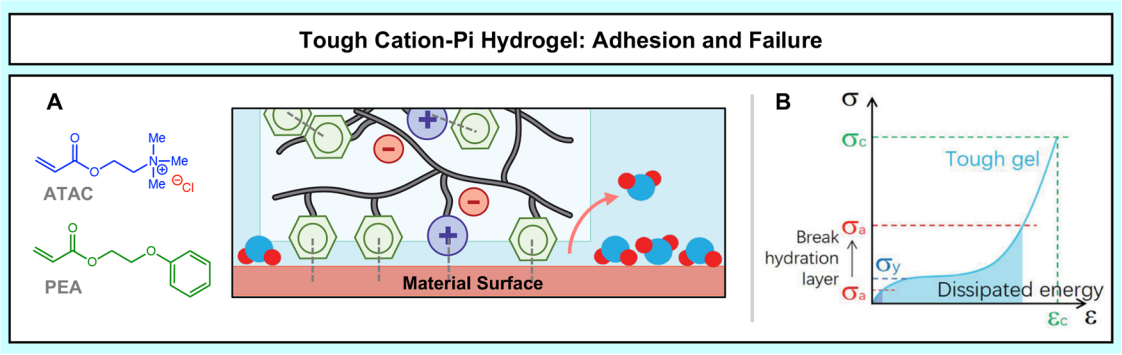

Figure 19. A) Polymerized from cationic 2-(acryloyloxy)ethyl trimethylammonium chloride (ATAC), and 2-phenoxyethyl acrylate (PEA), A tough cation-π hydrogel capable of underwater adhesion to an interface, inducing the expulsion of water and local dielectric reduction. B) The graph of bulk stress—strain for a song adhesive indicates fracture stress (σ_c), yielding stress (σ_y) fracture strain (ε_c), and debonding stress (σ_a) at the interface of adhesion. Cation-π and π-π interactions allow energy dissipation such that cohesive failure is not reached, and can achieve high σ_a in water, overcoming high interfacial hydration. Adapted from Fan et al., 2021 (ref 304, Copyright 2020 John Wiley and Sons).

proteins, barnacle proteins, and analogous mimetic structures, long-range charge-based repulsion competes with the much shorter range cation-π interaction, which additionally makes the formation of cation-π interactions dependent on salt content and will be later discussed as a distinct opportunity for programming polymeric assembly (Section 3.2).

The lifetime and exchange rate of cation-π interactions in aqueous media are difficult to measure as a result of the strongly hydrophobic arene groups.[320] A simulation on small molecule benzene and monovalent Na^+ in water showed an average contact time of ~0.3 ns, but the pair underwent such rapid exchange that a Na^+ cation was in contact for roughly 40% of the lifetime of the simulation (15 ns).[321] Cation-π interactions are interesting in that the strength of interaction does not fully agree with trends in the degree of polarizability or quadrupole of arene, nor the charge density of the cation.[322] This is an effect of the aqueous media, as the hydrophobic and yet locally polar nature of arene groups endow them with complex hydration characteristics. This is important, as a cation-π bond is established via the competition of dehydration and hydration in the interstitial space between components. Displacement of water from the cation hydration shell by hydrophobic π group allows more direct electrostatic interactions to occur, with hydration rather than charge established as the primary driver of forming strong cation-π interactions (Figure 19).[304,322]

While the balance among charge, hydration, and configurational variability has been established as crucial for modulating the timescale of cation-π interactions, current discussions of their existence in hydrogels remains limited. For example, consider the cooperativity of cation-π interactions in biological systems. Isolated cation-π interaction energies are much different than those observed in biology due to the involvement of several other groups that can interact with either species.[323] Engineering ternary style interactions may provide additional handles to program directionality in cation-π interactions. This could be achieved by incorporating other interacting motifs such as halogen bonding, the involvement of additional arene groups, or studying the effect of counterion on the dynamics of bond exchange in these hydrogels (Figure 20).[323,324] In addition to higher order complexation structures, incorporation of unconventional π groups (carbonyl and

https://doi.org/10.1021/acs.chemrev.5c00466
Chem. Rev. XXXX, XXX, XXX−XXX

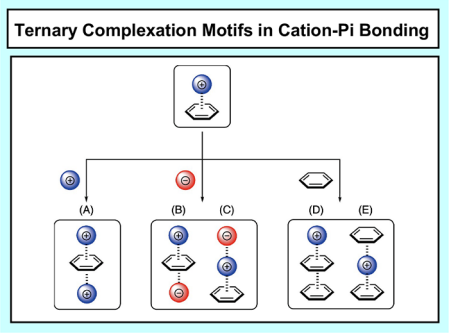

Figure 20. Potential for cation-πinteractions to form ternary style complexes in the form of A) cation-π-cation, B) cation-π-anion, C) anion−cation-π, D) cation-π-π, or E) π-cation-π. Adapted from Fundamentals of Cation−π Interactions. Adapted from Yamada, 2022 (ref 324, Copyright 2022 Springer Nature).

thiocarbonyl)[325] which create conformational rigidity, remain unexplored as potential means to modulate timescale of cation-π interactions in hydrogels.

3.2.5. Hydrogen Bonding. Hydrogen bonding is a noncovalent, intermolecular force that occurs when a dipole forms between an electronegative atom and covalently bonded hydrogen atom, allowing the hydrogen atom to experience an attractive force to another electronegative atom.[326] While weaker than covalent bonding, this interaction is stronger than a typical dipole and contributes to the structure and characteristics of polymer networks, including hydrogels. Solvent−solute hydrogen bonds measured in *N*-methylacetimide-methanol are shown to break and reform within 10−20 ps.[327] The bond activation energy of disassociation individual hydrogen bonds has been determined by X-ray crystallography and computational methods to be between 10 and 65 kJ mol^{-1}.[232,328,329] In hydrogels, the directionality and density of these hydrogen bonds affects their summative strength.[330] Relative to ionic interactions, hydrogen bonds are intrinsically directional, due to the electronegative dipoles that form them.[331]

In a case study using poly(methacrylamide-*co*-methacrylate) (P(MAM-*co*-MAA)) hydrogels, the relative strength and time of both bond cleavage as well as relaxation and viscoelastic behavior was determined using a variety of pure shear and extension stress tests in a variety of directions (Figure 21).[332] Energy dissipation and relaxation within the P(MAM-*co*-MAA) hydrogel, held together purely by dynamic and directional hydrogen bonds, was found to be dependent on the rate of applied strain. This study found that as strain rate approached the same rate of bond breaking t_r, the hydrogel began to exhibit dynamic bond behavior, and subsequently became more viscoelastic and tough. At strain rates less than the bond breaking rate, more fluid and soft hydrogel behavior dominated. In the P(MAM-*co*-MAA) hydrogels described above, it was found that energy required for flow was approximately 80 kJ mol^{-1}, compared to that of pure sticker disassociation of around 46 kJ mol^{-1}, due to the hydrogen bonding interactions between polymers hindering disentanglement.[332] The energy required for flow was positively correlated to the concentration of polar acrylamide, contributing to directional hydrogen bonding.[77]

Cooperativity, enforced by macromolecular structure, can enhance the strength of hydrogen bonds, influencing the gelation and mechanical properties of constituent polymers.

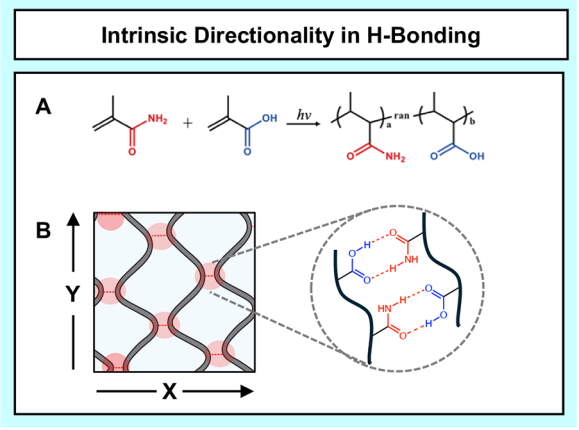

Figure 21. A) Chemical structure of monomers MAM and MAA, and resulted polymers P(MAM-*co*-MAA). B) Structural diagram of equilibrated hydrogels. Adapted from Liu et al., 2023 (ref 332, Copyright 2023 Informa UK Limited).

The chemical structure of the hydrogen boding unit in homopolymers, modulates the balance between polymer/solvent and polymer/polymer interactions. This is an important consideration when evaluating chemical architectures to develop a tough hydrogen bond based hydrogel. Acrylamides provide a simple platform for such a systematic examination. Polyacrylamide (PAM) is characterized by unsubstituted amide and the polymer−solvent interaction is much stronger than the polymer−polymer interaction and thus the material shows no retention of network structure when solvated. The incorporation of another amide-like unit introduces a second, complementary H-bonding group, as seen in Figure 22. By modulating the structure of this secondary interacting unit, a series of polymers with increasing interaction strength and macroscopic strength and toughness have been developed, poly(*N*-acroyl beta-alaninamide) (pNAAA),[333] poly(*N*-acroyl glycinamide) (pNAGA),[334,335] poly(*N*-acroyl semicarbazide) (pNASC).[336] A dramatic increase in stiffness is observed from pNAAA to pNAGA, which entails the removal of a single methylene unit. This can be attributed to the removal of rotational freedom and the overall configurational variability. Additionally, substitution of a methylene with a N−H unit in the pendant chain of pNAGA transforms the terminal amide into the urea motif characteristic of pNASC. This transforms the resulting hydrogels into stiff, thermoplastic materials. Notably, these materials are relatively resistant to salt concentration, providing additional advantages relative to ionically crosslinked networks.

Finally, the strong propensity for hydrogen bonding with water results in its localization within interstitial spaces of hydrogel polymer meshes.[326] As these polymer−water interactions strongly compete with polymer−polymer interactions, the resulting equilibrium structure depends on the overall balance between the energy of these interactions. In cases where these are relatively balanced, water can act as a bridging molecule, contributing to the overall stiffness and toughness of a hydrogel. However, given its bulk fluid properties, it is difficult to quantify the contribution of individual hydrogen bonds between solvent and polymer. In analogy to the great interest in "biological water",[337] *i.e.*, the hydration shell of proteins, understanding the role of water in such systems is needed. Identifying the overall saturation of polymer, relative to the volume of available hydrogen bonds is

https://doi.org/10.1021/acs.chemrev.5c00466
Chem. Rev. XXXX, XXX, XXX−XXX

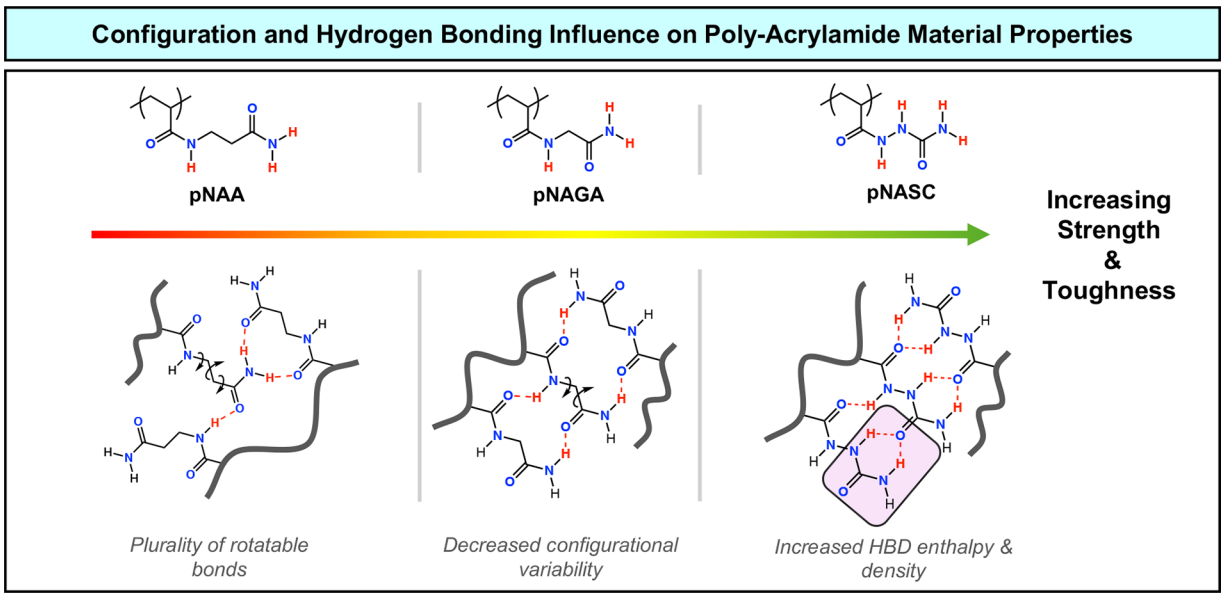

Figure 22. Comparison of acrylamide hydrogen bonding motifs based on beta-alanamide, glycinamide, and semicarbazide, demonstrating how configurational variability and hydrogen bonding density influence properties.

a quantifiable method of understanding how water acts as a toughener or plasticizer in a hydrogel. Furthermore, hydrogen bonds will likely remain a central motif in hydrogels, with latent potential in their combination with other motifs to engender dynamic modulation of polymer−polymer interactions that result in triggerable assembly and/or remodeling.

Hydrogen bonds can also provide tunable uniaxial tensile stress−strain behavior provided there is sufficient density of these interactions to provide overall mechanical integrity. For instance, in 2013 Guo et al. introduced a UPy bonded PEG network in which the UPy's exhibit self-complementary quadruple hydrogen bonding.[338] This polymer is effectively hyperelastic through a strain of 200% (much larger than the metal ligand and ionic systems discussed above), and then rolls over to modest strain hardening, indicating first backbone stretching and then a progressive breakdown of the hydrogen bonding. Consistent with this mechanism, the elastic region extends to lower strains and higher stresses when the PEG chains are shortened. Wang et al. synthesized poly(methacrylamide-*co*-methacrylic acid) copolymers that formed hydrogen bonds between the carboxylic acid and amide groups.[339] In contrast to the PEG-based system, this gel exhibits a sharp yield event at small strain (<10%), similar to the behavior of a glassy polymer, which is followed by substantial strain softening and then eventually strain hardening again starting at 100% strain. This copolymer however exhibited strain rate dependence of the yield stress typical of a thermoplastic gel and much more extreme than a typical glassy polymer—3× increase over 1000× strain rate increase.

3.2.6. Dipolar and Quadrupolar Interactions. Dipolar and quadrupolar interactions span an array of noncovalent interactions, including ion-dipole, dipole−dipole, and π-π interactions. While diverse in chemical motifs, these interactions have been grouped together due to their mechanistic similarity as well as their similar role as "reinforcing" interactions in hydrogels,[340] *i.e.*, they are not traditionally utilized as primary interactions to enforce shape and stiffness, but rather to enhance energy dissipation and/or recovery after deformation. For the purpose of this review, "dipole" refers to persistent dipoles (rather than induced dipoles), and are typically made up of electronegative atoms, such as oxygen, nitrogen, sulfur, and fluorine, attached to carbon atoms. As such, common dipole motifs are amides, nitriles, and esters.

Ion-dipole interactions are ubiquitous in solution and polymer chemistry, defined as the electrostatic attraction between a molecule with a dipole and an ion. The directionality of ion-dipole interactions can vary, with the directionality of interactions with spherical ions moderately directional, while planar structures such as pyridinium and imidazoliums have their cationic charge much more spatially defined, resulting in much more directional interactions. Notably, the strong dipole moment of water results in strong competition of solvent−polymer interactions with polymer−polymer interactions in hydrogels, making these interactions substantially weaker than in the gas phase and therefore more transient. This is particularly relevant for ion-dipole interactions, wherein water competes with the polymeric dipole motif for interaction with the ionic species. As ion-dipole interactions in gels play central roles in technological applications such as electrochemical devices for energy harvesting and storage and consideration of the intrinsic time−temperature relationships is important for engineering critical properties such as ionic conductivity and stiffness, strength, and toughness (Figure 23).[341] As a result, these properties may vary due to environmental variation, *e.g.*, placement on human body or changes in season, as well as operation of the device itself. Notable examples of molecular design driven solutions to these challenges have recently emerged. With the observation that entropic considerations are primary drivers of interaction energy at the elevated temperature associated with electrochemical devices (>100 °C) valency along with strength of ion-dipole interaction were utilized to tune the temperature sensitivity of ionogel mechanical properties.[341]

Dipole−dipole interactions are short-range, noncovalent intermolecular forces that have been reported to improve the mechanical properties of hydrogels and other polymer networks.[232] Dipole−dipole interactions, which are moderately

https://doi.org/10.1021/acs.chemrev.5c00466
Chem. Rev. XXXX, XXX, XXX−XXX

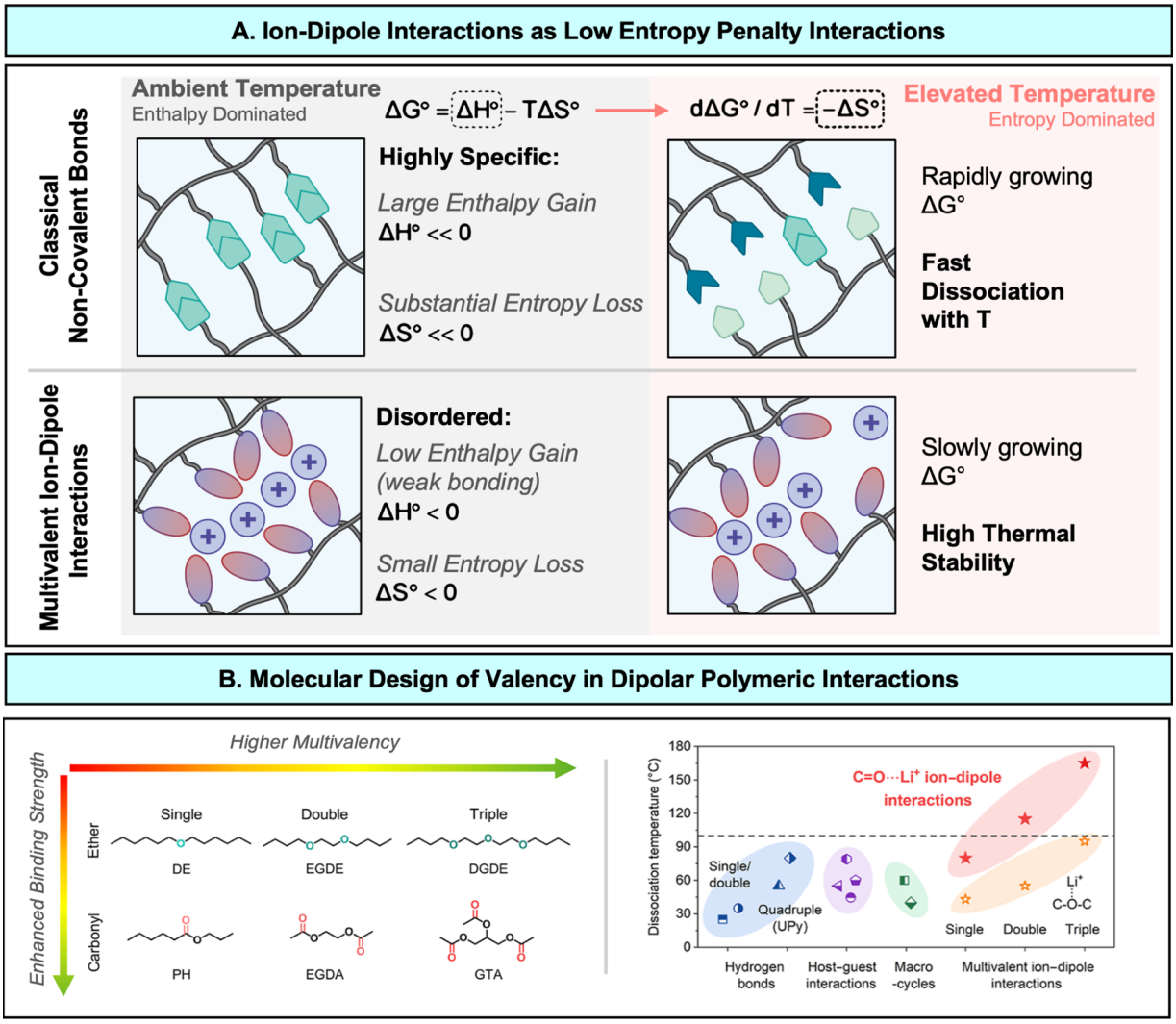

Figure 23. Illustrating the unique properties of dipolar interactions. A) The lower directionality of ion-dipole interactions relative to other noncovalent bonds results in a lower entropic penalty and enhanced thermal stability. B) Multiple axes of molecular structure, such as functional group identity and density, enable the tuning of disassociation strength of ion-dipole interactions in polymeric materials. Modified from Jin et al., 2023 (ref 341, Copyright American Chemical Society).

directional, can create dynamic and reversible supramolecular networks. Though weaker than dynamic covalent interactions and hydrogen bonds, dipoles can still tune the mechanical properties of hydrogels.[9,326,342]

The timescales of dipole and quadrupole are not often reported in current literature. Computational studies suggest that dipole−dipole interactions in hydrogels are more dynamic than hydrogen bonds, with the lowest relaxation time and activation energy compared to other physical interactions.[342] Due to their highly dynamic nature, dipole−dipole interactions can increase the flexibility of gels and can limit energy dissipation at low strains. These interactions have also been reported to increase the apparent activation energy of H-bonded hydrogels, providing a synergistic benefit to both dipole−dipole and H-bond strength.[342] Leveraging both H-bonds and dipole−dipole interactions has been shown to toughen hydrogels with shape memory.[326]

Moving beyond the canonical use of acrylonitrile as a dipole−dipole bonding motif,[342−345] Lei and Huo create a sulfone functionalized monomer to achieve tough and fatigue resistant hydrogels.[346] A copolymer of 2-(methylsulfonyl)ethyl acrylate and acrylamide was crosslinked with α,ω-diacryloyl poly(ethylene glycol). While hydrogen bonding is also accessible to this system, modulating the fraction of sulfone dipoles yield more pronounced shifts in the mechanical properties of the hydrogel, indicating they are critical in toughening this material. The sulfone bond is multivalent and hydrophilic, which is exploited to protect hydrogen bonding within the network from disruption via water. The authors find an ideal toughness (107 ± 7 kJ m^{-3}) when the fraction of sulfone to acrylamide is 50−60%, and above which (50−100%) the hydrogel transitions from strong and tough to strong and brittle (26.6 ± 4 kJ m^{-3}) due to the high concentration of sulfone bonds restricting polymer chain and water mobility under deformation. Monitoring via FTIR-spectroscopy revealed the sulfone bond strength increased as the fraction of 2-(methylsulfonyl)ethyl acrylate increased from 20 to 60%, but then decreased as the fraction approached 100%. Additionally, an increase in the concentration of chaotropic KSCN was found to disrupt sulfone bonds, decreasing the work of extension (toughness) to 6.5 ± 0.8 kJ m^{-3}.[346]

https://doi.org/10.1021/acs.chemrev.5c00466
Chem. Rev. XXXX, XXX, XXX−XXX

Another critical technological area that polymers with engineered ion-dipole and dipole−dipole interactions contribute to is the design of robust electrolyte membranes in aqueous Zn metal batteries.[347−349] Polymeric electrolytes with sufficient mechanical strength and toughness are needed to preventing dendrites from piercing the separator and causing device failure but additionally must solvate zinc in a fashion that ensures rapid transport and even deposition onto the electrode, factors that involve modulation of polymer segmental motion as well as Zn ion solvation. Currently, polymeric gel electrolytes either lack conductivity (solid) or mechanical properties (gel).[347−349] Thus, the incorporation of emerging studies on metal ion solvation with polymer design are needed to bridge this gap to realize the potent potential of aqueous Zn batteries.

3.2.7. Dispersion Interactions and Hydrophobicity. Hydrophobic interactions are both common and extremely vital motifs within biological systems such as the phospholipid bilayer of cell membranes,[350] protein folding,[351] and highly extensible elastin of aortic tissue.[352] While an individually weak, nondirectional force, hydrophobic interactions often occur in entropically driven aggregates, as aggregation minimizes the need for water molecules to organize into a H-bonding network around the nonpolar structures, thereby maximizing the overall configurability of the system.[353] The dissociation energy of hydrophobic interactions is on the order of k_BT (~0.1−20 kJ mol^{-1}),[38] indicating a facile exchange process within aggregates that function as an energy dissipation mechanism(Figure 24, **A**).[354,355] For example, a hydrophilic PEG polymer alone has toughness 130.2 ± 45.4 kJ m^{-3}, but when incorporating a hydrophilic trimethylene carbonate block, the toughness is greatly improved (215.3 ± 46.4 kJ/m^{-3}) due to energy dissipation via uncoiling of collapsed hydrophobic lengths (Figure 24, **B**).[356] Below a critical concentration of hydrophobic groups, intrapolymer associations dominate, whereas above that critical concentration, the hydrophobic pockets take a three-dimensional shape, bridging interpolymer interactions.[357] In aqueous solutions, micellular crosslinks can range from spherical, to rod-like, to layered structures.[358,359] The size and concentration of hydrophobic groups and their resultant micelles have been identified as modulating the timescale of these interactions in aqueous media.[355] Small molecule pairs have association lifetimes as short as 2−4 ns, but the favorability of forming larger aggregates extends association lifetimes from milliseconds to hundreds of seconds long.[360,361] Larger hydrophobic blocks form larger aggregates with higher association strength, longer timescales of interaction, and higher penalty to rearrangement and dissociation.[359,362] Later discussions in this section will address how the multiscale structures that result from hydrophobic phase separations and aggregations can be leveraged in the spatiotemporal regulation of hydrogel toughness.

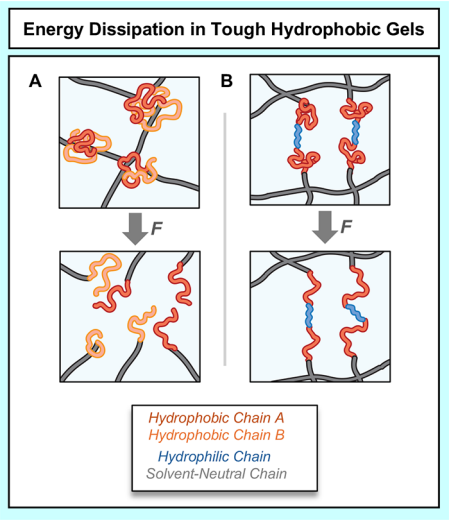

Figure 24. Possible modes of energy dissipation in tough hydrophobic hydrogels, including A) aggregates of hydrophobic moieties which dissociate under mechanical deformation (adapted from Zhao et al., 2021, ref 366, Copyright 2021 American Chemical Society), and B) the uncoiling of hidden hydrophobic lengths under mechanical deformation. Adapted from Zhang et al., 2009 (ref 356, Copyright 2009 Royal Chemical Society).

Hydrophobicity can be difficult to balance in gel design, however, as some amount of hydrophilicity is needed for water permeability of the hydrogel.[358] Salt and surfactants are common strategies used to improve solubility, aggregate size, and toughness. Hydrophobic groups in water alone have a high penalty to dissociation and exchange, but the introduction of a surfactant allows micelles to undergo more dynamic exchange within soluble pockets, resulting in a comparatively shorter bond lifetime and improved energy dissipation under mechanical deformation.[363,364] Salt may be used to help disrupt the water network local to the hydrophobic groups, allowing better mobility through aqueous media and the formation of larger aggregates.[358] The true advantages of hydrophobic association are brought out in combination with other bonds, most commonly hydrophilic associations, and the reader is directed to the expert review by Jiang et al. for a comprehensive survey of hydrophobic association in hydrogels.[359]

Although individually weak, the entropic drive for aggregation in aqueous media makes hydrophobic crosslinks tough on the macromolecular scale. The strength and timescale of these interactions are highly subject to changes in the solvent environment, such as pH and ionic content. As previously discussed in Section 2.2.3, pH can be used as a trigger to switch hydrophobic interactions on or off, typically accompanied by large entropic changes to the system via the formation or dissociation of hydrophobic aggregates.[365] Hydrophobic interactions are often used in conjunction with hydrophilic motifs to produce the greatest effect on toughness via the use of multiple dynamic bond motifs, as will be explored in the next section.

3.2.8. Systems with Multiple Dynamic Bonding Motifs. As exemplified by the routine use of primary covalent and secondary dynamic motifs within single network hydrogels to manipulate small strain rheological behavior, the combination of different types of interactions can yield a dramatic increase in toughness. By incorporating multiple dynamic motifs, materials begin to access higher order structures and assemblies that synergistically improve energy distribution and dissipation.[366] Additionally, should those dynamic bonds have substantially different lifetimes, the resultant material will undergo multiple relaxation and exchange pathways. These reversible linkers can coexist either orthogonally to each other, or in direct synergy. Orthogonal dynamic bonds do not influence each other's exchange kinetics and experience well resolved separate relaxations, whereas pairs of the latter will

https://doi.org/10.1021/acs.chemrev.5c00466
Chem. Rev. XXXX, XXX, XXX−XXX

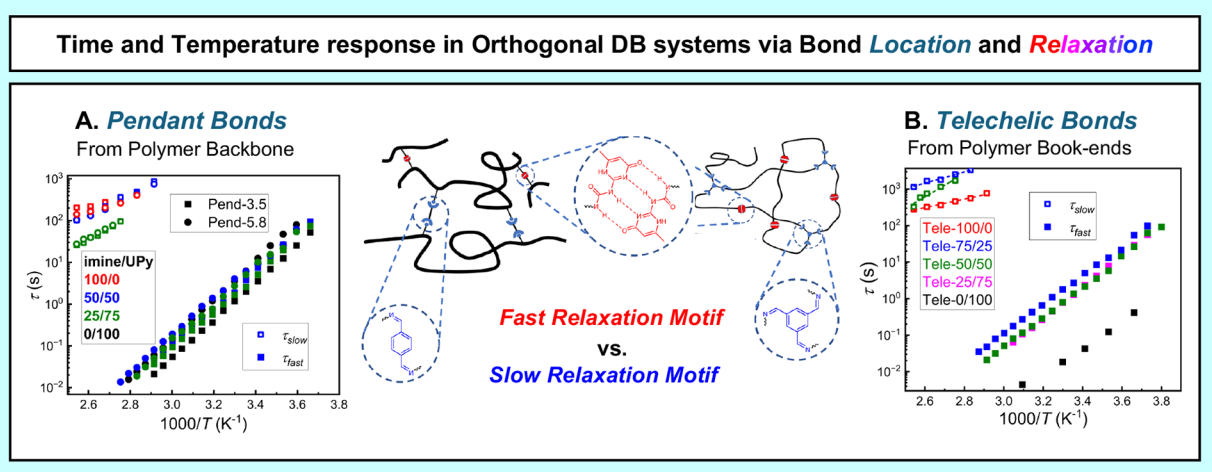

Figure 25. Timescale and temperature response of A) pendant with 3.5 and 5.8 mol % amine groups per chain and B) telechelic polymers with dual relaxation motifs (fast UPy, slow imine) and 2.9 mol % amine groups per chain. Different imine/UPy ratios are color coded. Adapted from Ge et al., 2023 (ref 367, Copyright 2023 Springer Nature).

have a cooperative (or disruptive) effect, influencing each other's relaxation and exchange.[367]

Common orthogonal systems utilize a combination of hydrogen bonding and dynamic-covalent linkages, as they exist on dramatically different timescales of relaxation and exchange. Ge et al. study the effect of imine crosslinkers (τ_{slow}) and a relatively strong 2-ureido-4[1H]-pyrimidone (UPy, τ_{fast}) hydrogen bonding motif in polydimethylsiloxane (PDMS) with various mole percents of amine (NH_2) incorporated into the backbone, noting that the relaxation timescales of the dynamic bonds differ by 1−2 orders of magnitude depending on the nature and functionalization of amine sites with imine crosslinker (Figure 25).[367] Through small amplitude oscillatory shear (SAOS) rheology, the authors observed two critical timescales: a fast timescale for the hydrogen bonds, and a slow timescale for dynamic covalent bonds. In this instance, energy dissipated via the breaking of reversible hydrogen bonds is the primary contribution to toughness, while the imine bond influences the overall network structure and final terminal relaxation. In a pendent network without UPy, lower concentration of imine crosslinker results in a shorter exchange timescale, as the availability of unfunctionalized amine groups allows exchange of imine bonds to proceed via both imine transesterification and metathesis. While the concentration of dynamic covalent linkage does not seem to effect UPy dynamics to a significant degree, it was noted that increasing UPy concentration does indeed shorten imine bond exchange similarly to pendant networks containing no UPy (Figure 25, **A**). This is attributed to a lower effective imine crosslink density, which presents as a lower plateau modulus and slightly faster imine exchange. The authors also investigated differences between ∼7332 g/mol and ∼5000 g/mol PDMS, with 3.5 and 5.8 mol % amine groups per chain (respectively). SAOS rheology indicated that the high frequency plateau of the rubbery plateau modulus is independent of dynamic bond ratio and is only impacted by the initial concentration of amine sites in the PDMS chains (effective crosslink density). Meanwhile, the low frequency plateau is dependent on both amine and imine concentration, which determines the final network structure just before its terminal relaxation (τ_{slow}). By comparison, 3-arm imine crosslinks formed in a telechelic network create a denser structure, which is theorized to undergo a form of associative pair exchange via aggregates, thereby extending the terminal relaxation timescale (Figure 25, **B**).[367]

The telechelic network is structured such that there are two amine sites per PDMS chain (∼5000 g/mol), effectively capping both ends of the polymer. Exchange is initiated when multiple amine groups aggregate around 3-arm imine crosslinks, merge, and separate with new partners attached. Thus, for this architecture, imine bonds dictate the network structure and appearance of distinct relaxation timescales. Since the imine bond has a comparatively long timescale of exchange, it can be said that the 3-arm crosslink acts as nearly static. 100% UPy forms head-to-tail linear network structures, whose exchange results in major rearrangement of the network. Below 50% imine functionalization, the network is a sparsely joined collection of hyperbranched structures, resulting in macroscopic flow via the dominant exchange of UPy motifs. The high frequency, short relaxation of these hyperbranched structures occurs via UPy relaxation within the arms, whereas low frequency relaxation only occurs via a major network rearrangement stemming from diffusion of the central 3-arm imine star polymer segments. Typically, only one significant relaxation timescale is apparent, τ_{fast} (Figure 25, B). The relaxation timescale, τ_{slow}, for imine exchange only appears above 50% imine concentration, and is determined by the imine network's ability to percolate throughout the gel. In adherence with the Flory Stockmayer theory, fewer dynamic crosslinks per unit volume significantly impede aggregate pair exchange. Above 50% functionalization with imine crosslinker, both imine and UPy timescales of exchange are extended. These observations are reflected by the activation energy for exchange in each scenario significantly.[367]

Additionally, separate dynamic interactions can influence each other's timescales. For example, Zhang et al. state that the hydrogen bonding capabilities of acrylamide are stabilized when copolymerized with the acrylonitrile due to synergy with the dipolar interactions.[326] However, it can also be argued that this is truly an effect of the hydrophobic character of acrylonitrile rather than dipole−dipole interactions, with further studies needed to clarify the underpinnings of this system. In either case, acrylonitrile serves as a motif to spatially restrict H-bonding units in microdomains inaccessible to

https://doi.org/10.1021/acs.chemrev.5c00466
Chem. Rev. XXXX, XXX, XXX−XXX

water, leading to network contraction and promoting polymer−polymer rather than polymer−solvent hydrogen bond exchange. Authors sought to balance this dehydrating effect by incorporating an anionic monomer into the network, ensuring solvent permeability and inducing compensatory swelling. The resultant material undergoes successful dynamic bond exchange to achieve full recovery in 6 h, one-quarter of the time needed to reach full healing without acrylonitrile groups. Higher extensibility and toughness of hydrogels with (5.5 kJ/m^2) and without acrylonitrile (0.48 kJ/m^2) are indicative of longer effective hydrogen bond lifetimes.[326]

Multibond type single network configurations have also been explored for their large deformation behavior and self-healing ability. For example, Fan et al. fabricated cation-π and π-π gels with 2-(acryloyloxy)ethyl trimethylammonium chloride (ATAC, cationic), and 2-phenoxyethyl acrylate (PEA, π group). Excess π groups create π-π stacking opportunities which act as another form of dynamic crosslink. The resultant material is highly stretchable, with a failure strain >800%, and full recovery from 200% applied strain after only 2 min. Wei et al. formed a chitosan-based gel with dynamic imine and acylhydrazone bonds and showed that the degree and rate of healing from a cut and reassemble test could be significantly modulated through pH, by acidification decreasing the stability of the acylhydrazone crosslinks.[368]

3.3. Spatiotemporal Regulation of Toughness

Throughout this review, the discussion of hydrogels as tough materials and the dynamic molecular interactions that determine toughness have largely been consistent with single network architectures. However, the incorporation of multiscale, complex, and/or heterogeneous structures (Figure 26)

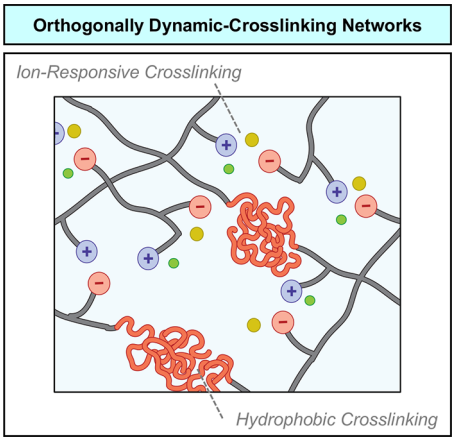

Figure 26. Schematic structure of hydrophobically modified ionic hydrogel.

into hydrogel networks provides opportunities for further enhancement of toughness through spatiotemporal regulation of those structures. In this context, spatiotemporal regulation refers to the control of the distribution components in the network of the hydrogel in space (*e.g.*, network density or microstructure) and time (*e.g.*, the dynamic regulation of interaction energy and timescale using stimuli at a given time relative to deformation). As discussed previously, hydrogel mechanical behaviors such as relaxation kinetics, fatigue resistance, and recovery require both spatial and temporal considerations when assessing their components with respect to hydrogel toughness. Section 3.2 detailed spatial aspects from a molecular perspective, wherein the directionality dependence of dynamic bonds directly contributes to their exchange kinetics, thermodynamic penalties, and timescales.

Further spatial regulation of hydrogel networks extends beyond the molecular motifs into the multiscale regime. Spatial elements of this nature include both network architectures and multiscale macromolecular structure, *i.e.*, conformation and topology. Higher order architectures and structural motifs may be integrated into hydrogels as a mechanism for enhanced energy distribution during deformation; the pronounced spatial aspects of higher order structures (such as microstructural surface area, anisotropy, network volume percentage and density) lead to compounding hierarchical effects associated with fracture resistance or fatigue resistance.[38] While the spatial contributions of higher order structures introduce more considerations and potential complications when compared to molecular-scale spatial components such as bond directionality, they also provide opportunities for nuanced tunability. By leveraging dynamic bonds within these spatial elements, hydrogels containing complex architectures and higher order structures can be transformed into temporally regulated, multiscale mechanisms for energy dissipation. The timescales for the spatial regulation of multiscale structures are direct products of the hierarchies in dynamic molecular interactions, their respective timescales, as well as their environmental sensitivity. The temporal component encompasses different points in time as they relate to deformation of the hydrogel, including the timescale of strain application (relaxation/energy dissipation kinetics), after deformation occurs (recovery/healing kinetics) or during fracture and hydrogel failure (crack blunting/propagation). Importantly, understanding the relationship between molecular interactions and multiscale structure in determining overall material mechanical behaviors provides a handle to program the assembly of hydrogels for multiscale construction (Section 4) as well as dynamically modulate hydrogel mechanical behaviors (Section 5).

In relation to this review, network architectures should be considered as modalities or strategies to introduce multiscale structures that interact synergistically with dynamic bonds to maximize hydrogel toughness. Architectures include single networks, interpenetrating networks (IPNs), and composite networks which add one or more separate phases consisting of polymeric or nanomaterials (Figure 27). These are not exclusive, and multiple architectures may be found within a single hydrogel system. As the impact of network structure on the mechanical properties of hydrogels has been extensively reviewed, these will only be overviewed to provide a framework for contextualizing these structures with dynamic bonds. The reader is directed to these excellent reviews for a more in-depth understanding of the effects of network architectures on hydrogel toughening.[12,37,38] The following sections introduce multiscale motifs commonly used as energy dissipation mechanisms within hydrogels, drawing attention to their effect on toughening. While a diverse number of structural motifs/strategies exist, their spatiotemporal tunability and mechanistic contributions to toughness can be broadly grouped into three main categories: 1) Complex network structures, 2) microphase separation, and 3) induction of anisotropy.

3.3.1. Complex Network Structures. Increasing the complexity of network architecture from a standard, single network is a well-known strategy for introducing toughening multiscale motifs within hydrogels, and can largely be

https://doi.org/10.1021/acs.chemrev.5c00466
Chem. Rev. XXXX, XXX, XXX−XXX

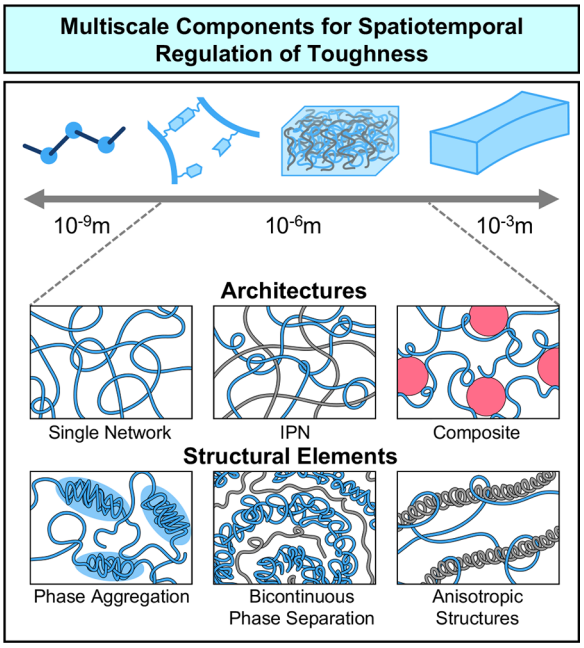

Figure 27. Toughness can result from synergy that occurs across the multiscale regime. Included are network architectures and structural elements that can be used as multiscale motifs for spatiotemporal regulation of toughness.

accomplished in two ways: 1) introduce additional polymer networks in the form of IPNs or 2) introduce a separate phase by adding nanoparticle or polymeric materials. These heterogeneous networks should be conceptualized in terms of intranetwork, internetwork, and/or filler-network interactions that combine synergistically into specific structural motifs that enhance hydrogel toughness. Understanding the nature and role of each interaction within the system as a whole is necessary for the intentional design of spatiotemporally regulated hydrogels.

IPNs are hybrid hydrogels comprised of two or more interpenetrating networks that differ in molecular and/or structural composition. The term IPN was introduced in 1960,[369] and although their use in hydrogels began as a method of adhering hydrogels to silicone surfaces,[370] modern research has explored hydrogel IPNs for their enhanced mechanical properties as well as their ability to combine chemical and physical properties of multiple materials.[371−374] Depending on the chain length and bond strengths of their constituent networks, one network can function as a source of sacrificial bonds to dissipate energy, while the other maintains the original shape of the network, producing a form of shape memory.[372] Additionally, different mechanical properties can be accessed by synthetically adjusting the degree of network interpenetration. Double network (DN) hydrogels, first introduced by Gong et al. in 2003, are a subclass of IPNs that are fully interpenetrating and composed of an abundantly crosslinked brittle network, and a sparsely crosslinked ductile network.[375] Under load, the brittle network fractures to dissipate energy and forms a large damage zone around the crack tip, hindering further crack propagation, while the ductile network elongates to maintain the structural integrity of the gel. Because of their structure, DNs can achieve fracture toughness upward of 1000 J m^{-2} and maintain high extensibility while returning to the initial shape after deformation.[43] The energy dissipation mechanism of IPNs can also shift due to stoichiometric effects, particularly when constituent networks have disparate relaxation regimes, making them highly tunable architectures.[235] Traditional IPNs with covalent networks rely on the breaking of bonds to dissipate energy, meaning they rapidly fatigue, even after a single deformation cycle.[43] By replacing one or both of these networks with dynamic networks, the spatial contributions of IPNs can be temporally regulated to reduce fatigue, introduce self-healing and increase fracture toughness.

Hybrid hydrogels composed of dense, ionically crosslinked alginate and sparse, covalently crosslinked polyacrylamide (PAM) highlight how spatial elements like chain length and volume ratio of the networks can be used to decouple stiffness and fracture toughness in DNs containing dynamic interactions. Li et al. synthesized alginate and PAM DNs that achieved simultaneously high stiffness (∼1 MPa) and fracture toughness (4000 J m^{-2}). Increasing the total volume ratio of alginate resulted in an increase in both stiffness and strength, but a decrease in toughness. By increasing the ratio of short to long alginate chains while keeping total volume of alginate constant, a significant decrease in strength was observed without an accompanying decrease in stiffness or toughness.[207] Sun et al. showed that the impressive mechanical behaviors characteristic of these networks are due to crack bridging by the PAM network and the large dissipative deformation region created by the separation of the dynamically bonded alginate network,[206] leading to notch insensitivity that maintains toughness, stiffness, and extensibility even when damaged. In the previous example, decreasing the ratio of crosslinked poly(acrylamide) reduces structural integrity and its availability for crack bridging, which decrease fracture energy. Introducing short chains leads to enhanced interaction within the dissipative region, where the rupture of ionic crosslinks allows for energy dissipation. The role of each component network underscores how the composition of spatial elements contributes to multiscale motifs that participate in network toughening. Such tunability of dynamic IPN and DN mechanical properties is also seen through network topology, due to changes in the distribution of bond strengths and characteristic length scales. For example, Huang et al., using the synthetic tunability of PEG to investigate the topological dependence of DN hydrogels comprised of alginate and covalent PEG networks.[376] In this study, alginate dramatically strengthened and stiffened linear PEG networks when compared to its effect on nonlinear, 4-arm PEG networks, even accounting for the molecular weight differences, highlighting the way that dynamic bonds interact synergistically with network topology.

The effect of dynamic interactions on IPN mechanical properties is even more pronounced when both networks are fully dynamic. Yuan et al. designed a dynamic DN composed of hydrophobically crosslinked PAM and ionically crosslinked xanthan gum that demonstrated faster recovery, reduced hysteresis after deformation, and new self-healing ability compared to previous DN gels discussed.[377] This fully noncovalent DN showed near complete recovery from loading to 300% strain after 5 h, with most of that occurring within the first 2 h. In this system, the hydrophobic interactions within PAM have low energetic barriers for disassociation and reassociation, allowing them to act as weak dynamic crosslinks with fast reformation timescales; the xanthum gum contains strong ionic crosslinks that reform slowly over time. By

https://doi.org/10.1021/acs.chemrev.5c00466
Chem. Rev. XXXX, XXX, XXX−XXX

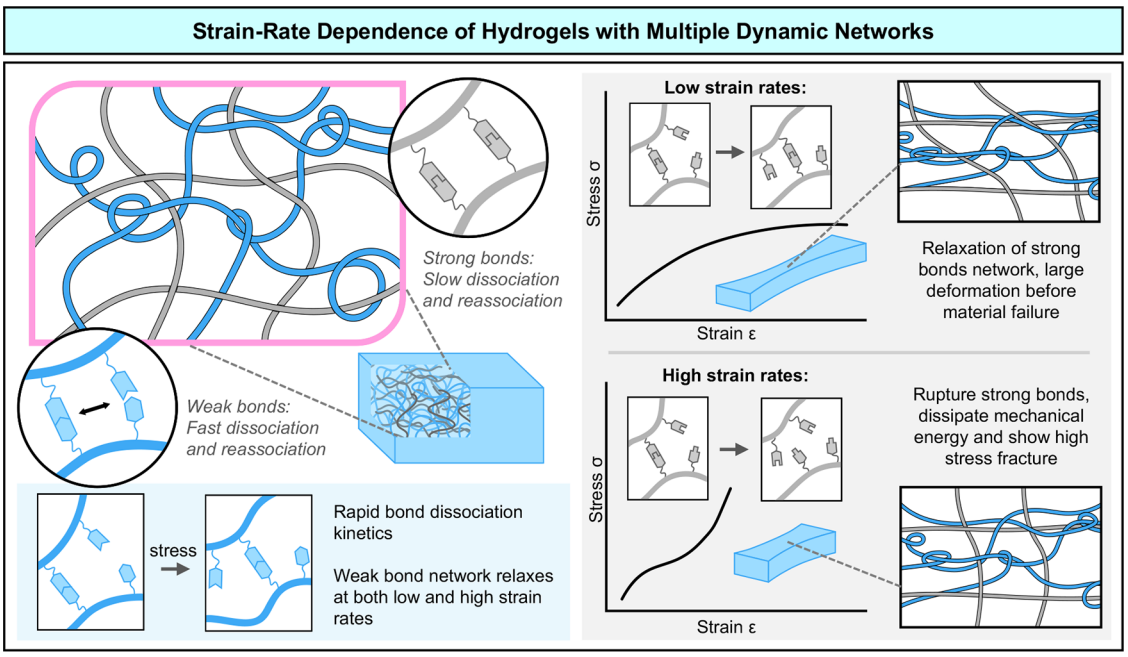

Figure 28. Strain-rate dependence of dynamic networks containing bonds with distinct reformation timescales and bond strengths. Weaker bonds with fast reformation timescales act as dynamic crosslinkers that relax quickly across strain rates. Strong bonds with slow reformation timescales act as dynamic crosslinkers under slow strain rates, allowing a large amount of deformation. Under fast strain rates, these bonds act as static crosslinkers that rupture and dissipate mechanical energy, resulting in high stress fracture and strain-induced toughening.

incorporating multiple dynamic networks with distinct reformation timescales and bond strengths, fully dynamic DNs benefit from enhanced energy dissipation through plastic deformation of the weakly bonded network as well as enhanced recovery due to shape memory and self-healing of the strongly bonded network.[378] Additionally, the mechanical properties and recovery of DNs containing dynamic bonds show high strain-rate dependence due to the physical nature of their sacrificial bonds. Covalent DNs show strain-rate independent behavior, with fragmentation of the covalent networks occurring at a certain strain regardless of velocity.[43] However, when dynamic networks are incorporated, toughness tends to scale in proportion to strain-rate, where fast relaxation of one network allows greater deformation of the hydrogel at longer timescales without fragmentation of the network (Figure 28). This can be seen both in hybrid DNs consisting of one covalent and one dynamic network,[379] and in fully dynamic DNs.[76]

Moving on from IPNs, complex network architectures formed by introducing a separate phase of nanoparticle additives or polymeric materials are broadly considered as composite networks. Nanoparticles made from materials such as silica, metals, metal oxides, polymers, clay, and more recently 1D and 2D conjugated materials such as graphene oxide and transition metal chalcogenides, have been used to enhance the mechanical properties of hydrogels as well as add additional functionality such as electrochemical conductivity. Improved control over nanoparticle size, shape, and composition has enabled a broad range of properties in nanoparticle composite gels. Through the physical interaction of these particles within the hydrogel network, nanocomposite hydrogels can reach stiffness, toughness, and elongation several times that of the pure polymer network.[380−382] Whether by noncovalent adsorption of polymer chains, coordination of exposed metal sites, hydrogen bonding, or other interactions, the large surface area of nanoparticles allows them to interact with many polymer chains at once, essentially opening vast opportunities for the introduction of new and interesting dynamic bonding motifs at the multiscale. The versatility of composite networks has led to the creation of nanoparticle composite gels with fracture toughness upward of 6000 J m^{-2}, and while some of the mechanical enhancement is due to the interactions of filler particles with each other, the increased toughness is largely attributable to the functionality of nanoparticle fillers as crosslinking junctions for the polymer network.[383] Toughening effects as a result of anisotropic alignment of fillers with high aspect ratios are discussed later in Section 3.3.3.

The dynamic bonding that accompanies filler particulate is an inherent component of composite networks and is key to toughness enhancement seen in such systems. Assessment and tailoring of the interactions introduced by a selected filler can lead to the intentional design of specific toughening regimes. For instance, Song et al., used metal nanoparticles that functioned as both fillers and dynamic crosslinking junctions, enabling different mechanical properties compared to inert filler particles.[384] In this system, the nanoparticles delay relaxation, creating a plateau region in G' at low frequencies; interestingly, nanoparticle incorporation also delays fast relaxation modes. The nanoparticle dynamic crosslinking also drives substantial strain-rate dependence at large strain, with the gel transitioning from fluid-like to solid-like behavior when the strain-rate is increased 10×.[384] Liu et al. in 2023 used coordination nanoparticles—tight clusters of polymer dynamically crosslinked with metal ions—and poly(vinyl alcohol) (PVA) to create a simultaneously tough (3500 J m^{-2}), highly extensible (2300%), and self-healing hydrogel film.[385] Under load, these clusters contribute to improved mechanical properties through particle reinforcement, reshaping of the

https://doi.org/10.1021/acs.chemrev.5c00466
Chem. Rev. XXXX, XXX, XXX−XXX

broader network, and by changing their internal network structure to dissipate energy.[385]

3.3.2. Microphase Separation. Phase separation can be used to introduce multiscale structural elements into hydrogel networks that participate in numerous toughening mechanisms. Controlled microstructures in the form of phase-separated aggregates, nanocrystalline regions, and bicontinuous phase separations result from the combination of molecular design, such as polymer composition and topology, and environmental factors, such as solvation environment or external stimuli. In Section 4, the specific methods for utilizing the dynamically reconfigurable, environmentally sensitive energy landscape of dynamic bonds will be outlined. More broadly, hydrogels with microphase separation consist of relatively stiff polymer dense regions and relatively soft polymer sparse regions.[76,386,387] Polymer dense regions act as physical crosslinks, lending structural support that can distribute mechanical energy across the network while also providing sacrificial bonds for energy dissipation. This is particularly evident when phase separation results in nanocrystalline domains, as is the case for freeze−thawed PVA and salt-induced crystallization of chitosan.[388]

In conjunction with the incorporation of sacrificial bonds (a previously discussed mechanism for toughening), the dynamic interactions that lead to phase separation can further provide tuning opportunities to enhance toughening. Within the stiff phase of phase separated hydrogels, dynamic interactions can be tailored to rupture or dissociate under specific mechanical loads or timescales, interacting synergistically with the broader network structure to dissipate mechanical energy and blunt crack tips in a manner like double network gels.[389] For example, crystalline domains in PVA gels improve toughness by introducing an interconnected physical network structure. In addition to crystallinity, freeze−thawing results in phase separation. PVA gels prepared via this process benefit from the introduction of crystalline regions that act as strong physical crosslinkers, while phase separation enhances the distribution of mechanical energy across the network. Meanwhile, PVA gels that are aged at room temperature do not experience phase separation and therefore show less mechanical enhancement at the same crystallinity (Holloway et al. 2013).[390] Directed phase separation for spatiotemporally controlled relaxation can also be accomplished when constituent networks support topologically complex architectures, such as bottlebrush polymers, which dictate hydrogel structure and properties. This topological confinement results in the spatial organization of immiscible components relative to one another at controlled distances and length scales, creating designated energy dissipation routes. For example, incorporating hydrophobic content in the bottlebrush backbones results in their collapse under aqueous conditions, creating hidden lengths that extend under specific strains as well as reduce strain hardening.[391]

The spatial contributions of phase separation within the hydrogel matrix can be deliberately tuned to form microphase regions with low surface energy, introducing fully or semi-bicontinuous structures that enhance hydrogel toughening. As a result of a substantial energy difference between polymer solvation and polymer−polymer interactions, phase separation of chain segments into polymer rich and polymer poor regions becomes thermodynamically favorable,[392−394] and structures such as densely packed or entangled aggregates and microcrystalline domains form to minimize a hydrogel's free energy and reduce contact with water.[392−394] Uniquely, although phase separation introduces inherent heterogeneity into microstructures, the macrostructure of hydrogels containing bicontinuous phase separation is uniform, which enables uniform energy distribution and improved energy dissipation through the network.[393,395]

Similarly to phase separated aggregates or nanocrystalline regions, the bicontinuous microphase separations function as dynamic crosslinks capable of enhancing toughness via rearrangements or induction of anisotropy.[395] Interestingly, such phase separations can be accessed through DN architectures comprised of one hydrophobic and one hydrophilic polymer network,[392−394] as well as polyampholyte single networks. Hydrogen bonding, hydrophobic, host−guest, cation-pi, and ionic interactions have been used to form nominally single network gels that are susceptible to forming aggregates, micelles, or participating in additional interactions. For example, Tuncaboylu et al. used salt to drive physical assembly of hydrophilic−hydrophobic copolymers[358] and found that there was a range of increasing salt content over which the storage/loss modulus crossover could be tuned to lower frequency (greater stability)—below this threshold salt content, the micelles did not fully form and above this threshold large scale phase segregation occurred. Polyampholyte hydrogels with a mix of strong and weak ionic interactions can form this kind of phase separated structure, and have achieved fracture energy as high as 4000 J m^{-2} with stiffness around 1.8 MPa.[76,261]

3.3.3. Anisotropy as a Structural Motif. When structural elements with high aspect ratios, such as fibrillar or planar structures, are incorporated into the hydrogel matrix, new multiscale motifs for toughening arise depending on the element's length scale, alignment, spatial (conformational/translational/rotational) mobility and network percolation. Fibrils and fibers are a ubiquitous phenomenon in tough biological tissues such as muscle, ligament, and cartilage; just the addition of fibrillar components to a hydrogel tends to greatly enhance mechanical properties. For instance, Baniasadi and Minary-Jolandan reported alginate/collagen fibril composite gels in which nanoscale collagen fibrils are incorporated into an ionically crosslinked alginate network. The resulting gel had storage and loss moduli of 7 and 3.8 kPa respectively at 1 Hz, compared to 2.5 and 0.4 kPa for a pure alginate gel under the same ionic conditions, showing that even the addition of relatively small amounts of fibrils (1 mg fibrils per mL deionized water) increased elasticity and energy dissipation by several times.[396] Such toughening effects stem from two main multiscale motifs: structural reinforcement and induction of anisotropy.

Similar to IPNs and composite networks, reinforcement of the hydrogel structure by fibrillar or planar components is a result of network percolation, the strength/stiffness of the components, and the introduction of new physical crosslinks through entanglement and high surface area interactions. High network percolation allows for fast mechanical energy distribution and dissipation, and stiff anisotropic networks also participate in crack blunting and propagation. The effectiveness of fibril reinforcement was demonstrated by Fang et al., who synthesized a hydrogel consisting of a PAM network covalently crosslinked by acrylated agarose fibrils to form an interpenetrating network that showed a toughness of 55 MJ m^{-3} compared to single network PAM, which showed a toughness of 4 MJ m^{-3}. The rigid agarose reduced network deformation under high strains, while the covalent crosslinks

https://doi.org/10.1021/acs.chemrev.5c00466
Chem. Rev. XXXX, XXX, XXX−XXX

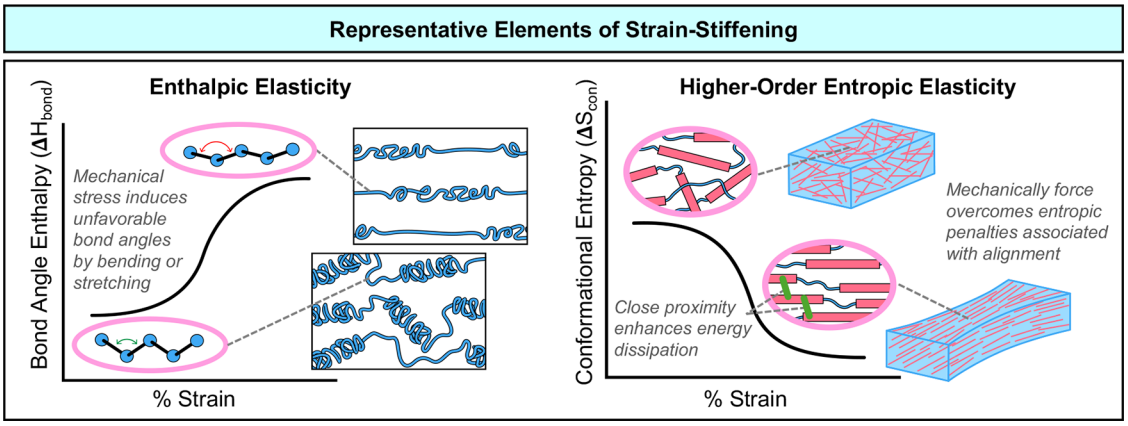

Figure 29. Anisotropic effects can lead to strain-stiffening, *i.e.*, nonlinear elasticity. Hydrogels containing structures that cannot readily undergo changes in entropy are driven by the enthalpic storage of mechanical energy through the induction of high energy, unfavorable bond angles at crosslinking junctions through bending or stretching. Hydrogels with flexible, anisotropic higher order structures that can readily access states with higher translational entropy store mechanical energy through a loss conformational entropy. Mechanical force brings together anisotropic alignments, where increased proximity of energy dissipation or distribution mechanisms within the hydrogel network contributes to hydrogel toughness.

increased interfacial interaction between the two networks, which resulted in efficient stress transfer.[397]

These hydrogels synthesized by Fang and co-workers also benefitted from the second aforementioned multiscale structural motif: induction of anisotropy. When incorporating anisotropic structures into a hydrogel, the propensity to form aligned anisotropic regions greatly increases. In this case, *in situ* small-angle X-ray scattering (SAXS) measurements showed scattering patterns indicative of high anisotropy for the PAM hydrogels that were crosslinked with agarose fibrils with strong intensity along the equatorial axis of applied strain, even at low strains. Conversely, the significantly less tough single network covalent PAM hydrogels showed isotropic scattering patterns regardless of applied strains.[397] Geonzon et al. synthesized tough hydrogels that show anisotropic alignment by utilizing salt induced κ-carrageenan double helix bundles.[398] These bundles are isotropic within a covalently crosslinked network but achieve anisotropic directionality along the axis of strain. With a further increase in strain, the bundles themselves form a local crystalline-like order. As a result, both toughness (7.15 kJ m^{-2}, 7.0 MJ m^{-3}) and Young's modulus (17 MPa) are greatly enhanced.[398]

Materials that undergo anisotropic induction under mechanical stress participate in strain-stiffening, a rate dependent phenomenon that has been reported for numerous tough hydrogels and previously mentioned in Section 2. It can generally be conceptualized as a dramatic increase in a material's stiffness and elastic modulus above a critical stress and strain[399−401] (Figure 29). The thermodynamic driving force of strain-stiffening is attributed to elasticity within the hydrogel that can be grouped as entropic or enthalpic.[402] Gels that are driven by entropic elasticity are composed of flexible or semiflexible higher order structural components which become aligned in the direction of the critical strain, reducing conformational entropy in favor of translational entropy.[400,401] The strain-stiffening of entropic gels results in a higher local density of polymer−polymer interactions whose effect on mechanics dramatically increases as they progress in length scale. In tough hydrogels, energy dissipation mechanisms are forced closer together in the same orientation, increasing interactions with increased network anisotropy.[400,401] As a result, a higher maximum stiffening index, or the rate at which a gel stiffens as stress is increased, can be achieved.[401,403] In contrast, enthalpic gels are typically composed of more rigid networks which cannot readily access a shift from conformational to translational entropy at high strain rates.[401] Rather than participate in entropic strain-stiffening, these network filaments are instead forced to bend and stretch asymmetrically between crosslinking points, which can perturb bond lengths and angles.[399,402] While low strain rates may still yield anisotropic-like alignments within the macromolecular network structure, a lower stiffening index is routinely the outcome of these gels when compared to those that also participate in entropic strain-stiffening mechanisms.[399,403]

3.3.4. Multimodal. Given the breadth of possible combinations of polymers and interactions, hydrogels with multimodal energy dissipation structures can access a broad space of mechanical properties.[377,404,405] Biological organisms utilize several forms of dynamic physical bonds simultaneously in combination with an array of multiscale, hierarchical structures as a basis for tough tissues and structural materials. For example, mussel byssus core fibers are known for their incredible toughness and near spontaneous healing, attributable to a semicrystalline structure comprised of preCol protein units with three domains: 1) histidine rich terminal residues that engage in metal coordination with Zn^{2+} and aspartate, 2) flanking domains of a β sheet-like structure that are formed via hydrogen bonding and 3) triple helix collagen domains formed through geometrically staggered H-bonding associations.[406] Notably, the mussel uses pH to spatiotemporally regulate the formation of Zn^{2+}-complex formation, such that only in the mildly basic environment of seawater can zinc-histidine bonds form.[407,408] The combination of these dynamic interactions *and* a complex arrangement of multiscale structural motifs provide numerous avenues for energy dissipation; including weak and strong reversible bonds, structural reinforcement at multiple length scales from spatial contributions of both sheet-like and collagen domains, and interfacial interactions externally regulated through pH, water salinity, and complex biofabrication.[406]

While the toughness of mussel byssus core fibers benefits from the combination of dynamic bonds with disparate

https://doi.org/10.1021/acs.chemrev.5c00466
Chem. Rev. XXXX, XXX, XXX−XXX

relaxation timescales, other systems may contain dynamic bonds of similar lifetimes and E_d, which can undergo relaxation on similar timescales while still synergistically improving toughness. Notably, even seemingly simple combinations can yield complex materials with exceptional properties. For example, a hybrid hydrogel that combines poly(diallyldimethylammonium chloride) (PDDACl)/branched poly(ethylenimine) (PEI) with a polyelectrolyte mixture of poly(sodium 4-styrenesulfonate) (NaPSS)/poly(acrylic acid) forms a phase-separated network composed of several dynamic bonding pairs. Proton exchange between PAA and PEI make a hydrogen-bonded ion pair, while release of NaCl drives the complexation of PDDA and PSS, making system with four different ion pairs and four different combinations of polymer−polymer hydrogen bonds (precipitation and rehydration likely led to the removal of NaCl).[409]

The hierarchy of interaction strengths in these potential pairings further defines the equilibrium structure, wherein strong interactions of PDDA−PSS lead to phase separation and dense PEC nanoparticles, which serve as structural reinforcement and dissipating motif to the weaker PAA−PEI network (Figure 30). The strong association of PSS and PDAA

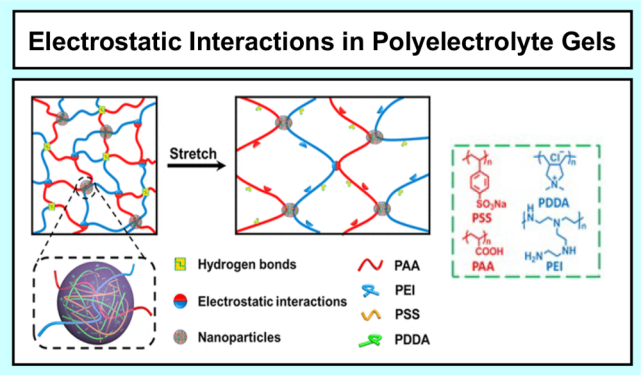

Figure 30. Physical crosslink structure and energy dissipation mechanism of a polyelectrolyte formed from weak electrostatic interactions (PEI−PAA) and strong electrostatic PSS−PDDA nanoparticle entanglements. Adapted with permission from Yuan et al., 2019 (ref 409, Copyright 2019 American Chemical Society).

is a result of their poor hydration, which results in ionic bond strength of 136.2 kJ/mol (see Section 3.2 for more details).[410] The more hydrophilic PEI−PAA primary network is characterized by weak electrostatic interactions (63.6 kJ/mol) and hydrogen bonding (26.7 kJ/mol) that additionally depending on local pH. This results in a tensile strength of 1.26 ± 0.06 MPa, strain at break of 2434.2 ± 150.3%, and a toughness of 19.53 ± 0.48 MJ/m^3. Incredibly, the toughness of these quaternary mixtures is ∼5.2 and ∼108 times higher than that of the binary PEI−PAA and PDDA−PSS hydrogels, respectively.[409] Additionally, self-healing occurs within this system due to the dynamic rearrangement of hydrogen bonding in water, followed by slower electrostatic interactions between PEI−PAA.[409]

Multimodal dissipation can also be seen at the microstructural level by including varied spatial elements within the network. For example, incorporating fibrillar structures at different orthogonal or complementary length scales within a hydrogel network can achieve significant mechanical improvement due to synergistic mechanical enhancement from dynamic interactions between the various fibers and the hydrogel.[411] Lin et al. combined macroscale fiber reinforcement using 3D-printed flexible poly(lactic acid) (PLA) fibers with a hybrid double network composed of ionically crosslinked alginate fibrils and covalently crosslinked polyacrylamide to create an extremely tough and stiff hydrogel that maintained good extensibility. The gel had a stiffness of over 6 MPa and toughness over 30,000 J m^{-2}, and could be stretched 2.6 times the original length before the fiber network failed. Even after the fibers were severed, the secondary toughening mechanism and shape recovery properties of the double network hydrogel allowed the composite to retain structural integrity at even greater deformation.[412]

The synergy that results from network architecture, multiscale structural motifs, and rational incorporation of dynamic interactions leads to universal toughening strategies across hydrogel systems that create opportunities for spatiotemporal regulation of toughening in hydrogels. Most importantly, these synergistic interactions across the multiscale regime should be considered as tools for energy distribution and dissipation; providing precision in mechanical behaviors and responses. The mechanisms for assembly (Section 4) and modulation (Section 5) of these synergetic interactions are key frontiers in hydrogel toughening, with stimuli-responsive materials being a critical element in future development and applications.

3.4. Summary—Molecular Structure Defines Dynamic Bond Timescale and Environmental Sensitivity

A material's timescale is intimately linked to its molecular structure. Dynamic bonds offer multiple avenues to enhance the toughness of hydrogels, with reversible bond formation and breaking that dissipates mechanical energy. The exchange dynamics of these bonds define the material's macroscopic properties, as the dynamic bond must strike a balance: strong enough to resist deformation but sufficiently weak to break and dissipate energy. In the design of hydrogels, a range of dynamic interactions have been leveraged—from dynamic covalent bonds and metal−ligand coordination; to hydrogen bonding and dipole−dipole interactions. As highlighted in the above sections, each bond has unique exchange dynamics that have potential to endow gels with increased toughness. Still, for each of these bond types, several factors must be considered: directionality and steric effects, as well as sensitivity to environmental factors such as temperature and cosolute identity. From these foundations, the properties of dynamic bonds can be modulated to achieve specific material structural elements and toughness. The dynamic nature of bonds can also lead to stimuli-responsive materials, changing their structure and mechanical properties in response to light, temperature, or pH. Through material design or external stimuli, the energy landscape of dynamic interactions can be influenced, and the timescale can be altered. These properties of dynamic hydrogels offer a path forward for a range of emerging applications—from tissue engineering to soft robotics. As will be explored in Section 4, the utilization of the intrinsic molecular structure defined properties can be utilized to dictate the assembly and formation of multiscale structures that further enhance the toughness and overall robustness of hydrogels.

https://doi.org/10.1021/acs.chemrev.5c00466
Chem. Rev. XXXX, XXX, XXX−XXX

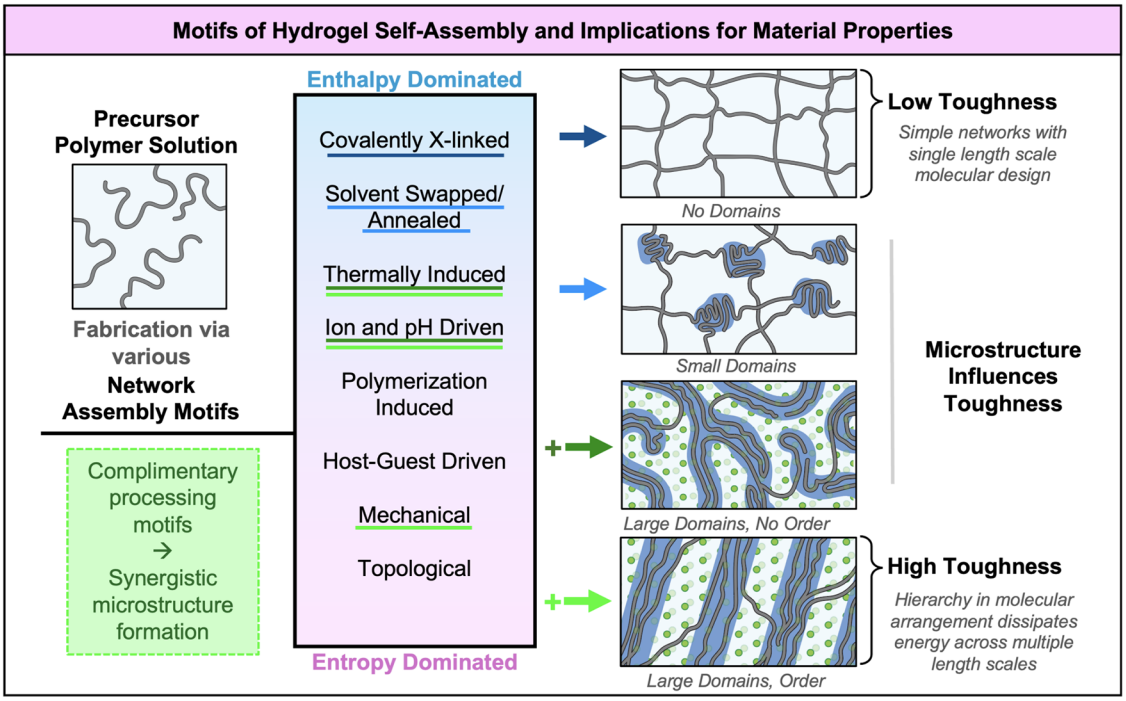

Figure 31. Motifs for the programmable assembly of hydrogels. Energy of solvation changes upon stimuli induction result in gelation for flexible polymers. Variations in configurational entropy drive the assembly of rigid polymers wherein solvent exclusion provides driving force for gelation. Depending on motif of gelation, assembly pathway provides access to close-to- or far-from equilibrium structures. Critically, these motifs of interaction may be coupled to provide dynamic access to a broader scope of hydrogel architectures.

4. DYNAMIC MODULATION OF BONDING TO TAILOR ASSEMBLY, STRUCTURE, AND TOUGHNESS

The structural parameters for creating high toughness hydrogels with network architectures that maximize extensibility as well as distribute and dissipate mechanical energy extend well beyond the length scale of dynamic bonds into multiscale structures.[12,38] As overviewed in the prior section, mechanical performance is directly determined by the structure of the network gel framework across length scales, *i.e.*, hierarchies of molecular functionality, macromolecular structural topology, as well as network microstructure defines the energetic favorability and exchange timescales of dynamic bonds. Superimposing these perspectives results in considering the relationship between the manipulation of the strength and timescale of intermolecular interactions to create the very multiscale structures that engender toughness. While currently an emerging perspective in soft material chemistry, it is the basis of the biofabrication of tissues and structural composites such as silk, connective tissue, and bone.[406,413,414] To incite further exploration of the exciting area, this section surveys the manipulation of chemical interactions, both in time and space, which are required to assemble tough hydrogels materials. Furthermore, this investigation will showcase the intrinsic and inextricable relationship between building block structure, assembly/fabrication, and macroscale properties as templated by the structure and functions of natural materials.[415−417]

As a general overview, the construction of a hydrogel can be generally described as taking an aqueous solution of polymer precursors or polymers, and physically or chemically manipulating them to form a percolated, solvent swollen network—a gel. Referred to as "sol-gel", the reversibility of this process is dependent on the physical and chemical basis of the formation of the gel. In this way, the entire process of gel formation depends on the evolution of chemical structure through time, *i.e.*, while the physical properties of the resulting networks depends on their molecular and macromolecular structure,[38] the formation of these structures should be viewed as an evolution through time that is programmed by the chemical interactions discussed in Section 3.

Theoretical descriptions of this behavior, developed by Flory−Stockmayer theory (as an extension of Carothers' work), first considered the case of chemical crosslinking, treating the network as growing in time as the chemical reaction of monomers progresses.[418−420] Thus, at a critical degree of reaction progress, which is determined by the number of reaction sites per monomer, the extremely large molecule/network would transition from being soluble to insoluble or "gelled" products. Sol−gel transitions must also consider noncovalent interactions wherein enthalpy of attractive interactions versus available thermal energy dictates the number of crosslinks at a given time, meaning there is a critical temperature of gelation, as formalized by the seminal work by Rubinstein et al.[421] In general, these considerations are useful for creating an equilibrium picture of hydrogels and indeed have been expanded to rationalize the solution behavior of biomacromolecules, an emerging topic in biology, biomedical engineering, and material science.[153,154,422,423] However, it has been recently recognized that the network scale structures that provide exceptional mechanical properties in hydrogels, particularly in biological structural materials, are not always the equilibrium structures.[424,425] Taken in sum, this represents an historical transition from the design of equilibrium to nonequilibrium structures, occurring via stimuli-induced phase separation that is often kinetically arrested. This underscores and extends the core theme of Section 3, molecular and macromolecular structure plays a central role in dictating the thermodynamics and kinetics of

https://doi.org/10.1021/acs.chemrev.5c00466
Chem. Rev. XXXX, XXX, XXX−XXX

assembly, thereby dictating structure and resulting properties (Figure 31).

In this section, we provide a perspective on classical systems of hydrogel synthesis by considering the contributions and implications of nonequilibrium and time-dependent nature of gel formation techniques from a fundamental chemistry perspective. Further, we contrast them with the time-tested strategies that biology employs to create exceptional hydrogels.[406]

4.1. Thermal and Solvation Triggered Assembly

The early discovery of gelatin-based hydrogels historically marks how polymer interaction equilibria can be dictated by thermo-temporal processing to afford polymeric assemblies that are locked in nonequilibrium conformations. Initial applications of gelatin-based hydrogels have advanced primarily from culinary modifiers (dating back to the 10th century)[426] to a range of functional applications such as photosensitive films,[427] drug delivery,[428] and synthetic tissue scaffolds.[429] General processing of gelatin-based hydrogels exploits the thermo-reversible helix−coil transition of tropocollagen driven by an increase of thermal energy.[430] Above a critical temperature (~40 °C), weak noncovalent interactions, *e.g.*, hydrogen bonding and dipolar interactions, stabilizing the quaternary structure of tropocollagen are disrupted, resulting in denaturation into individual random chains, known as gelatin.[430−432] Upon cooling, a reduction of thermal energy favors renaturation to partially ordered triple helices driving gelation into a translucent hydrogel. This translucency is noteworthy relative to the opacity of tissues such as connective tissue and the brilliant colors of avian facial structures, both of which directly indicate the presence of dense collagenous structures larger than the wavelength of visible light.[433]

Thus, temperature is one of the simplest parameters to tune the balance of interpolymer vs polymer−solvent interactions for the programmable assembly of hydrogels. This perspective encompasses the traditional enthalpy mediated processing of polymeric materials for which the input of thermal energy affords a reduction in populated states of interpolymer interactions for processing into desired architectures. It was not long after these initial studies on gelatin-based hydrogels that researchers sought to tune molecular structure to advance the capabilities of hydrogel systems.

4.1.1. Upper Critical Solution Temperature Behavior.

Upper critical solution temperature (UCST) type phase behavior describes the phase separation (or coil-to-globule transition) of a polymeric system induced by a reduction of thermal energy. In binary mixtures (solvent/polymer), the UCST is characterized by the maximum point on a polymer solubility curve (Figure 32),[154] below which intermolecular interactions between polymer chains are more favorable than polymer solvation and drive demixing.[434] The theoretical basis for understanding UCST behavior has long been rationalized through the lens of Flory−Huggins theory,[435−438] which describes the thermodynamics of polymer phase behavior as a balance between entropically favored mixing and the enthalpic penalty of disrupting polymer−polymer interactions for solvation, typically quantified by the parameter, χ. Therefore, UCST behavior is generally considered to be enthalpically driven with spontaneous demixing, *i.e.*, spinodal decomposition, occurring above a critical χ value. As discussed in Section 3.2, environmental conditions such as ionic strength,

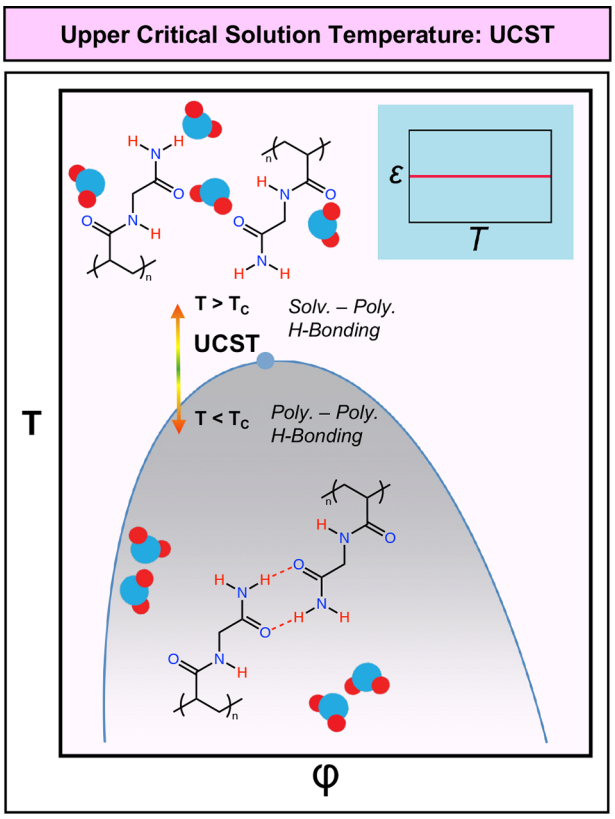

Figure 32. UCST phase diagram obtained for binary polymer/solvent systems. Below the UCST, the system is characterized with favorable polymer−polymer interactions. Above the UCST, temperature invariant interpolymer interactions, denoted as ϵ, result in miscibility driven by an increase of thermal energy. φ is the volume fraction of polymer. Figure modified from Lin et al., 2018 (ref 154, Copyright 2018 American Chemical Society).

pH and concentration modulate polymer−solvent interaction equilibria and have been used as a handle to dictate the UCST transition temperature for programmable hydrogel assembly. Among factors such as concentration, solvent, and added salt, molecular weight has a pronounced effect on the UCST, as it directly shifts a polymer's entropy of mixing.[439] An increased molecular weight generally reduces entropy of mixing, thus decreasing the temperature at which a polymer's storage modulus surpasses the loss modulus and undergoes gelation. However, this topic remains unexplored as a means of tuning gel mechanical properties. The reader is encouraged to explore the following comprehensive reviews for a deeper understanding of factors employed to tune UCST behavior.[439,440]

The molecular structures giving rise to UCST behavior have been well reviewed with polymeric side chains featuring the propensity to form strong intermolecular interactions identified as key motifs.[434] A prominent example is encompassed in poly(NAGA). The dual amide motif in NAGA is characterized with hydrogen bonding interactions an order of magnitude higher in binding energy relative to that of a single amide,[441] highlighting it as a versatile building block for the fabrication of hydrogels with applications ranging from injectable drug delivery and theragnostic systems[442,443] to mechanically robust thermoplastics.[441] Alternative structures are comprised by poly(zwitterions) and polyelectrolytes which form dipolar and ionic interactions that outcompete solvation.[434]

https://doi.org/10.1021/acs.chemrev.5c00466
Chem. Rev. XXXX, XXX, XXX−XXX

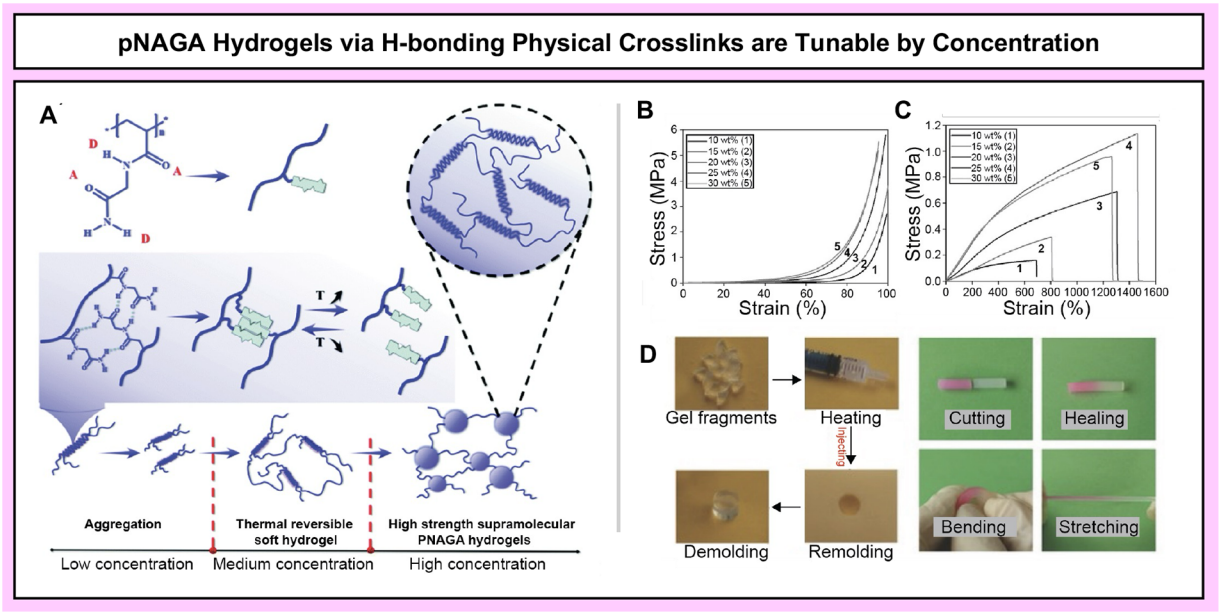

Figure 33. Left, A) Characterization of poly(NAGA) phase behavior across three concentration regimes, adapted from Xu et al., 2018 (ref 334, Copyright 2018 Royal Society of Chemistry). Versatility of poly(NAGA) as a thermoresponsive polymer. B) Tensile and C) compressive stress−strain curves for poly(NAGA) hydrogels as a function of polymer weight fraction, respectively. D). Self-healing and thermal processing of poly(NAGA) hydrogels prepared at (10 wt %). Characterization of poly(NAGA) phase behavior across three concentration regimes. B−D adapted with permission from Dai et al., 2015 (ref 335, Copyright 2015 John Wiley and Sons).

Approaching the toughness standard required for the next generation of hydrogels remains challenging with UCST-based assembly. Hydrogel architectures assembled by this pathway typically feature porous networks which limits the degree of energy dissipation across scales. The traditionally enthalpically mediated transitions also result in high strength polymer interactions with timescales that limit structural reorganization upon deformation, further limiting toughness. The success of poly(NAGA) hydrogels is an exemplary case demonstrating the applications of UCST driven hydrogel fabrication. Within the high concentration regime (∼10−30 wt %), its hydrogels display impressive mechanical behavior under tension and compression tailored by the density of hydrogen bonding within the network, *i.e.*, modulation of concentration (Figure 33, **A,B**).[434] The supramolecular nature of these networks also engenders a degree of self-healing (Figure 33, **C**) with up to 80% recovery of mechanical properties after reformation of hydrogen bonds at the fracture edge. Until recently, work in polymers with UCST behavior has been relatively limited which may describe the dearth of its application within hydrogel assembly. This may arise from a need for a broader scope of molecular structures displaying UCST type behavior which has remained challenging owing to the fundamental limitations of balancing the energy of polymer−polymer and polymer−solvent interactions and their scaling with temperature, with the relative water insolubility of poly(NASC) an exemplary case (Figure 22 for structural comparison and Sections 3.2.5 and 4.1.3 for further discussion). While current research efforts largely focus on expanding the scope of available structures exhibiting UCST behavior, it could be advantageous to consider how this assembly mechanism can be combined and/or modulated by other external stimuli. Additionally, the field would benefit from this broadened molecular scope as it would provide an area rich in polymer physics for further opportunities of nonequilibrium hydrogel assembly. For example, the phase diagram of polymers with a UCST can be altered by incorporating high T_g side chains which gives rise to interesting vitrification effects if quenched below a characteristic Bergham's point.[434]

4.1.2. Induced Crystallization. While the UCST driven assembly of hydrogels offers a thermal handle to modulate interpolymer interactions for hydrogel assembly, the toughness in these systems is typically limited by low fracture energies. Induced crystallization, driven by a reduction of thermal energy in specific macromolecular systems where the enthalpic benefits of ordered packing outweigh the entropic penalty, represents an alternative thermally induced assembly pathway for hydrogels with enhanced toughness. The crystalline domains resulting from induced crystallization are characterized as high functionality crosslinks (*e.g.*, incorporating >10 chains/crosslink), increasing the energy required for fracture per unit area.[38,104] This has enabled access to decoupled mechanical properties and extremely high values of fracture toughness comparable to that of biological tissues.[38,444] Moreover, the enthalpic and entropic contributions toward induced crystallization differ from UCST. Induced crystallization is typically characterized with much greater heats of transformation and reductions in configurational entropy during the sol−gel transition, which has implications for thermal stability and mass transport,[104,434] as will be discussed in Section 4.2.2.

A prominent synthetic example of hydrogels assembled by induced crystallization is PVA processed by freeze−thaw cycling or thermal annealing.[104,445,446] Notably, solutions of PVA above a critical concentration (∼30 wt %) are known to undergo spontaneous crystallization at room temperature potentially arising from random thermal fluctuations.[390] Freeze−thaw processing of PVA solutions, however, provides a thermo-temporal handle over crystallization by controlling the spatial organization of PVA chains resulting from phase separation during freezing.[390] During the freezing of PVA solutions (−20 °C), growing ice fronts expel PVA,

https://doi.org/10.1021/acs.chemrev.5c00466
Chem. Rev. XXXX, XXX, XXX−XXX

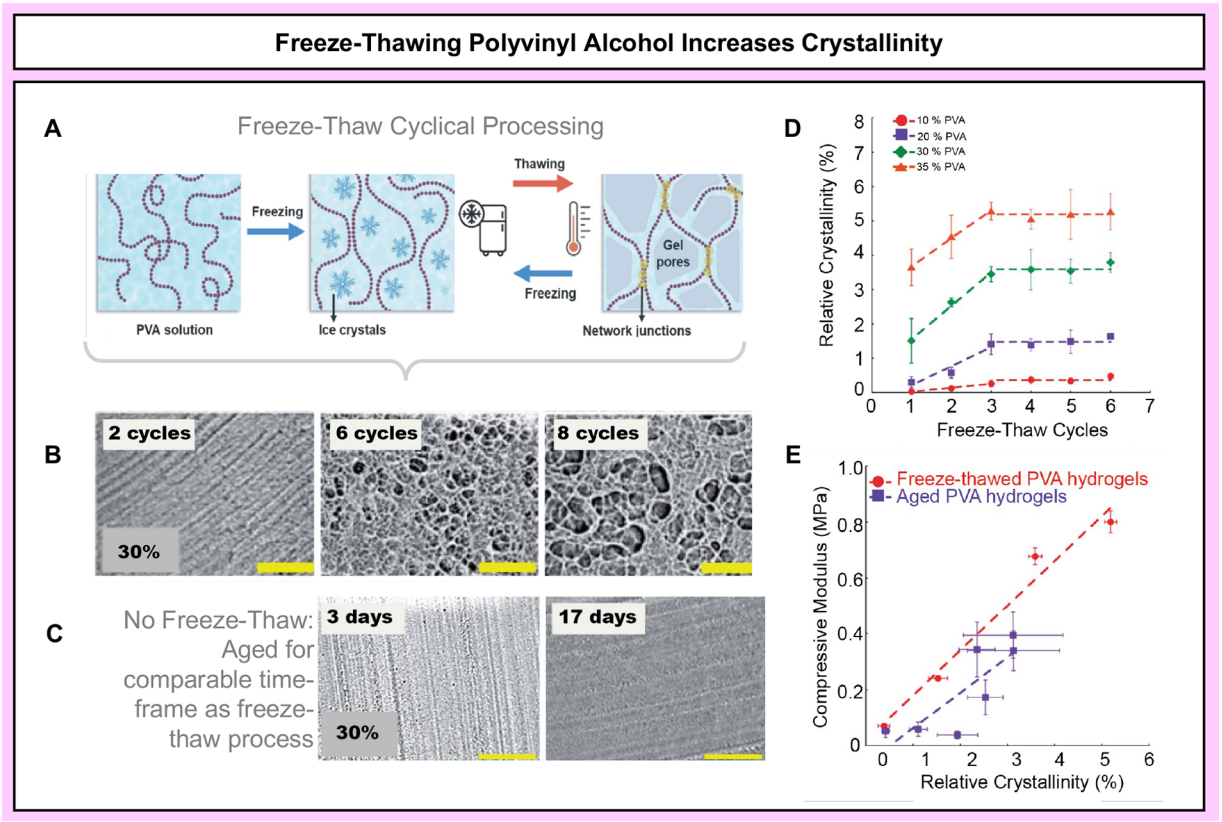

Figure 34. Freeze−thawing as a pathway to fabricate porous and tough hydrogels. A) Expulsion of solute from growing icefronts during freezing induces microphase separation and crystallization in PVA solutions. Reproduced with modifications from Adelnia et al., 2022 (ref 448, Copyright 2022 Elsevier). B) Freeze−thawing induces porous PVA microstructure formation as a result of phase separation which is not seen in C) aged hydrogels (scale bar = 80 μm) where D) degree of crystallinity in PVA hydrogels reaches a plateau after three cycles of freeze−thawing and increasing the weight fraction of PVA results in higher degrees of crystallinity owing to reduced interaxial distances of polymer chains. E) PVA hydrogels produced by freeze−thawing are characterized with higher moduli compared to aged hydrogels with similar degrees of crystallinity as a result of densification from phase separation. Adapted with permission from Holloway et al., 2013 (ref 390, Copyright 2013 Royal Society of Chemistry).

concentrating it in polymer rich domains wherein the reduced interaxial distance between polymers drives hydrogen bonding, inducing crystallization and thus physical crosslinking of the hydrogel (Figure 34, **A**).[447,448] Dissolution of amorphous PVA upon thawing results in swelling to a degree limited by the fraction of crystalline domains which can be increased by cycling the freeze−thaw process or increasing PVA concentration, resulting in a stronger, more crystalline hydrogel (Figure 34, **D**).[390,445] Thus, freeze−thaw cycling of PVA represents a fundamentally nonequilibrium hydrogel fabrication pathway as the structure and mechanical properties are a direct function of the time, temperature, and number of cycles used throughout fabrication. The results from Holloway et al.[390] beautifully demonstrate the impact of nonequilibrium processing on hydrogel architecture and mechanical properties by comparing freeze−thawed PVA hydrogels with those formed by aging. Phase separation occurring throughout freeze−thaw cycling results in porous networks whereas aged hydrogels are homogeneous. Additionally, this porous architecture results in PVA enriched domains which is hypothesized to enhance compressive modulus relative to aged samples with similar degrees of crystallinity. (Figure 34, **B**,**C**).[390]

Spatiotemporal control over the induced crystallization of PVA hydrogels has been realized via directional freezing and/or patterned annealing. This has broadened the programmability of structure and mechanical properties in these systems, which is crucial for biomedical applications such as synthetic tissue mimics or substrates for stem cell differentiation. Directional freezing of PVA solutions was developed as early as 2005 for the fabrication of oriented, porous PVA monoliths.[449] Simply accomplished by slow immersion of a specimen into a freezing bath, the oriented structures arise as a function of variations in ice growth rate during directional freezing resulting in diffusion of dissolved solute into interstitial areas for templated growth.[449−451] While this material was not applied as a hydrogel, it was recently demonstrated that the directional freezing process enhances the toughness of PVA hydrogels relative to those produced by freeze−thawing.[452] This is likely to arise from extrinsic toughening mechanisms, such as crack deflection, resulting from structural orientation. Recently, Lin et al.[104] realized patterned annealing post freeze−thawing for the enhancement of crystallinity in PVA hydrogels. This was demonstrated to increase fracture energy via enhanced crystallinity while maintaining a relatively soft modulus and high-water content for biological applications.

While robust, the applications of this process are limited by the relatively sparse array of competent polymer structures and processing methodologies to control crystallization in a spatiotemporally defined fashion. The codevelopment of

https://doi.org/10.1021/acs.chemrev.5c00466
Chem. Rev. XXXX, XXX, XXX−XXX

polymer functionality with processing methods could provide new opportunities in this area.

4.1.3. Solvent Swapping/Annealing. In analogy to using thermal energy to disrupt attractive polymer−polymer interactions, solvent choice can modulate the balance of cohesive polymer interactions and solvation. This is particularly advantageous relative to UCST because the range of polymer−solvent and polymer−polymer interactions is expanded, *i.e.*, stronger polymer−polymer interactions can be included in the final hydrogel. Literature reported examples commonly use the hydrogen bond accepting (HBA) propensity of DMSO to disrupt cohesive interpolymer hydrogen bonding for triggered assembly upon immersion in water. In this way, pregel solutions, *i.e.*, solutions of polymer in DMSO, characterized by extended polymer chain conformations can be subsequently kinetically trapped upon restoration of noncovalent interactions in an aqueous environment (Figure 35). This has resulted in hydrogels with enhanced toughness with a prominent example comprised by poly(NASC). The substitution of NH for the methylene spacer in NAGA results in a 2-fold enhancement of intermolecular interaction strength rendering polymers of NASC water insoluble.[453] The DMSO-to-water solvent-swap approach has facilitated its fabrication into highly stiff and tough hydrogels with fracture energies of ∼10 kJ m^{-2}. Similar approaches with PVA have demonstrated networks with homogeneity in crystalline domain distribution providing a 2-fold enhancement of fracture toughness relative to freeze−thawed hydrogels with similar water content.[454] Thus, solvent-exchange presents opportunities the fabrication of hydrogels with nonequilibrium network/microstructures. It would be interesting to consider how polymer conformation could be altered by external stimuli such as salt or temperature prior to solvent-exchange for the fabrication of hydrogels with a broader range of morphologies.

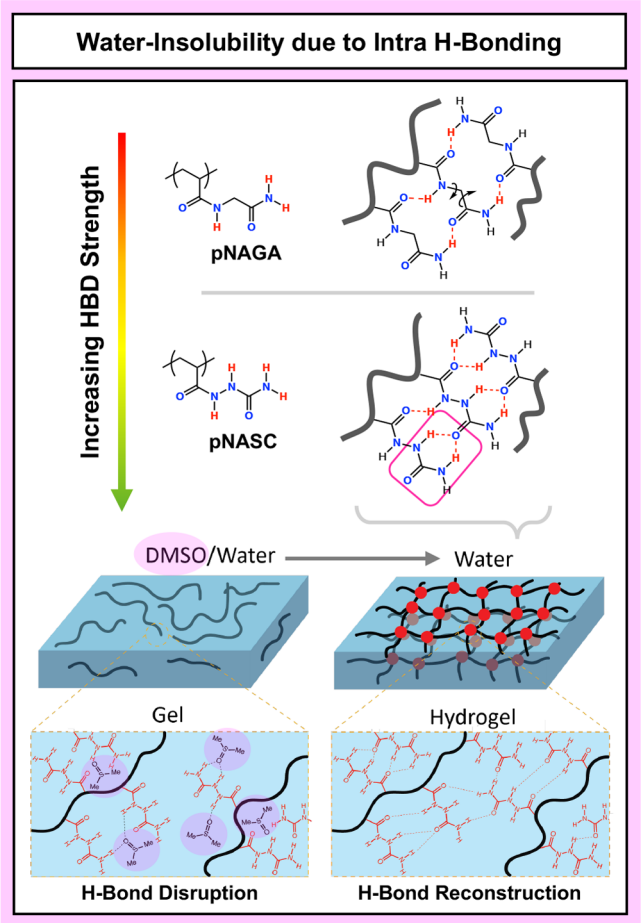

Figure 35. Ureido motif in poly(NASC) engenders increased hydrogen bonding strength resulting in water immiscibility. General strategy for the fabrication of poly(NASC) hydrogels follows polymerization in DMSO/Water mixture to reduce interpolymer interactions via enhanced hydrogen bond acceptance from solvent. Immersion of polymerized poly(NASC) organogels results in enhanced interpolymer interaction and phase separation driven by decreased propensity of hydrogen bond acceptance from solvent. Adapted from Fan et al., 2020 (ref 336, Copyright 2020 Royal Society of Chemistry).

Solvent swapping is also highly relevant for the self-assembly of nanostructured hydrogels of block copolymers, *i.e.*, polymers consisting of two or more incompatible sequences covalently bound together. In the melt, block copolymer nano morphology is driven by mixing entropy based on covalent attachment, and minor incompatibility between blocks results in microphase separation.[455] In aqueous solutions, this phase separation is achieved through ABA-type block copolymer architectures where A represents a hydrophobic segment and B a hydrophilic segment.[456] Such ABA-blocks favor microphase separation to minimize hydrophobe-water contacts and often resulting in characteristic micelle formation. Notably, above a critical concentration, microphase separation in micelles yields a physical hydrogel through entropically favored bridging interactions between the outer micelle layers that link the hydrophobic cores of adjacent micelles (Figure 36).[457−459] Bridging is entropically favored at higher concentrations as it relieves the crowding of polymer chains around the core.

Typically, to control assembly of block-polymer hydrogels, polymer solvation can be manipulated from a dually A-B compatible system via evaporation,[460] vapor-phase treatment,[461] or immersion[462] to yield an aqueous environment that drives selective solvation of each block. Thus, solvent-based assembly of block polymer hydrogels is traditionally an equilibrium-based process consisting of lengthy exchange. Lang et al.[457] marks a notable shift from this equilibrium perspective with the development of solvent−nonsolvent rapid injection for the preparation of nanostructured hydrogels. Utilizing a series of ABA block copolymers consisting of PEO midblocks with styrene (SOS), isoprene (IOI), or butadiene (BOB) end-blocks dissolved in tetrahydrofuran (THF) a range of hydrogels were fabricated via rapid injection into water (Figure 36). Interestingly, the resulting material was found to be dictated by the initial concentration of block copolymer, allowing Lang et al.[457] to develop universal design rules for the nonequilibrium processing of block copolymer hydrogels and providing a route to industrial scale fabrication. Block copolymer solutions were demonstrated to form hydrogels if the initial concentration was above the entanglement regime (c_e), determined by viscometry. Below c_e, rapid injection resulted in micelles and microgel formation denoting the dilute and semidilute regimes, respectively. Notably, the hydrogels produced from this pathway displayed a hierarchical structure consisting of nanoscale hydrophobic domains embedded in a cellular network composed of the hydrophilic bridges. Further, the properties of the hydrophobic core, dictated by choice of end-block, were shown to govern the mechanical properties of the hydrogels with glass end-blocks favoring enhanced fracture energy and strain at break. This work represents a hallmark for

https://doi.org/10.1021/acs.chemrev.5c00466
Chem. Rev. XXXX, XXX, XXX−XXX

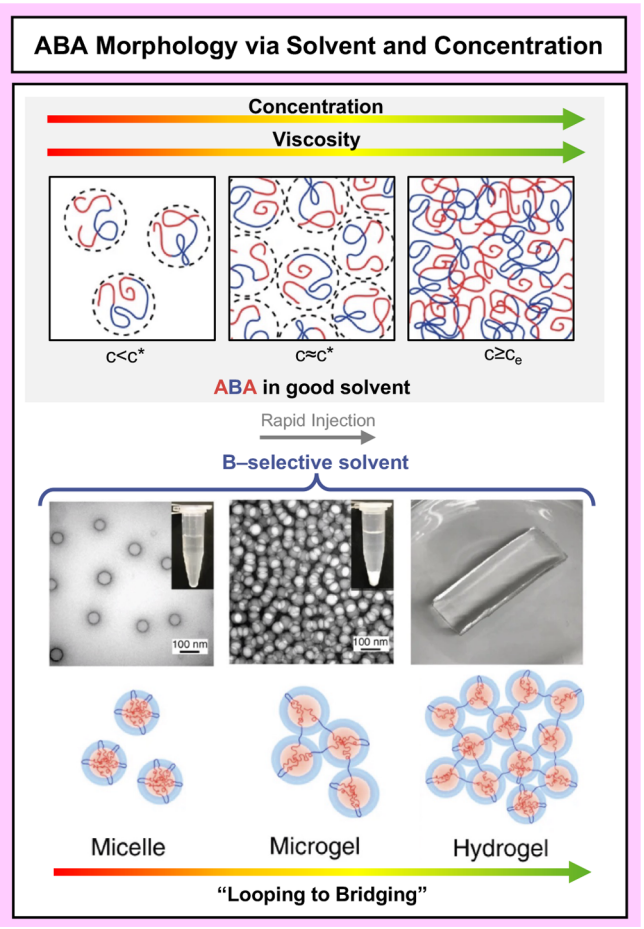

Figure 36. Rapid injection of ABA copolymers into B-selective solvent results in self-assembly into micellar structures. Triblock copolymer concentration dictates resulting material morphologies ranging from micellar solutions to microgels to hydrogels relating to the dilute, semidilute, and entanglement regimes, respectively. Adapted with modifications from Lang et al., 2019 (ref 456, Copyright 2019 Springer Nature).

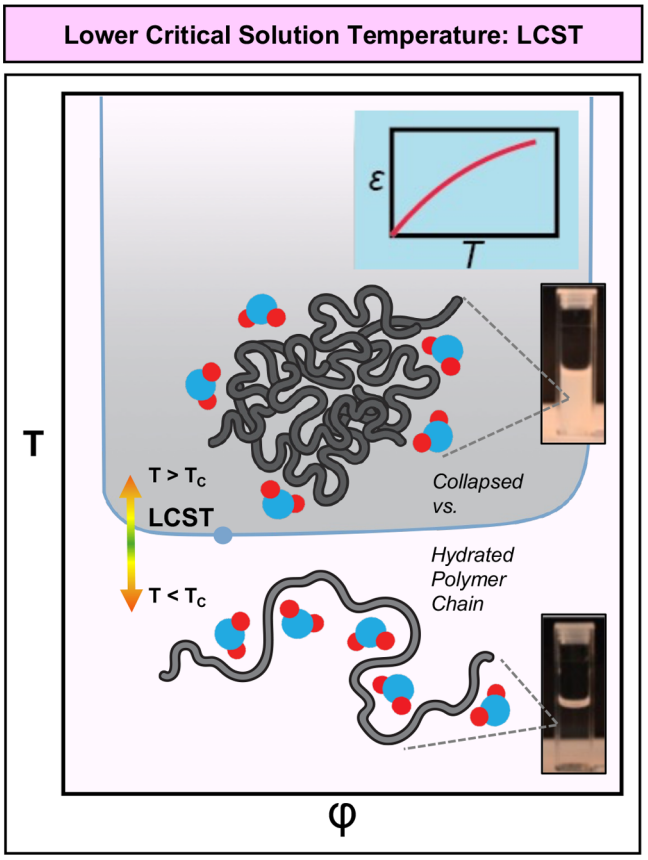

Figure 37. Phase diagram of binary solvent/polymer mixtures displaying LCST upon increase in temperature. Below LCST the system is in 1-phase, above the LCST interpolymer interaction favorability, denoted by ϵ, increases via disruption of weak solvation interactions resulting in demixing into 2-phases. Adapted with modifications from Lin et al., 2018 (ref 154, Copyright 2018 American Chemical Society) and de la Rosa et al., 2015 (ref 465, Copyright 2016 Elsevier).

the industrial production of nanostructured and functional hydrogels with potential applications in drug delivery, synthetic tissue development, and energy storage. However, the injection process inherently limits the dimensions and overall scope of assembling nonequilibrium hydrogel structures, with other analogous methods of triggering phase separation are required.

4.1.4. Lower Critical Solution Temperature. Lower critical solution temperature (LCST)-type phase behavior describes the phase separation of polymer solutions induced by an increase of thermal energy. The LCST thus represents the minimum temperature above which polymer solvation is energetically unfavorable[463−465] (Figure 37). In contrast to UCST and solvent-swapping driven phase separation, LCST transitions are entropically driven, arising from the entropically costly formation of organized solvation shells around polymer chains,[466] compared to entropically favorable free-rotation and translation of the solvent molecules once expelled from direct interaction with the polymer.

In the context of LCST, it is beneficial to analyze solvation as the formation of interactions between solvent and polymer (*e.g.*, hydrogen bonding, dipolar interactions, etc.) that are energetically more favorable than solvent−solvent interactions.[466−468] The molecular requisites for LCST-type transitions are polymer motifs with favorable polymer−solvent interactions shielded/enshrouded by motifs with unfavorable interactions that additionally require solvent ordering to be spatially accommodated. This imposed solvent ordering must be sufficiently small to enable solvation, but substantial enough to impose an entropic penalty. This structural parameter space provides a much broader scope for molecular design as opposed to UCST-type systems.[464] Thus, structures exhibiting an LCST are generally characterized with a degree of amphiphilicity providing favorable polymer−solvent interactions below a critical temperature.

A prominent example is poly(*N*-isopropylacrylamide) (PNIPAM), which features a hydrophobic isopropyl functional group coupled with a hydrophilic amide motif. Aqueous solutions of PNIPAM are reported to have an LCST of ∼32 °C, making it an attractive material for biomedical applications that require gelation upon contact with body temperature.[469−471] The characteristic isopropyl amide of PNIPAM mimics the structure of valine, a key motif in the hydrophobic domains of tropoelastin which comprises the elastic fibers in the connective tissues of vertebrates.

It is widely known that elastic fiber assembly is driven by the LCST induced phase separation of tropoelastin.[414,472] Critically, phase separation compartmentalizes tropoelastin into spherical droplets (∼2−6 μm) that undergo coalescence

https://doi.org/10.1021/acs.chemrev.5c00466
Chem. Rev. XXXX, XXX, XXX−XXX

and maturation into higher order fibers stabilized by crosslinking via lysyl oxidase (LOX).[414,473,474] The resulting elastic fibers endow a range of biological tissues with superior mechanical resiliency allowing for cyclic stress−relaxation on the order of a billion cycles in some tissues.[475] Further, single elastin fibers have displayed toughness values of up to almost 2 MJ m^{-3}.[476] Thus, LCST is vital for the biofabrication of elastic fibers with mutations to tropoelastin known to disrupt LCST-behavior having major implications in elastogenesis.[477,478]

Elastin-like peptides (ELPs) are a class of synthetic macromolecule designed to mimic the assembly of natural tropoelastin. Comprised of repeating units of Val-Pro-Gly-X_1-Gly (where X_1 is a residue other than proline), these macromolecular constructs offer programmability over LCST transition temperature by modulating the hydrophobicity of the X_1 residue.[479] As such, ELPs have been targeted for the development of synthetic tissues and have found success in mimicking the architecture and mechanical properties of elastic fibers when crosslinked via chemical,[480] enzymatic,[481] or photobased[482] processes. Recently, physical ELP networks have been realized by LCST-induced assembly above a critical weight fraction resulting in kinetically arrested phase separation.[483] This was attributed to impeded macromolecular dynamics from specific ELP sequences which were found to arrest macrophase separation into bicontinuous structures. Further, the mechanical properties of the resulting hydrogels could be tuned via hydrophobicity, rate of heating, and molecular weight providing hydrogels with moduli on the order of 1 MPa. Additionally, block copolymers of ELPs have been used for the fabrication of physically crosslinked biomimetic hydrogels. Silk-elastin-like-peptides (SELP)[484,485] are a notable example that display two-step assembly driven by micellization of silk domains at low temperature followed by LCST driven assembly of elastin domains. This has enabled the fabrication of SELP hydrogels with tunable architectures by controlling the ratio of silk to elastin-like domains (Figure 38).[485] The structural programmability in these systems demonstrates promise for the use of LCST-induced assembly in the architecting of tough hydrogels.

Poly(oligoethylene glycol[methyl ether][meth]acrylates) are an alternative class of polymers characterized by LCST-type behavior.[464,486−488] Notably, the pendant chain length is known to dictate LCST. As the number of ethylene glycol repeats increases, the polymer trends toward higher transition temperatures driven by enhanced polymer−solvent interactions via hydrogen bonding or dipolar interactions.[486,487] Additional parameters to tune LCST-type transitions include copolymerization,[489] ionic strength,[490,491] molecular weight,[492] concentration,[493] and pH.[494,495]

Recently, Zheng et al.[496] utilized a thermoresponsive tetrabutylphosphonium bromide electrolyte to induce LCST behavior in solutions of poly(2,2'-disulfonyl-4−4'-benzidine terephthalamide) (PBDT) (Figure 39, **A**) for the fabrication of thermoreversible fibrous hydrogels (Figure 39, **B**). Gelation and architecture were shown to be dictated by the rigidity of PBDT, characterized by a persistence length of 1 μm as driven by a double-helical conformation.[497] The lack of conformational freedom in this system engendered a three-step gelation characterized by nucleation and growth of branched aggregates resulting in a dense and fibrillar network structure (Figure 39, **B**). LCST was demonstrated to be tuned by the identity of the quaternary alkylphosphonium counterion where butyl side chains provided an optimized balance of hydrophobicity

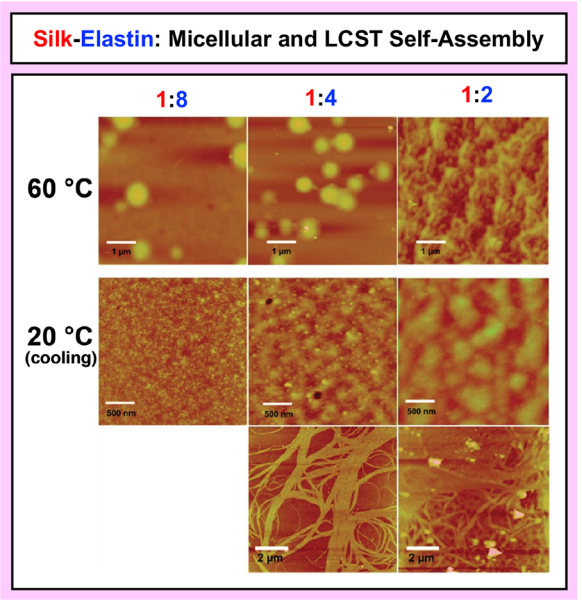

Figure 38. Tunable structures of SELP as a function of silk-to-elastin ratio upon heating (60 °C) and cooling (20 °C) characterized by atomic force microscopy (AFM). Ratios at top of image correspond to silk:elastin ratio. As fraction of silk increases, structures trend to fibrillar morphologies hypothesized to arise from crosslinking of silk domains. Adapted with permission from Xia et al., 2011 (ref 485, Copyright 2011 American Chemical Society).

inducing thermally driven electrostatic interactions at ∼45 °C via hydrophobic collapse of the cation side chains. Interestingly, tetrabutylammonium counterions lack this thermal response owing to enhanced hydrophilicity requiring longer alkyl chains to induce LCST behavior. Rapid gelation, afforded by the rigid structure of PBDT, enabled these formulations to be applied as aerosols for the coating of heated, inert substrates with applications in fire suppression and antibacterial coatings[496] (Figure 39, **C**).

4.2. Ion and pH Induced Assembly Pathways

Macromolecular solvation is profoundly impacted by the presence of analytes such as ions or acids and bases. The addition or removal of these species modulates the physicochemical properties of macromolecular solutions (*i.e.*, zeta potential, interfacial tension), offering dynamic control over solvation. In this way, ions and pH can be used to elicit the assembly of hydrogels into a variety of architectures spanning from porous synthetic hydrogels to fibrillar biomaterials.

4.2.1. Ion Specific Effects. Macromolecular solubility can be enhanced (salting-in) or reduced (salting-out) according to trends in specific ion effects (SIE), which have been well tabulated in the characteristic Hofmeister series. Salting-out is generally observed upon the addition of kosmotropic ions to macromolecular solutions, which has been attributed to the polarization of water interacting with hydrophilic segments on the polymer chain (See Section 3.2.3 for further discussion). This has been correlated with ion hydration entropy (ΔS_{hyd}), providing an entropic driving force for desolvation rooted in the gain of ion and water configurational entropy upon macromolecular association.[288,498,499] Kosmotropic ions have thus been utilized to shift the favorability of polymer−water interactions for the assembly of hydrogels via manipulation of LCST or UCST to lower or higher temperatures, respectively,

https://doi.org/10.1021/acs.chemrev.5c00466
Chem. Rev. XXXX, XXX, XXX−XXX

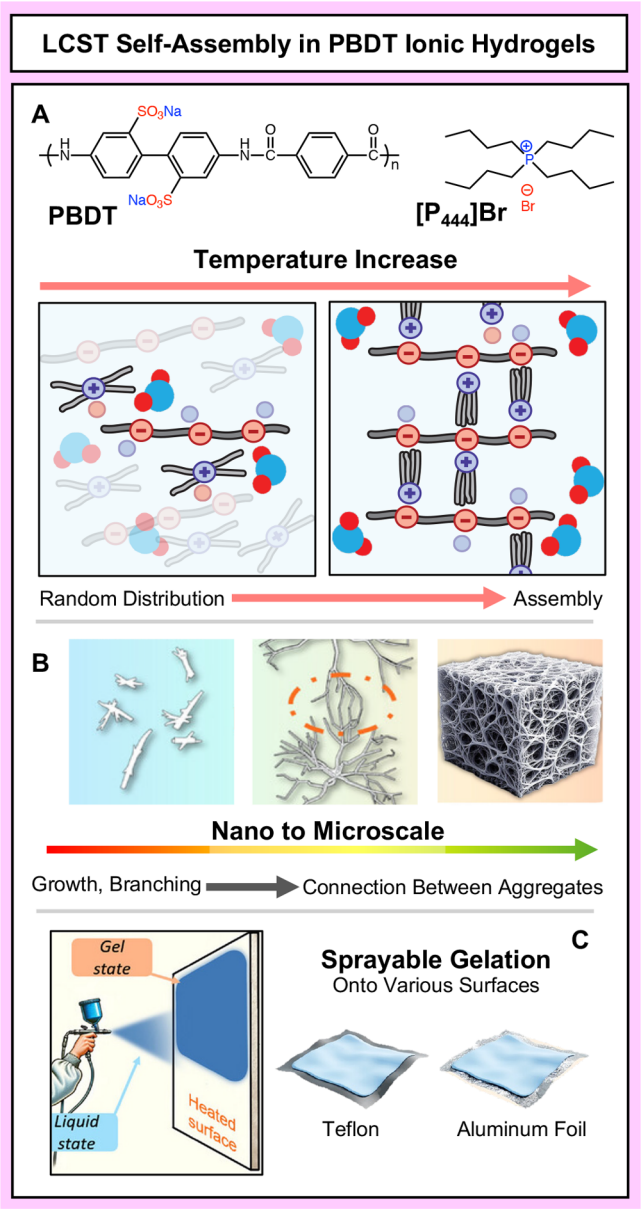

Figure 39. A) Temperature induced collapse of tetrabutylphosphonium cation side chains induces hydrophobic transition for assembly of PBDT via electrostatic interactions. B) Mechanism of gelation in PBDT phosphonium cation systems. C) Sprayable formulations of PBDT/phosphonium cations applied on heated substrates induces rapid gelation for coating inert substrates. Reproduced with modifications from Zheng et al., 2025 (ref 496, Copyright 2025 John Wiley and Sons).

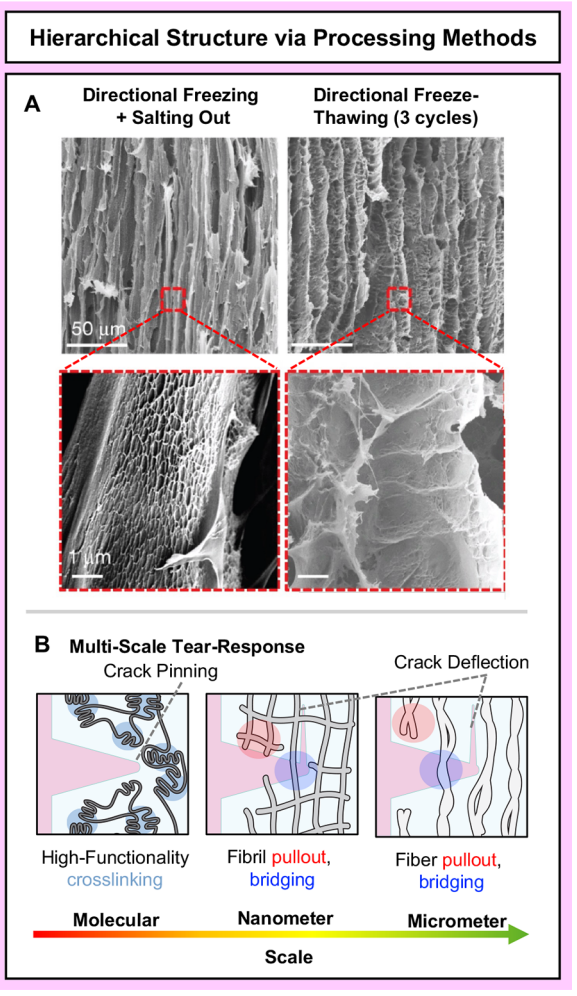

Figure 40. A) Microstructures of directionally freeze–thawed PVA hydrogels with (left) and without (right) salting-out. (Left) Salting-out post directional freeze–thawing provides hierarchical hydrogels resulting from densification of PVA. (Right) Directionally freeze–thawed hydrogels are characterized with oriented porous structures that lack nanoscale structuring (top scale bar = 50 μm, bottom scale bar = 1 μm. B) Hypothesized modes of multiscale energy dissipation resulting from hierarchical structures. Reproduced with modifications from Hua et al., 2021 (ref 452, Copyright 2021 Springer Nature).

or for the modification of aggregation state during freeze–thawing.[452,500] Manipulation in this way enables access to a broader window of hydrogel processing parameters as salting-out via kosmotropic ions should apply across polymer systems.

Hua et al.[452] marks a notable example of salting-out in conjunction with directional freeze–thawing for the fabrication of hierarchical PVA hydrogels with high toughness (~175 MJ m^{-3}). Structure of the obtained hydrogels was dictated by a synergy of directional freeze–thawing providing a porous PVA gel template that underwent further crystallization induced aggregation to yield a nanofibrillar network driven by salting-out with trivalent citrate (Figure 40, **A, left**). Interestingly, PVA hydrogels fabricated from directional freeze–thawing without treatment with citrate resulted in oriented porous networks that lacked fibrillar structures (Figure 40, **A, right**). The hierarchical structuring resulting from directional freeze–thawing in conjunction with salting out was demonstrated to enhance toughness via multiscale energy dissipation encompassed by crack deflection and bridging at the micro- to nanoscale and crack pinning by crystalline crosslinks (Figure 40, **B**). This fabrication pathway was further adapted to gelatin and alginate hydrogels, which also displayed similar hierarchical architectures and enhanced toughness.

Comparatively, chaotropic ions generally enhance the solubility of macromolecules via binding to nonpolar polymer interfaces resulting in enhanced hydrophilicity or electrostatic repulsion from an increased zeta-potential.[501] Isothermal titration calorimetry (ITC) has elucidated the driving force for chaotropic association to nonpolar interfaces to be enthalpic, arising from the reformation of the hydrogen bonded structure of water upon desolvation.[502] This

https://doi.org/10.1021/acs.chemrev.5c00466
Chem. Rev. XXXX, XXX, XXX−XXX

phenomenon has been more broadly recognized as a distinct supramolecular assembly motif, referred to as the chaotropic effect, which has been utilized in the construction of hierarchical supramolecular complexes and general soft matter engineering.[501]

There has been increasing interest in the utilization of nanoions, such as polyoxometalates and boron clusters, as chaotropic species for the assembly of hydrogels. The charge densities of nanoions are unprecedentedly low owing to delocalization across the ∼1 nm sized anions, engendering what has been described as superchaotropic behavior. A prominent example was demonstrated by Hohenschutz et al.[503] in the assembly of cellulose ether (CE) hydrogels with the polyoxometalate nanoanion, $SiW_{12}O_{40}^{-4}$, (SiW). Gelation was shown to be a balance between electrostatic repulsion and aggregation that was dictated by SiW concentration. Intermediate concentrations engendered electrostatic repulsion between CE chains from SiW adsorption to the neutral backbone. Further increase of SiW concentration screens the electrostatic repulsion and drives gelation via hydrophobic association. This is an exciting area of research as network formation via nanoion association enables the incorporation of additional functionalities such as catalysis and energy storage.[504]

Notably, these ion−polymer interaction motifs are specifically for neutral macromolecules. Biological and synthetic charged polymers, or polyelectrolytes, have been documented to show a reversion in SIE trends hypothesized to arise from direct ion−ion interactions which are dictated by the hydration enthalpy mismatch of the ion pair. Initially proposed by Collins,[292] the law of matching water affinities (LMWA) provides the basis for understanding ion pairing in aqueous solutions; contact ion pairs are formed when ions share similar hydration enthalpies whereas solvent separated ion pairs are favored when there is a hydration enthalpy mismatch. Progress in LMWA has demonstrated that these trends are also applicable in organic solvents, shifting the perspective of governance by hydration enthalpy to affinities being governed by likeness of ion size.[505]

Aubrecht et al.[265] utilized these trends for the programmable assembly of cationic polyelectrolytes containing tetraalkylammonium motifs. Mixing with sodium salts of varying anion identity resulted in a range of architectures spanning fluid coacervates to rubber-like solids (Figure 41). Mechanical properties of crosslinked hydrogels comprised of these polyelectrolytes were also shown to follow a reversed Hofmeister effect providing stiffer hydrogels as chaotropicity of the anion increased, hypothesized to result from tighter ion pairing with the tetraalkylammonium cation, typically characterized as chaotropic.[506]

4.2.2. pH Induced Assembly. Macromolecules containing weakly acidic or basic side chains are susceptible to modulations in solvation energy as a function of pH.[507] Such macromolecules, deemed pH-responsive, undergo changes in ionization state in response to variations in pH which can enhance or reduce solubility. Generally, increased charge density, resulting from ionization of side chains, enhances solvation via electrostatic repulsion between polymer chains favoring polymer−solvent interactions. Comparatively, decreased charge density, resulting from deionization, reduces solubility from the enthalpic incentive of favorable intermolecular interactions (*e.g.*, hydrogen bonding) between polymer chains. In this way, pH can be utilized as a handle to

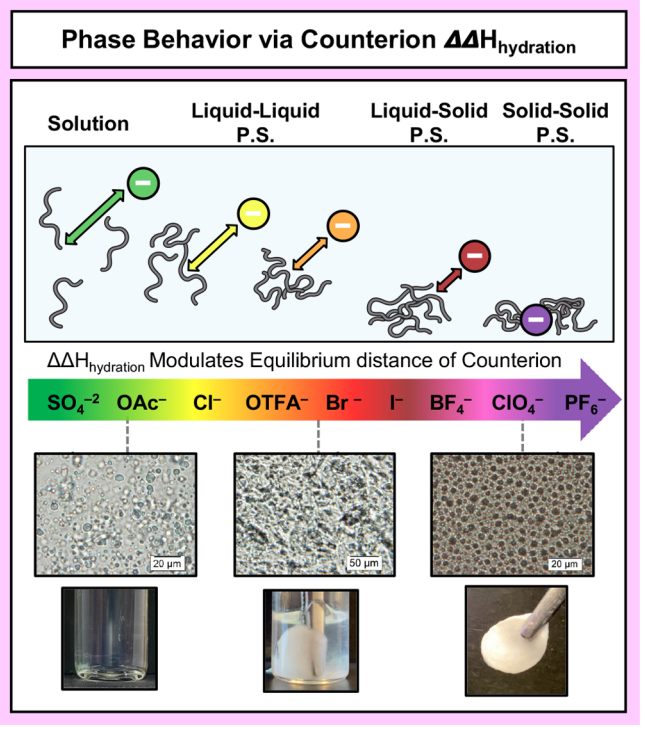

Figure 41. Phase behavior of polycationic structure is dictated by enthalpy of hydration mismatch between tetraalkylammonium cation and added anion. Large differences in hydration enthalpy between ions results in large equilibration distances favoring fluid-like phase behavior (left). As enthalpy of hydration mismatch trends toward smaller values equilibration distance of the ion is reduced resulting in gel behavior from enhanced interpolymer interactions. Small hydration enthalpy mismatch results in tight ion pairing driving the formation of cohesive solids with micellar structures. Adapted from Aubrecht et al., 2024 (ref 265, Copyright 2024 John Wiley and Sons).

dynamically control the spatial organization of macromolecules via modulation of attractive/repulsive interactions, ultimately enabling the triggered assembly of hydrogels.

A prominent example of the pH induced assembly of hydrogels is found in the treatment of polysaccharide solutions with acids or bases. Such biomacromolecules are rich in hydroxyl, carboxyl, and amino motifs, enabling triggerable protonation/deprotonation events for pH induced assembly. Cellulose nanofibers have been assembled into micro- and nanoporous hydrogels via immersion in sodium hydroxide (NaOH) solutions.[508,509] Gelation was attributed to the disruption of intramolecular hydrogen bonding upon immersion in NaOH resulting in conversion of cellulose's crystal structure, *e.g.*, mercerization, forming interdigitated crystalline crosslinks between nanofibers that are trapped upon neutralization.[509−512]

Chitosan (CS), a deacetylation product of chitin, has also been demonstrated to undergo pH induced assembly via the controlled diffusion of hydroxide (OH^-) into CS solutions[513,514] (Figure 42, **A**). Interestingly, hydrogels produced from this pathway are characterized with layered structures resulting from a Liesegang ring phenomenon which arises when the diffusion of small molecule reagents (*e.g.*, NaOH) is coupled with precipitation/gelation, thus affording the spatiotemporal assembly of nonequilibrium structures[515] (Figure 42, **B**). The work of Nie et al.[514] elucidated that CS concentration and rate of OH^- diffusion could be used to

https://doi.org/10.1021/acs.chemrev.5c00466
Chem. Rev. XXXX, XXX, XXX−XXX

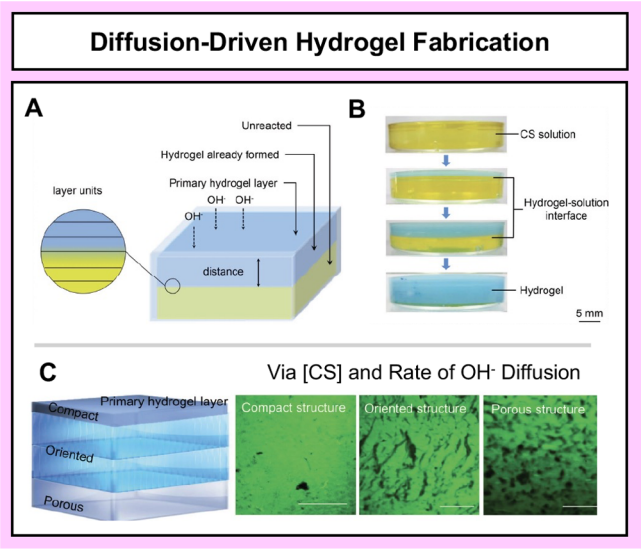

Figure 42. Fabrication of chitosan hydrogels by treatment with sodium hydroxide. A) General scheme of hydrogel fabrication by directional diffusion of hydroxide. B) Progression of hydrogel development as a function of hydroxide diffusion time. C) Blue regions correspond to methylene blue tagged chitosan in the gel phase. Adapted with permission from Nie et al., 2015 (ref 514, Copyright 2015 Springer Nature).

afford orientation within the layered structures of CS hydrogels (Figure 42, **C**). It was demonstrated that CS concentrations above the entanglement regime impeded macromolecular relaxation between layers resulting in oriented structures dictated by the direction of OH^- diffusion. Complexation of metal cations with the amino and hydroxyl motifs of CS has also been realized as a pathway to modulate network structure.[516] The complexation of high affinity metals (*e.g.*, Cu^{2+}), prior to treatment with NaOH, induces contraction of CS, driving disentanglement that engendered the formation of multilayered structures via enhanced mobility at the gelation front. Comparatively, complexation with low affinity metals (*e.g.*, Ca^{2+}) resulted in unaltered structures.[516] This is interesting as the incorporation of metals enables the fabrication of inorganic hydrogel composites via precipitation of metal cations in basic solution, providing a pathway toward the multiscale composite structures found in nature, such as bone or nacre, which are characterized by excellent damage tolerance.

Alternative load-bearing soft biological materials, such as ligaments and tendon, are generally characterized with excellent toughness hypothesized to arise from the crystalline structures comprising these materials.[104] The toughness of such materials has been mimicked, for example, by the crystalline crosslinks characteristic of PVA hydrogels[390,447] (Section 4.1.2), however, achieving similar degrees of hydration typical of soft tissues remains a challenge. Recently, Huang et al.[517] realized a deprotonation-complexation-protonation approach (Figure 43, **A**) for the fabrication of PVA hydrogels that display high equilibrium water content (EWC) while maintaining the excellent fracture energies characteristic of PVA systems. Controlling the nucleation of crystallites via ion-complexation in basic PVA solutions

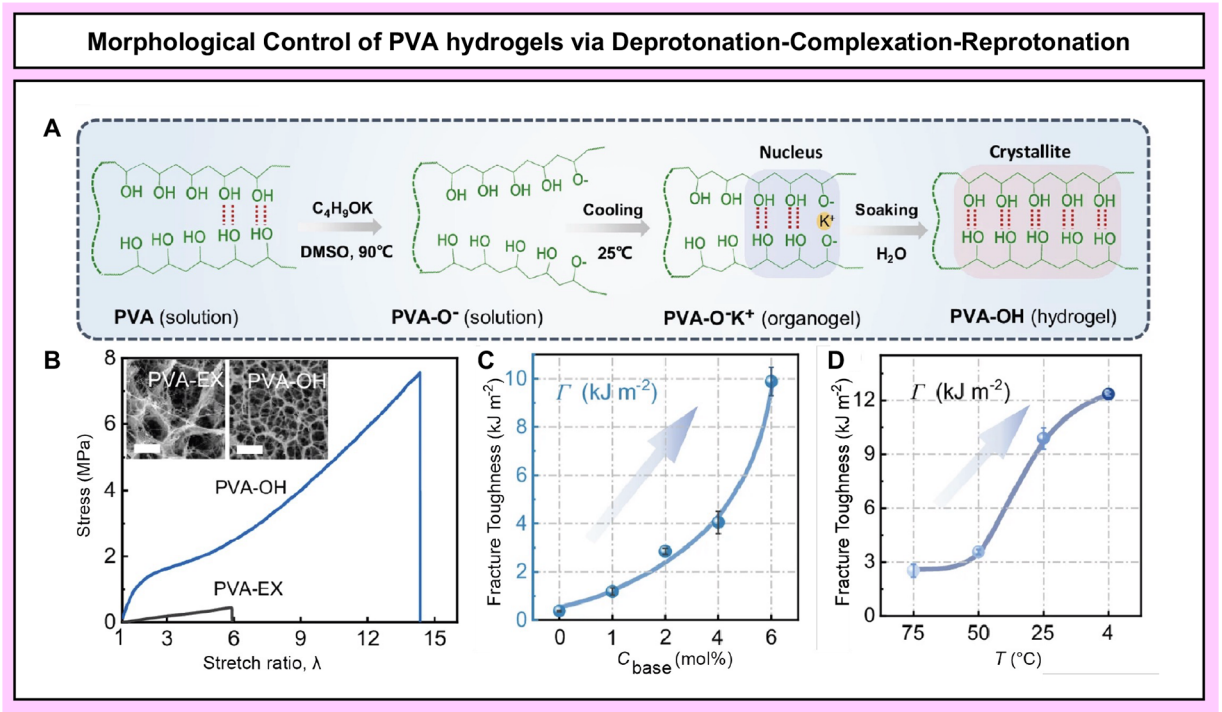

Figure 43. A) Pathway to control crystal morphology in PVA hydrogels via deprotonation-complexation-reprotonation (DCR) approach. B) Representative stress−strain curves and microstructural characterization of PVA hydrogels obtained via DCR approach (PVA−OH) and solvent exchange (PVA-EX) (scale bar = 2 μm). C) Fracture toughness of PVA−OH as a function of potassium t-butoxide concentration. Increased basicity results in higher toughness engendered by an increase of nucleation sites providing denser crystalline morphologies. D) Fracture toughness of PVA−OH as a function of complexation temperature. Toughness increases upon a decrease of complexation temperature as a result of denser nucleation. Adapted with permission from Huang et al., 2024 (ref 517, Copyright 2024 Springer Nature).

https://doi.org/10.1021/acs.chemrev.5c00466
Chem. Rev. XXXX, XXX, XXX−XXX

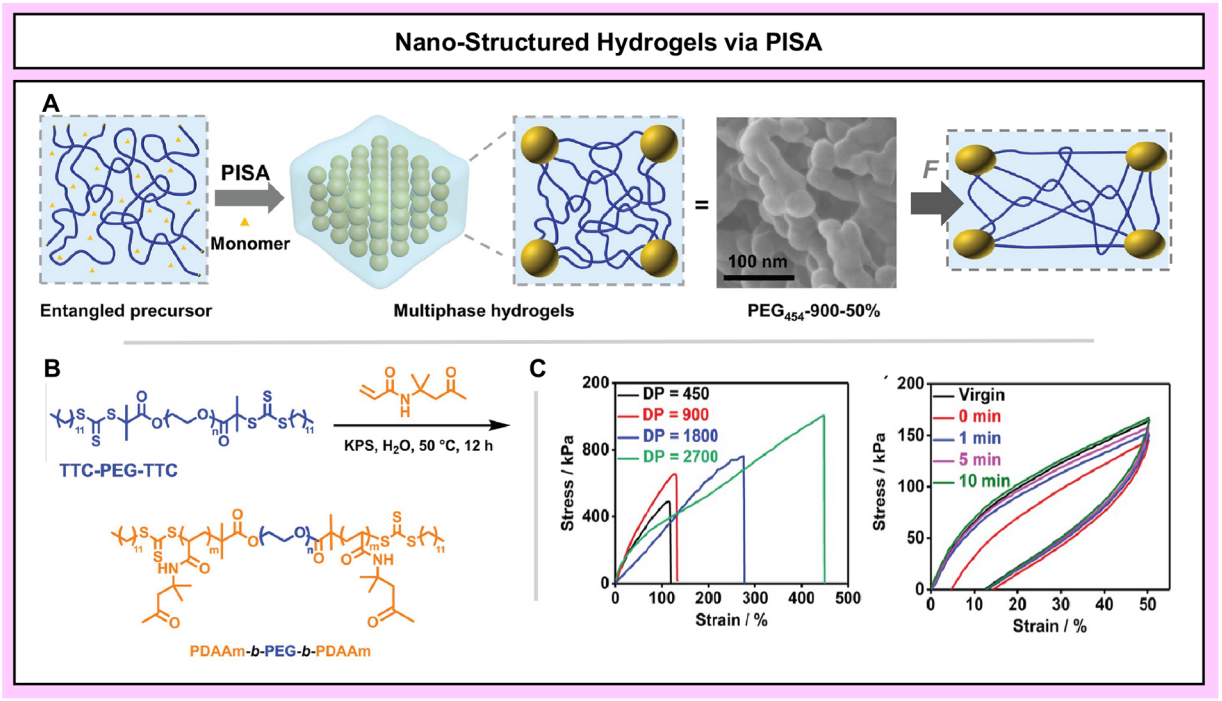

Figure 44. A) General pathway to nanostructured hydrogels produced by PISA. Predicted mechanism of energy distribution via hydrophilic midblock and dissipation via rupture of hydrophobic cores. B) PISA formulations for fabrication of nanostructured hydrogels. C) Representative stress−strain curves of PDAAm-*b*-PEG-*b*-PDAAm hydrogels as a function of PDAAm degree of polymerization (hydrogels produced at a solids content of 50 wt % and constant PEG degree of polymerization of 454). Recovery of hydrogels as a function of rest-time in between cycles. Adapted from Zeng et al., 2023 (ref 519, Copyright 2023 John Wiley and Sons).

allowed homogeneous distribution of crosslinks throughout the network which were trapped upon immersion in aqueous environments. In this way, volume shrinkage is limited via a reduction in configurational entropy from precrosslinked PVA chains prior to crystal growth providing access to enhanced EWC. Additionally, this system displays excellent fracture toughness (12.4 kJ m^{-2}) via enhanced energy distribution and dissipation engendered by homogeneity in crystal domain spacing and enhanced interchain hydrogen bonding relative to solvent-exchange or annealed PVA hydrogels (Figure 43, **B**). Moreover, the mechanical properties and architecture of the obtained hydrogels were governed by the concentration of base and temperature during complexation, underscoring that this approach as a highly programmable pathway toward the fabrication of tough hydrogels with programmable structures (Figure 43, **C, D**).

4.3. Polymerization-Induced Assembly

Polymerization induced self-assembly (PISA) has been a more recent pathway for the construction of strong and tough hydrogels with architectures defined at the nanometer length scale.[518,519] PISA can be conducted in a range of solvents with a wide range of monomer identities; however, this discussion will be limited to aqueous systems. For aqueous PISA, a macroinitiator is chain extended with a hydrophobic monomer, thus triggering assembly into nano-objects above a critical degree of polymerization to minimize hydrophobe-water contact.[520−523] Notably, this monomer is carefully selected to be soluble or dispersible, with the resulting homopolymer characterized by limited solubility in water. The resulting morphology of aggregates produced via PISA are dictated by a balance of minimizing interfacial and interaction energy while maximizing configurational entropy, analogous to block copolymer assembly.[455,524−526] Generally, the morphology can be predicted by

$$p = v/al \tag{10}$$

where p represents the molecular packing parameter, v the volume of the hydrophobic block, a the interfacial area between hydrophilic/hydrophobic blocks, and l the chain length of the hydrophobic block.[527,528] In practice, tuning morphology is generally achieved by varying the hydrophobic monomer feed ratio (*e.g.*, impacting the hydrophobic block length), changing molecular structure, or utilizing external stimuli such as pH, salt, or temperature to tune the interfacial interactions between the hydrophilic/hydrophilic blocks.

Recently, work from the Huo group has realized the fabrication of tough hydrogels via the construction of multiphase networks driven by aqueous PISA[519] (Figure 44, **A**). A prominent example utilized a bifunctional PEG-based macro-chain transfer agent (CTA) extended by hydrophobic diacetone acrylamide (DAAm) to yield a BAB triblock copolymer[519] (Figure 44, **B**). Systematic investigation via SAXS, SEM, and tensile testing elucidated the dependence of weight percent and hydrophilic and hydrophobic chain length on the architecture and mechanical properties of the resulting PISA formulations. PISA above a critical weight fraction (*i.e.*, solids content) (∼30 wt %) resulted in nanostructured hydrogels consisting of spherical micellar nanodomains comprised by hydrophobic DAAm blocks bridged by hydrophilic PEG. These results are consistent with prior work in hydrogels fabricated from triblock copolymers which predicts network formation via physical entanglements if the polymer concentration is above a threshold entanglement concentration.[457] Obtained hydrogels were characterized with architectures and mechanical properties dependent on both

https://doi.org/10.1021/acs.chemrev.5c00466
Chem. Rev. XXXX, XXX, XXX−XXX

hydrophilic and hydrophobic chain length, underscoring the tunability of this assembly pathway (Figure 44, **C, left**). The fracture toughness of obtained hydrogels reached fracture energies as high as 14 kJ m^{-2} comparable, if not exceeding, current work in hydrogel fabrication from triblock copolymers.[519] Further, cyclic tensile testing revealed architecture dependent energy dissipation via the distribution and reversible or irreversible dissipation of stress from the hydrophilic PEG bridges and hydrophobic micellar domains, respectively (Figure 44, **C, right**). While PISA driven hydrogel fabrication may be in its infancy, it is reasonable to expect that through strategic chemical design of noncovalent interactions between copolymer blocks,[518] PISA will contribute significant advances in the development of tough hydrogels with programmable architectures.

Polymerization induced microphase separation (PIMS) is an alternative polymerization induced assembly pathway that has recently gained attention for the fabrication of hydrogels with programmable architectures. The theoretical basis for PIMS is well described by Flory–Huggins theory[435,437] wherein the molecular weight dependence of the interaction parameter, χ, provides a driving force for demixing once a polymer reaches a critical degree of polymerization.[529,530] Examples of PIMS for the fabrication of polymeric materials typically focused on nonaqueous systems, however, there has recently been renewed interest for the fabrication of hydrogels.

Recently, Dudaryeva et al.[531] realized the application of PIMS for the assembly of hydrogels with tunable porosity by tuning the polymerization kinetics in PEG-based thiol–ene systems. Cross-linking star-based PEG decorated with norbornene utilizing dithiothreitol (DTT) in the presence of dextran (DEX) (exclusion agent) resulted in the formation of porous hydrogels. Control over hydrogel morphology was achieved by varying UV light intensity which is well-known to dictate polymerization kinetics in thiol–ene systems.[532] Fundamentally, Dudaryeva et al. demonstrated that porosity in this system was a competition between two different timescales: percolation and phase separation. Reduction of polymerization kinetics, achieved by a low irradiation intensity, allows the timescale of phase separation to outcompete percolation, resulting in a microporous hydrogel with relatively large pore sizes (~70 μm) while increasing polymerization kinetics results in a hydrogel with relatively smaller pores (~10 μm) (Figure 45). More broadly, Dudaryeva et al. elucidated general design rules for the fabrication of hydrogels with tunable porosity by developing scaling laws based on the timescale of polymer-rich domain diffusion (τ_{pd}) and merging (τ_m) during spinodal decomposition. These timescales are dictated by parameters such as polymerization kinetics (dictating the crosslinking density and thus τ_m) as well as solution viscosity (dictating polymer diffusion and thus τ_{pd}) providing a general handle over hydrogel porosity. More recently, PIMS/PISA formulations have been translated to additive manufacturing.[533−536] This has elucidated the multiscale engineering of bulk gel-like materials with nano- to mesoscale structuring mediated by PIMS/PISA and macroscale structure governed by the additive manufacturing process. In this way, access to the multiscale programming of material properties such as toughness, strength, and stiffness should be enabled for the fabrication of multifunctional hydrogels.

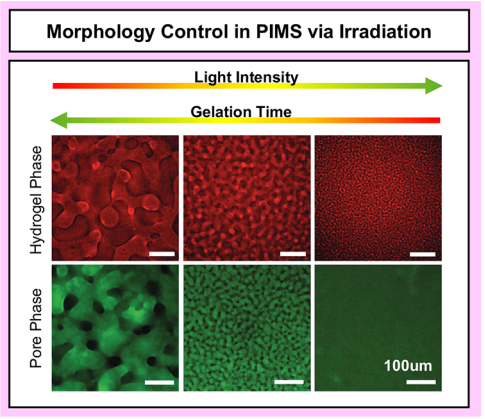

Figure 45. UV intensity dictates polymerization kinetics in PEG-based thiol–ene systems for fabrication of tunable bicontinuous structures (Red phase = PEG, green phase = dextran, scale bar = 100 μm). Adapted with permission from Dudaryeva et al., 2025 (ref 531, Copyright 2025 John Wiley and Sons).

4.4. Host–Guest interactions

Host–Guest interactions are a broad class of supramolecular interactions defined by a cooperative and dynamic combination of noncovalent forces between distinct complementary molecular species attracted to each other by hydrophobic interactions, van der Waals forces, ionic interactions, or other weak physical bonds.[537,538] Materials that utilize host–guest attractions in their design typically demonstrate high reversibility and responsiveness, enabled by macromolecular structures that react to external stimuli like temperature, pH, light, and mechanical force.[539−541] This programmability enables the assembly of advanced structures with applications in drug delivery, adaptive materials, self-healing systems, and molecular machines (Figure 46).[542]

For many macrocyclic host–guest systems involving small-molecule guests, equilibrium binding constants span from millisecond timescale dissociation to ultrahigh-affinity such that complex remains stable for hours or longer.[543] This broad kinetic window underscores the programmability of host–guest lifetime and stability and offers opportunities to design supramolecular materials with tailored dynamics, from transient and highly dynamic, to long-lived, kinetically persistent architectures through tuning entropic and enthalpic contributions of each component on the host–guest pairing. As such, when these interactions are utilized to connect polymer chains or multifunctional monomers in crosslinked networks, they are particularly notable for their reversible and self-healing properties, the noncovalent crosslinks can break and rearrange under applied force, then reform, enabling the material to enhance toughness and recover from mechanical damage.[544,545]

Common examples of host–guest systems driven by hydrophobic association include cyclodextrins and pillararrene, while cucurbiturils or calixarenes form via hydrogen bonding and polar interactions(Figure 47, **A**).[546−548] Crown ethers are another popular motif which utilize ion-dipole and electrostatic interactions that invite cations (Figure 47, **B**).[549,550] Other existing systems use π-π stacking or charge-transfer interactions (Figure 47, **C**),[547] and even shape complementarity such as dendrimer-like designs that maximizes van der Waals contacts.[551]

https://doi.org/10.1021/acs.chemrev.5c00466
Chem. Rev. XXXX, XXX, XXX−XXX

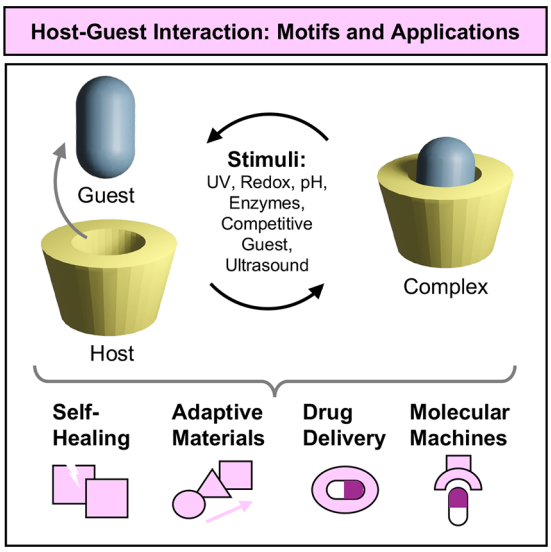

Figure 46. Schematic representation of a stimulus-responsive host–guest system and its multifunctional applications. A dynamic host–guest interaction framework, where supramolecular assembly is driven or reversed by diverse external inputs such as UV light, pH, redox changes, or biomolecular signals. These reversible interactions underpin diverse functionalities including controlled drug delivery (left), cargo release and reuptake (bottom left), energy harvesting or dissipation (top right), and signal transduction or molecular switching in materials (bottom right).

Host–guest interactions are an effective and well-studied approach for enhancing the toughness of supramolecular polymer gels via the precise tuning of material dynamic timescales. The resulting materials can efficiently dissipate mechanical energy while maintaining structural integrity by combining short-timescale dynamic bonds (host–guest interactions) with long-timescale interactions (*e.g.*, covalent).[49] A notable example includes slide-ring gels, in which polyrotaxane-based crosslinkers allow topological sliding of ring-shaped molecules along a polymer backbone. These crosslinkes are referred to as a "figure-of-eight" given the putative dimeric structure of the linked polyrotaxanes. This mobility enables stress redistribution and energy dissipation without bond scission, exemplified by cyclodextrin-threaded poly(ethylene glycol) systems that display both high stretchability and toughness.[552] Prospects for the improvement of toughness likely center on further developing these interactions as stimuli-triggerable assembly motifs to precisely architect network structure at both mesoscopic and macroscopic length scales. This would require the development of more sophisticated synthetic methods involving higher order polymer topologies, such as bottlebrush or comb polymers in conjunction with precisely tailored polymer network connectivity. Together, these provide latent opportunities for enhanced precision in controlling mechanical properties via structure and material timescales. Furthermore, the integration of theoretical and experimental methodologies will facilitate the forecasting and actualization of innovative topologies,[553] thereby offering a comprehensive toolkit for the development of supramolecular polymer gels with exceptional mechanical properties and functional responsiveness.

4.5. Topological Impacts on Assembly and Properties

While the manipulation of noncovalent interactions broadly underpins assembly mechanics and timescales, the spatial

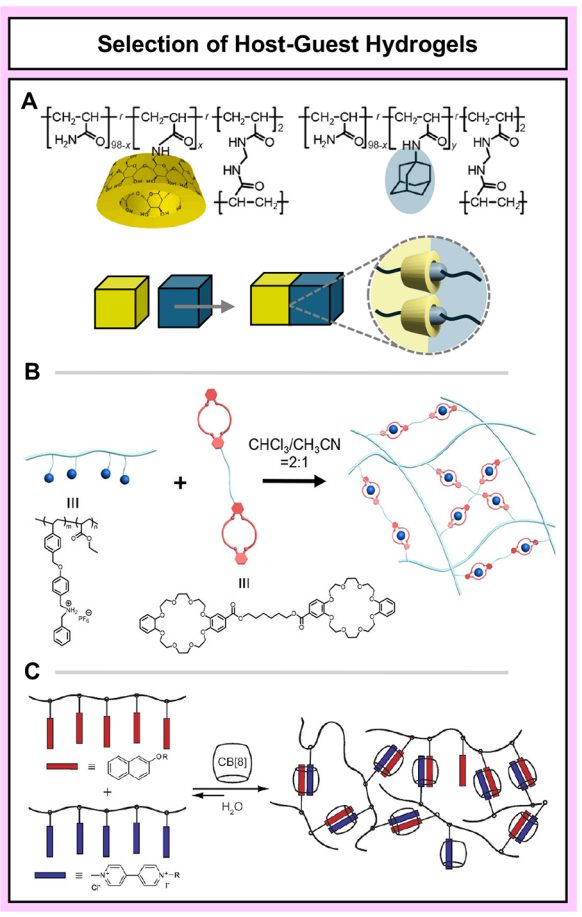

Figure 47. Representative examples of supramolecular hydrogel formation via host–guest interactions. A) Schematic of a polymer functionalized with β-cyclodextrin (host) and adamantane (guest) units enabling reversible crosslinking through host–guest complexation. A xerogel matrix illustrating the progressive formation of inclusion complexes between host–guest in the self-healing capability. Reproduced with modifications from Kakuta et al., 2015 (ref 546, Copyright 2015 American Chemical Society). B) Formation of a supramolecular polymer network via threading of linear polymers with macrocyclic hosts through noncovalent interactions. Reproduced from Xia et al. 2020 (ref 550, Copyright 2020 American Chemical Society). C) Assembly of hydrogels based on cucurbit[8]uril (CB[8])-mediated ternary complexation of electron-rich and electron-deficient aromatic guests appended to polymer chains in aqueous media. Reproduced from Appel et al., 2010 (ref 547, Copyright 2010 American Chemical Society).

organization of these interactions, *i.e.*, polymer architectural features such as size and topology, are a significant means to modulate their material properties. The resulting spatial confinement reshapes the energetic landscape by creating kinetic and entropic barriers as well as energetic incentives to drive macroscale formation and assembly into structures that enhance toughness as well as strength. Copolymerization is a classic method of controlling molecular interactions by templating the covalent combination, thereby independently or synergistically driving higher-order polymer organization and assembly. Moreover, block copolymer structures, as discussed previously in Sections 4.1.3 and 3.3 on solvent swapping and polymerization induced self-assembly, enable a larger scale spatial enforcement of functional group presentation and enable the assembly of unique nano- and micro-

https://doi.org/10.1021/acs.chemrev.5c00466
Chem. Rev. XXXX, XXX, XXX–XXX

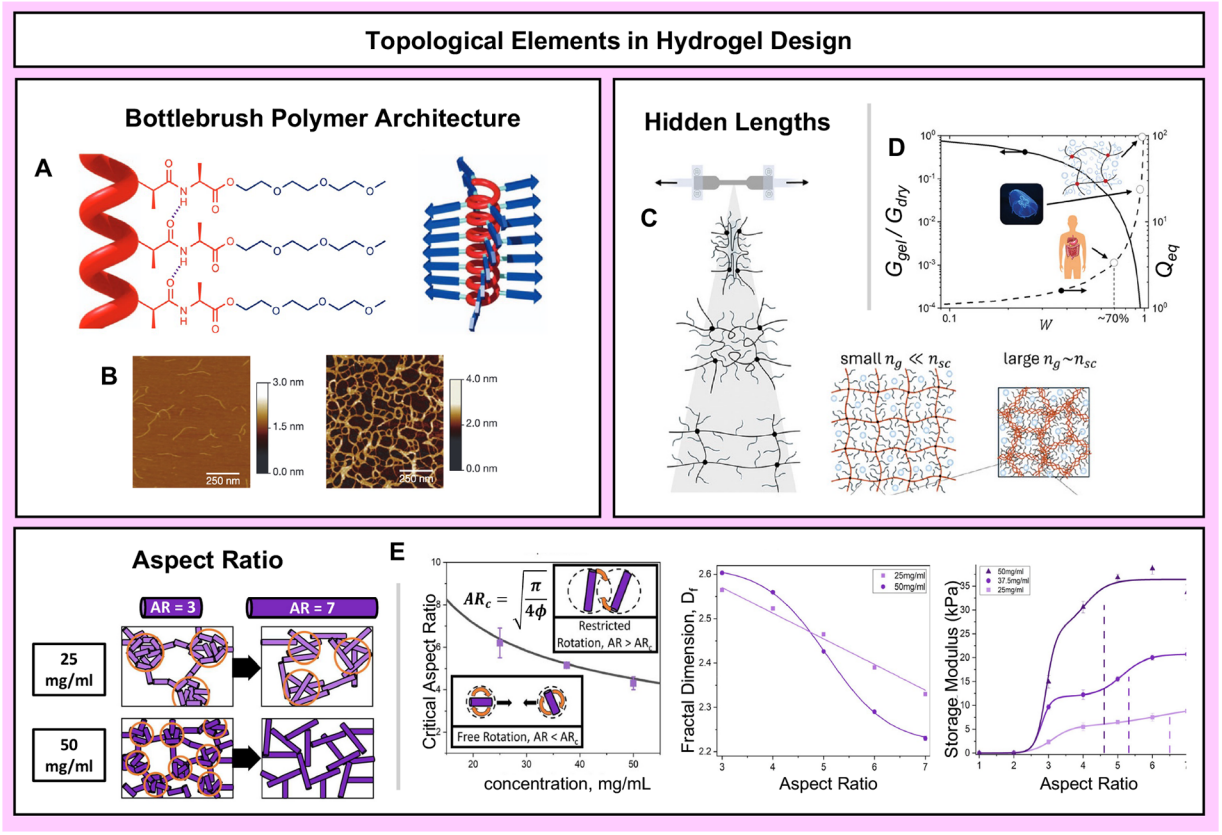

Figure 48. A) Representation of a stiff helical polyisocyanide backbone stabilized with the hydrogen-bonded dialanyl groups and ethylene glycol peptide substituent 'tails', represented in blue. B) AFM image of isolated polymer chains (*left*), and a 'monolayer' of bundles of the polymer gel (*right*) transferred to mica. Figure A,B and caption reproduced with modifications from Kouwer et al., 2013 (ref 562, Copyright 2013 Springer Nature). C) Unraveling of hidden length reservoirs during stretching (*top*), and phase separation of hydrophobic backbone from hydrophilic side chains in water during stretching (*bottom*). D) Relative gel modulus (left) and Equilibrium swelling ratio (*right*) versus water content. At small n_g, or high grafting density, phase separation may occur within the backbones of independent network strands, while at large n_g, multistrand aggregation may occur. Figure C, D and caption reproduced with modifications from Wang et al., 2024 (ref 391, Copyright 2024 John Wiley and Sons). E) Schematic representation of structural changes as building block AR is increased while at a constant concentration, critical aspect ratio (at which rod-like polyproteins can no longer freely rotate in solution) as a function of polyprotein concentration in solution (*left graph*), extracted fractal dimension of hydrogels as a function of building block AR at protein concentrations (*middle graph*), and the storage modulus of hydrogels as a function of building block AR at varying polyprotein concentrations, where solid lines show fits using a double sigmoidal fit, and dashed lines show the extracted ARc points for each protein concentration (*right graph*). Figure and caption adapted with permission from Hughes et al., 2023 (ref 563, Copyright 2023 Springer Nature).

structures. In this way, control over molecular connectivity controls the timescale and dynamic requirements of hierarchical assembly.

The development of robust and simple living-like polymerization strategies, *e.g.*, ATRP, RAFT, and ROMP, has rendered structurally complex graft polymers such as combs and bottlebrush polymers (BBP) readily accessible and has catalyzed a surge in sophisticated hydrogel design with unique topologies.[554] Comb polymers have been recently demonstrated to decouple stiffness and extensibility, while the unique characteristics of bottlebrush polymers, namely low entanglement at high molecular weights, enables ultrasoftness and tissue-like strain stiffening behavior.[555−560] As an alternative to linear polymers, and via discrete avenues of inter- and intramolecular interactions not possible in the former, these macromolecular constructs offer biologically relevant physical models of network interaction, most often contributing entropic incentives for assembly by virtue of preferential solvent exclusion within the BBP framework.

For example, an elegantly simple copolymerization of small molecule monomers and macromonomers creates a covalently linked, brush-like network that folds to create hidden, extensible lengths which endow the network with tissue-like strain-stiffening[391] (Figure 48, **C,D**). In other examples, BBP hydrogels are made with LCST-sensitive PEG or PNIPAM side chain constituents to use temperature as a trigger on the ultimate topology as tuned by relationship between the identity and length of the side chains and backbone.[561] With numerous stimuli, there forms a hierarchy of entropically driven processes, first by which solvent exclusion within the side chains then creates larger order structures controlled by the species rotational and translational diffusion and entanglement behavior.

Kouwer et al. 2013[562] marks an early example of the power of a BBP-like copolymer design, distinguished for creating synthetic strain-stiffening tissue-like hydrogel networks (Figure 48, **A**). With a rigid and chiral polyisocyanopeptide (PIC) core polymer decorated with a PEG outer shell, or "brush'"-like substituents, the LCST behavior of PEG is harnessed to promote thermal gelation, while topology controls bundling of the network. The length of the 'backbone' defines network formation: reducing backbone lengths results in precipitated

https://doi.org/10.1021/acs.chemrev.5c00466
Chem. Rev. XXXX, XXX, XXX−XXX

polymer aggregates at the LCST. Critically, increasing the backbone lengths results in gel formation via kinetically trapping the entropically favored network formed upon LCST due to the longer chains being trapped in the network structure before their precipitation. Aspects of this assembly process are beginning to be isolated and explored in other biologically relevant contexts, for example Hughes et al. specifically examine how the aspect ratio of rod-like polymeric building blocks defines network architecture and mechanics, based on the rotational and translational diffusion requirements during network formation. Mechanical rigidity increases as the polymers increase in aspect ratio and reduce their ability to rotate freely and instead favors maximizing solvent entropy; the topology of the network changes from fractal-like clusters driven by rotational diffusion in the macromolecule to homogeneous and interconnected segments driven by translational diffusion as a function of concentration given a critical aspect ratio[563] (Figure 48, **E**).

In the work of Kouwer et al. the nature of the PIC backbone limits itself to a constant bundle thickness due to the chiral backbone design; despite that this allows for a mesh size as a direct function of concentration, it ultimately limits hierarchical assembly of the system.[562] While able to form structures with tissue-like mechanics, this framework is missing the ability to dissipate substantial amounts of mechanical energy.

Regarding stimuli-response, current developments in BBP architecture are helping to overcome the limitations in network design. Many stimuli-responsive hydrogels are formed by the assembly of linear block copolymers, wherein one or more units demonstrate LCST behavior and gel assembly can either proceed through physical entanglements or micellar structure periodicity. However, while there is much versatility in these systems, they often suffer from high concentrations of polymer required for gelation, as well as gel syneresis (the expulsion of water upon collapse).[564] Conversely, the BBP architecture alone is not necessarily enough to drive the formation of a sol–gel transition, where solution phase anisotropic ordering is observed with PNIPAM brushes in the work of Li et al., yet the highly turbid systems are prevented from forming networks due to systemic inhomogeneity from aggregation and a lack of precise bonding interactions.[565] Instead, incorporating BBP architecture in combination with block copolymerization techniques allows for high control over network mesh size and stimuli response. For example Vohidov et al. report hydrophobic PLA, hydrophilic PEG, and LCST PNIPAM ABC triblock brush copolymers, which can form hydrogels at biological temperatures for sustained drug delivery at low critical micelle concentrations and high tunability based on each block identity.[566]

Additionally, the unique property modulation that arises from the BBP topology has been explored in numerous contexts.[567−569] In one example particularly relevant to tailoring the properties of hydrogels, Deng et al. demonstrate the impact of the bottlebrush architecture in promoting zwitterion-interaction of the side chains resulting in UCST behavior. This was attributed to the conformational restriction created by the dense topology of the bottlebrush and is not observed in linear analogs.[570] As researchers continue to elucidate topology specific properties, there have been clear advancements in the ability to correlate BBP molecular features such as grafting density, side chain length, and distance between sites of self-interaction, with hierarchically developed material properties, such as the slope of strain-stiffening and soft-to-hard transition[571,572] (Figure 49, **A**).

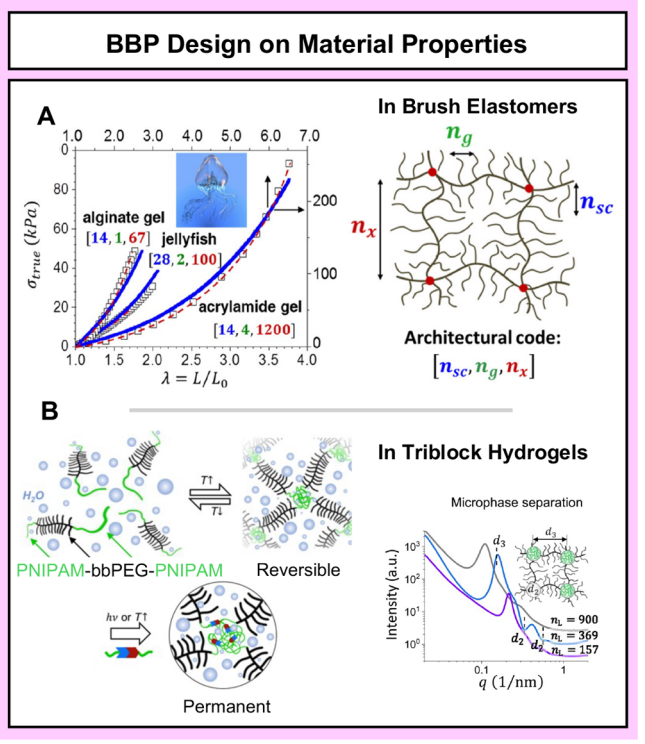

Figure 49. A) Stress–strain data for alginate gel, jellyfish tissue, and poly(acrylamide-*co*-urethane) gel are shown together with curves for PDMS bottlebrush and comb with the corresponding architectural triplets [nsc, ng, nx] (left) and where covalent network architecture is defined by degrees of polymerization (DP) of side chains (nsc), backbone spacer between side chains (ng), and backbone between two crosslink junctions (nx) (right); Figure and caption reproduced with modifications from Sheiko et al., 2019 (ref 571, Copyright 2019 American Chemical Society). B) Linear-bottlebrush-linear(LBL) triblock copolymers with linear PNIPAM and bottlebrush PEG blocks form a homogeneous solution in water at 25 °C. Upon heating above LCST, gelation occurs. LBL hydrogels can be either dissociated through network cooling or permanently crosslinked by reactive monomeric units purposely incorporated within L-blocks (left), where 1D SAXS curves of selected LBLs show PNIPAM domain size increases with nL and the dashed lines mark the minima of the sphere form factor (d2) and the interference peak (d3), related to the diameter and ordering of PNIPAM domains, respectively (right). Figure and caption reproduced with modifications from Vashahi et al., 2022 (ref 573, Copyright 2022 The American Association for the Advancement of Science).

These advancements in polymer design give rise to the current benchmark of topologically motivated biological hydrogel design. Materials such as injectable linear-BBP hydrogel networks made by Vashahi et al. have distinctly low solution viscosities due to low entanglement, strong microphase separation via the combination of linear and BBP scaffolds capable of sustaining high rates of deformation and preventing against gel syneresis, and can access strain stiffening response due to the composition of the brush network[573] (Figure 49, **B**).

While approaching the soft-to-hard material standards set by biological counterparts, there is still room for development in these materials, among which is the dynamicity of the system,

https://doi.org/10.1021/acs.chemrev.5c00466
Chem. Rev. XXXX, XXX, XXX−XXX

including stress relaxation and self-healing behaviors. Synthesis of aldehyde-imine dynamic covalent chemistries (DCvC) shown in linear copolymers demonstrates a tunable control over the material's viscoelastic profile in time as explored in Section 2.2,[574] yet these promising chemistries have not been deeply explored in their topography as the chemical development of such systems is lacking. Future materials may benefit from incorporating DCvCs into the advances made by molecular topology in the formation of tough hydrogel design and synthesis.

It is worth noting that topological association has been correlated with colloidal liquid crystalline (LC) transitions, *i.e.*, concentration triggered entropy-driven spontaneous ordering, which have been demonstrated to template the fibrillar structures found in a range of exceptionally robust biological materials.[406,414,575,576] A specific example, highlighted in work from the Harrington group, elucidated the importance of smectic LC phases in the fabrication of byssal threads, the adhesive fibers used by mussels for anchoring to the seafloor.[577] The requisite for such organization was demonstrated to be 2-fold; association of byssus core proteins (preCols) into hierarchical bundles provides sufficient rigidity to enable an LC transition via the entropic incentive of translational entropy gain upon solvent exclusion,[578,579] while a symmetric ABCBA primary sequence allows access to the high degree of order characteristic of a smectic phase.[577] Kinetic trapping is then driven by pH triggered metal coordination via terminal protein domains enriched in histidine resulting in a semicrystalline, tough, self-healing, and fibrillar core structure.[406,577]

The macroscale anisotropy characteristic of mussel byssus, among many other biological materials, engenders unprecedented energy distribution and dissipation.[416,580] As these structures are driven, in part, by colloidal LC assembly,[406,414] translation to synthetic hydrogels may offer opportunities for enhancing strength and toughness. However, current examples and chemistries are limited, typically focusing on chemically crosslinking LC phases of 1D[581,582] or 2D[583−585] nanomaterials which provide the topological requisite for LC transitions.[578] Development of novel pathways to access LC assembly in synthetic hydrogels will enable the spatial programming of hydrogel networks for enhanced mechanical and functional properties.

4.6. Mechanical Force Induced Network Formation and Structuring

As exemplified by biological structural materials, hydrogels and soft materials with anisotropic and hierarchical ordering enable the creation of exceptional materials from relatively ordinary macromolecules. While the macromolecular shape/topology provides a means for ordered assembly, another handle to create order within materials is shear force. In many biological materials, shear is used to induce anisotropy in the process of aligning nanomaterials and polymer chains for network formation.[406,586]

One of the most well-known natural shear-driven assembly phenomena is spider silk, which has long been a gold standard of material strength and toughness.[587] The silk production organ, known as the ampullate gland, acts as a flow reactor where pH and ion content are modified to induce phase separation and additional spatial constriction in the gland diameter creates shear induced assembly.[406,588] This process has inspired synthetic control over bulk solutions of polymer (Figure 50, **A, B**). These polymer systems are amenable to solidification and assemblies of polymer sheets by shear-induced interactions, tunable by the composition of the polymers (such as their capacity for hydrogen bonding, π-π and multivalent interactions),[589] as well as by the intensity and duration of shear force imparted on the system.[590] While the specific assembly mechanics of spider silk and its precursors continue to be further elucidated, advances in the knowledge of its building block constituents and modes of supramolecular interactions has shaped the development of the status quo for shear aligned self-assembled hydrogels.[591−593]

As described in the previous section, polymer topology can be a tool to access controlled self-assemblies via molecular anisotropy. However, these rod-like architectures can be challenging and inherently inaccessible to some materials without some specific input, *i.e.*, consider cellulose strands arranging into randomly coiled and unordered entangled networks via traditional gelation techniques. In fact, these hydrogels can be reprogrammed under shear force to reorient isotropic constituents to anisotropic networks without covalent chemical modification. Simple handles such as displacement during stretching and time during drying have been shown by Mredha et al. as powerful techniques to tune the design of superstructures and supramolecular interactions by using physical input to coordinate hydrogen bonding or other noncovalent IMF's for enthalpic gain and lasting material properties in complex biological materials such as cellulose and alginate[594] (Figure 50, **C**). Enhancements in hydrogen bonding density, afforded by extended chain conformations, resulted in a 2-fold increase in toughness relative to hydrogels fabricated via nontemplated driven assembly.

Typical supramolecular handles like ionic and hydrogen bonding (Hofmeister effect, etc.) can be utilized in tandem with shear-based alignment. In this way, a broader range of hydrogel architectures and mechanical properties are made available with further tunability enabled by the timing of shear as well as the order of operations. For example, Zhang et al.[595] tuned the entanglement density and aggregation state of PVA-carboxymethyl cellulose gels via a salting out approach post shear-processing, which resulted in two-orders of magnitude tunability in toughness (0.19−30.39 MJ m^{-3}). The anisotropic architectures coupled with a broad range of mechanical tunability should enable this assembly strategy to be utilized for synthetic tissue engineering.

These simple, physical modification pathways render a number of methods accessible to tune the inherent supramolecular interactions within a polymer system. For example, Qiao et al. systematically combine pressure and time via rate, loading, and duration to promote and even fine-tune the thermodynamically driven physical crosslinking of a PVA network.[596] PVA hydrogels with nanocrystalline domains have also been enhanced via mechanical training, which dramatically increased the fatigue threshold by aligning the crystalline domains into nanofibril structures. In 2019, Lin et al. reported the creation of muscle-like hydrogels which achieved a high fatigue threshold of 1,250 J m^{-2} and high ultimate tensile strength of 5.2 MPa, while maintaining a low elastic modulus of 0.2 MPa. The freeze−thaw process results in dendritic growth of ice crystals, which contribute to the formation of randomly oriented crystalline nanofibril structures. By repeated stretching of the gel (on the order of 1000 times), these regions can be aligned along the training axis, resulting in a dramatic increase in fracture toughness.[104] Considering the

https://doi.org/10.1021/acs.chemrev.5c00466
Chem. Rev. XXXX, XXX, XXX−XXX

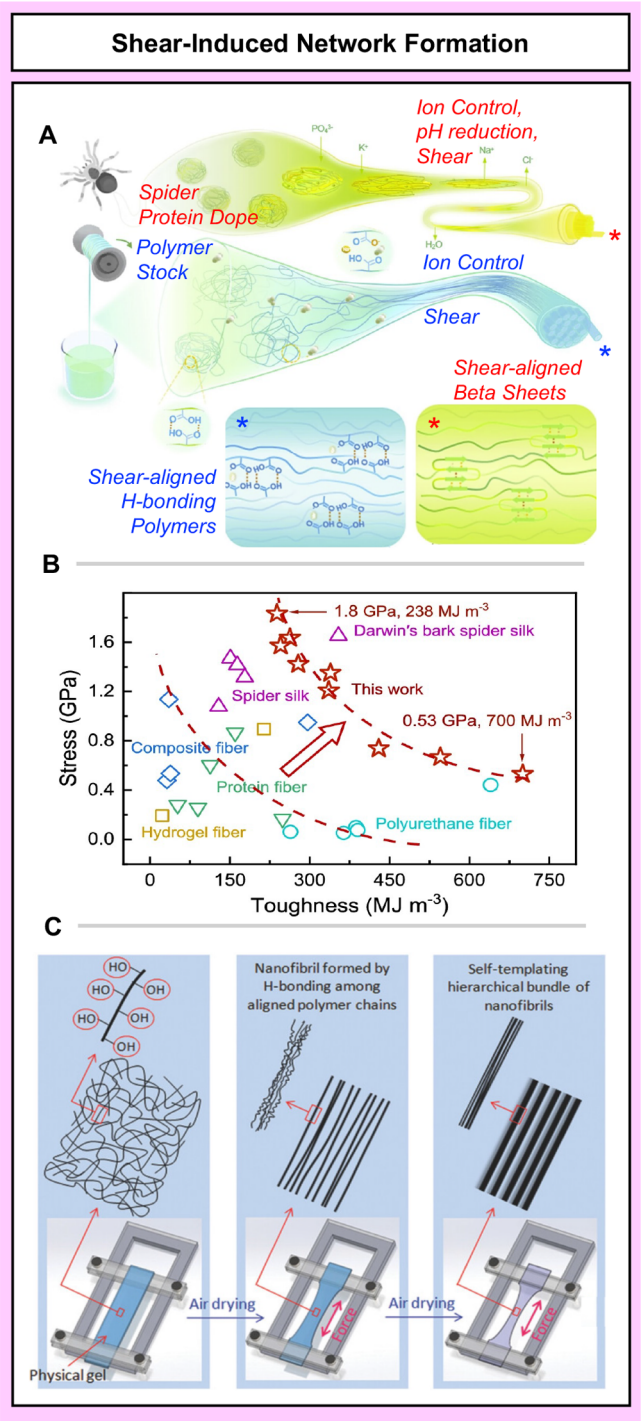

Figure 50. A) Schematic of the spinning of spider silk and the PAA fiber artificial spider silk system, where modulation of the nanofibrils of the PAA fiber can be achieved by tuning the polymer chain flexibility, and B) the breaking stress and toughness of the artificial spider silk fibers using PAA fiber can be compared with those of typical robust fiber materials reported in the literature. Figure and caption reproduced with modifications from He et al., 2024 (ref 588, Copyright 2024 Springer Nature). C) Schematic of drying in confined conditions method for creating aligned fibrous hydrogels with hierarchical superstructures. A rectangular piece of hydrogel with fiber-forming H-bonding sites is clamped to a sample holder. During air drying, the gel's width and thickness shrink and the gel experiences tension, which aligns the polymer chains in the length direction. Thin fibrils are formed along the tensile direction through H-bond formation as drying increases the concentration of polymer. Further drying induces aggregation of nanofibrils to form thick fibers and reswollen gels maintain their structure due to the formation of stable H-bonds. Figure and caption adapted from Mredha et al., 2018 (ref 594, Copyright 2018 John Wiley and Sons).

sheer number of number of dynamic bonding modalities, mechanical manipulation dramatically expands the opportunities to create toughening and strengthening network structures, overall offering more versatility to a given network composition.[597,598]

However, most shear aligned hydrogels are limited by scale as shear alignment is an intrinsically scale-dependent phenomenon. Along these lines, specimen uniformity poses a considerable challenge in scale-up. Additionally, the material compositions being tested with this strategy are often limited to biological materials such as cellulose and collagen,[599,600] and PVA.[594,596] As this field develops, the execution of shear force can be implemented in smarter processing designs such as flow-induced alignment,[601] which might increase the accessibility to underexplored chemical designs, motifs, and compositions.

4.7. Summary—Programming Hydrogel Assembly and Multiscale Structure via Manipulation of Dynamic Bonds

As discussed in Section 4, external stimuli (*i.e.*, salt, temperature, pH, mechanical force, solvent) provide a handle to dynamically regulate the energetics of polymer solvation for the triggered assembly of hydrogels. An exemplary system is represented by PVA which has been utilized as a framework for the stimuli-induced assembly of hydrogels with architectures ranging from porous gels to fibrous multiscale networks. Distilled concepts from these investigations suggest that synergy in hydrogel assembly is obtained with the conjoined application of stimuli which affords precision over the balance of solvation energy and configurational entropy for the fabrication of hydrogels with programmable structures. This is akin to the biofabrication of natural materials wherein the implementation of stimuli is used to dictate polymer dynamics for triggered liquid-to-solid transitions into multiscale energy dissipating structures.

We believe exciting areas of development for future advances in the assembly of tough hydrogels include a broader implementation of the dynamic bonding schemes discussed in Section 3 as well as their patterning across a variety of macromolecular topologies, *i.e.*, bottlebrush, comb, or star frameworks. This will provide greater programmability over the timescale of interpolymer interactions, as well as the driving force for assembly, enabling precision in bottom-up soft matter engineering. Additional stimuli that have demonstrated promise for the spatiotemporal assembly of hydrogels include light, magnetic and electric fields, which in combination enable programmable, multistimuli construction of high-order hydrogel architectures with enhanced toughness through dynamic force-dissipating interactions.

The next section focuses on the dynamic reconfiguration of hydrogel architecture as a function of applied external stimuli. This contrasts with hydrogel assembly as this reconfiguration occurs on already assembled hydrogel networks and therefore provides the opportunity to modulate hydrogel mechanics across time via thermodynamic and kinetic incentives. As will be discussed, this perspective of hydrogel remodeling will

https://doi.org/10.1021/acs.chemrev.5c00466
Chem. Rev. XXXX, XXX, XXX−XXX

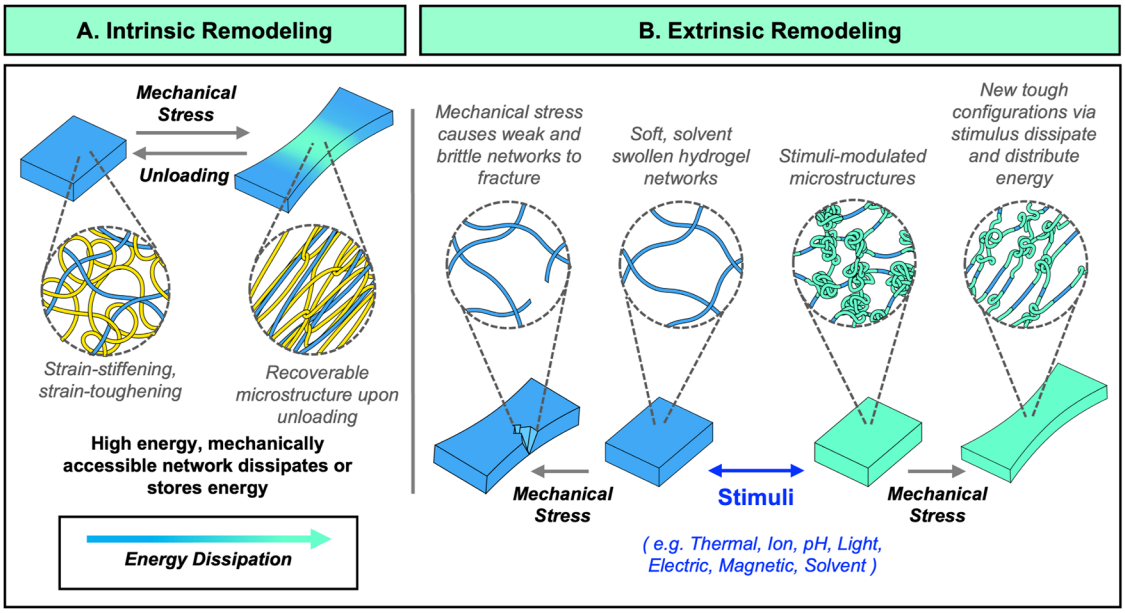

Figure 51. Diagrams illustrating A) the evolution of hydrogel microstructures before and during mechanical stress for intrinsic remodeling and B) before and after stimulus modulation and mechanical stress for extrinsic remodeling. During mechanical stimulus, hydrogels that undergo intrinsic remodeling access high-energy configurations that dissipate, distribute or store mechanical energy, followed by recovery of the microstructure upon unloading. Hydrogels that undergo extrinsic remodeling require an external stimulus to reconfigure the microstructure for energy dissipation or distribution, *i.e.*, toughening is independent of mechanical stimulus, allowing for interesting thermodynamic and kinetic manipulation of toughening through extrinsic remodeling.

enable new opportunities for enhancing toughness while expanding also enabling additional functionalities such as recycling.

5. RECOVERY AND REMODELING

The design of tough hydrogels that meet application-specific mechanical property requirements, such as stiffness and strength at given loading timescale, requires deep consideration of their dynamic structural components. While biological material systems provide inspirations to address these design challenges via hierarchical structuring of polymeric materials,[602] additional investigation reveals that organisms can also dynamically modulate existing material to access sophisticated hierarchical structures. This process, referred to here as dynamic remodeling, requires an external stimulus to introduce toughening, strengthening, and stiffening microstructures into materials.[603−606] The process of remodeling is distinct from assembly (as discussed in Section 4), as it supposes a pre-existing network that undergoes property evolution upon introduction of a stimulus. Notably, it follows the same chemical and thermodynamic bases as those outlined for assembly. Additionally, for the purposes of this review, remodeling is considered distinct from postloading structural recovery and postfracture self-healing.

5.1. Framework for Dynamic Remodeling

For hydrogels, remodeling takes place at the microstructural level in response to energy/mass input that occurs in the form of mechanical deformation or external stimuli such as light, heat, or ions. From a chemical perspective, these stimuli elicit molecular and macromolecular scale changes such as the formation of dynamic crosslinks,[607,608] phase separations,[609−611] and conformational shifts.[612] Dynamic microstructural remodeling processes can be classified into two distinct processes, *intrinsic* and *extrinsic*. Intrinsic remodeling is stress or strain induced, whereas extrinsic remodeling involves a nonmechanical stimulus (Figure 51). In intrinsic remodeling processes, such as the strain-toughening mechanisms and multimodal bond regimes for energy dissipation previously introduced in Section 3, the hydrogel network contains higher energy toughening/strengthening configurations that are accessed through microstructural reorganization induced by mechanical stress (Figure 51, **A**). Often, dynamic bonds are leveraged in hydrogel networks to access common intrinsic remodeling toughening mechanisms such as strain- and impact-stiffening.

Strain-induced crystallization, where aligned crystalline polymer chains form transiently in response to mechanical stimuli, is a form of intrinsic remodeling and a well-investigated strengthening mechanism observed in natural rubber. Liu and co-workers[613] developed a tough hydrogel featuring strain-induced crystallization via hydroxypropyl-α-cyclodextrin slide-ring crosslinks that dynamically slide along PEG chains, causing reversible and rapid PEG crystallization under mechanical deformation, The hydrogels achieved exceptional toughness (6.6−22 MJ m^{-3}), which is 1 order of magnitude larger than the toughness of covalently crosslinked PEG hydrogels, with near-complete mechanical energy recovery superior to covalently crosslinked gels. As another example of intrinsically remodeled hydrogel, Zhu and co-workers[614] developed a highly entangled double-network hydrogel (HEDN) using physical entanglements as dynamic crosslinks, enabling anisotropic chain orientation under tension to store mechanical energy via entropy loss, achieving near-total reversibility, minimal hysteresis over 1000 cycles, high tensile strength (~3 MPa), exceptional fracture energy (8340 J m^{-2}), and notable strain-stiffening behavior.

Mechanically induced directional bonds are another example of intrinsic remodeling. The previously introduced work of Qiao et al.[607] is demonstrative of such directional dynamic

https://doi.org/10.1021/acs.chemrev.5c00466
Chem. Rev. XXXX, XXX, XXX−XXX

bonds. They synthesized a supramolecular polymer network (SPN) composed of poly(α-thioctic acid) (polyTA) and arginine clusters, where directional guanidinium−carboxylate salt-bridge H-bonds control chain dynamics. Due to the competition between polyTA−arginine and arginine−arginine interactions, the material forms a highly directional salt-bridge H-bonding hierarchical structure that maximizes interfacial bonding. Upon impact-induced remodeling, the formation of salt-bridge H-bonds was accompanied by a substantial entropic penalty, resulting in a simultaneous stiffening and toughening of the polymer network. This feature allows SPNs to show strong dependence on strain rate, allowing them to rapidly transition from compliant to rigid under impact. Based on the principle of time−temperature equivalency, the strain rate dependence can be effectively regulated by manipulating the entropy penalty (penalty increases as going from nondirectional bonds to highly directional bonds formation), which is the slope of the Gibbs free energy (ΔG)−temperature curve. This enables the supramolecular polymer network to exhibit an extraordinary ∼2100-fold increase in storage modulus, transitioning from a compliant state (21 kPa at 0.1 Hz) to a stiffened state (45.3 MPa at 100 Hz) under increasing strain rates.

Incorporating dynamic bonds with varying relaxation times was discussed previously in Section 3, and it is recognized as another way to access strain-stiffening regimes as a function of strain. Wang et al. designed a tissue-like, hierarchically structured single network hydrogel consisting of the one-pot copolymerization of acrylamide, acrylonitrile, and maleic acid followed by immersion in aqueous $FeCl_3$ solution.[343] The Fe^{3+} cations physically crosslink the hydrogel network with dynamic bonds supporting two separate relaxation modes—a fast relaxation from weaker mono- and bis-ligand coordination, and a slow relaxation from stronger tris-ligand coordination—while also causing acrylamide rich domains to salt out, forming curled chains. Additionally, the acrylonitrile rich domains aggregate in clusters dominated by dipole−dipole interactions. At small strain, an initial elastic deformation regime that consists of unfurling chains and fast elastic deformation of the acrylonitrile clusters yields a Young's modulus of 0.08 MPa. As the strain increases a second regime is introduced, where the breaking of weaker mono- and bis-ligand-Fe^{3+} coordination bonds and disruption of dipole−dipole interactions within the acrylonitrile clusters dissipate energy, and the unfurled acrylamide chains undergo anisotropic alignment, resulting in energy storage due to entropy loss and significant strain-stiffening (tangent stiffness 2.6−3.6 MPa). Even higher strain exposes a third regime, where the strong tis-ligand-Fe^{3+} coordination bonds are ruptured and further disruption of the acrylonitrile clusters is seen until hydrogel failure. The incorporation of varying dynamic bond strengths results in an overall toughness of 6.5 MJ m^{-3}.

It should be noted that for intrinsic remodeling, the nature of the hydrogel's energetic landscape is not fundamentally changed upon mechanical stimulus; rather, the mechanisms of energy distribution or dissipation change as a function of mechanical force applied. Therefore, toughening introduced by intrinsic remodeling is inextricably coupled with mechanical stressors.

5.2. Mechanisms of Extrinsic Remodeling

In extrinsic remodeling processes, the external stimulus can be conceptualized as *reconfiguring* the energy landscape of the network, resulting in a different set of dynamics and structure, in both the unloaded and loaded state (Figure 51, B). Thus, to enhance toughness, these dynamic bonds and/or microstructures are remodeled to maximize energy dissipation and distribution without the application of mechanical stress. Extrinsic remodeling provides unique opportunities for kinetic and thermodynamic manipulations of hydrogel structures and mechanical responses. For a hydrogel that is designed to undergo extrinsic remodeling, a stimulus could speed up or slow down intrinsic processes during deformation for fracture prevention or fracture blunting,[615−618] or introduce microstructures that increase a hydrogel's stiffness or elasticity.[316,619,605,38] Additionally, these changes could advantageously modulate the timescale of recovery or introduce an external source of network repair.[612,620,621] Furthermore, stimuli-responsive hydrogels create opportunities for materials that are tough and strong while also being reprocessable, recyclable and/or degradable.[387,622]

This section will examine hydrogels that undergo non-mechanical stimuli-induced toughening and/or stiffening,[623] grouped by remodeling mechanism. The discussion for each mechanism considers thermodynamic contributions of the stimulus to the hydrogel microstructure, what stimuli-induced microstructures result in hydrogel toughness and/or stiffness, factors determining network recovery and reprocessability, as well as the functional applications of the system. Because dynamic remodeling is a frontier in advanced hydrogel design, the aim of this section is to convey a broad understanding of extrinsic remodeling, and provide important considerations for the development of stimuli-responsive tough and strong hydrogels.

5.2.1. Paired Physical Cross-Linking. Hydrogel remodeling through physical crosslinking is a category of mechanisms that enables toughening of hydrogels and possesses its own advantages. Ion-specific interactions, host−guest interactions, hydrogen bonding, and other interactions can be induced via external stimulus to form paired physical crosslinks, which alter the network thermodynamic equilibrium through noncovalent interactions. For example, Cui et al. explores the use of metal ion coordination to enhance the mechanical properties of alginate-based hydrogels.[624] A double network hydrogel composed of multivalent cation-sensitive alginate and kosmotropic anion-sensitive PVA is prepared. The initial alginate/PVA hydrogel is soft, with an elastic modulus of 0.013 MPa and fracture stress of 0.26 MPa. However, by optimizing the ion content, under the synergistic effect of cations and anions, formation of PVA microstructures induced by salting-out of SO_4^{2-} anion, and cation-alginate paired physical crosslinks, the alginate/PVA-2 hydrogel achieves a remarkable increase in fracture toughness of 39 kJ m^{-2}, which is 3 orders of magnitude greater than that of the untreated hydrogel, and an elastic modulus of 3.71 MPa.

As introduced in Section 3, hydrogen bonding is another common type of physical crosslink that can dynamically tune the mechanical properties of hydrogels. These noncovalent interactions serve the function of sacrificial bonds that can dissipate energy under mechanical stress, resulting in hydrogel toughening. Yue et al.[640] reported a strategy to progressively tune the toughness of hydrogels through dynamic H-bonds. The gel layers consist of polyacrylamide (PAM) and sodium polyacrylate (PAANa) copolymers, containing fixed amide ($-CONH_2$) and carboxylate ($-COO^-$) groups within the polymer network. The mobile Na^+ ions associated with

https://doi.org/10.1021/acs.chemrev.5c00466
Chem. Rev. XXXX, XXX, XXX−XXX

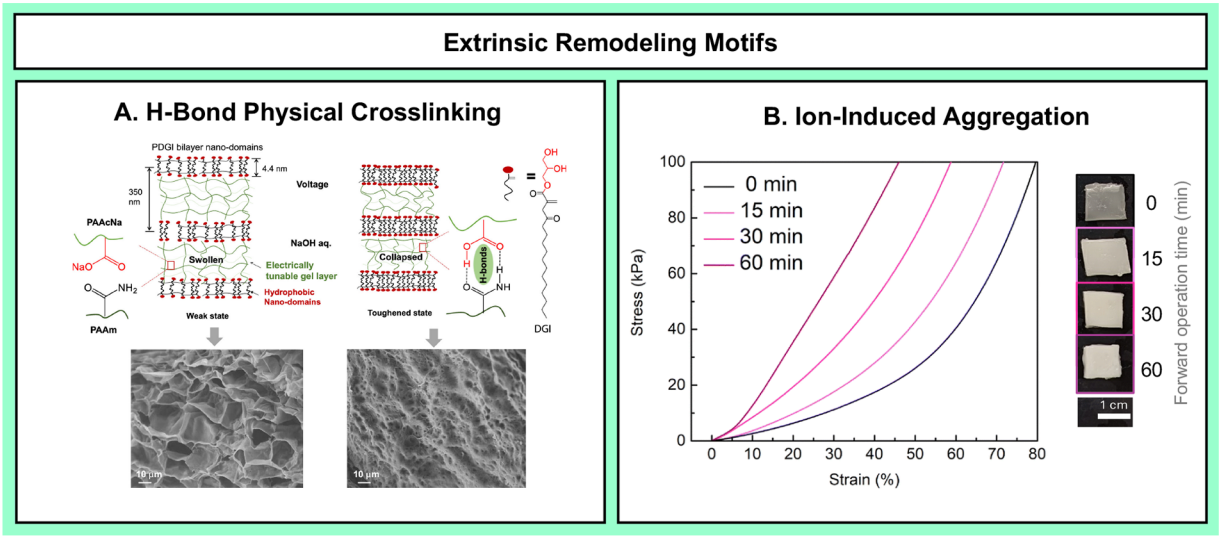

Figure 52. Various strategies for extrinsic remodeling. A) Schematic showing stimuli-responsive PAM−PAANa and poly(dodecyl glyceryl itaconate) bilayer hydrogels that undergo entropically penalized directional hydrogen-bonding when an electric field is applied. SEM images of the hydrogel in weak and toughened states before and after an applied voltage of −1.7 V. Figure adapted with permission from Yue et al., 2022 (ref 608, Copyright 2022 American Chemical Society). B) Ion-responsive IPN hydrogels showing increasing opacity as time duration of an applied voltage (∼5 V) is increased. Compression stress−strain curves of IPNs held under voltage for different time durations indicate increased stiffening over longer time frames. Figure adapted with permission from Cai et al., 2025 (ref 642, Copyright 2025 Royal Society of Chemistry).

$-COO^-$ groups readily exchange with H^+ ions due to the high cation selectivity of these groups (Figure 52, **A**). Under an applied voltage above ∼1.7 V, water electrolysis generates H^+ ions that exchange with Na^+ ions, creating carboxylic acid groups (−COOH) which readily form additional dynamic H-bonds with $-CONH_2$ groups. As the treatment time increases, toughness increases due to the gradual increase in the number of H-bonds within the duration of the applied electric field, offering a temporal remodeling strategy for hydrogel toughening.

Lu et al. reported a dynamic hydrogel network consisting of dual functionalized dynamic crosslinkers, enabling on-demand switching between two distinct toughening states of the hydrogel, and spatiotemporal regulation of the network's viscoelasticity.[619] The dual dynamic crosslinker contains aldehydes at the ends, capable of forming dynamic Schiff base bonds with the amine sites in the polymer network, and when exposed to light, triggers a radical-induced dynamic disulfide metathesis. Through altering the structure of the aldehyde component, the hydrogel's intrinsic stress relaxation time can be tuned from 3400 to 500 s via a reversible imine metathesis reaction. Extrinsic remodeling is triggerable utilizing visible light by incorporating thiuram disulfide (TDS) moieties into the hydrogel network. While TDS undergoes slow disulfide metathesis under ambient conditions, light exposure significantly accelerates this exchange, reducing the hydrogel's stress relaxation time by half. Both mechanisms allow for a crosslinker dose-dependent reorganization of polymer network microstructures which enables spatiotemporal control over the exchange rates of hydrogel's dynamic crosslinks.

5.2.2. Physical Cross-Linking through Phase Separation. Solvent-induced phase separation was discussed in terms of solvent annealing and solvent swapping in Section 4, where balancing the solvation energies of polymers of specific solvents can enhance intra- and interpolymer interaction, resulting in the assembly of physical hydrogel networks from a pregel sol. In remodeling, solvents can be used as a stimulus to restructure existing networks by inducing areas of polymer aggregation, crystallization, and/or chain entanglements[625] within those networks.[626,627] From an ecological perspective, hydrogels without covalent crosslinks tend to be less toxic, highly reprocessable and/or recyclable.[628] Dynamic remodeling of hydrogel strength and toughness through physical interactions is one way to increase the functionality and broaden the applications of more environmentally friendly and sustainable materials.

Hydrophobic associating hydrogels are an example of weak physically associating hydrogels that display minimal strength or toughness.[629] Cui and co-workers demonstrated the effectiveness of dynamic remodeling by introducing polymer aggregates into a simple, random copolymer hydrogel matrix via solvent-induced phase separation.[387] Acrylamide and steryl methacrylate monomers were copolymerized in water in the presence of surfactant using free radical polymerization. The incorporation of both hydrophobic and hydrophilic groups results in hydrophobic associations that act as a weak, dynamic microstructure within the hydrogel. Introduction of poor solvent THF at some critical concentration enthalpically drives the aggregation of partial polymer chains after replacing some of the water that surrounds the hydrogel. The resulting dense phases of polymer act as physical crosslinks between sparse polymer phases, and the degree of aggregation—measured as the volume fraction of polymer in the hydrogel—can be tuned by adjusting the concentration of THF. Upon 70 wt % THF in water, the hydrogel experiences a steep increase in volume fraction, from 0.14 to about 0.35. This remodeling process was shown to be reversible, where hydrogels can be soaked in pure water and regain their original volume fraction, with the degree of healing largely dependent on the amount of time allowed for enthalpic rearrangement of the hydrogel species. The mechanical properties of the remodeled hydrogel could be controlled based on THF concentration; at 70 wt %, the elastic modulus jumps to 100 MPa, approximately 4 orders of magnitude higher than the original hydrogel. Increasing the

https://doi.org/10.1021/acs.chemrev.5c00466
Chem. Rev. XXXX, XXX, XXX−XXX

THF concentration to 90 wt %, however, yields an abrupt decrease in fracture strain. Additionally, the remodeled hydrogel at 70 wt % THF shows pronounced hysteresis compared to the original hydrogel under tensile loading−unloading testing, 2.82 MJ m^{-3} versus 0.021 MJ m^{-3}, respectively. Cui and co-workers suggest that at 70 wt % THF, phase separation is not so extreme, allowing aggregates to act as sacrificial bonds for energy dissipation and enhanced toughness. Increasing to 90 wt %, the closely packed, dense regions of the polymer form crystalline features, and upon rupture induce crack propagation and decrease polymer toughness.

Sophisticated remodeling of physically associated hydrogels through solvent-induced phase separation can be achieved using physically entangled double networks with different solvent responses. Zhao and co-workers, inspired by the stiffness-switching behaviors of sea cucumber tissues, showed extreme and reversible solvent-stimulated stiffening of cellulose-poly(acrylamide) supramolecular hydrogels upon exposure to ethanol.[612] Acrylamide was polymerized via free radical polymerization *in situ* inside a self-assembled cellulose network. The stiffening mechanism induced by ethanol stimulus was shown to be a synergistic combination of polymer conformation and interpolymer interactions with no damage to the hydrogel network, occurring in only a few hours. Cellulose networks and linear polyacrylamide are individually soluble in ethanol, however molecular dynamics simulations (MD) showed that cellulose maintains an extended chain conformation in both water and ethanol, while polyacrylamide (PAM) undergoes a conformational shift from an extended chain in water to curled in ethanol (Figure 53). MD also indicated that the presence of ethanol results in increased hydrogen bonding interactions between cellulose and PAM. Additionally, DFT calculations showed that the hydrogen bonding interaction energy of ethanol in water was 1.77 eV, larger than cellulose and ethanol (1.65 eV) or PAM and ethanol (1.25 eV). Therefore, the introduction of ethanol disrupts the hydrogen bonding network of cellulose and PAM in water, while simultaneously inducing conformational curling in PAM chains and promoting interchain interactions. Dynamic restructuring of hydrogel microstructure takes place; cellulose strands are wrapped in semicrystalline PAM chain armor, resulting in a dramatic reinforcement of the cellulose network and subsequent stiffening of the hydrogel. This process of disruption followed by reinforcement takes place over approximately 2.5 h, after which the remodeled hydrogel shows a 21-fold increase in tensile strength (from 0.86 to 18.39 MPa) and an almost 500-fold increase in stiffness (from 0.51 to 243.6 MPa). Even with such high stiffness, the material was still tough and malleable, showing no embrittlement or cracking after severe deformations such as folding. Similar to the previous example, these hydrogels also showed high reversibility, where self-healing from scratches or other structural damage could be repaired upon submersion in pure water, followed by stiffening in ethanol.[612]

Phase separation through solvent stimulus does not always require a second solvent. By tuning the solvation kinetics of hydrophilic, physically entangled double networks, Xu and co-workers dynamically toughened hydrogels through simple dehydration and rehydration.[622] Sodium styrenesulfonate (NaSS) and sodium sulfobetaine methacrylate (SBMA) were copolymerized via free radical polymerization *in situ* inside a concentrated linear PVA suspension. The microstructure

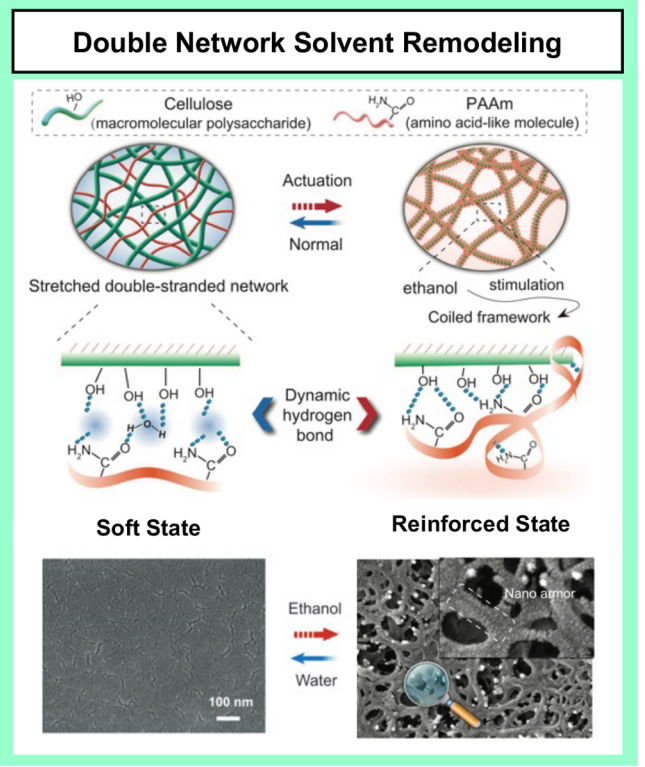

Figure 53. Solvent reconfigurable double-stranded supramolecular networks undergo extreme stiffness-switching behaviors. Upon ethanol exposure, PAAm chains undergo conformational shifts that reinforce the cellulose network, resulting in enhanced hydrogel stiffness. Figure adapted from Zhao et al., 2022 (ref 612, Copyright 2022 John Wiley and Sons).

consists of weak dynamic hydrogen bonding between PVA and the copolymer poly(NaSS-*co*-SMBA). Upon air-drying, hydrophobic interactions between the PVA and poly(NaSS-*co*-SMBA) are activated, forming a stiff, opaque solid material. Rehydration of the hydrogel is possible due to the charged anionic and zwitterionic species, which facilitate the re-entry of water into the polymer matrix while preserving the hydrophobic aggregations formed during dehydration. This results in a phase-separated, microporous, highly percolated network, where hydrophobic polymer domains are stabilized in water via the hydrophilic ionic and zwitterionic moieties. While not reversible, the phase separated, physically entangled networks are easily reprocessed by heating the hydrogel to 80 °C and reperforming the dehydration−rehydration process. Upon remodeling, hydrogels showed a 2.5-fold increase in fracture stress as well as high fatigue resistance, where the hydrogel showed almost no change in hysteresis after 50 cycles of tensile and compact stress testing, respectively. Additionally, the ionic and zwitterionic stabilization of the phase separated domains made hydrogels stable in harsh conditions. Remodeled hydrogels displayed structural integrity under pH 1, 10 and 14, saline solution, and mixed solvents, including DMSO, ethanol, and isopropyl alcohol. The manufacturing implications of simple hydrogels dynamically toughened through dehydration−rehydration is highlighted by Liu et al. utilizing crosslinking PAM and linear PVA composite hydrogels.[630] An aqueous solution of acrylamide, crosslinker and initiator is crosslinked in the presence of linear PVA at 60 °C, where the thermal evaporation of water from the hydrogel precursor

https://doi.org/10.1021/acs.chemrev.5c00466
Chem. Rev. XXXX, XXX, XXX−XXX

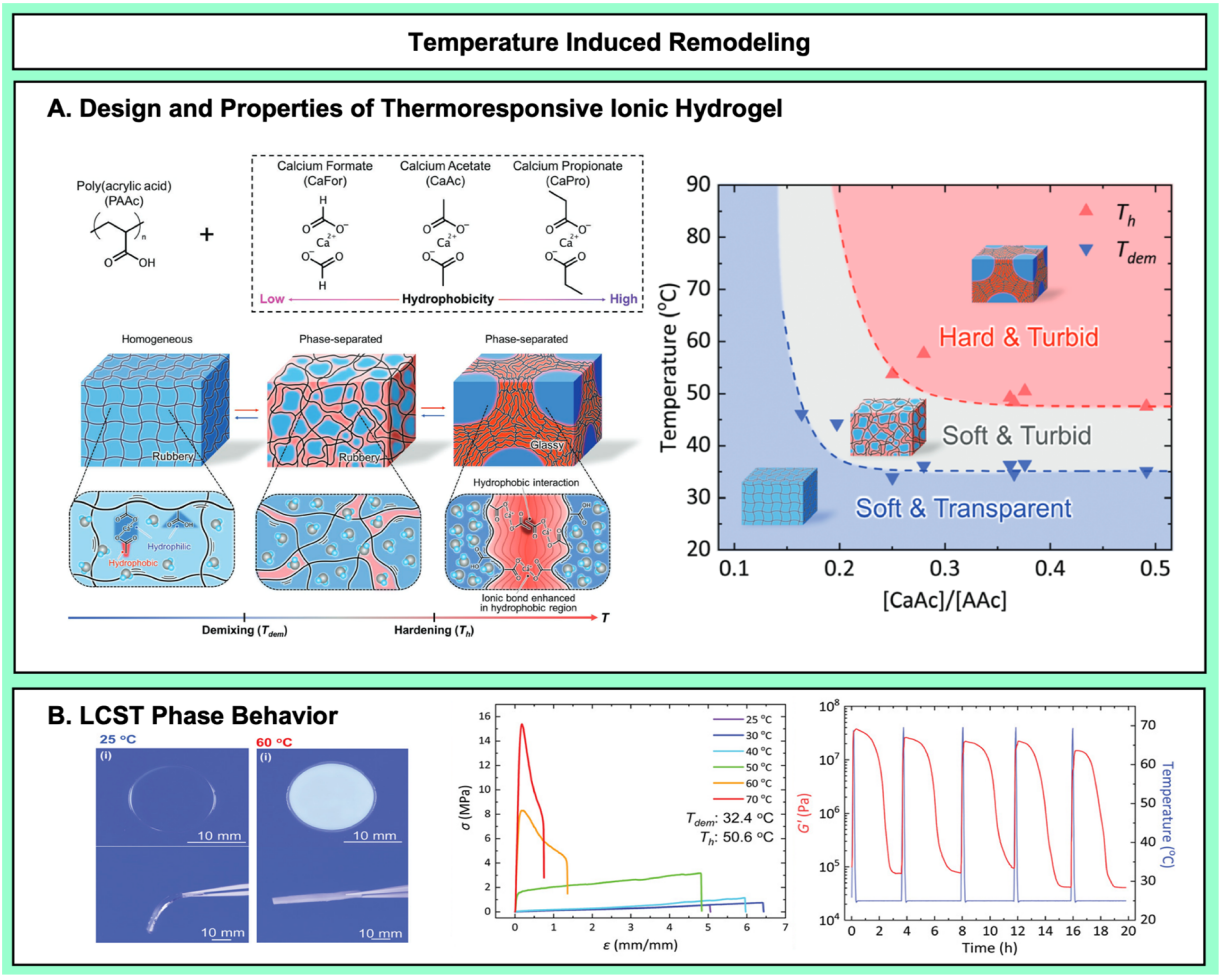

Figure 54. A) Mechanism for instant isochoric thermal stiffening of of PAAc-calcium acetate hydrogels gels when exposed to 60 °C. B) Uniaxial tensile stress−strain curves show dramatic stiffening and toughening response as a function of temperature. Storage modulus (G') as a function of temperature upon repeated heating and cooling cycles shows high reversibility. Figure adapted with permission from Nonoyama et al., 2019 (ref 222, Copyright 2019 John Wiley and Sons).

solution drives the formation of PVA semicrystalline regions within the crosslinked PAM. After fabrication, the toughened hydrogel is swollen in water and can undergo switchable mechanical properties: soaking in a heated water bath disrupts the semicrystalline PVA, and the hydrogel softens (Young's modulus ∼1.0 kPa, toughness 0.02 MJ m^{-3}). Upon thermal evaporation of the water, the semicrystalline regions are reintroduced, and the hydrogel demonstrates regained toughness when it is swollen with water (Young's modulus 100 kPa, toughness 2.39 MJ m^{-3}). The degree of crystallinity (therefore, hydrogel toughness) can be directly controlled by heating temperature and time during the thermal evaporation process, showing a dynamic toughening regime for processing and manufacture.

Thermally induced phase separation is a well-known and frequently used strategy in the assembly and fabrication of tough hydrogels, as outlined in Section 4. However, controlling the rate of mechanical property evolution over time, as well as large volume changes, present particular challenges for thermally induced phase separation in dynamically remodeled hydrogels. Strategies such as IPNs, composites and salt additives have been used to tailor thermoresponsiveness for hydrogels. Polymers that display LCST phase behavior undergo phase separation above some temperature, where the energy input as a result of increased temperature overcomes the entropically favored solvation of hydrophobic functional groups, resulting in dehydration and partitioning into hydrophobic aggregates.[631,470,467] Phase separation triggered by LCST tends to be highly sensitive and very tunable; well-studied polymers like PNIPAM are known to display massive variation in phase boundaries depending on molecular weight, dispersity, tacticity, and branching.[632,633] Additionally, kinetically arrested demixing and thermal hysteresis of PNIPAM[634] point to slow thermodynamic equilibration that may be considered in the functional design of thermally remodeled hydrogels.

PNIPAM and derivative polymers undergo phase separation at or around biologically relevant temperatures, between 25 and 40 °C.[288,467] However, upon reaching their LCST, PNIPAM hydrogels will undergo rapid volume changes,[635] expelling solvent (syneresis) and making it unattractive for applications like drug delivery. Motloung and co-workers demonstrated a cellulose nanofibril (CNF) and PNIPAM based, thermo-stiffening semi-IPN hydrogel for biomedical applications that showed tunable stiffening and deswelling kinetics depending on the concentration of salts introduced into the hydrogel matrix.[636] High molecular weight PNIPAM and CNF suspension were mixed, forming semi-IPNs that

https://doi.org/10.1021/acs.chemrev.5c00466
Chem. Rev. XXXX, XXX, XXX−XXX

consisted of physically entangled and hydrogen bonded PNIPAM and CNF. Cellulose does not exhibit LSCT behavior, however temperature sweeps of the storage modulus of the hybrid hydrogels still showed an abrupt phase transition slightly above PNIPAM hydrogel LCST, due to the small amounts of CNF added for structural support. Gelation was induced through salt addition, where different concentrations of NaCl were investigated for their influence on deswelling kinetics of the hydrogel upon thermally stimulated phase separation. NaCl addition enhanced physical interactions within the hydrogel, attributed to the electrostatic screening effect of the Na^+ on the negative carboxylate motif of the CNFs, which allowed for greater interfibrillar entanglement. These hydrogels showed significant increase in storage modulus at room temperature when compared to the hybrid hydrogels without salt. More importantly, however, the NaCl hydrogels showed both decrease in volume and elastic modulus change, as well as a time-delayed onset of thermo-stiffening, depending on the concentration of salt used to induce gelation. The no-salt hydrogels experienced a 224% increase in storage modulus after temperatures were raised to 37 °C (above LCST) and held for approximately 12 min. However, with 10 mM NaCl addition, the storage modulus only increased 88%, and required almost 20 min to achieve after temperature increase. A 25 mM addition of NaCl resulted in little change to either volume or storage modulus at 37 °C, due to the time−temperature superposition shift in LCST resulting from the chain entanglements and aggregation induced by increased ionic strength. Simply through enhanced interpolymer physical entanglement, Motloung and co-workers demonstrated both tunable stiffening upon thermal stimulus and delayed equilibration through kinetic entrapment of the hydrogel microstructure.[636]

The molecular motif characteristic of PNIPAM—entropically costly hydrophobic groups stabilized by well-solvated hydrophilic groups—has been the genesis of a slew of thermo-stiffening polymers displaying LCST behavior in the last 55 years.[467] Impressive developments in the enhancement of the stiffening and toughening response of these hydrogels have been made by controlling the kinetics of phase separation through careful manipulation of hydrophobic and hydrophilic groups. Nonoyama and co-workers developed instant, isochoric thermo-stiffening and -toughening hydrogels with crosslinked polyelectrolyte poly(acrylic acid) (PAA) complexed with retrograde soluble salt calcium acetate (Figure 54, **A**).[618] The temperature-inverse solubility of the acetate anion means that it undergoes dehydration at a critical temperature.[637] This causes a decrease in the relative permittivity of the Ca^{2+} environment and stabilizes the PAA-COO^- and Ca^{2+} ionic bond, resulting in rapid partitioning into polymer dense and polymer sparse phases. The enhanced stabilization of ionic bonds in the hydrogel matrix upon reaching the LCST favors a rubbery to glassy state transition of the polymer dense phase, which quenches macro phase separation and kinetically traps the aqueous solution phase in the hydrogel matrix. The lack of solvent escape prevents volume changes characteristic of LCST phase behavior, and so these gels undergo isochoric phase separation. LCST phase behavior is diffusion-based, and because PNIPAM does not undergo rubbery to glassy transitions under 100 °C, the operating temperature for aqueous systems, time of equilibration for PNIPAM hydrogels upon phase separation is long (as mentioned in the previous example) and proportional to the square of area size. Consequently, PNIPAM and other similar thermoresponsive polymers do not show such dramatic and instant phase separation, making these PAA-calcium acetate hydrogels exceptionally tough and strong. When the temperature was raised to 60 °C, the hydrogels displayed 20- and 80-fold increases in both toughness and strength, respectively (Figure 54, **B**). Due to the reversible nature of LCST behavior, Nonoyama and co-workers were able to fabricate athletic armor using a composite material of glass fabrics and PAA-calcium acetate hydrogels. Abrasion tests on asphalt showed instant toughening and stiffening of the composite material upon frictional heating, demonstrating a practical and reusable application of dynamically remodeled thermoresponsive hydrogels.

The applications of thermo-stiffening of hydrogels can also extend beyond enhancing toughness or strength. By surface-functionalizing hydrogels containing PAA-calcium acetate complexes with polyelectrolyte brushes, Zhang and co-workers demonstrated instant thermoresponsive surface lubrication, inspired by instant lubrication of catfish skin upon muscle hardening.[610] A copolymer hydrogel consisting of poly(acrylic acid) and poly(2-hydroxyethyl methacrylate-bromine) was crosslinked under UV light and then treated with calcium acetate to form a thermo-stiffening network. Then, a polyelectrolyte lubricating layer was added by polymerizing 3-sulfopropyl methacrylate potassium to the hydrogel surface via ATRP. At room temperature, the hydrogel underlayer is soft, resulting in large contact area at the relaxed polyelectrolyte surface, leading to a frictional coefficient of approximately 1.8. However, upon a temperature increase to 80 °C, the hydrogel rapidly stiffens, reducing deformation dissipation and decreasing the contact area of the polyelectrolyte surface by mechanically confining the polyelectrolyte surface chains perpendicular to the hydrogel surface. This results in a 3-fold decrease in frictional coefficient to approximately 0.6; the rapid kinetics of the PAA-calcium acetate LCST phase behavior allows the instant lubrication response.

Thermo-softening can be achieved by manipulating glass transition temperature (T_g), as demonstrated by Lin et al. in the fabrication of thermoresponsive glassy hydrophobic hydrogels.[638] Isobornyl acrylate and acrylamide were copolymerized in organic solvent with crosslinker to form a network containing hydrophobic and hydrophilic regions. Solvent swapping with water yielded bicontinuous networks comprised of hydrophobic regions flanked by water-solvated hydrophilic regions. The osmotic pressure of the water limiting polymer chain segmental motion combined with the high T_g of the hydrophobic polymer provides a rigid network that toughens the hydrogel at room temperature. However, as the temperature increases, the glassy hydrophobic regions transition to a rubbery state and the hydrogel softens. Hydrogels showed a Young's modulus decrease from 50.5 to 0.031 MPa and decrease in toughness from 35.2 to 2.3 MJ m^{-3} when the temperature was increased from 25 to 80 °C. The degree of phase separation and T_g can be tuned by varying hydrophobic and hydrophilic comonomer identity and crosslinker ratio, resulting in hydrogels with variable modulation in toughness and recovery. Another interesting way that thermo-softening behavior can be achieved is through UCST phase behavior, although it rarely used for toughening applications in hydrogels due to the limitations described in Section 4. However, ionogels (gel networks swollen with ionic liquids) have shown impressive thermoresponsiveness,[639] accessed by introducing

https://doi.org/10.1021/acs.chemrev.5c00466
Chem. Rev. XXXX, XXX, XXX−XXX

bicontinuous microstructures through polymer vitrification when the heating of the ionogel is quenched just below Berghmans' point (liquid−liquid phase transition). Such phase behavior manipulations in ionogels may provide inspiration for UCST-type toughening responses in hydrogels.

5.2.3. Ion-Mediated Phase Separations. Dynamic toughening of hydrogels via ion-mediated phase separation consists of polymer−polymer interactions that are modified as a result of salt or pH stimulus. Similar to solvent-induced phase separation and LCST phase separation behavior, ion-mediated phase separation can form polymer aggregates or microcrystalline regions that behave as physical crosslinks, providing energy dissipation mechanisms for toughening and/or increased crosslink density for stiffening or strengthening.[640] The driving forces for ion-mediated phase separations are complex and not entirely understood. However, theoretical models such as Hofmeister salting-in/out and LMWA (as were discussed in Sections 3 and 4), provide some insight into the enthalpic and entropic contributions of these complicated systems. The size, hydrophobicity, and charge density and distribution of polymer functional groups and salt ion pairs determine the interaction affinity of polymer−polymer, polymer−solvent, polymer−ion, ion−ion, ion−solvent, and solvent−solvent interactions. Broad trends for aqueous systems include 1) large, hydrophobic and charge disperse species preferentially interact with each other entropically, through van der Waals and dipole interactions, and 2) small, hydrophilic, and charge dense species interact with each other and water molecules enthalpically, through solvation energy, hydrogen bonding and electrostatic interactions.[246] Properties of polymers in solution, such as interfacial tension and zeta-potential can be tuned through introduction of salts, where solvated charged species can cause disruptions to the polymer hydration sphere as well as electrostatic screening.[527] Altogether, it is understood that the mechanism for ion-mediated phase separation is highly specific to the species within the system, making it a rich, diverse space full of opportunity for tunable toughening and stiffening of hydrogels through remodeling strategies.

Controlling the degree of crystallinity within hydrogels that undergo ion-mediated phase-separation is one way to enhance or tune material toughening and strength. Yang and co-workers fabricated ion-responsive double network chitosan-polyacrylamide hydrogels, where the degree of toughening was correlated to whether the ion stimulus was saline or alkaline.[611] Short chain chitosan was incorporated into a covalently crosslinked polyacrylamide network *in situ* by forming a suspension of chitosan with acrylamide monomer and polymerizing the acrylamide via free radical polymerization. Upon addition of 1 M NaCl, hydrogels experienced an almost 5-fold increase in fracture energy, from 1.8 to 8.3 kJ m^{-2}, and a 13-fold increase in tensile strength, from 0.15 to 1.94 MPa. 1 M NaOH remodeled hydrogels, however, showed an even greater increase in fracture energy at 12.9 kJ m^{-2}, and higher tensile strength at 2.12 MPa. The difference in response can be attributed to the ion-sensitive, un-crosslinked, short chain chitosan. Chitosan is known to undergo classic salting out behavior, where mildly kosmotropic ions such as chloride result charge screening and the aggregation of chitosan chains.[641] Hydroxide ions, on the other hand, entirely deprotonate the amine groups, resulting in neutral, hydrophobic chitosan chains that form microcrystalline regions.[616] NaCl soaked chitosan gels showed few diffraction features aside from the NaCl crystals, however the NaOH soaked chitosan gels and DN gels presented peaks indicative of (020) and (110) chitosan lattice diffraction. These findings agree well with the mechanical differences in the remodeled hydrogels. Phase separation induced by NaCl addition results in physical crosslinks made of weaker polymer associations and amorphous aggregates, introducing sacrificial bonds for energy dissipation. NaOH addition results in physical crosslinks made up of microcrystalline regions that require greater mechanical energy before rupture, greatly increasing fracture energy as well as strength compared to the NaCl hydrogels. It was noted, however, that upon lengthened soaking time—increased from 20 min to 1 h—the NaCl hydrogels showed enhanced tensile strength as well as lower ductility. The longer soaking times allowed enhanced phase separation in the NaCl gels, further equilibrating into more dense polymer phases and toughening the hydrogel by strengthening the physical crosslinks.

Cai et al. demonstrated electric field-driven tuning of stiffness and strain hardening a semi-IPN of polycationic and polyanionic chains in a PAA matrix, saturated with NaCl.[642] A 5-fold stiffness change was attainable with a voltage of 5 V applied over 1 h (Figure 52, **B**), and this stiffness change could be fully reversed over the same time period by changing the direction of the applied field. The electric field is used to control the concentration of mobile ions in the gel. The compliant state corresponds to a saturation of mobile ions that screen ionic interactions among the polymer chains, and the stiff state corresponds to the absence of mobile ions. Prior work on a gel of the same chemistry showed that mechanical property dependence on salt concentration is related to a heterogeneous microstructure that forms from polyelectrolyte chain aggregation around the neutral PAA matrix when salt is removed.[643] The phase segregation effect is apparent in the transformation of the gel in each of these works from transparent to opaque.

Ion-specific behavior along the Hofmeister series is a common way to demonstrate tunable toughening and strengthening of hydrogels,[644,645] and it can be used to extend mechanical modulation via thermal phase separation in hydrogels. By combining the synergetic effects of both organic additives and Hofmeister salts, Lin and co-workers were able to dynamically toughen hydrogels nearly isochorically through time−temperature superposition manipulation of rubbery and glassy phases.[615] A tough, crosslinked copolymer was synthesized using hydrophobic isobornyl acrylate and hydrophilic acrylamide as comonomers. Poly(isobornyl acrylate) (PIBA) exhibits a glass transition of 94 °C, meaning that the hydrophobic PIBA aggregates within the Poly(IBA-*co*-AM) hydrogel act as strong, glassy physical crosslinks, leading to an elastic modulus of 25.9 MPa at room temperature. Addition of organic additives as plasticizers shifts the time−temperature superposition of the hydrophobic glassy regions, resulting in a glassy to rubbery transition that allows increased chain movement of the hydrophobic physical crosslinks and a subsequent decrease in elastic modulus to only a few hundred kPa depending on the identity of the organic additive. The addition of Hofmeister salts, however shows remarkable change in the opposite direction, where kosmotropic salts disrupt the solvation of the hydrophilic PAM, resulting in salting-out type phase separation that increases the physical crosslinking of the hydrogel (even akin to a glassy phase, Lin and co-workers suggest) and can increase the elastic modulus to 150 MPa depending on the anion identity of the salt.[615] Additionally, the hydrophobic aggregates, acting as physical

https://doi.org/10.1021/acs.chemrev.5c00466
Chem. Rev. XXXX, XXX, XXX−XXX

crosslinks inherent to the hydrogel matrix, supply shape memory that is retained during remodeling, and so the polymers experience relatively low volume changes upon large changes in elastic modulus. The incredible tunable range of elastic modulus for these hydrogels, from 0.0042 to 150 MPa, demonstrates the opportunity for versatile applications in ion-mediated phase separation for hydrogel remodeling.

Ion-mediated phase separation can also act as a stabilizing force in nonequilibrium systems to prolong material structural integrity and functionality over greater lengths of time. Jiang and co-workers fabricated toughened regenerated silk fibroin and gelatin composite hydrogels for bone healing and regeneration purposes that can undergo ion-controlled degradation.[617] Biomedical applications often require that synthetic wound dressings and drug delivery systems undergo biodegradation to reduce toxicity and facilitate tissue growth.[646] Gelatin and regenerated silk fibroin (RSF) degrade in biological conditions over time, however gelatin undergoes rapid structural degradation within minutes, while RSF networks may take weeks or months to degrade, depending on the composition. While initial rapid degradation may be attractive for drug delivery in wound dressings, mechanical properties are sacrificed. Conversely, a dressing that degrades too slowly can impede healing and prevent tissue regeneration. In an attempt to merge the degradation properties of these two species, composite hydrogels of 3, 6, and 9 wt % RSF and 9, 6, 3 wt % gelatin, respectively, were formed by combining both polymers of their respective concentrations in solution and enzymatically crosslinking using horseradish peroxidase and hydrogen peroxide. The hydrogels were then toughened through ionic crosslinking via 1.1 M ammonium sulfate addition. When the 3%RSF/9%gelatin composite hydrogels were soaked in 1.1 M sodium salt solutions, they showed remarkable differences in degradation time based on anion identity. Sodium iodide resulted in complete degradation in just a few hours. Increasing kosmotropicity of the anion to chloride lengthened the degradation time to over 40 h, and hydrogels in monosodium phosphate solution degraded after approaching 100 h. Increasing the RSF content resulted in even longer degradation times, with the 6%RSF/6%gelatin hydrogels showing degradation times of approximately 30, 100, and 170 h for sodium iodide, sodium chloride, and monosodium phosphate, respectively. The mechanism for controlled degradation is a synergistic combination of the gelatin and RSF undergoing a salting out phase separation in response to kosmotropic ions,[647] which increases interactions such as hydrogen bonding between the two networks, and the suppression of gelatin diffusion out of the hydrogel matrix as the RSF content is increased. While the primary toughening mechanism for these hydrogels is through ionic crosslinking, stabilizing the structural properties of materials programmed for degradation through ion-responsive remodeling is one way to enhance functionality and broaden applications of tough and strong hydrogels.

5.3. Summary—Final Outlook on Remodeling of Hydrogel Networks

Extrinsic dynamic remodeling is an excellent way to introduce toughening post-fabrication into otherwise unremarkable and featureless hydrogel networks. The decoupling of mechanical stimulus from network toughening provides handles for instantaneous, isochoric, and switch-like transformations in mechanical behavior and recovery.

New directions in extrinsic toughening lie in highly anisotropic and hierarchical materials, where stimuli-responsive, macrostructural conformational shifts result in microstructures that undergo intrinsic toughening under mechanical stress. This has already been demonstrated in elastomers; for example, Li et al. developed a photoresponsive supramolecular gel network[648] where upon stretching, the gel's azo-bridged bipedal host molecules enable extreme stretchability by sliding along polymer chains and undergoing strain-induced crystallization. When exposed to UV light, azobenzene mesogens undergo trans-to-cis isomerization, disrupting the crystallized structures by deconstructing the aligned crystalline region to an isotropic macrostructure, which leads to release of stored strain energy. Similar photostimulated trans-to-cis isomerization of azobenzene for mechanical strain stiffening has been demonstrated in liquid crystal elastomers (LCE), where Ohzono et al. showed photoinduced nematic phase switching in crosslinked diacrylate mesogens. The disruption of the nematic phase under UV irradiation allowed the LCE to undergo elastic rearrangement upon mechanical deformation, resulting in photoswitchable strain-induced crystallization.[649] Developments in the assembly of hydrogels containing hierarchical or anisotropic microstructures, including complex hydrogel composites,[650] elastomer-hydrogels hybrids,[651] and elastomer-like hydrogels,[652,653] create opportunities for similar externally modulated intrinsic toughening.

Extrinsic remodeling also allows for spatiotemporal modulation of toughening toward advancement of soft robotics and living-like synthetic chemical systems. The localized adjusting, diverting and stabilizing of thermodynamic equilibria through stimulus across bulk materials gives rise to time-dependent, kinetically influenced, *spatially* separated toughening responses (Figure 55), similar to isolated or localized tissue stiffening in biological materials. Early development in next-generation, stimulus-induced and spatiotemporally controlled toughening over mechanical properties in materials is already underway, with some examples mentioned in this section. Recall the work done by Nonoyama et al., where instant toughening of thermoresponsive hydrogel composites showed reversible, localized toughening in response to asphalt abrasion.[618] Or

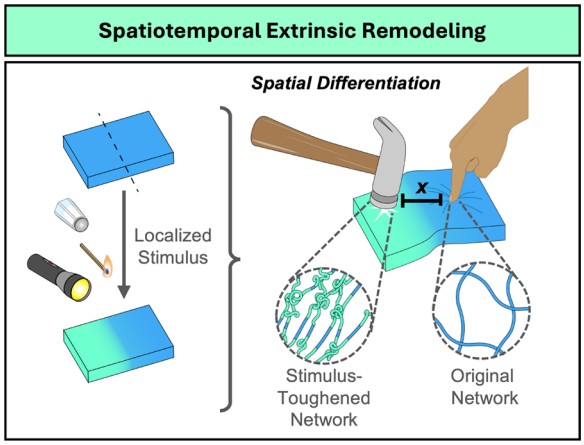

Figure 55. Diagram illustrating spatiotemporal opportunities in extrinsic remodeling. Localized stimulus input results in spatially differentiated microstructures across the bulk hydrogel with different mechanical properties. Distance between two points on the same hydrogel designated with *x*.

https://doi.org/10.1021/acs.chemrev.5c00466
Chem. Rev. XXXX, XXX, XXX−XXX

the work performed by Cai et al., where spatially variable stiffness was achieved in response to localized electrical current application.[642] Beyond the spatial tailoring of properties, the capability to dynamically alter material properties can address critical challenges in the design of materials, such as the trade-off between strength and toughness seen in many materials,[602] or the trade-off between strength and timescale of self-healing. The extraordinary functionality stemming from extrinsically toughened and strengthened hydrogels cements dynamic remodeling as an important strategy for the fabrication of advanced, responsive and adaptive materials.

6. OUTLOOK ON THE MODULATION OF TIME SCALE TO PROGRAM STRUCTURE, PROPERTIES, AND DYNAMIC HYDROGEL RESPONSES

As described throughout this review, tough dynamic hydrogels are a broad category of materials encompassing multiple length scales and hierarchical interactivity, sharing one critical feature: time-dependent mechanical properties tunable by manipulation of the fundamental kinetics and thermodynamic equilibria of constituent energy dissipation motifs. While many excellent reviews have highlighted the intrinsic relationship between multiscale structuring of polymer network and the mechanical properties of hydrogels, this review has sought to holistically explore the impact of molecular structure, both of polymers and solvent, on material timescale (Section 3) and the resulting relationship with network structure formation (Section 4), as well as the time-dependent mechanical response of these networks (Section 2), and the ability to dynamically reconfigure mechanical properties for mechanical response in response to or independently of mechanical deformation (Section 5). In addition to reviewing established schemes for hydrogels, the authors have highlighted examples of non(hydro)gel systems and dynamics which may prove useful to future works or to frame a deeper understanding of temporal behaviors within hydrogel systems.

Moreover, the goal of this structure is to encourage and enable researchers engaging in the development and/or application of hydrogels to maintain a basic, molecularly informed understanding of the fundamental parameters dictating the dynamics underlying their formation and behavior. These fundamentals include:

1) That dynamic bonds have a characteristic timescale of exchange that depends on factors such as bond enthalpy, entropic penalties or solvent restructuring, and external stimuli (dielectric of the medium, temperature, light, and cosolutes) and that these molecular scale dynamics are reflected on a macroscopic scale to determine mechanical properties. Furthermore, that the combination of multiple dynamic bonds can further improve toughness, introducing multirelaxation regimes into the material.
2) The central role of molecular structure in determining the thermodynamics, kinetics, and environmental sensitivity of dynamic bonds, which can be simplified to enthalpic or entropic bases, and further defines temperature responses and ions, pH, fields, and mechanical force in a chemical context specific fashion.
3) The defining influence of water in modulating the strength and dynamics of the reconfigurable bonds underlying hydrogels, *i.e.*, the solvation induced reordering of the relative bond hierarchy strengths as compared to that of the gas phase, providing context to key observations like the "weakest" bonds provide the toughest hydrogels.
4) The identification and classification of the thermodynamic bases underpinning workhorse as well as emerging hydrogel fabrication techniques, specifically whether polymer solvation energy or polymer configurational entropy were being manipulated to induce assembly and network formation.
5) Broadly understanding how these molecular structure shaped thermodynamic bases further inform response to external stimuli, which illustrates not only the conserved mechanistic bases of assembly regimes such as UCST, LCST, and solvent swapping, but also the intrinsic similarity between toughening mechanisms like strain-induced crystallization and assembly mechanisms such as mechanical force induced gelation.

In illustrating the consistent role of molecular structure in defining the energetic landscape of hydrogels across the broad contexts of structure and function, the authors hope to further provide a fundamental basis to leverage the design principles outlined in the comprehensive and impactful reviews on the structuring of hydrogels to maximize their toughness, ultimately catalyzing the entry to and mastery of an exceptionally diverse scientific and technological space that interweaves chemistry and materials science to directly influence biomedical engineering, soft robotics, and energy storage, among a number of other domains.

Furthermore, these fundamentals are useful not only to rationalize the state-of-the-art of hydrogels but also stimulate new insights that will drive the development of the next generation of hydrogel centered technologies. The emerging trends in the application of molecular fundamentals and toughness were specifically highlighted, such as the impact of bonding directionality, which introduces an entropic penalty and a commensurate mechanical response driven property evolution, as well as the emerging effect of ion specific interactions, which modulate the association strength of ion pairs and competitive interactions that can introduce dynamicity. Although seemingly counterintuitive, the affinity of ions may be exploited to achieve weaker polymer−polymer interactions in what is typically a strongly interacting regime, therefore achieving higher rates of dissociation, facile exchange, and improving toughness. Additionally, this can be incorporated into the fabrication of materials, which by concurrently manipulating polymer topology could enable the dual programming of network structure and material timescales for synergistic enhancement of mechanical properties. Furthermore, considering these in conjunction with the emerging ability to use multiple wavelengths of light to inscribe network connectivity in 3D dimensions opens intriguing opportunities to access the next generation of hydrogels with programed structure and dynamics. Finally, combining this hydrogel structural programming with the spatiotemporal control of its properties via remodeling, perhaps controlled by an integrated autonomously sensing and reacting computational platform and internal stimuli application system will move the distinction between a soft robot with tissue-like mechanics and life-like preparation, adaptation, and response to environments with naturally occurring organisms away from property and behavior based criteria to more fundamental questions of information propagation.

https://doi.org/10.1021/acs.chemrev.5c00466
Chem. Rev. XXXX, XXX, XXX−XXX

■ ASSOCIATED CONTENT

Supporting Information

The Supporting Information is available free of charge at https://pubs.acs.org/doi/10.1021/acs.chemrev.5c00466.

Data points and their respective sources as compiled within the Ashby Plots of Figure 2 (XLSX)

■ AUTHOR INFORMATION

Corresponding Authors

Meredith Silberstein − *Sibley School of Mechanical and Aerospace Engineering, Cornell University, Ithaca, New York 14853, United States;* orcid.org/0000-0002-6853-9796; Email: meredith.silberstein@cornell.edu

Benjamin R. McDonald − *Department of Chemistry, Brown University, Providence, Rhode Island 02912, United States;* orcid.org/0000-0002-2408-2448; Email: mcdonabe@brown.edu

Authors

Hana Tabit − *Department of Chemistry, Brown University, Providence, Rhode Island 02912, United States*

Aiden Saul − *Department of Chemistry, Brown University, Providence, Rhode Island 02912, United States*

Kennalee Orme − *Department of Chemistry, Brown University, Providence, Rhode Island 02912, United States*

Timea Kolozsvary − *Department of Chemistry, Brown University, Providence, Rhode Island 02912, United States;* orcid.org/0000-0002-0960-9985

Zachary A. Bernheimer − *Materials Science and Engineering, Cornell University, Ithaca, New York 14853, United States*

Hongyi Cai − *Materials Science and Engineering, Cornell University, Ithaca, New York 14853, United States*

Manto Lam − *Department of Chemistry, Brown University, Providence, Rhode Island 02912, United States*

Si Chen − *Materials Science and Engineering, Cornell University, Ithaca, New York 14853, United States*

Rebecca Tobias − *Department of Chemistry, Brown University, Providence, Rhode Island 02912, United States*

Manh Khang Trang − *Department of Chemistry, Brown University, Providence, Rhode Island 02912, United States*

Ryan Doherty − *Department of Chemistry, Brown University, Providence, Rhode Island 02912, United States*

Complete contact information is available at: https://pubs.acs.org/10.1021/acs.chemrev.5c00466

Author Contributions

The manuscript was written through contributions of all authors. All authors have given approval to the final version of the manuscript. CRediT: **Hana Tabit** conceptualization, writing - original draft, writing - review & editing; **Aiden Saul** conceptualization, visualization, writing - original draft, writing - review & editing; **Kennalee Orme** conceptualization, visualization, writing - original draft, writing - review & editing; **Timea Kolozsvary** visualization, writing - original draft, writing - review & editing; **Zachary Aaron Bernheimer** conceptualization, visualization, writing - original draft, writing - review & editing; **Hongyi Cai** writing - original draft; **Man To Lam** writing - original draft, writing - review & editing; **Si Chen** writing - original draft, writing - review & editing; **Rebecca Tobias** writing - original draft, writing - review & editing; **MANH KHANG TRANG** writing - original draft, writing - review & editing; **Ryan Doherty** writing - original draft, writing - review & editing; **Meredith N Silberstein** conceptualization, funding acquisition, project administration, resources, supervision, visualization, writing - original draft, writing - review & editing; **Benjamin McDonald** conceptualization, funding acquisition, project administration, resources, supervision, visualization, writing - original draft, writing - review & editing.

Notes

The authors declare no competing financial interest.

Biographies

Hana Tabit is a Ph.D. candidate in the Chemistry Department at Brown University. They completed their undergraduate studies in Chemistry at Worcester Polytechnic Institute. Hana's current research focuses on designing biomimetic ion responsiveness in synthetic macromolecules with the intent for usage in wastewater remediation.

Aiden Saul is a Ph.D. candidate in the Department of Chemistry at Brown University. He completed his undergraduate studies in Chemistry at Saint Joseph's University. He is currently focused on the design of specific-ion responsive polymers that mimic the assembly pathways of biological materials for the rational fabrication of hierarchical nanocomposites.

Kennalee Orme is a Ph.D. candidate in the Department of Chemistry at Brown University. She received her undergraduate degree in Biochemistry at Idaho State University. Her current research is focused on the development of biomimetic electrodes for green energy applications.

Timea Kolozsvary is a Ph.D. candidate in the Department of Chemistry at Brown University. She received her undergraduate degree in Chemistry from Northeastern University. Her research examines polymer topology, with a focus on bottlebrush polymers, in the design of hierarchically and self-assembled biomimetic materials.

Zachary Aaron Bernheimer is a Ph.D. student in Materials Science and Engineering at Cornell University. He received his Bachelor's degree in Chemical Physics from Hendrix College. His research focuses on understanding bioinspired and soft polymer materials through computational and experimental approaches.

Hongyi Cai received his B.E. in Macromolecular Materials and Engineering from Zhejiang University. He earned his Ph.D. in Materials Science and Engineering from Cornell University, completing his dissertation on polymer materials with dynamic bonds under the supervision of Prof. Meredith Silberstein. He is currently a research scientist in the specialty chemicals industry.

Manto Lam is a Ph.D. candidate in the Chemistry Department at Brown University. He completed his undergraduate studies in Chemistry at New York University. His current research focuses on the design and synthesis of novel polymer architectures for biomimetic hierarchical materials.

Si Chen is a postdoctoral fellow at the Engineered Living Materials Institute (ELMI) at Cornell University, where her research focuses on the mechanics of plant growth and morphogenesis. She earned her Ph.D. from UT Austin, studying mechanical properties of hydrogels. Her expertise lies at the intersection of mechanics of materials and plant biomechanics.

Rebecca Tobias is a Ph.D. candidate in the Department of Chemistry at Brown University. She completed her undergraduate studies at Austin College. Her current research interests are in high throughput characterization of polymeric material microenvironments.

https://doi.org/10.1021/acs.chemrev.5c00466
Chem. Rev. XXXX, XXX, XXX−XXX

Manh Khang Trang is a Postdoctoral Fellow in the Department of Chemistry at Brown University. He earned his undergraduate degree in Chemistry from Can Tho University and received his Ph.D. from National Yang Ming Chiao Tung University. His research is focused on programming network phase separation dynamics within ion interacting polymer gels.

Ryan Doherty is an undergraduate researcher in the Department of Chemistry at Brown University. His current research interests are in developing high-throughput polymer synthesis and characterization techniques.

Meredith Silberstein is a Professor in the Sibley School of Mechanical & Aerospace Engineering at Cornell University and Director of the Engineered Living Materials Institute. Her work on polymer multiphysics has led to the NSF CAREER, DOE Early Career, and DARPA Young Investigator awards. Meredith Silberstein's Mechanics for Materials Design Lab is devoted to using mechanical experiments and modeling methods in material design, with particular focus on multifunctional, living, and polymeric materials.

Benjamin R. McDonald is an Assistant Professor of Chemistry and Ph.D. trainer in Biomedical Engineering and Materials Engineering at Brown University. He received his Ph.D. from Northwestern University and subsequently conducted postdoctoral research in the laboratory of Prof. Timothy M. Swager at the Massachusetts Institute of Technology. He is the Principal Investigator of the BIOMM Laboratory, which seeks to translate the physicochemical principles of biomacromolecules that underly biofabrication and biofunction to synthetic material systems in order to provide new technological opportunities in the fields of biomedicine, energy, and materials science.

■ ACKNOWLEDGMENTS

A.S. and B.R.M. gratefully acknowledge the ACS Petroleum Research Fund for funding (66525-DNI7). K.M.T., M.N.S., Z.B., and B.R.M. gratefully acknowledge the NSF MOMS program for funding (CMMI-2334663 and CMMI-2334664). B.T. acknowledges the Brown Research Seed Award. H. C. and M.N.S. acknowledge the Department of Energy Biomolecular Materials Program (DE-SC0025354). S.C. acknowledges the Fleming Fellowship.

■ ABBREVIATIONS

AA (or Ac), acrylic acid; AFM, atomic force microscopy; Alg, alginate; AM (or Am), acrylamide; aq, aqueous; AR, aspect ratio; AR_c, critical aspect ratio at which rod like macromolecules can no longer rotate freely in solution; ATAC, 2-(acryloyloxy)ethyl trimethylammonium chloride; ATRP, atom transfer radical polymerization; BBP, bottlebrush polymer; BOB, triblock polymer poly(butadiene-*co*-PEO-*co*-butadiene); CB[8], cucurbit[8]uril; CE, cellulose ether; c_e, concentration of block copolymers required to enter the entanglement regime and form hydrogels; CNF, cellulose nanofibril; CS, chitosan; CTA, chain transfer agent; DA, dopamine; DAAm, diacetone acrylamide; DC, direct current; DCB, dynamic covalent bond; DCR, deprotonation-complexation-reprotonation; DCvC, dynamic covalent chemistry; De, Deborah number; DEX, dextran; DFT, density functional theory; DI, deionized; DMSO, dimethyl sulfoxide; DN, double network; DNLS, disordered natural liquid state; DTT, dithiothreitol; E_a, activation energy of bond association; ε_c, fracture strain; E_d, activation energy of bond dissociation; ELP, elastin-like polypeptide; EWC, equilibrium water content; FE-SEM, field-emission scanning electron microscopy; FTIR, Fourier Transform Infrared; G', storage modulus; G", loss modulus; Gly, glycene; GMA, glycerol monomethacrylate; H-field, magnetic field; HA, hyaluronic acid; HBA, hydrogen bond acceptor; HEDN, highly entangled double-network hydrogel; HPMA, 2-hydroxypropyl methacrylate; HSAB, Hard and Soft Acids and Bases theory; IEP, isoelectric point; IMF, intermolecular force; IOI, triblock polymer poly(isoprene-*co*-PEO-*co*-isoprene); IPN, interpenetrating network; ITC, isothermal calorimetry; k_a, rate constant for bond association; k_B, Boltzmann's constant; k_d, rate constant for bond dissociation; LBL, linear-bottlebrush-linear; LC, liquid crystalline; LCE, liquid crystal elastomer; LCST, lower critical solution temperature; LFTS, locally favored tetrahedral state; LMWA, Law of Matching Water Affinities; LOX, lysyl oxidase; MAA, methacrylate; MAM, methacrylamide; MD, molecular dynamics; MPTC, 3-(methacryloylamino)propyl-trimethylammonium chloride; NaOH, sodium hydroxide; NaPSS, poly(sodium 4-styrenesulfonate); NaSS, sodium styrenesulfonate; n_g, degree of polymerization (DP) of backbone spacer between side chains in an LBL network; n_{sc}, degree of polymerization (DP) of side chains in an LBL network; n_x, degree of polymerization (DP) of the backbone between two crosslink junctions in an LBL network; PAA, poly(acrylic acid); PAM, poly(acrylamide); PBDT, poly(2,2'-disulfonyl-4−4'-benzidine terephthalamide); PDDACl, poly(diallyldimethylammonium chloride); PDMS, polydimethylsiloxane; PEA, 2-phenoxyethyl acrylate; PEC, polyelectrolyte complex; PEG, poly(ethylene glycol); PEI, poly(ethlene imine); PEO, poly(ethylene oxide); PIBA, Poly(isobornyl acrylate); PIC, polyisocyanopeptide; PIMS, Polymerization induced microphase separation; PISA, polymerization induced self-assembly; PLA, poly(lactic acid); pNAAA, poly(*N*-acroyl beta-alaninamide); pNAGA, poly(*N*-acroyl glycinamide); pNASC, poly(*N*-acroyl semicarbazide); PnBA, poly(*n*-butyl acrylate); PMAA, poly(methacrylic acid); PMAM, poly(methacrylamide); PNIPAM, poly(*N*-isopropylacrylamide); polyTA, poly(α-thioctic acid); preCol, mussel byssus core proteins; Pro, proline; PSS, polystyrenesulfonate; PTMO, poly(tetramethylene oxide); PVA, poly(vinyl alcohol); PVA-EX, PVA hydrogels obtained via solvent exchange; PVA−OH, PVA hydrogels obtained via DCR approach; pVBIPS, poly(3-(1-(4-vinylbenzyl)-1H-imidazol-3-ium-3-yl)propane-1-sulfonate); RAFT, reversible addition−fragmentation chain-transfer; ROMP, ring-opening metathesis polymerization; RSF, regenerated silk fibroin; σ_a, debonding stress at the interface of adhesion; SAOS, small amplitude oscillatory shear rheology; SAXS, small-angle X-ray scattering; SBMA, sodium sulfobetaine methacrylate; σ_c, fracture stress at the interface of adhesion; SELP, Silk-elastin-like-peptide; SEM, scanning electron microscope; SIE, specific ion effects; SiW, nano ion $SiW_{12}O_{40}^{-4}$; SOS, triblock polymer poly(styrene-*co*-PEO-*co*-styrene); SP, spiropyran; SPN, supramolecular polymer network; σ_y, yielding stress at the interface of adhesion; t, time; T, temperature; TDS, thiuram disulfide; T_c, cloud point temperature; T_g, glass transition temperature; THF, tetrahydrofuran; τ_{pd}, timescale of polymer-rich domain diffusion during spinodal decomposition; τ_m, timescale of polymer-rich domain merging during spinodal decomposition; TTS, time−temperature-superposition; UCST, upper critical solution temperature; Upy, 2-ureido-4[1H]-pyrimidinone; UV, ultraviolet; Val, valine; Wi, Wissenberg numer; β-CD, β-cyclodextrin; ΔG, free energy; ΔG_{mix}, free energy of mixing; ΔH_a, enthalpy of bond association; ΔH_{mix}, enthalpy of mixing;

https://doi.org/10.1021/acs.chemrev.5c00466
Chem. Rev. XXXX, XXX, XXX−XXX

ΔS_{hyd}, entropy of hydration; Φ_1, volume fraction of solvent; Φ_2, volume fraction of polymer; χ, the dimensionless Flory parameter.; χ_c, a critical value of the Flory parameter, above which UCST behavior is enthalpically driven

REFERENCES

(1) Hyon, S.-H.; Cha, W.-I.; Ikada, Y.; Kita, M.; Ogura, Y.; Honda, Y. Poly(Vinyl Alcohol) Hydrogels as Soft Contact Lens Material. *J. Biomater. Sci., Polym. Ed.* **1994**, *5* (5), 397−406.

(2) Lee, K. Y.; Mooney, D. J. Hydrogels for Tissue Engineering. *Chem. Rev.* **2001**, *101* (7), 1869−1880.

(3) Kobayashi, M.; Hyu, H. S. Development and Evaluation of Polyvinyl Alcohol-Hydrogels as an Artificial Atrticular Cartilage for Orthopedic Implants. *Materials* **2010**, *3* (4), 2753−2771.

(4) Tavakoli, S.; Klar, A. S. Advanced Hydrogels as Wound Dressings. *Biomolecules* **2020**, *10* (8), 1169.

(5) Hoare, T. R.; Kohane, D. S. Hydrogels in Drug Delivery: Progress and Challenges. *Polymer* **2008**, *49* (8), 1993−2007.

(6) Zheng, W. J.; An, N.; Yang, J. H.; Zhou, J.; Chen, Y. M. Tough Al-Alginate/Poly(N-Isopropylacrylamide) Hydrogel with Tunable LCST for Soft Robotics. *ACS Appl. Mater. Interfaces* **2015**, *7* (3), 1758−1764.

(7) Jamnongkan, T.; Kaewpirom, S. Potassium Release Kinetics and Water Retention of Controlled-Release Fertilizers Based on Chitosan Hydrogels. *J. Polym. Environ* **2010**, *18* (3), 413−421.

(8) Zhuo, Y.; Chen, J.; Xiao, S.; Li, T.; Wang, F.; He, J.; Zhang, Z. Gels as Emerging Anti-Icing Materials: A Mini Review. *Mater. Horiz.* **2021**, *8* (12), 3266−3280.

(9) Wang, K.; Yao, Y.; Liu, H.; Wang, J.; Li, X.; Wang, X.; Yang, R.; Zhou, H.; Hu, X. Fabrication of Flexible Wearable Mechanosensors Utilizing Piezoelectric Hydrogels Mechanically Enhanced by Dipole−Dipole Interactions. *ACS Appl. Mater. Interfaces* **2024**, *16* (38), 51542−51553.

(10) Zhang, C.; Kwon, S. H.; Dong, L. Piezoelectric Hydrogels: Hybrid Material Design, Properties, and Biomedical Applications. *Small* **2024**, *20* (28), 2310110.

(11) Xue, B.; Bashir, Z.; Guo, Y.; Yu, W.; Sun, W.; Li, Y.; Zhang, Y.; Qin, M.; Wang, W.; Cao, Y. Strong, Tough, Rapid-Recovery, and Fatigue-Resistant Hydrogels Made of Picot Peptide Fibres. *Nat. Commun.* **2023**, *14* (1), 2583.

(12) Li, X.; Gong, J. P. Design Principles for Strong and Tough Hydrogels. *Nat. Rev. Mater.* **2024**, *9* (6), 380−398.

(13) Gu, Y.; Zhao, J.; Johnson, J. A. Polymer Networks: From Plastics and Gels to Porous Frameworks. *Angew. Chem., Int. Ed.* **2020**, *59* (13), 5022−5049.

(14) Rubinstein, M.; Colby, R. H. *Polymer Physics*; Oxford University Press, 2003.

(15) Osada, Y.; Gong, J.-P. Soft and Wet Materials: Polymer Gels. *Adv. Mater.* **1998**, *10* (11), 827−837.

(16) Almdal, K.; Dyre, J.; Hvidt, S.; Kramer, O. Towards a Phenomenological Definition of the Term 'Gel.'. *Polym. Gels Networks* **1993**, *1* (1), 5−17.

(17) Zhang, Y. S.; Khademhosseini, A. Advances in Engineering Hydrogels. *Science* **2017**, *356* (6337), eaaf3627.

(18) Kuzina, M. A.; Kartsev, D. D.; Stratonovich, A. V.; Levkin, P. A. Organogels versus Hydrogels: Advantages, Challenges, and Applications. *Adv. Funct. Mater.* **2023**, *33* (27), 2301421.

(19) Zeng, L.; Lin, X.; Li, P.; Liu, F.-Q.; Guo, H.; Li, W.-H. Recent Advances of Organogels: From Fabrications and Functions to Applications. *Prog. Org. Coat.* **2021**, *159*, 106417.

(20) Wang, H.; Heilshorn, S. C. Adaptable Hydrogel Networks with Reversible Linkages for Tissue Engineering. *Adv. Mater.* **2015**, *27* (25), 3717−3736.

(21) Drury, J. L.; Mooney, D. J. Hydrogels for Tissue Engineering: Scaffold Design Variables and Applications. *Biomaterials* **2003**, *24* (24), 4337−4351.

(22) Kopeček, J. Hydrogel Biomaterials: A Smart Future? *Biomaterials* **2007**, *28* (34), 5185−5192.

(23) Tibbitt, M. W.; Anseth, K. S. Hydrogels as Extracellular Matrix Mimics for 3D Cell Culture. *Biotechnol. Bioeng.* **2009**, *103* (4), 655−663.

(24) Peppas, N. A.; Hilt, J. Z.; Khademhosseini, A.; Langer, R. Hydrogels in Biology and Medicine: From Molecular Principles to Bionanotechnology. *Adv. Mater.* **2006**, *18* (11), 1345−1360.

(25) Spicer, C. D. Hydrogel Scaffolds for Tissue Engineering: The Importance of Polymer Choice. *Polym. Chem.* **2020**, *11* (2), 184−219.

(26) Li, X.; Luo, F.; Sun, T. L.; Cui, K.; Watanabe, R.; Nakajima, T.; Gong, J. P. Effect of Salt on Dynamic Mechanical Behaviors of Polyampholyte Hydrogels. *Macromolecules* **2023**, *56* (2), 535−544.

(27) Xian, S.; Webber, M. J. Temperature-Responsive Supramolecular Hydrogels. *J. Mater. Chem. B* **2020**, *8* (40), 9197−9211.

(28) Abdullah, T.; Okay, O. 4D Printing of Body Temperature-Responsive Hydrogels Based on Poly(Acrylic Acid) with Shape-Memory and Self-Healing Abilities. *ACS Appl. Bio Mater.* **2023**, *6* (2), 703−711.

(29) Cheng, R.; Xu, M.; Zhang, X.; Jiang, J.; Zhang, Q.; Zhao, Y. Hydrogen Bonding Enables Polymer Hydrogels with pH-Induced Reversible Dynamic Responsive Behaviors. *Angew. Chem., Int. Ed.* **2023**, *62* (23), No. e202302900.

(30) FitzSimons, T. M.; Anslyn, E. V.; Rosales, A. M. Effect of pH on the Properties of Hydrogels Cross-Linked via Dynamic Thia-Michael Addition Bonds. *ACS Polym. Au* **2022**, *2* (2), 129−136.

(31) Duan, T.; Bian, Q.; Li, H. Light-Responsive Dynamic Protein Hydrogels Based on LOVTRAP. *Langmuir* **2021**, *37* (33), 10214−10222.

(32) Wu, K.; Wu, X.; Zhang, Y.; Chen, S.; Qiao, Z.; Wei, D.; Sun, J.; Fan, H. Semiconvertible Hyaluronic Hydrogel Enabled Red-Light-Responsive Reversible Mechanics, Adhesion, and Self-Healing. *Biomacromolecules* **2022**, *23* (3), 1030−1040.

(33) Cui, N.; Han, K.; Zhou, C.; Seong, M.; Lu, T.; Jeong, H. E. A Tough Polysaccharide-Based Hydrogel with an On-Demand Dissolution Feature for Chronic Wound Care through Light-Induced Ultrafast Degradation. *ACS Appl. Bio Mater.* **2020**, *3* (12), 8338−8343.

(34) Fairbanks, B. D.; Singh, S. P.; Bowman, C. N.; Anseth, K. S. Photodegradable, Photoadaptable Hydrogels via Radical-Mediated Disulfide Fragmentation Reaction. *Macromolecules* **2011**, *44* (8), 2444−2450.

(35) Zhao, X. Multi-Scale Multi-Mechanism Design of Tough Hydrogels: Building Dissipation into Stretchy Networks. *Soft Matter* **2014**, *10* (5), 672−687.

(36) Bosnjak, N.; Silberstein, M. N. Pathways to Tough yet Soft Materials. *Science* **2021**, *374* (6564), 150−151.

(37) Creton, C. 50th Anniversary Perspective: Networks and Gels: Soft but Dynamic and Tough. *Macromolecules* **2017**, *50* (21), 8297−8316.

(38) Zhao, X.; Chen, X.; Yuk, H.; Lin, S.; Liu, X.; Parada, G. Soft Materials by Design: Unconventional Polymer Networks Give Extreme Properties. *Chem. Rev.* **2021**, *121* (8), 4309−4372.

(39) Amirthalingam, S.; Rajendran, A. K.; Moon, Y. G.; Hwang, N. S. Stimuli-Responsive Dynamic Hydrogels: Design, Properties and Tissue Engineering Applications. *Mater. Horiz.* **2023**, *10* (9), 3325−3350.

(40) Li, Z.-Y.; Liu, Y.-Y.; Li, Y.-J.; Wang, W.; Song, Y.; Zhang, J.; Tian, H. High-Preservation Single-Cell Operation through a Photo-Responsive Hydrogel-Nanopipette System. *Angew. Chem., Int. Ed.* **2021**, *60* (10), 5157−5161.

(41) Zhao, C.; Tian, S.; Liu, Q.; Xiu, K.; Lei, I.; Wang, Z.; Ma, P. X. Biodegradable Nanofibrous Temperature-Responsive Gelling Microspheres for Heart Regeneration. *Adv. Funct. Mater.* **2020**, *30* (21), 2000776.

(42) Cai, Z.; Huang, K.; Bao, C.; Wang, X.; Sun, X.; Xia, H.; Lin, Q.; Yang, Y.; Zhu, L. Precise Construction of Cell-Instructive 3D Microenvironments by Photopatterning a Biodegradable Hydrogel. *Chem. Mater.* **2019**, *31* (13), 4710−4719.

(43) Gong, J. P. Why Are Double Network Hydrogels so Tough? *Soft Matter* **2010**, *6* (12), 2583−2590.

https://doi.org/10.1021/acs.chemrev.5c00466
Chem. Rev. XXXX, XXX, XXX−XXX

(44) Li, B.; Cao, P.-F.; Saito, T.; Sokolov, A. P. Intrinsically Self-Healing Polymers: From Mechanistic Insight to Current Challenges. *Chem. Rev.* **2023**, *123* (2), 701−735.
(45) Long, R.; Mayumi, K.; Creton, C.; Narita, T.; Hui, C.-Y. Time Dependent Behavior of a Dual Cross-Link Self-Healing Gel: Theory and Experiments. *Macromolecules* **2014**, *47* (20), 7243−7250.
(46) Hu, Y.; Suo, Z. Viscoelasticity and Poroelasticity in Elastomeric Gels. *Acta Mechanica Solida Sinica* **2012**, *25* (5), 441−458.
(47) Sievers, J.; Mahajan, V.; Welzel, P. B.; Werner, C.; Taubenberger, A. Precision Hydrogels for the Study of Cancer Cell Mechanobiology. *Adv. Healthc. Mater.* **2023**, *12* (14), 2202514.
(48) Liu, S. Q.; Tay, R.; Khan, M.; Ee, P. L. R.; Hedrick, J. L.; Yang, Y. Y. Synthetic Hydrogels for Controlled Stem Cell Differentiation. *Soft Matter* **2010**, *6* (1), 67−81.
(49) Wanasinghe, S. V.; Dodo, O. J.; Konkolewicz, D. Dynamic Bonds: Adaptable Timescales for Responsive Materials. *Angew. Chem., Int. Ed.* **2022**, *61* (50), No. e202206938.
(50) Xu, Z.; Lu, J.; Lu, D.; Li, Y.; Lei, H.; Chen, B.; Li, W.; Xue, B.; Cao, Y.; Wang, W. Rapidly Damping Hydrogels Engineered through Molecular Friction. *Nat. Commun.* **2024**, *15* (1), 4895.
(51) Chen, K.; Wu, Z.; Liu, Y.; Yuan, Y.; Liu, C. Injectable Double-Crosslinked Adhesive Hydrogels with High Mechanical Resilience and Effective Energy Dissipation for Joint Wound Treatment. *Adv. Funct. Mater.* **2022**, *32* (12), 2109687.
(52) Sun, X.; Chwatko, M.; Lee, D.-H.; Bachman, J. L.; Reuther, J. F.; Lynd, N. A.; Anslyn, E. V. Chemically Triggered Synthesis, Remodeling, and Degradation of Soft Materials. *J. Am. Chem. Soc.* **2020**, *142* (8), 3913−3922.
(53) Lin, X.; Zhao, X.; Xu, C.; Wang, L.; Xia, Y. Progress in the Mechanical Enhancement of Hydrogels: Fabrication Strategies and Underlying Mechanisms. *J. Polym. Sci.* **2022**, *60* (17), 2525−2542.
(54) Xing, W.; Tang, Y. On Mechanical Properties of Nano-composite Hydrogels: Searching for Superior Properties. *Nano Materials Science* **2022**, *4* (2), 83−96.
(55) Liu, X.; Liu, J.; Lin, S.; Zhao, X. Hydrogel Machines. *Mater. Today* **2020**, *36*, 102−124.
(56) Xu, J.; Zhu, X.; Zhao, J.; Ling, G.; Zhang, P. Biomedical Applications of Supramolecular Hydrogels with Enhanced Mechanical Properties. *Adv. Colloid Interface Sci.* **2023**, *321*, 103000.
(57) Xu, C.; Chen, Y.; Zhao, S.; Li, D.; Tang, X.; Zhang, H.; Huang, J.; Guo, Z.; Liu, W. Mechanical Regulation of Polymer Gels. *Chem. Rev.* **2024**, *124* (18), 10435−10508.
(58) Fuchs, S.; Shariati, K.; Ma, M. Specialty Tough Hydrogels and Their Biomedical Applications. *Adv. Healthcare Mater.* **2020**, *9* (2), 1901396.
(59) Stojkov, G.; Niyazov, Z.; Picchioni, F.; Bose, R. K. Relationship between Structure and Rheology of Hydrogels for Various Applications. *Gels* **2021**, *7* (4), 255.
(60) Ward, I. M.; Sweeney, J. *Mechanical Properties of Solid Polymers*; Wiley, 2012.
(61) Calvet, D.; Wong, J. Y.; Giasson, S. Rheological Monitoring of Polyacrylamide Gelation: Importance of Cross-Link Density and Temperature. *Macromolecules* **2004**, *37* (20), 7762−7771.
(62) Zheng, D.; Lin, S.; Ni, J.; Zhao, X. Fracture and Fatigue of Entangled and Unentangled Polymer Networks. *Extreme Mech. Lett.* **2022**, *51*, 101608. .
(63) Buffinton, C. M.; Tong, K. J.; Blaho, R. A.; Buffinton, E. M.; Ebenstein, D. M. Comparison of Mechanical Testing Methods for Biomaterials: Pipette Aspiration, Nanoindentation, and Macroscale Testing. *J. the Mechanical Behavior of Biomedical Materials* **2015**, *51*, 367−379.
(64) Richbourg, N. R.; Rausch, M. K.; Peppas, N. A. Cross-Evaluation of Stiffness Measurement Methods for Hydrogels. *Polymer* **2022**, *258*, 125316.
(65) The Swollen Polymer Network Hypothesis: Quantitative Models of Hydrogel Swelling, Stiffness, and Solute Transport. *Prog. Polym. Sci.* **2020**, *105*, 101243. .
(66) Erman, B.; Mark, J. E. *Structures and Properties of Rubberlike Networks*; Oxford University Press, 1997.
(67) Slaughter, B. V.; Khurshid, S. S.; Fisher, O. Z.; Khademhosseini, A.; Peppas, N. A. Hydrogels in Regenerative Medicine. *Adv. Mater.* **2009**, *21* (32−33), 3307−3329.
(68) Peppas, N. A.; Reinhart, C. T. Solute Diffusion in Swollen Membranes. Part I. A New Theory. *J. Membr. Sci.* **1983**, *15* (3), 275−287.
(69) Boyce, M. C.; Arruda, E. M. Constitutive Models of Rubber Elasticity: A Review. *Rubber Chem. Technol.* **2000**, *73* (3), 504−523.
(70) Flory, P. J. Molecular Theory of Rubber Elasticity. *Polym. J.* **1985**, *17* (1), 1−12.
(71) Ross-Murphy, S. B. Rheological Characterization of Polymer Gels and Networks. *Polym. Gels Networks* **1994**, *2* (3), 229−237.
(72) Lake, G. J.; Thomas, A. G. The Strength of Highly Elastic Materials. *Proceedings of the Royal Society of London. Series A, Mathematical and Physical Sciences* **1967**, *300* (1460), 108−119.
(73) Tang, J.; Li, J.; Vlassak, J. J.; Suo, Z. Fatigue Fracture of Hydrogels. *Extreme Mechanics Letters* **2017**, *10*, 24−31.
(74) Bai, R.; Yang, J.; Morelle, X. P.; Yang, C.; Suo, Z. Fatigue Fracture of Self-Recovery Hydrogels. *ACS Macro. Lett.* **2018**, *7* (3), 312−317.
(75) Fullenkamp, D. E.; He, L.; Barrett, D. G.; Burghardt, W. R.; Messersmith, P. B. Mussel-Inspired Histidine-Based Transient Network Metal Coordination Hydrogels. *Macromolecules* **2013**, *46* (3), 1167−1174.
(76) Sun, T. L.; Kurokawa, T.; Kuroda, S.; Ihsan, A. B.; Akasaki, T.; Sato, K.; Haque, M. A.; Nakajima, T.; Gong, J. P. Physical Hydrogels Composed of Polyampholytes Demonstrate High Toughness and Viscoelasticity. *Nat. Mater.* **2013**, *12* (10), 932−937.
(77) Du, C.; Zhang, X. N.; Sun, T. L.; Du, M.; Zheng, Q.; Wu, Z. L. Hydrogen-Bond Association-Mediated Dynamics and Viscoelastic Properties of Tough Supramolecular Hydrogels. *Macromolecules* **2021**, *54* (9), 4313−4325.
(78) Zhong, D.; Xiang, Y.; Wang, Z.; Chen, Z.; Liu, J.; Wu, Z. L.; Xiao, R.; Qu, S.; Yang, W. A Visco-Hyperelastic Model for Hydrogels with Tunable Water Content. *J. the Mechanics and Physics of Solids* **2023**, *173*, 105206.
(79) Lu, T.; Wang, Z.; Tang, J.; Zhang, W.; Wang, T. A Pseudo-Elasticity Theory to Model the Strain-Softening Behavior of Tough Hydrogels. *J. the Mechanics and Physics of Solids* **2020**, *137*, 103832.
(80) Zheng, S. Y.; Yu, H. C.; Yang, C.; Hong, W.; Zhu, F.; Qian, J.; Wu, Z. L.; Zheng, Q. Fracture of Tough and Stiff Metallosupramolecular Hydrogels. *Mater. Today Phys.* **2020**, *13*, 100202.
(81) Baumberger, T.; Ronsin, O. Environmental Control of Crack Propagation in Polymer Hydrogels. *Mech. Soft Mater.* **2020**, *2* (1), 14.
(82) Creton, C.; Ciccotti, M. Fracture and Adhesion of Soft Materials: A Review. *Rep. Prog. Phys.* **2016**, *79* (4), 046601. .
(83) Starkova, O.; Aniskevich, A. Limits of Linear Viscoelastic Behavior of Polymers. *Mech Time-Depend Mater.* **2007**, *11* (2), 111−126.
(84) Lidor, G.; Maxwell, B. The Dynamic Properties of Elastomers above the Limit of Linear Viscoelastic Response. *Polym. Eng. Sci.* **1979**, *19* (15), 1092−1097.
(85) Dodda, J. M.; Deshmukh, K.; Bezuidenhout, D.; Yeh, Y.-C. Hydrogels: Definition, History, Classifications, Formation, Constitutive Characteristics, and Applications. In *Multicomponent Hydrogels: Smart Materials for Biomedical Applications;* Dodda, J. M., Deshmukh, K., Bezuidenhout, D., Eds.; The Royal Society of Chemistry, 2023.
(86) MITCHELL, J. R. THE RHEOLOGY OF GELS. *J. Texture Studies* **1980**, *11* (4), 315−337.
(87) Ward, I. M.; Sweeney, J. *Introduction to the Mechanical Properties of Solid Polymers 2e*; John Wiley & Sons Inc., 2004.
(88) Katashima, T. Rheological Studies on Polymer Networks with Static and Dynamic Crosslinks. *Polym. J.* **2021**, *53* (10), 1073−1082.
(89) Gaylord, N. G.; Van Wazer, J. R. Viscoelastic Properties of Polymers. *J. Polym. Sci.* **1961**, *51* (156), S77−S78.
(90) Tanaka, F.; Edwards, S. F. Viscoelastic Properties of Physically Crosslinked Networks Part 2. Dynamic Mechanical Moduli. *J. Non-Newtonian Fluid Mech.* **1992**, *43* (2−3), 273−288. .

https://doi.org/10.1021/acs.chemrev.5c00466
Chem. Rev. XXXX, XXX, XXX−XXX

(91) Grindy, S. C.; Learsch, R.; Mozhdehi, D.; Cheng, J.; Barrett, D. G.; Guan, Z.; Messersmith, P. B.; Holten-Andersen, N. Control of Hierarchical Polymer Mechanics with Bioinspired Metal-Coordination Dynamics. *Nat. Mater.* **2015**, *14* (12), 1210−1216.
(92) Webber, M. J.; Tibbitt, M. W. Dynamic and Reconfigurable Materials from Reversible Network Interactions. *Nat. Rev. Mater.* **2022**, *7* (7), 541−556.
(93) Tanner, R. I. A Test Particle Approach to Flow Classification for Viscoelastic Fluids. *AIChE J.* **1976**, *22* (5), 910−918.
(94) Poole, R. J. *The Deborah and Weissenberg Numbers*; Rheology Bulletin; The British Society of Rheology, 2012; Vol. *2*.
(95) Thompson, R. L.; Oishi, C. M. Reynolds and Weissenberg Numbers in Viscoelastic Flows. *J. Non-Newtonian Fluid Mech.* **2021**, *292*, 104550.
(96) Chen, Q.; Tudryn, G. J.; Colby, R. H. Ionomer Dynamics and the Sticky Rouse Modela. *J. Rheol.* **2013**, *57* (5), 1441−1462.
(97) Rouse, P. E., Jr. A Theory of the Linear Viscoelastic Properties of Dilute Solutions of Coiling Polymers. *J. Chem. Phys.* **1953**, *21* (7), 1272−1280.
(98) Liu, X. Y.; Liu, J.; Lin, S. T.; Zhao, X. H. Hydrogel Machines. *Mater. Today* **2020**, *36*, 102−124.
(99) Yu, G.; Yan, X.; Han, C.; Huang, F. Characterization of Supramolecular Gels. *Chem. Soc. Rev.* **2013**, *42* (16), 6697−6722.
(100) Zhao, Y.; Beck, J. B.; Rowan, S. J.; Jamieson, A. M. Rheological Behavior of Shear-Responsive Metallo-Supramolecular Gels. *Macromolecules* **2004**, *37* (10), 3529−3531.
(101) Oyen, M. L. Mechanical Characterisation of Hydrogel Materials. *International Materials Reviews* **2014**, *59* (1), 44−59.
(102) Cui, K.; Gong, J. P. How Double Dynamics Affects the Large Deformation and Fracture Behaviors of Soft Materials. *J. Rheol.* **2022**, *66* (6), 1093−1111.
(103) Bai, R. B.; Yang, J. W.; Suo, Z. G. Fatigue of Hydrogels. *EUROPEAN JOURNAL OF MECHANICS A-SOLIDS* **2019**, *74*, 337−370.
(104) Lin, S.; Liu, X.; Liu, J.; Yuk, H.; Loh, H.-C.; Parada, G. A.; Settens, C.; Song, J.; Masic, A.; McKinley, G. H.; Zhao, X. Anti-Fatigue-Fracture Hydrogels. *Sci. Adv.* **2019**, *5* (1), eaau8528.
(105) Zhan, L.; Qu, S.; Xiao, R. A Review on the Mullins Effect in Tough Elastomers and Gels. *Acta Mech. Solida Sin.* **2024**, *37* (2), 181−214.
(106) Münstedt, H. Rheological Experiments at Constant Stress as Efficient Method to Characterize Polymeric Materials. *J. Rheol.* **2014**, *58* (3), 565−587.
(107) Van Lijsebetten, F.; Debsharma, T.; Winne, J. M.; Du Prez, F. E. A Highly Dynamic Covalent Polymer Network without Creep: Mission Impossible? *Angew. Chem., Int. Ed.* **2022**, *61* (48), No. e202210405.
(108) Qiu, H. N.; Lin, J.; Hou, L. X.; Xiao, R.; Zheng, Q.; Wu, Z. L. Stress Relaxation and Creep Response of Glassy Hydrogels with Dense Physical Associations. *ACS Appl. Mater. Interfaces* **2025**, *17* (6), 9981−9991.
(109) Long, R.; Hui, C.-Y. Fracture Toughness of Hydrogels: Measurement and Interpretation. *Soft Matter* **2016**, *12* (39), 8069−8086.
(110) Rivlin, R. S.; Thomas, A. G. Rupture of Rubber. I. Characteristic Energy for Tearing. *J. Polym. Sci.* **1953**, *10* (3), 291−318.
(111) Yu, Y.; Bouklas, N.; Landis, C. M.; Huang, R. Poroelastic Effects on the Time- and Rate-Dependent Fracture of Polymer Gels. *J. Appl. Mech.* **2020**, *87*, 031005. .
(112) Bouklas, N.; Landis, C. M.; Huang, R. Effect of Solvent Diffusion on Crack-Tip Fields and Driving Force for Fracture of Hydrogels. *J. Appl. Mech.* **2015**, *82*, 081007. .
(113) Knauss, W. G. A Review of Fracture in Viscoelastic Materials. *Int. J. Fract.* **2015**, *196* (1), 99−146.
(114) Chen, S.; Ravi-Chandar, K. Rate-Dependent Fracture Behavior of Gelatin-Based Hydrogels. *Int. J. Fract.* **2023**, *243* (2), 185−202.
(115) Qi, Y.; Li, X.; Venkata, S. P.; Yang, X.; Sun, T. L.; Hui, C.-Y.; Gong, J. P.; Long, R. Mapping Deformation and Dissipation during Fracture of Soft Viscoelastic Solid. *J. the Mechanics and Physics of Solids* **2024**, *186*, 105595.
(116) Knauss, W. G. Stable and Unstable Crack Growth in Viscoelastic Media. *Transactions of The Society of Rheology* **1969**, *13* (3), 291−313.
(117) Knauss, W. G. Delayed Failure—the Griffith Problem for Linearly Viscoelastic Materials. *International J. Fracture Mechanics* **1970**, *6* (1), 7−20.
(118) Knauss, W. G. On the Steady Propagation of a Crack in a Viscoelastic Sheet: Experiments and Analysis. In *Deformation and Fracture of High Polymers*; Kausch, H. H., Hassell, J. A., Jaffee, R. I., Eds.; Springer US: Boston, MA, 1973; pp 501−541.
(119) Schapery, R. A. A Theory of Crack Initiation and Growth in Viscoelastic Media. *Int. J. Fract.* **1975**, *11* (4), 549−562.
(120) Schapery, R. A. A Theory of Crack Initiation and Growth in Viscoelastic Media II. Approximate Methods of Analysis. *Int. J. Fract.* **1975**, *11* (3), 369−388.
(121) Schapery, R. A. A Theory of Crack Initiation and Growth in Viscoelastic Media. *Int. J. Fract.* **1975**, *11* (1), 141−159.
(122) Persson, B. N. J.; Brener, E. A. Crack Propagation in Viscoelastic Solids. *Phys. Rev. E* **2005**, *71* (3), No. 036123.
(123) Tobolsky, A.; Eyring, H. Mechanical Properties of Polymeric Materials. *J. Chem. Phys.* **1943**, *11* (3), 125−134.
(124) Taylor, D. L.; in het Panhuis, M. Self-Healing Hydrogels. *Adv. Mater.* **2016**, *28* (41), 9060−9093.
(125) Zhang, H.; Wang, C.; Zhu, G.; Zacharia, N. S. Self-Healing of Bulk Polyelectrolyte Complex Material as a Function of pH and Salt. *ACS Appl. Mater. Interfaces* **2016**, *8* (39), 26258−26265.
(126) Samanta, S.; Kim, S.; Saito, T.; Sokolov, A. P. Polymers with Dynamic Bonds: Adaptive Functional Materials for a Sustainable Future. *J. Phys. Chem. B* **2021**, *125* (33), 9389−9401.
(127) Mozhdehi, D.; Neal, J. A.; Grindy, S. C.; Cordeau, Y.; Ayala, S.; Holten-Andersen, N.; Guan, Z. Tuning Dynamic Mechanical Response in Metallopolymer Networks through Simultaneous Control of Structural and Temporal Properties of the Networks. *Macromolecules* **2016**, *49* (17), 6310−6321.
(128) Dong, L.; Li, L.; Chen, H.; Cao, Y.; Lei, H. Mechanochemistry: Fundamental Principles and Applications. *Adv. Sci.* **2025**, *12*, 2403949.
(129) Rakshit, S.; Zhang, Y.; Manibog, K.; Shafraz, O.; Sivasankar, S. Ideal, Catch, and Slip Bonds in Cadherin Adhesion. *Proc. Natl. Acad. Sci. U. S. A.* **2012**, *109* (46), 18815−18820.
(130) Bell, G. I. Models for the Specific Adhesion of Cells to Cells: A Theoretical Framework for Adhesion Mediated by Reversible Bonds between Cell Surface Molecules. *Science* **1978**, *200* (4342), 618−627.
(131) Stukalin, E. B.; Cai, L.-H.; Kumar, N. A.; Leibler, L.; Rubinstein, M. Self-Healing of Unentangled Polymer Networks with Reversible Bonds. *Macromolecules* **2013**, *46* (18), 7525−7541.
(132) Thomas, S.; Surendran, A. *Self-Healing Polymer-Based Systems*; Elsevier, 2020.
(133) Zhao, Y. H.; Jie, Y. S.; Xue, Y. C.; Shi, Z. W.; Dong, Y. C.; Muthukumar, M.; Jia, D. Universal Law of Hierarchical Dynamics in Gels Arising from Confluence of Local Physically Dynamic Bonds. *Nat. Commun.* **2025**, *16* (1), 3247.
(134) Tito, N. B.; Creton, C.; Storm, C.; Ellenbroek, W. G. Harnessing Entropy to Enhance Toughness in Reversibly Crosslinked Polymer Networks. *Soft Matter* **2019**, *15* (10), 2190−2203.
(135) Marco-Dufort, B.; Iten, R.; Tibbitt, M. W. Linking Molecular Behavior to Macroscopic Properties in Ideal Dynamic Covalent Networks. *J. Am. Chem. Soc.* **2020**, *142* (36), 15371−15385.
(136) Appel, E. A.; del Barrio, J.; Loh, X. J.; Scherman, O. A. Supramolecular Polymeric Hydrogels. *Chem. Soc. Rev.* **2012**, *41* (18), 6195−6214.
(137) Parada, G. A.; Zhao, X. Ideal Reversible Polymer Networks. *Soft Matter* **2018**, *14* (25), 5186−5196.

https://doi.org/10.1021/acs.chemrev.5c00466
Chem. Rev. XXXX, XXX, XXX−XXX

(138) Tang, S.; Wang, M.; Olsen, B. D. Anomalous Self-Diffusion and Sticky Rouse Dynamics in Associative Protein Hydrogels. *J. Am. Chem. Soc.* **2015**, *137* (11), 3946−3957.
(139) Zhang, Z.; Chen, Q.; Colby, R. H. Dynamics of Associative Polymers. *Soft Matter* **2018**, *14* (16), 2961−2977.
(140) McLeish, T. The Science of Softness. In *Soft Matter: A Very Short Introduction*; McLeish, T., Ed.; Oxford University Press, 2020.
(141) Elling, B. R.; Dichtel, W. R. Reprocessable Cross-Linked Polymer Networks: Are Associative Exchange Mechanisms Desirable? *ACS Cent. Sci.* **2020**, *6* (9), 1488−1496.
(142) Zhang, X.; Vidavsky, Y.; Aharonovich, S.; Yang, S. J.; Buche, M. R.; Diesendruck, C. E.; Silberstein, M. N. Bridging Experiments and Theory: Isolating the Effects of Metal−Ligand Interactions on Viscoelasticity of Reversible Polymer Networks. *Soft Matter* **2020**, *16* (37), 8591−8601.
(143) Xiang, S.-L.; Hua, Q.-X.; Gong, W.-L.; Xie, N.-H.; Zhao, P.-J.; Cheng, G. J.; Li, C.; Zhu, M.-Q. Photoplastic Transformation Based on Dynamic Covalent Chemistry. *ACS Appl. Mater. Interfaces* **2019**, *11* (26), 23623−23631.
(144) Cai, D.; Xia, R.; Shao, Y.; Chen, G.; Liu, L.; Li, Y.; Zhang, P.; Zhi, Y.; Li, C.; Wen, Y.; Cheng, X.; Liu, J.; Yu, Y. Mechanically Compatible Sealing of Hydrogel with Coherent Interface. *Adv. Mater.* **2025**, *37* (12), 2414515.
(145) Yu, A. C.; Lian, H.; Kong, X.; Lopez Hernandez, H.; Qin, J.; Appel, E. A. Physical Networks from Entropy-Driven Non-Covalent Interactions. *Nat. Commun.* **2021**, *12* (1), 746.
(146) Ashter, S. A. 6 - Mechanics of Materials. In *Thermoforming of Single and Multilayer Laminates*; Ashter, S. A., Ed.; William Andrew Publishing: Oxford, 2014; pp 123−145.
(147) Liu, M.; Guo, J.; Hui, C.-Y.; Creton, C.; Narita, T.; Zehnder, A. Time-Temperature Equivalence in a PVA Dual Cross-Link Self-Healing Hydrogel. *J. Rheol.* **2018**, *62* (4), 991−1000.
(148) Söntjens, S. H. M.; Sijbesma, R. P.; van Genderen, M. H. P.; Meijer, E. W. Stability and Lifetime of Quadruply Hydrogen Bonded 2-Ureido-4[1H]-Pyrimidinone Dimers. *J. Am. Chem. Soc.* **2000**, *122* (31), 7487−7493.
(149) Sun, P.; Li, Y.; Qin, B.; Xu, J.-F.; Zhang, X. Super Strong and Multi-Reusable Supramolecular Epoxy Hot Melt Adhesives. *ACS Materials Lett.* **2021**, *3* (7), 1003−1009.
(150) Zhao, C.; Gong, X.; Wang, S.; Jiang, W.; Xuan, S. Shear Stiffening Gels for Intelligent Anti-Impact Applications. *Cell Rep. Phys. Sci.* **2020**, *1* (12), 100266.
(151) Hiemenz, P. C. *Polymer Chemistry: The Basic Concepts*; M. Dekker: New York, 1984.
(152) Miller-Chou, B. A.; Koenig, J. L. A Review of Polymer Dissolution. *Prog. Polym. Sci.* **2003**, *28* (8), 1223−1270.
(153) Pappu, R. V.; Cohen, S. R.; Dar, F.; Farag, M.; Kar, M. Phase Transitions of Associative Biomacromolecules. *Chem. Rev.* **2023**, *123*, 8945. .
(154) Lin, Y.-H.; Forman-Kay, J. D.; Chan, H. S. Theories for Sequence-Dependent Phase Behaviors of Biomolecular Condensates. *Biochemistry* **2018**, *57* (17), 2499−2508.
(155) Pettersson, L. G. M.; Henchman, R. H.; Nilsson, A. Water—The Most Anomalous Liquid. *Chem. Rev.* **2016**, *116* (13), 7459−7462.
(156) Gallo, P.; Amann-Winkel, K.; Angell, C. A.; Anisimov, M. A.; Caupin, F.; Chakravarty, C.; Lascaris, E.; Loerting, T.; Panagiotopoulos, A. Z.; Russo, J.; Sellberg, J. A.; Stanley, H. E.; Tanaka, H.; Vega, C.; Xu, L.; Pettersson, L. G. M. Water: A Tale of Two Liquids. *Chem. Rev.* **2016**, *116* (13), 7463−7500.
(157) Kontogeorgis, G. M.; Holster, A.; Kottaki, N.; Tsochantaris, E.; Topsøe, F.; Poulsen, J.; Bache, M.; Liang, X.; Blom, N. S.; Kronholm, J. Water Structure, Properties and Some Applications—A Review. *Chem. Thermodyn. Therm. Anal.* **2022**, *6*, 100053.
(158) Breynaert, E.; Houlleberghs, M.; Radhakrishnan, S.; Grübel, G.; Taulelle, F.; Martens, J. A. Water as a Tuneable Solvent: A Perspective. *Chem. Soc. Rev.* **2020**, *49* (9), 2557−2569.
(159) Gonella, G.; Backus, E. H. G.; Nagata, Y.; Bonthuis, D. J.; Loche, P.; Schlaich, A.; Netz, R. R.; Kühnle, A.; McCrum, I. T.; Koper, M. T. M.; Wolf, M.; Winter, B.; Meijer, G.; Campen, R. K.; Bonn, M. Water at Charged Interfaces. *Nature Reviews Chemistry* **2021**, *5* (7), 466−485.
(160) Gregory, J. K.; Clary, D. C.; Liu, K.; Brown, M. G.; Saykally, R. J. The Water Dipole Moment in Water Clusters. *Science* **1997**, *275* (5301), 814−817.
(161) Shi, R.; Tanaka, H. Direct Evidence in the Scattering Function for the Coexistence of Two Types of Local Structures in Liquid Water. *J. Am. Chem. Soc.* **2020**, *142* (6), 2868−2875.
(162) Suarez-Martinez, P. C.; Batys, P.; Sammalkorpi, M.; Lutkenhaus, J. L. Time−Temperature and Time−Water Superposition Principles Applied to Poly(Allylamine)/Poly(Acrylic Acid) Complexes. *Macromolecules* **2019**, *52* (8), 3066−3074.
(163) Fabre, V.; Quandalle, G.; Billon, N.; Cantournet, S. Time-Temperature-Water Content Equivalence on Dynamic Mechanical Response of Polyamide 6,6. *Polymer* **2018**, *137*, 22−29.
(164) Ishisaka, A.; Kawagoe, M. Examination of the Time−Water Content Superposition on the Dynamic Viscoelasticity of Moistened Polyamide 6 and Epoxy. *J. Appl. Polym. Sci.* **2004**, *93* (2), 560−567.
(165) Levin, M.; Cohen, N. Thermo-Mechanics of PNIPAM Gels: From a Single Chain to a Network Response. *Macromolecules* **2025**, *58*, 5187. .
(166) Biedermann, F.; Schneider, H.-J. Experimental Binding Energies in Supramolecular Complexes. *Chem. Rev.* **2016**, *116* (9), 5216−5300.
(167) Hobza, P. Calculations on Noncovalent Interactions and Databases of Benchmark Interaction Energies. *Acc. Chem. Res.* **2012**, *45* (4), 663−672.
(168) Steiner, T. The Hydrogen Bond in the Solid State. *Angew. Chem., Int. Ed.* **2002**, *41* (1), 48−76.
(169) Markovitch, O.; Agmon, N. Structure and Energetics of the Hydronium Hydration Shells. *J. Phys. Chem. A* **2007**, *111* (12), 2253−2256.
(170) Ye, J.; Fu, S.; Zhou, S.; Li, M.; Li, K.; Sun, W.; Zhai, Y. Advances in Hydrogels Based on Dynamic Covalent Bonding and Prospects for Its Biomedical Application. *Eur. Polym. J.* **2020**, *139*, 110024.
(171) Xianyu, B.; Xu, H. Dynamic Covalent Bond-Based Materials: From Construction to Biomedical Applications. *Supramolecular Materials* **2024**, *3*, 100070.
(172) Zhang, V.; Kang, B.; Accardo, J. V.; Kalow, J. A. Structure−Reactivity−Property Relationships in Covalent Adaptable Networks. *J. Am. Chem. Soc.* **2022**, *144* (49), 22358−22377.
(173) Majumdar, S.; Mezari, B.; Zhang, H.; van Aart, J.; van Benthem, R. A. T. M.; Heuts, J. P. A.; Sijbesma, R. P. Efficient Exchange in a Bioinspired Dynamic Covalent Polymer Network via a Cyclic Phosphate Triester Intermediate. *Macromolecules* **2021**, *54* (17), 7955−7962.
(174) Li, L.; Peng, X.; Zhu, D.; Zhang, J.; Xiao, P. Recent Progress in Polymers with Dynamic Covalent Bonds. *Macromol. Chem. Phys.* **2023**, *224* (20), 2300224.
(175) Han, Y.; Cao, Y.; Lei, H. Dynamic Covalent Hydrogels: Strong yet Dynamic. *Gels* **2022**, *8* (9), 577.
(176) Escobar, F. I.; Anseth, K. S.; Schultz, K. M. Dynamic Changes in Material Properties and Degradation of Poly(Ethylene Glycol)−Hydrazone Gels as a Function of pH. *Macromolecules* **2017**, *50* (18), 7351−7360.
(177) Kathan, M.; Kovaříček, P.; Jurissek, C.; Senf, A.; Dallmann, A.; Thünemann, A. F.; Hecht, S. Control of Imine Exchange Kinetics with Photoswitches to Modulate Self-Healing in Polysiloxane Networks by Light Illumination. *Angew. Chem., Int. Ed.* **2016**, *55* (44), 13882−13886.
(178) Self, J. L.; Dolinski, N. D.; Zayas, M. S.; Read de Alaniz, J.; Bates, C. M. Brønsted-Acid-Catalyzed Exchange in Polyester Dynamic Covalent Networks. *ACS Macro Lett.* **2018**, *7* (7), 817−821.
(179) Cromwell, O. R.; Chung, J.; Guan, Z. Malleable and Self-Healing Covalent Polymer Networks through Tunable Dynamic Boronic Ester Bonds. *J. Am. Chem. Soc.* **2015**, *137* (20), 6492−6495.

https://doi.org/10.1021/acs.chemrev.5c00466
Chem. Rev. XXXX, XXX, XXX−XXX

(180) Delahaye, M.; Winne, J. M.; Du Prez, F. E. Internal Catalysis in Covalent Adaptable Networks: Phthalate Monoester Transesterification As a Versatile Dynamic Cross-Linking Chemistry. *J. Am. Chem. Soc.* **2019**, *141* (38), 15277−15287.
(181) Reisinger, D.; Kriehuber, M. U.; Bender, M.; Bautista-Anguís, D.; Rieger, B.; Schlögl, S. Thermally Latent Bases in Dynamic Covalent Polymer Networks and Their Emerging Applications. *Adv. Mater.* **2023**, *35* (24), 2300830.
(182) Jourdain, A.; Asbai, R.; Anaya, O.; Chehimi, M. M.; Drockenmuller, E.; Montarnal, D. Rheological Properties of Covalent Adaptable Networks with 1,2,3-Triazolium Cross-Links: The Missing Link between Vitrimers and Dissociative Networks. *Macromolecules* **2020**, *53* (6), 1884−1900.
(183) Webber, M. J.; Appel, E. A.; Meijer, E. W.; Langer, R. Supramolecular Biomaterials. *Nat. Mater.* **2016**, *15* (1), 13−26.
(184) Scheutz, G. M.; Lessard, J. J.; Sims, M. B.; Sumerlin, B. S. Adaptable Crosslinks in Polymeric Materials: Resolving the Intersection of Thermoplastics and Thermosets. *J. Am. Chem. Soc.* **2019**, *141* (41), 16181−16196.
(185) De Alwis Watuthanthrige, N.; Chakma, P.; Konkolewicz, D. Designing Dynamic Materials from Dynamic Bonds to Macromolecular Architecture. *Trends in Chemistry* **2021**, *3* (3), 231−247.
(186) Zheng, N.; Xu, Y.; Zhao, Q.; Xie, T. Dynamic Covalent Polymer Networks: A Molecular Platform for Designing Functions beyond Chemical Recycling and Self-Healing. *Chem. Rev.* **2021**, *121* (3), 1716−1745.
(187) Podgórski, M.; Fairbanks, B. D.; Kirkpatrick, B. E.; McBride, M.; Martinez, A.; Dobson, A.; Bongiardina, N. J.; Bowman, C. N. Toward Stimuli-Responsive Dynamic Thermosets through Continuous Development and Improvements in Covalent Adaptable Networks (CANs). *Adv. Mater.* **2020**, *32* (20), 1906876.
(188) Zhang, V.; Accardo, J. V.; Kevlishvili, I.; Woods, E. F.; Chapman, S. J.; Eckdahl, C. T.; Stern, C. L.; Kulik, H. J.; Kalow, J. A. Tailoring Dynamic Hydrogels by Controlling Associative Exchange Rates. *Chem.* **2023**, *9* (8), 2298−2317.
(189) Lou, J.; Friedowitz, S.; Will, K.; Qin, J.; Xia, Y. Predictably Engineering the Viscoelastic Behavior of Dynamic Hydrogels via Correlation with Molecular Parameters. *Adv. Mater.* **2021**, *33* (51), 2104460.
(190) Mukherjee, S.; Hill, M. R.; Sumerlin, B. S. Self-Healing Hydrogels Containing Reversible Oxime Crosslinks. *Soft Matter* **2015**, *11* (30), 6152−6161.
(191) Wang, C.; Shen, Z.; Hu, P.; Wang, T.; Zhang, X.; Liang, L.; Bai, J.; Qiu, L.; Lai, X.; Yang, X.; Zhang, K. Facile Fabrication and Characterization of High-Performance Borax-PVA Hydrogel. *J. Sol-Gel Sci. Technol.* **2022**, *101* (1), 103−113.
(192) Liu, Y.; Liu, Y.; Wang, Q.; Han, Y.; Chen, H.; Tan, Y. Doubly Dynamic Hydrogel Formed by Combining Boronate Ester and Acylhydrazone Bonds. *Polymers* **2020**, *12* (2), 487.
(193) Yesilyurt, V.; Ayoob, A. M.; Appel, E. A.; Borenstein, J. T.; Langer, R.; Anderson, D. G. Mixed Reversible Covalent Crosslink Kinetics Enable Precise, Hierarchical Mechanical Tuning of Hydrogel Networks. *Adv. Mater.* **2017**, *29* (19), 1605947.
(194) Cornellà, A. C.; Furia, F.; Van Assche, G.; Brancart, J. Controlling the Relaxation Dynamics of Polymer Networks by Combining Associative and Dissociative Dynamic Covalent Bonds. *Adv. Mater.* **2024**, *36* (46), 2407663.
(195) Liu, X.; Wu, J.; Tang, Z.; Wu, J.; Huang, Z.; Yin, X.; Du, J.; Lin, X.; Lin, W.; Yi, G. Photoreversible Bond-Based Shape Memory Polyurethanes with Light-Induced Self-Healing, Recyclability, and 3D Fluorescence Encryption. *ACS Appl. Mater. Interfaces* **2022**, *14* (29), 33829−33841.
(196) Petelinšek, N.; Mommer, S. Tough Hydrogels for Load-Bearing Applications. *Adv. Sci.* **2024**, *11* (12), 2307404.
(197) Knight, A. S.; Larsson, J.; Ren, J. M.; Bou Zerdan, R.; Seguin, S.; Vrahas, R.; Liu, J.; Ren, G.; Hawker, C. J. Control of Amphiphile Self-Assembly via Bioinspired Metal Ion Coordination. *J. Am. Chem. Soc.* **2018**, *140* (4), 1409−1414.
(198) Zha, X.; Chen, Y.; Fan, H.; Yang, Y.; Xiong, Y.; Xu, G.; Yan, K.; Wang, Y.; Xie, Y.; Wang, D. Handedness Inversion of Chiral 3-Aminophenol Formaldehyde Resin Nanotubes Mediated by Metal Coordination. *Angew. Chem., Int. Ed.* **2021**, *60* (14), 7759−7769.
(199) Park, S. H.; Jung, S. H.; Ahn, J.; Lee, J. H.; Kwon, K.-Y.; Jeon, J.; Kim, H.; Jaworski, J.; Jung, J. H. Reversibly Tunable Helix Inversion in Supramolecular Gels Trigged by Co2+. *Chem. Commun.* **2014**, *50* (88), 13495−13498.
(200) Henderson, K. J.; Zhou, T. C.; Otim, K. J.; Shull, K. R. Ionically Cross-Linked Triblock Copolymer Hydrogels with High Strength. *Macromolecules* **2010**, *43* (14), 6193−6201.
(201) Irving, H.; Williams, R. J. P. 637. The Stability of Transition-Metal Complexes. *J. Chem. Soc.* **1953**, No. 0, 3192−3210.
(202) Irving, H.; Williams, R. J. P. Order of Stability of Metal Complexes. *Nature* **1948**, *162* (4123), 746−747.
(203) Grant, G. T.; Morris, E. R.; Rees, D. A.; Smith, P. J. C.; Thom, D. Biological Interactions between Polysaccharides and Divalent Cations: The Egg-Box Model. *FEBS Lett.* **1973**, *32* (1), 195−198.
(204) Morris, E. R.; Rees, D. A.; Thom, D.; Boyd, J. Chiroptical and Stoichiometric Evidence of a Specific, Primary Dimerisation Process in Alginate Gelation. *Carbohydr. Res.* **1978**, *66* (1), 145−154.
(205) Thom, D.; Grant, G. T.; Morris, E. R.; Rees, D. A. Characterisation of Cation Binding and Gelation of Polyuronates by Circular Dichroism. *Carbohydr. Res.* **1982**, *100* (1), 29−42.
(206) Sun, J.-Y.; Zhao, X.; Illeperuma, W. R. K.; Chaudhuri, O.; Oh, K. H.; Mooney, D. J.; Vlassak, J. J.; Suo, Z. Highly Stretchable and Tough Hydrogels. *Nature* **2012**, *489* (7414), 133−136.
(207) Li, J.; Illeperuma, W. R. K.; Suo, Z.; Vlassak, J. J. Hybrid Hydrogels with Extremely High Stiffness and Toughness. *ACS Macro Lett.* **2014**, *3* (6), 520−523.
(208) Fang, Y.; Al-Assaf, S.; Phillips, G. O.; Nishinari, K.; Funami, T.; Williams, P. A.; Li, L. Multiple Steps and Critical Behaviors of the Binding of Calcium to Alginate. *J. Phys. Chem. B* **2007**, *111* (10), 2456−2462.
(209) Pearson, R. G. Hard and Soft Acids and Bases, HSAB, Part 1: Fundamental Principles. *J. Chem. Educ.* **1968**, *45* (9), 581.
(210) Pearson, R. G. Hard and Soft Acids and Bases, HSAB, Part II: Underlying Theories. *J. Chem. Educ.* **1968**, *45* (10), 643.
(211) Dharmapriya, T. N.; Lee, D.-Y.; Huang, P.-J. Novel Reusable Hydrogel Adsorbents for Precious Metal Recycle. *Sci. Rep.* **2021**, *11* (1), 19577.
(212) Tang, S.; Olsen, B. D. Relaxation Processes in Supramolecular Metallogels Based on Histidine−Nickel Coordination Bonds. *Macromolecules* **2016**, *49* (23), 9163−9175.
(213) Ahmadi, M.; Seiffert, S. Coordination Geometry Preference Regulates the Structure and Dynamics of Metallo-Supramolecular Polymer Networks. *Macromolecules* **2021**, *54* (3), 1388−1400.
(214) Zheng, S. Y.; Ding, H.; Qian, J.; Yin, J.; Wu, Z. L.; Song, Y.; Zheng, Q. Metal-Coordination Complexes Mediated Physical Hydrogels with High Toughness, Stick−Slip Tearing Behavior, and Good Processability. *Macromolecules* **2016**, *49* (24), 9637−9646.
(215) Barrett, D. G.; Fullenkamp, D. E.; He, L.; Holten-Andersen, N.; Lee, K. Y. C.; Messersmith, P. B. pH-Based Regulation of Hydrogel Mechanical Properties Through Mussel-Inspired Chemistry and Processing. *Adv. Funct. Mater.* **2013**, *23* (9), 1111−1119.
(216) Tang, Q.; Zhao, D.; Yang, H.; Wang, L.; Zhang, X. A pH-Responsive Self-Healing Hydrogel Based on Multivalent Coordination of Ni2+ with Polyhistidine-Terminated PEG and IDA-Modified Oligochitosan. *J. Mater. Chem. B* **2019**, *7* (1), 30−42.
(217) Lu, L.; Tian, T.; Wu, S.; Xiang, T.; Zhou, S. A pH-Induced Self-Healable Shape Memory Hydrogel with Metal-Coordination Cross-Links. *Polym. Chem.* **2019**, *10* (15), 1920−1929.
(218) Holten-Andersen, N.; Harrington, M. J.; Birkedal, H.; Lee, B. P.; Messersmith, P. B.; Lee, K. Y. C.; Waite, J. H. pH-Induced Metal-Ligand Cross-Links Inspired by Mussel Yield Self-Healing Polymer Networks with near-Covalent Elastic Moduli. *Proc. Natl. Acad. Sci. U. S. A.* **2011**, *108* (7), 2651−2655.
(219) Yount, W. C.; Loveless, D. M.; Craig, S. L. Strong Means Slow: Dynamic Contributions to the Bulk Mechanical Properties of

https://doi.org/10.1021/acs.chemrev.5c00466
Chem. Rev. XXXX, XXX, XXX−XXX

Supramolecular Networks. *Angew. Chem., Int. Ed.* **2005**, *44* (18), 2746−2748.
(220) Loveless, D. M.; Jeon, S. L.; Craig, S. L. Chemoresponsive Viscosity Switching of a Metallo-Supramolecular Polymer Network near the Percolation Threshold. *J. Mater. Chem.* **2007**, *17* (1), 56−61.
(221) Rao, Y.-L.; Chortos, A.; Pfattner, R.; Lissel, F.; Chiu, Y.-C.; Feig, V.; Xu, J.; Kurosawa, T.; Gu, X.; Wang, C.; He, M.; Chung, J. W.; Bao, Z. Stretchable Self-Healing Polymeric Dielectrics Cross-Linked Through Metal−Ligand Coordination. *J. Am. Chem. Soc.* **2016**, *138* (18), 6020−6027.
(222) Nonoyama, T.; Lee, Y. W.; Ota, K.; Fujioka, K.; Hong, W.; Gong, J. P. Instant Thermal Switching from Soft Hydrogel to Rigid Plastics Inspired by Thermophile Proteins. *Adv. Mater.* **2020**, *32* (4), 1905878.
(223) Takahashi, R.; Wu, Z. L.; Arifuzzaman, M.; Nonoyama, T.; Nakajima, T.; Kurokawa, T.; Gong, J. P. Control Superstructure of Rigid Polyelectrolytes in Oppositely Charged Hydrogels via Programmed Internal Stress. *Nat. Commun.* **2014**, *5* (1), 4490.
(224) Fan, H. L.; Wang, J. H.; Tao, Z.; Huang, J. C.; Rao, P.; Kurokawa, T.; Gong, J. P. Adjacent Cationic-Aromatic Sequences Yield Strong Electrostatic Adhesion of Hydrogels in Seawater. *Nat. Commun.* **2019**, *10*, 5127.
(225) Yin, H.; You, M.; Shi, X.; Yu, H.; Chen, Q. New Insights into Pure Zwitterionic Hydrogels with High Strength and High Toughness. *MATERIALS HORIZONS* **2024**, *11* (16), 3946−3960.
(226) Deng, Y.; Zhou, J.; Si, M.; Wang, G.; Tang, Y.; Zhang, Z. R.; Hu, J.; Wang, Y.; Yang, J.; Zheng, S. Y. Ferric Salt-Mediated Tough Zwitterionic Hydrogel. *Macromolecules* **2025**, *58* (6), 2860−2869.
(227) Muthukumar, M. 50th Anniversary Perspective: A Perspective on Polyelectrolyte Solutions. *Macromolecules* **2017**, *50* (24), 9528−9560.
(228) Wang, Y.; Zhao, Y.; Bollas, A.; Wang, Y.; Au, K. F. Nanopore Sequencing Technology, Bioinformatics and Applications. *Nat. Biotechnol.* **2021**, *39* (11), 1348−1365.
(229) Hu, Z.-L.; Liu, Y.-H.; Xin, K.-L.; Yu, R.-J.; Zhang, L.-M.; Ying, Y.-L. Nanopore Deciphering Single Digital Polymers Towards High-Density Data Storage. *Chem.—Eur. J.* **2023**, *29* (27), No. e202203919.
(230) Morales, D.; Palleau, E.; Dickey, M. D.; Velev, O. D. Electro-Actuated Hydrogel Walkers with Dual Responsive Legs. *Soft Matter* **2014**, *10* (9), 1337−1348.
(231) Tepermeister, M.; Silberstein, M. N. Harnessing Ionic Complexity: A Modeling Approach for Hierarchical Ionic Circuit Design. *Phys. Rev. Appl.* **2025**, *23* (5), No. 054047.
(232) Mendes, A. C.; Baran, E. T.; Reis, R. L.; Azevedo, H. S. Self-Assembly in Nature: Using the Principles of Nature to Create Complex Nanobiomaterials. *WIREs Nanomedicine and Nanobiotechnology* **2013**, *5* (6), 582−612.
(233) Fu, J.; Schlenoff, J. B. Driving Forces for Oppositely Charged Polyion Association in Aqueous Solutions: Enthalpic, Entropic, but Not Electrostatic. *J. Am. Chem. Soc.* **2016**, *138* (3), 980−990.
(234) Wang, Q.; Schlenoff, J. B. The Polyelectrolyte Complex/Coacervate Continuum. *Macromolecules* **2014**, *47* (9), 3108−3116.
(235) Yin, H.; King, D. R.; Sun, T. L.; Saruwatari, Y.; Nakajima, T.; Kurokawa, T.; Gong, J. P. Polyzwitterions as a Versatile Building Block of Tough Hydrogels: From Polyelectrolyte Complex Gels to Double-Network Gels. *ACS Appl. Mater. Interfaces* **2020**, *12* (44), 50068−50076.
(236) *Oxford English Dictionary. Zwitterion, n.*; Oxford University Press, 2025.
(237) Mei, W.; Colby, R. H.; Hickey, R. J. Enhancing the Dielectric Constant of Zwitterionic Liquids via Dipole Moment and Anion Chemistry. *J. Chem. Phys.* **2024**, *161* (1), No. 014506.
(238) Shao, Q.; Jiang, S. Effect of Carbon Spacer Length on Zwitterionic Carboxybetaines. *J. Phys. Chem. B* **2013**, *117* (5), 1357−1366.
(239) Sarker, P.; Lu, T.; Liu, D.; Wu, G.; Chen, H.; Sajib, M. S. J.; Jiang, S.; Chen, Z.; Wei, T. Hydration Behaviors of Nonfouling Zwitterionic Materials. *Chem. Sci.* **2023**, *14* (27), 7500−7511.
(240) Zhang, S.; Ao, H.; Dong, J.; Wang, D.; Wang, C.; Xu, X.; Hou, Z.; Yang, J. Dipole Moment Dictates the Preferential Immobilization in Gel Electrolytes for Ah-Level Aqueous Zinc-Metal Batteries. *Angew. Chem., Int. Ed.* **2025**, *64* (2), No. e202414702.
(241) Zheng, W.; Xu, S.; Radisic, D.; Stokes, S.; Li, X.; Bowen, K. H., Jr. On the Interaction of Electrons with Betaine Zwitterions. *J. Chem. Phys.* **2005**, *122* (10), 101103.
(242) Lee, H.; Puodziukynaite, E.; Zhang, Y.; Stephenson, J. C.; Richter, L. J.; Fischer, D. A.; DeLongchamp, D. M.; Emrick, T.; Briseno, A. L. Poly(Sulfobetaine Methacrylate)s as Electrode Modifiers for Inverted Organic Electronics. *J. Am. Chem. Soc.* **2015**, *137* (1), 540−549.
(243) Knoesel, R.; Ehrmann, M.; Galin, J. C. Poly(Ammonium Sulfopropylbetaine)s: 5. Interactions in Dilute Aqueous Solution with Low Molecular Weight Salts or Zwitterions and with Poly(Electrolyte)s. *Polymer* **1993**, *34* (9), 1925−1932.
(244) Muthukumar, M. Double Screening in Polyelectrolyte Solutions: Limiting Laws and Crossover Formulas. *J. Chem. Phys.* **1996**, *105* (12), 5183−5199.
(245) Muthukumar, M. Ordinary−Extraordinary Transition in Dynamics of Solutions of Charged Macromolecules. *Proc. Natl. Acad. Sci. U. S. A.* **2016**, *113* (45), 12627−12632.
(246) Gregory, K. P.; Elliott, G. R.; Robertson, H.; Kumar, A.; Wanless, E. J.; Webber, G. B.; Craig, V. S. J.; Andersson, G. G.; Page, A. J. Understanding Specific Ion Effects and the Hofmeister Series. *Phys. Chem. Chem. Phys.* **2022**, *24* (21), 12682−12718.
(247) Salis, A.; Ninham, B. W. Models and Mechanisms of Hofmeister Effects in Electrolyte Solutions, and Colloid and Protein Systems Revisited. *Chem. Soc. Rev.* **2014**, *43* (21), 7358−7377.
(248) Muthukumar, M. Theory of Counter-Ion Condensation on Flexible Polyelectrolytes: Adsorption Mechanism. *J. Chem. Phys.* **2004**, *120* (19), 9343−9350.
(249) Medda, L.; Barse, B.; Cugia, F.; Boström, M.; Parsons, D. F.; Ninham, B. W.; Monduzzi, M.; Salis, A. Hofmeister Challenges: Ion Binding and Charge of the BSA Protein as Explicit Examples. *Langmuir* **2012**, *28* (47), 16355−16363.
(250) Wang, M.; Xiao, X.; Siddika, S.; Shamsi, M.; Frey, E.; Qian, W.; Bai, W.; O'Connor, B. T.; Dickey, M. D. Glassy Gels Toughened by Solvent. *Nature* **2024**, *631* (8020), 313−318.
(251) Zhang, Z.; Huang, C.; Weiss, R. A.; Chen, Q. Association Energy in Strongly Associative Polymers. *J. Rheol.* **2017**, *61* (6), 1199−1207.
(252) Chen, Q.; Tudryn, G. J.; Colby, R. H. Ionomer Dynamics and the Sticky Rouse Model. *J. Rheol.* **2013**, *57* (5), 1441−1462.
(253) Huang, C.; Chen, Q.; Weiss, R. A. Rheological Behavior of Partially Neutralized Oligomeric Sulfonated Polystyrene Ionomers. *Macromolecules* **2017**, *50* (1), 424−431.
(254) Gudla, H.; Shao, Y.; Phunnarungsi, S.; Brandell, D.; Zhang, C. Importance of the Ion-Pair Lifetime in Polymer Electrolytes. *J. Phys. Chem. Lett.* **2021**, *12* (35), 8460−8464.
(255) Wei, R.; Song, W.; Yang, F.; Zhou, J.; Zhang, M.; Zhang, X.; Zhao, W.; Zhao, C. Bidirectionally pH-Responsive Zwitterionic Polymer Hydrogels with Switchable Selective Adsorption Capacities for Anionic and Cationic Dyes. *Ind. Eng. Chem. Res.* **2018**, *57* (24), 8209−8219.
(256) Zhang, Y.; Liao, J.; Wang, T.; Sun, W.; Tong, Z. Polyampholyte Hydrogels with pH Modulated Shape Memory and Spontaneous Actuation. *Adv. Funct. Mater.* **2018**, *28* (18), 1707245.
(257) Zhang, Y.; Hu, Q.; Yang, S.; Wang, T.; Sun, W.; Tong, Z. Unique Self-Reinforcing and Rapid Self-Healing Polyampholyte Hydrogels with a pH-Induced Shape Memory Effect. *Macromolecules* **2021**, *54* (11), 5218−5228.
(258) Qu, K.; Yuan, Z.; Wang, Y.; Song, Z.; Gong, X.; Zhao, Y.; Mu, Q.; Zhan, Q.; Xu, W.; Wang, L. Structures, Properties, and Applications of Zwitterionic Polymers. *ChemPhysMater.* **2022**, *1* (4), 294−309.
(259) Zhang, Y.; Hu, Q.; Sun, W.; Sun, T.; Wang, T.; Liu, H.; Tong, Z. pH-Induced Mechanical Transition in Polyion Complex Hydro-

https://doi.org/10.1021/acs.chemrev.5c00466
Chem. Rev. XXXX, XXX, XXX−XXX

gels: Shifting from Ionic Association to Hydrophobic Association. *Macromolecules* **2024**, *57* (2), 574−585.
(260) Petelinšek, N.; Mommer, S. Tough Hydrogels for Load-Bearing Applications. *Adv. Sci. (Weinh)* **2024**, *11* (12), 2307404.
(261) Sun, T. L.; Luo, F.; Kurokawa, T.; Karobi, S. N.; Nakajima, T.; Gong, J. P. Molecular Structure of Self-Healing Polyampholyte Hydrogels Analyzed from Tensile Behaviors. *Soft Matter* **2015**, *11* (48), 9355−9366.
(262) Karobi, S. N.; Sun, T. L.; Kurokawa, T.; Luo, F.; Nakajima, T.; Nonoyama, T.; Gong, J. P. Creep Behavior and Delayed Fracture of Tough Polyampholyte Hydrogels by Tensile Test. *Macromolecules* **2016**, *49* (15), 5630−5636.
(263) Zhao, X.; Huebsch, N.; Mooney, D. J.; Suo, Z. Stress-Relaxation Behavior in Gels with Ionic and Covalent Crosslinks. *J. Appl. Phys.* **2010**, *107* (6), 63509.
(264) He, X.; Ewing, A. G. Hofmeister Series: From Aqueous Solution of Biomolecules to Single Cells and Nanovesicles. *ChemBioChem* **2023**, *24* (9), No. e202200694.
(265) Aubrecht, F. J.; Orme, K.; Saul, A.; Cai, H.; Ranathunge, T. A.; Silberstein, M. N.; McDonald, B. R. Ion-Specific Interactions Engender Dynamic and Tailorable Properties in Biomimetic Cationic Polyelectrolytes. *Angew. Chem., Int. Ed.* **2024**, *63* (41), No. e202408673.
(266) Jin, Y.; Lu, S.; Chen, X.; Fang, Q.; Guan, X.; Qin, L.; Chen, C.; Zhao, C. Time-Salt Type Superposition and Salt Processing of Poly(Methacrylamide) Hydrogel Based on Hofmeister Series. *Macromolecules* **2024**, *57* (6), 2746−2755.
(267) Wanasinghe, S. V.; Dodo, O. J.; Konkolewicz, D. Dynamic Bonds: Adaptable Timescales for Responsive Materials. *Angew. Chem., Int. Ed.* **2022**, *61* (50), No. e202206938.
(268) Liu, L.; Kou, R.; Liu, G. Ion Specificities of Artificial Macromolecules. *Soft Matter* **2017**, *13* (1), 68−80.
(269) Jenkins, H. D. B.; Marcus, Y. Viscosity B-Coefficients of Ions in Solution. *Chem. Rev.* **1995**, *95* (8), 2695−2724.
(270) Marcus, Y. Effect of Ions on the Structure of Water: Structure Making and Breaking. *Chem. Rev.* **2009**, *109* (3), 1346−1370.
(271) Hribar, B.; Southall, N. T.; Vlachy, V.; Dill, K. A. How Ions Affect the Structure of Water. *J. Am. Chem. Soc.* **2002**, *124* (41), 12302−12311.
(272) Mancinelli, R.; Botti, A.; Bruni, F.; Ricci, M. A.; Soper, A. K. Hydration of Sodium, Potassium, and Chloride Ions in Solution and the Concept of Structure Maker/Breaker. *J. Phys. Chem. B* **2007**, *111* (48), 13570−13577.
(273) Balos, V.; Kaliannan, N. K.; Elgabarty, H.; Wolf, M.; Kuhne, T. D.; Sajadi, M. Time-Resolved Terahertz-Raman Spectroscopy Reveals That Cations and Anions Distinctly Modify Intermolecular Interactions of Water. *Nat. Chem.* **2022**, *14* (9), 1031.
(274) Zangi, R. Can Salting-In/Salting-Out Ions Be Classified as Chaotropes/Kosmotropes? *J. Phys. Chem. B* **2010**, *114* (1), 643−650.
(275) Chen, Y.; Okur, H. I.; Gomopoulos, N.; Macias-Romero, C.; Cremer, P. S.; Petersen, P. B.; Tocci, G.; Wilkins, D. M.; Liang, C.; Ceriotti, M.; Roke, S. Electrolytes Induce Long-Range Orientational Order and Free Energy Changes in the H-Bond Network of Bulk Water. *Sci. Adv.* **2016**, *2* (4), e1501891. .
(276) Schwaab, G.; Sebastiani, F.; Havenith, M. Ion Hydration and Ion Pairing as Probed by THz Spectroscopy. *Angew. Chem., Int. Ed.* **2019**, *58* (10), 3000−3013.
(277) Tielrooij, K. J.; van der Post, S. T.; Hunger, J.; Bonn, M.; Bakker, H. J. Anisotropic Water Reorientation around Ions. *J. Phys. Chem. B* **2011**, *115* (43), 12638−12647.
(278) Waluyo, I.; Huang, C.; Nordlund, D.; Bergmann, U.; Weiss, T. M.; Pettersson, L. G. M.; Nilsson, A. The Structure of Water in the Hydration Shell of Cations from X-Ray Raman and Small Angle x-Ray Scattering Measurements. *J. Chem. Phys.* **2011**, *134* (6), No. 064513.
(279) Shalit, A.; Ahmed, S.; Savolainen, J.; Hamm, P. Terahertz Echoes Reveal the Inhomogeneity of Aqueous Salt Solutions. *Nature Chem.* **2017**, *9* (3), 273−278.
(280) Paschek, D.; Ludwig, R. Specific Ion Effects on Water Structure and Dynamics beyond the First Hydration Shell. *Angew. Chem., Int. Ed.* **2011**, *50* (2), 352−353.
(281) Chialvo, A. A. On the Solute-Induced Structure-Making/Breaking Phenomena: Myths, Verities, and Misuses in Solvation Thermodynamics. *Liquids* **2024**, *4* (3), 592−623.
(282) Oh, S. H.; Ryoo, R.; Jhon, M. S. Iodine-127 and Potassium-39 NMR Study of the Interaction of Ions with Water-Soluble Polymers. *Macromolecules* **1990**, *23* (6), 1671−1675.
(283) Livney, Y. D.; Ramon, O.; Kesselman, E.; Cogan, U.; Mizrahi, S.; Cohen, Y. Swelling of Dextran Gel and Osmotic Pressure of Soluble Dextran in the Presence of Salts. *J. Polym. Sci., Part B: Polym. Phys.* **2001**, *39* (22), 2740−2750.
(284) Livney, Y. D.; Portnaya, I.; Faupin, B.; Ramon, O.; Cohen, Y.; Cogan, U.; Mizrahi, S. Interactions between Inorganic Salts and Polyacrylamide in Aqueous Solutions and Gels. *J. Polym. Sci., Part B: Polym. Phys.* **2003**, *41* (5), 508−519.
(285) Zhang, Y.; Furyk, S.; Bergbreiter, D. E.; Cremer, P. S. Specific Ion Effects on the Water Solubility of Macromolecules: PNIPAM and the Hofmeister Series. *J. Am. Chem. Soc.* **2005**, *127* (41), 14505−14510.
(286) Zhang, Y.; Furyk, S.; Sagle, L. B.; Cho, Y.; Bergbreiter, D. E.; Cremer, P. S. Effects of Hofmeister Anions on the LCST of PNIPAM as a Function of Molecular Weight. *J. Phys. Chem. C* **2007**, *111* (25), 8916−8924.
(287) Shechter, I.; Ramon, O.; Portnaya, I.; Paz, Y.; Livney, Y. D. Microcalorimetric Study of the Effects of a Chaotropic Salt, KSCN, on the Lower Critical Solution Temperature (LCST) of Aqueous Poly(N-Isopropylacrylamide) (PNIPA) Solutions. *Macromolecules* **2010**, *43* (1), 480−487.
(288) Zhang, Y.; Furyk, S.; Bergbreiter, D. E.; Cremer, P. S. Specific Ion Effects on the Water Solubility of Macromolecules: PNIPAM and the Hofmeister Series. *J. Am. Chem. Soc.* **2005**, *127* (41), 14505−14510.
(289) Hamabata, A.; Von Hippel, P. H. Model Studies on the Effects of Neutral Salts on the Conformational Stability of Biological Macromolecules. II. Effects of Vicinal Hydrophobic Groups on the Specificity of Binding of Ions to Amide Groups. *Biochemistry* **1973**, *12* (7), 1264−1271.
(290) Wang, L.-H.; Zhang, Z.-D.; Hong, C.-Y.; He, X.-H.; You, W.; You, Y.-Z. Anion−Dipole Interactions Make the Homopolymers Self-Assemble into Multiple Nanostructures. *Adv. Mater.* **2015**, *27* (20), 3202−3207.
(291) Wang, L.-H.; Wu, T.; Zhang, Z.; You, Y.-Z. Unconventional Transitions of Poly(N-Isopropylacrylamide) upon Heating in the Presence of Multiple Noncovalent Interactions. *Macromolecules* **2016**, *49* (1), 362−366.
(292) Collins, K. D. Charge Density-Dependent Strength of Hydration and Biological Structure. *Biophys. J.* **1997**, *72* (1), 65−76.
(293) Hutskalov, I.; Linden, A.; Čorić, I. Directional Ionic Bonds. *J. Am. Chem. Soc.* **2023**, *145* (15), 8291−8298.
(294) Ma, J. C.; Dougherty, D. A. The Cation-Pi Interaction. *Chem. Rev.* **1997**, *97* (5), 1303−1324.
(295) Dougherty, D. A. The Cation-Pi Interaction. *Acc. Chem. Res.* **2013**, *46* (4), 885−893.
(296) Mecozzi, S.; West, A. P.; Dougherty, D. A. Cation-Pi Interactions in Aromatics of Biological and Medicinal Interest: Electrostatic Potential Surfaces as a Useful Qualitative Guide. *P Natl. Acad. Sci. USA* **1996**, *93* (20), 10566−10571.
(297) Cubero, E.; Luque, F. J.; Orozco, M. Is Polarization Important in Cation-Pi Interactions? *P Natl. Acad. Sci. USA* **1998**, *95* (11), 5976−5980.
(298) Torrice, M. M.; Bower, K. S.; Lester, H. A.; Dougherty, D. A. Probing the Role of the Cation−π Interaction in the Binding Sites of GPCRs Using Unnatural Amino Acids. *Proc. Natl. Acad. Sci. U.S.A.* **2009**, *106* (29), 11919−11924.
(299) Zhong, W.; Gallivan, J. P.; Zhang, Y.; Li, L.; Lester, H. A.; Dougherty, D. A. From Ab Initio Quantum Mechanics to Molecular

https://doi.org/10.1021/acs.chemrev.5c00466
Chem. Rev. XXXX, XXX, XXX−XXX

Neurobiology: A Cation−π Binding Site in the Nicotinic Receptor. *Proc. Natl. Acad. Sci. U.S.A.* **1998**, *95* (21), 12088−12093.
(300) Geng, H.; Zhang, P.; Peng, Q.; Cui, J.; Hao, J.; Zeng, H. Principles of Cation−π Interactions for Engineering Mussel-Inspired Functional Materials. *Acc. Chem. Res.* **2022**, *55* (8), 1171−1182.
(301) Mahadevi, A. S.; Sastry, G. N. Cation−π Interaction: Its Role and Relevance in Chemistry, Biology, and Material Science. *Chem. Rev.* **2013**, *113* (3), 2100−2138.
(302) Maier, G. P.; Rapp, M. V.; Waite, J. H.; Israelachvili, J. N.; Butler, A. Adaptive Synergy between Catechol and Lysine Promotes Wet Adhesion by Surface Salt Displacement. *Science* **2015**, *349* (6248), 628−632.
(303) Li, Y.; Cheng, J.; Delparastan, P.; Wang, H.; Sigg, S. J.; DeFrates, K. G.; Cao, Y.; Messersmith, P. B. Molecular Design Principles of Lysine-DOPA Wet Adhesion. *Nat. Commun.* **2020**, *11* (1), 3895.
(304) Fan, H.; Wang, J.; Gong, J. P. Barnacle Cement Proteins-Inspired Tough Hydrogels with Robust, Long-Lasting, and Repeatable Underwater Adhesion. *Adv. Funct. Mater.* **2021**, *31* (11), 2009334.
(305) Kennedy, C. R.; Lin, S.; Jacobsen, E. N. The Cation-Pi Interaction in Small-Molecule Catalysis. *Angew. Chem. Int. Edit* **2016**, *55* (41), 12596−12624.
(306) Yamada, S. Cation−π Interactions in Organic Synthesis. *Chem. Rev.* **2018**, *118* (23), 11353−11432.
(307) Liang, Z.; Li, Q. X. π−Cation Interactions in Molecular Recognition: Perspectives on Pharmaceuticals and Pesticides. *J. Agric. Food. Chem.* **2018**, *66* (13), 3315−3323.
(308) Lu, Q.; Oh, D. X.; Lee, Y.; Jho, Y.; Hwang, D. S.; Zeng, H. Nanomechanics of Cation−π Interactions in Aqueous Solution. *Angew. Chem., Int. Ed.* **2013**, *52* (14), 3944−3948.
(309) Arias, S.; Freire, F.; Quiñoá, E.; Riguera, R. The Leading Role of Cation−π Interactions in Polymer Chemistry: The Control of the Helical Sense in Solution. *Polym. Chem.* **2015**, *6* (26), 4725−4733.
(310) Hofman, A. H.; van Hees, I. A.; Yang, J.; Kamperman, M. Bioinspired Underwater Adhesives by Using the Supramolecular Toolbox. *Adv. Mater.* **2018**, *30* (19), 1704640.
(311) Fan, H.; Gong, J. P. Bioinspired Underwater Adhesives. *Adv. Mater.* **2021**, *33* (44), 2102983.
(312) Luo, F.; Sun, T. L.; Nakajima, T.; Kurokawa, T.; Zhao, Y.; Sato, K.; Bin Ihsan, A.; Li, X. F.; Guo, H. L.; Gong, J. P. Oppositely Charged Polyelectrolytes Form Tough, Self-Healing, and Rebuildable Hydrogels. *Adv. Mater.* **2015**, *27* (17), 2722.
(313) Yang, L.; Li, Y.; Du, M.; He, Y.; Lan, Y.; Yin, Q.; Zhu, F.; Chang, G. Force-Reversible and Energetic Indole-Mg-Indole Cation-π Interaction for Designing Toughened and Multifunctional High-Performance Thermosets. *Adv. Funct. Mater.* **2022**, *32* (14), 2111021.
(314) Anichini, C.; Czepa, W.; Pakulski, D.; Aliprandi, A.; Ciesielski, A.; Samorì, P. Chemical Sensing with 2D Materials. *Chem. Soc. Rev.* **2018**, *47* (13), 4860−4908.
(315) Geng, H.; Zhong, Q.-Z.; Li, J.; Lin, Z.; Cui, J.; Caruso, F.; Hao, J. Metal Ion-Directed Functional Metal−Phenolic Materials. *Chem. Rev.* **2022**, *122* (13), 11432−11473.
(316) Mahmudov, K. T.; Kopylovich, M. N.; Guedes da Silva, M. F. C.; Pombeiro, A. J. L. Non-Covalent Interactions in the Synthesis of Coordination Compounds: Recent Advances. *Coord. Chem. Rev.* **2017**, *345*, 54−72.
(317) Yamada, S. *The Cation−π Interaction*; Springer Nature: Singapore, 2022.
(318) Fan, H.; Wang, J.; Tao, Z.; Huang, J.; Rao, P.; Kurokawa, T.; Gong, J. P. Adjacent Cationic−Aromatic Sequences Yield Strong Electrostatic Adhesion of Hydrogels in Seawater. *Nat. Commun.* **2019**, *10* (1), 5127.
(319) Gebbie, M. A.; Wei, W.; Schrader, A. M.; Cristiani, T. R.; Dobbs, H. A.; Idso, M.; Chmelka, B. F.; Waite, J. H.; Israelachvili, J. N. Tuning Underwater Adhesion with Cation−π Interactions. *Nature Chem.* **2017**, *9* (5), 473−479.
(320) Fan, H.; Guo, H.; Kurokawa, T.; Gong, J. P. Quantitative Determination of Cation−π Interactions between Metal Ions and Aromatic Groups in Aqueous Media by a Hydrogel Donnan Potential Method. *Phys. Chem. Chem. Phys.* **2022**, *24* (10), 6126−6132.
(321) Yang, Y.; Liang, S.; Wu, H.; Shi, G.; Fang, H. Revisit the Hydrated Cation−π Interaction at the Interface: A New View of Dynamics and Statistics. *Langmuir* **2022**, *38* (8), 2401−2408.
(322) Park, S.; Lee, Y.; Jho, Y.; Hwang, D. S. Molecular Hydration Tunes the Cation−π Interaction Strength in Aqueous Solution. *Adv. Mater. Interfaces* **2023**, *10* (4), 2201732.
(323) Wu, R.; McMahon, T. B. Investigation of Cation-π Interactions in Biological Systems. *J. Am. Chem. Soc.* **2008**, *130* (38), 12554−12555.
(324) Yamada, S. Fundamentals of Cation−π Interactions. In *The Cation−π Interaction*; Yamada, S., Ed.; Springer Nature: Singapore, 2022; pp 7−41.
(325) Yamada, S.; Misono, T.; Tsuzuki, S. Cation−π Interactions of a Thiocarbonyl Group and a Carbonyl Group with a Pyridinium Nucleus. *J. Am. Chem. Soc.* **2004**, *126* (31), 9862−9872.
(326) Zhang, Y.; Li, Y.; Liu, W. Dipole−Dipole and H-Bonding Interactions Significantly Enhance the Multifaceted Mechanical Properties of Thermoresponsive Shape Memory Hydrogels. *Adv. Funct Materials* **2015**, *25* (3), 471−480.
(327) Woutersen, S.; Mu, Y.; Stock, G.; Hamm, P. Hydrogen-Bond Lifetime Measured by Time-Resolved 2D-IR Spectroscopy: *N*-Methylacetamide in Methanol. *Chem. Phys.* **2001**, *266* (2), 137−147.
(328) Grzybowski, B. A.; Wilmer, C. E.; Kim, J.; Browne, K. P.; Bishop, K. J. M. Self-Assembly: From Crystals to Cells. *Soft Matter* **2009**, *5* (6), 1110−1128.
(329) Hoeben, F. J. M.; Jonkheijm, P.; Meijer, E. W.; Schenning, A. P. H. J. About Supramolecular Assemblies of π-Conjugated Systems. *Chem. Rev.* **2005**, *105* (4), 1491−1546.
(330) Giubertoni, G.; Burla, F.; Bakker, H. J.; Koenderink, G. H. Connecting the Stimuli-Responsive Rheology of Biopolymer Hydrogels to Underlying Hydrogen-Bonding Interactions. *Macromolecules* **2020**, *53* (23), 10503−10513.
(331) SHAHI, A.; ARUNAN, E. Why Are Hydrogen Bonds Directional? *J. Chem. Sci.* **2016**, *128* (10), 1571−1577.
(332) Liu, Y.; Chen, Y.; Zhu, J.; Lu, M.; Jiang, C.; Fan, Z.; Sun, T. Time-Dependent Mechanical Behavior of Tough Hydrogels under Multiaxial Stretching. *International J. Smart and Nano Materials* **2023**, *14* (4), 460−473.
(333) Yu, J.; Wang, K.; Fan, C.; Zhao, X.; Gao, J.; Jing, W.; Zhang, X.; Li, J.; Li, Y.; Yang, J.; Liu, W. An Ultrasoft Self-Fused Supramolecular Polymer Hydrogel for Completely Preventing Postoperative Tissue Adhesion. *Adv. Mater.* **2021**, *33* (16), No. e2008395.
(334) Xu, Z.; Liu, W. Poly(N -Acryloyl Glycinamide): A Fascinating Polymer That Exhibits a Range of Properties from UCST to High-Strength Hydrogels. *Chem. Commun.* **2018**, *54* (75), 10540−10553.
(335) Dai, X.; Zhang, Y.; Gao, L.; Bai, T.; Wang, W.; Cui, Y.; Liu, W. A Mechanically Strong, Highly Stable, Thermoplastic, and Self-Healable Supramolecular Polymer Hydrogel. *Adv. Mater.* **2015**, *27* (23), 3566−3571.
(336) Fan, C.; Liu, B.; Xu, Z.; Cui, C.; Wu, T.; Yang, Y.; Zhang, D.; Xiao, M.; Zhang, Z.; Liu, W. Polymerization of N-Acryloylsemicarbazide: A Facile and Versatile Strategy to Tailor-Make Highly Stiff and Tough Hydrogels. *Mater. Horiz.* **2020**, *7* (4), 1160−1170.
(337) Raschke, T. M. Water Structure and Interactions with Protein Surfaces. *Curr. Opin. Struct. Biol.* **2006**, *16* (2), 152−159.
(338) Guo, M.; Pitet, L. M.; Wyss, H. M.; Vos, M.; Dankers, P. Y. W.; Meijer, E. W. Tough Stimuli-Responsive Supramolecular Hydrogels with Hydrogen-Bonding Network Junctions. *J. Am. Chem. Soc.* **2014**, *136* (19), 6969−6977.
(339) Wang, Y. J.; Zhang, X. N.; Song, Y.; Zhao, Y.; Chen, L.; Su, F.; Li, L.; Wu, Z. L.; Zheng, Q. Ultrastiff and Tough Supramolecular Hydrogels with a Dense and Robust Hydrogen Bond Network. *Chem. Mater.* **2019**, *31* (4), 1430−1440.
(340) Wang, W.; Zhang, Y.; Liu, W. Bioinspired Fabrication of High Strength Hydrogels from Non-Covalent Interactions. *Prog. Polym. Sci.* **2017**, *71*, 1−25.

https://doi.org/10.1021/acs.chemrev.5c00466
Chem. Rev. XXXX, XXX, XXX−XXX

(341) Jin, Z.; Chen, T.; Liu, Y.; Feng, W.; Chen, L.; Wang, C. Multivalent Design of Low-Entropy-Penalty Ion−Dipole Interactions for Dynamic Yet Thermostable Supramolecular Networks. *J. Am. Chem. Soc.* **2023**, *145* (6), 3526−3534.
(342) Yuan, W.; He, Y.; Liang, Q.; Lv, H.; Wang, Z.; Wu, H.; Wu, J.; Zhao, L.; Wang, Y. Ultra-Stretchable, Self-Recoverable, Notch-Insensitive, Self-Healable and Adhesive Hydrogel Enabled by Synergetic Hydrogen and Dipole−Dipole Crosslinking. *Mater. Horiz.* **2025**, *12* (7), 2223−2233.
(343) Wang, Y.; Xie, Y.; Xie, X.; Wu, D.; Wu, H.; Luo, X.; Wu, Q.; Zhao, L.; Wu, J. Compliant and Robust Tissue-Like Hydrogels via Ferric Ion-Induced of Hierarchical Structure. *Adv. Funct. Mater.* **2023**, *33* (12), 2210224.
(344) Bai, T.; Zhang, P.; Han, Y.; Liu, Y.; Liu, W.; Zhao, X.; Lu, W. Construction of an Ultrahigh Strength Hydrogel with Excellent Fatigue Resistance Based on Strong Dipole−Dipole Interaction. *Soft Matter* **2011**, *7* (6), 2825−2831.
(345) Cai, S.; Niu, B.; Ma, X.; Wan, S.; He, X. High Strength, Recyclable, Anti-Swelling and Shape-Memory Hydrogels Based on Crystal Microphase Crosslinking and Their Application as Flexible Sensor. *Chem. Eng. J.* **2022**, *430*, 132957.
(346) Lei, S.; Huo, M. Sulfone-Bond-Toughened Multifunctional Hydrogels with Ion-Modulated Fluorescence and Mechanical Properties. *ACS Macro Lett.* **2025**, *14*, 1382−1388.
(347) Lv, Y.; Xiao, Y.; Ma, L.; Zhi, C.; Chen, S. Recent Advances in Electrolytes for "Beyond Aqueous" Zinc-Ion Batteries. *Adv. Mater.* **2022**, *34* (4), 2106409.
(348) Zhao, S.; Zuo, Y.; Liu, T.; Zhai, S.; Dai, Y.; Guo, Z.; Wang, Y.; He, Q.; Xia, L.; Zhi, C.; Bae, J.; Wang, K.; Ni, M. Multi-Functional Hydrogels for Flexible Zinc-Based Batteries Working under Extreme Conditions. *Adv. Energy Mater.* **2021**, *11* (34), 2101749.
(349) Zeng, Y.; Luan, D.; Lou, X. W. Recent Advances in Electrode Engineering Strategies for Aqueous Zn-Based Batteries. *Chem.* **2023**, *9* (5), 1118−1146.
(350) Budin, I.; Szostak, J. W. Physical Effects Underlying the Transition from Primitive to Modern Cell Membranes. *Proc. Natl. Acad. Sci. U. S. A.* **2011**, *108* (13), 5249−5254.
(351) Camilloni, C.; Bonetti, D.; Morrone, A.; Giri, R.; Dobson, C. M.; Brunori, M.; Gianni, S.; Vendruscolo, M. Towards a Structural Biology of the Hydrophobic Effect in Protein Folding. *Sci. Rep* **2016**, *6* (1), 28285.
(352) Muiznieks, L. D.; Sharpe, S.; Pomès, R.; Keeley, F. W. Role of Liquid−Liquid Phase Separation in Assembly of Elastin and Other Extracellular Matrix Proteins. *J. Mol. Biol.* **2018**, *430* (23), 4741−4753.
(353) Xiao, F.; Chen, Z.; Wei, Z.; Tian, L. Hydrophobic Interaction: A Promising Driving Force for the Biomedical Applications of Nucleic Acids. *Adv. Sci.* **2020**, *7* (16), 2001048.
(354) Miquelard-Garnier, G.; Creton, C.; Hourdet, D. Synthesis and Viscoelastic Properties of Hydrophobically Modified Hydrogels. *Macromol. Symp.* **2007**, *256* (1), 189−194.
(355) Abdurrahmanoglu, S.; Can, V.; Okay, O. Design of High-Toughness Polyacrylamide Hydrogels by Hydrophobic Modification. *Polymer* **2009**, *50* (23), 5449−5455.
(356) Zhang, C.; Aung, A.; Liao, L.; Varghese, S. A Novel Single Precursor-Based Biodegradable Hydrogel with Enhanced Mechanical Properties. *Soft Matter* **2009**, *5* (20), 3831−3834.
(357) Yang, J.; Shi, F.-K.; Gong, C.; Xie, X.-M. Dual Cross-Linked Networks Hydrogels with Unique Swelling Behavior and High Mechanical Strength: Based on Silica Nanoparticle and Hydrophobic Association. *J. Colloid Interface Sci.* **2012**, *381* (1), 107−115.
(358) Tuncaboylu, D. C.; Sari, M.; Oppermann, W.; Okay, O. Tough and Self-Healing Hydrogels Formed via Hydrophobic Interactions. *Macromolecules* **2011**, *44* (12), 4997−5005.
(359) Jiang, H.; Duan, L.; Ren, X.; Gao, G. Hydrophobic Association Hydrogels with Excellent Mechanical and Self-Healing Properties. *Eur. Polym. J.* **2019**, *112*, 660−669.
(360) Yang, H.; Elcock, A. H. Association Lifetimes of Hydrophobic Amino Acid Pairs Measured Directly from Molecular Dynamics Simulations. *J. Am. Chem. Soc.* **2003**, *125* (46), 13968−13969.
(361) Miquelard-Garnier, G.; Hourdet, D.; Creton, C. Large Strain Behaviour of Nanostructured Polyelectrolyte Hydrogels. *Polymer* **2009**, *50* (2), 481−490.
(362) Mihajlovic, M.; Staropoli, M.; Appavou, M.-S.; Wyss, H. M.; Pyckhout-Hintzen, W.; Sijbesma, R. P. Tough Supramolecular Hydrogel Based on Strong Hydrophobic Interactions in a Multiblock Segmented Copolymer. *Macromolecules* **2017**, *50* (8), 3333−3346.
(363) Tuncaboylu, D. C.; Sahin, M.; Argun, A.; Oppermann, W.; Okay, O. Dynamics and Large Strain Behavior of Self-Healing Hydrogels with and without Surfactants. *Macromolecules* **2012**, *45* (4), 1991−2000.
(364) Patist, A.; Oh, S. G.; Leung, R.; Shah, D. O. Kinetics of Micellization: Its Significance to Technological Processes. *Colloids Surf., A* **2001**, *176* (1), 3−16.
(365) Hao, X.; Liu, H.; Lu, Z.; Xie, Y.; Yang, H. Endowing the Conventional HMPAM Hydrogel with pH-Responsive and Self-Healing Properties. *J. Mater. Chem. A* **2013**, *1* (23), 6920−6927.
(366) Zhao, X.; Chen, X.; Yuk, H.; Lin, S.; Liu, X.; Parada, G. Soft Materials by Design: Unconventional Polymer Networks Give Extreme Properties. *Chem. Rev.* **2021**, *121* (8), 4309−4372.
(367) Ge, S.; Tsao, Y.-H.; Evans, C. M. Polymer Architecture Dictates Multiple Relaxation Processes in Soft Networks with Two Orthogonal Dynamic Bonds. *Nat. Commun.* **2023**, *14* (1), 7244.
(368) Wei, Z.; Yang, J. H.; Liu, Z. Q.; Xu, F.; Zhou, J. X.; Zrínyi, M.; Osada, Y.; Chen, Y. M. Novel Biocompatible Polysaccharide-Based Self-Healing Hydrogel. *Adv. Funct Materials* **2015**, *25* (9), 1352−1359.
(369) Millar, J. R. Interpenetrating Polymer Networks. Styrene−Divinylbenzene Copolymers with Two and Three Interpenetrating Networks, and Their Sulphonates. *J. Chem. Soc.* **1960**, *0* (0), 1311−1317.
(370) Predecki, P. A Method for Hydron Impregnation of Silicone Rubber. *J. Biomed. Mater. Res.* **1974**, *8* (6), 487−489.
(371) Kim, Y. J.; Min, J. Property Modulation of the Alginate-Based Hydrogel via Semi-Interpenetrating Polymer Network (Semi-IPN) with Poly(Vinyl Alcohol). *Int. J. Biol. Macromol.* **2021**, *193*, 1068−1077.
(372) Zeng, Y.; Yang, W.; Liu, S.; Shi, X.; Xi, A.; Zhang, F. Dynamic Semi IPNs with Duple Dynamic Linkers: Self-Healing, Reprocessing, Welding, and Shape Memory Behaviors. *Polymers* **2021**, *13* (11), 1679.
(373) Lin, S.; Zhou, Y.; Zhao, X. Designing Extremely Resilient and Tough Hydrogels via Delayed Dissipation. *Extreme Mechanics Letters* **2014**, *1*, 70−75.
(374) Yu, Z.; Zhang, Y.; Gao, Z. J.; Ren, X. Y.; Gao, G. H. Enhancing Mechanical Strength of Hydrogels via IPN Structure. *J. Appl. Polym. Sci.* **2017**, *134* (8), app.44503.
(375) Gong, J. P.; Katsuyama, Y.; Kurokawa, T.; Osada, Y. Double-Network Hydrogels with Extremely High Mechanical Strength. *Adv. Mater.* **2003**, *15* (14), 1155−1158.
(376) Huang, Y.; Jayathilaka, P. B.; Islam, M. S.; Tanaka, C. B.; Silberstein, M. N.; Kilian, K. A.; Kruzic, J. J. Structural Aspects Controlling the Mechanical and Biological Properties of Tough, Double Network Hydrogels. *Acta Biomaterialia* **2022**, *138*, 301−312.
(377) Yuan, N.; Xu, L.; Wang, H.; Fu, Y.; Zhang, Z.; Liu, L.; Wang, C.; Zhao, J.; Rong, J. Dual Physically Cross-Linked Double Network Hydrogels with High Mechanical Strength, Fatigue Resistance, Notch-Insensitivity, and Self-Healing Properties. *ACS Appl. Mater. Interfaces* **2016**, *8* (49), 34034−34044.
(378) Zhang, H. J.; Sun, T. L.; Zhang, A. K.; Ikura, Y.; Nakajima, T.; Nonoyama, T.; Kurokawa, T.; Ito, O.; Ishitobi, H.; Gong, J. P. Tough Physical Double-Network Hydrogels Based on Amphiphilic Triblock Copolymers. *Adv. Mater.* **2016**, *28* (24), 4884−4890.
(379) Yin, H.; You, M.; Yu, H.; Si, X.; Zheng, Y.; Cui, W.; Zhu, L.; Chen, Q. Rate-Dependent Fracture Behaviors of Agar-Based Hybrid

https://doi.org/10.1021/acs.chemrev.5c00466
Chem. Rev. XXXX, XXX, XXX−XXX

Double-Network Hydrogels. *Macromolecules* **2024**, *57* (9), 4024−4033.
(380) Yang, J.; Zhao, J.-J.; Han, C.-R.; Duan, J.-F. Keys to Enhancing Mechanical Properties of Silica Nanoparticle Composites Hydrogels: The Role of Network Structure and Interfacial Interactions. *Compos. Sci. Technol.* **2014**, *95*, 1−7.
(381) Zou, H.; Wu, S.; Shen, J. Polymer/Silica Nanocomposites: Preparation, Characterization, Properties, and Applications. *Chem. Rev.* **2008**, *108* (9), 3893−3957.
(382) Haraguchi, K.; Takehisa, T. Nanocomposite Hydrogels: A Unique Organic−Inorganic Network Structure with Extraordinary Mechanical, Optical, and Swelling/De-Swelling Properties. *Adv. Mater.* **2002**, *14* (16), 1120.
(383) Klein, A.; Whitten, P. G.; Resch, K.; Pinter, G. Nanocomposite Hydrogels: Fracture Toughness and Energy Dissipation Mechanisms. *J. Polym. Sci., Part B: Polym. Phys.* **2015**, *53* (24), 1763−1773.
(384) Song, J.; Li, Q.; Chen, P.; Keshavarz, B.; Chapman, B. S.; Tracy, J. B.; McKinley, G. H.; Holten-Andersen, N. Dynamics of Dual-Junction-Functionality Associative Polymer Networks with Ion and Nanoparticle Metal-Coordinate Cross-Link Junctions. *J. Rheol.* **2022**, *66* (6), 1333−1345.
(385) Liu, X.; Chen, D.; Feng, S.; Yang, M.; Yang, M. Super-Stretchable Hydrogel Films with High Fracture Energy Enabled by Coordination Nanoparticles as Multifunctional Wound Dressings. *ACS Appl. Polym. Mater.* **2023**, *5* (9), 7318−7327.
(386) Cui, K.; Gong, J. P. Aggregated Structures and Their Functionalities in Hydrogels. *Aggregate* **2021**, *2* (2), e33.
(387) Cui, W.; Cai, Y.; Zheng, Y.; Ran, R. Mechanical Enhancement of Hydrophobically Associating Hydrogels by Solvent-Regulated Phase Separation. *Polymer* **2020**, *210*, 123042.
(388) Tsai, C.-C.; Morrow, B. H.; Chen, W.; Payne, G. F.; Shen, J. Toward Understanding the Environmental Control of Hydrogel Film Properties: How Salt Modulates the Flexibility of Chitosan Chains. *Macromolecules* **2017**, *50* (15), 5946−5952.
(389) Cui, K.; Sun, T. L.; Liang, X.; Nakajima, K.; Ye, Y. N.; Chen, L.; Kurokawa, T.; Gong, J. P. Multiscale Energy Dissipation Mechanism in Tough and Self-Healing Hydrogels. *Phys. Rev. Lett.* **2018**, *121* (18), 185501.
(390) Holloway, J. L.; Lowman, A. M.; Palmese, G. R. The Role of Crystallization and Phase Separation in the Formation of Physically Cross-Linked PVA Hydrogels. *Soft Matter* **2013**, *9* (3), 826−833.
(391) Wang, C. J.; Vashahi, F.; Moutsios, I.; Umarov, A. Z.; Ageev, G. G.; Wang, Z.; Ivanov, D. A.; Dobrynin, A. V.; Sheiko, S. S. Bottlebrush Hydrogels with Hidden Length: Super-Swelling and Mechanically Robust. *Adv. Funct. Mater.* **2024**, *34* (52), 2410905.
(392) Wang, S.; Yu, Z.; Sun, X.; Panahi-Sarmad, M.; Yang, P.; Zhu, P.; Zhu, Y.; Liu, H.; Jiang, F. A Universal Strategy to Mitigate Microphase Separation via Cellulose Nanocrystal Hydration in Fabricating Strong, Tough, and Fatigue-Resistant Hydrogels. *Adv. Mater.* **2025**, *37* (7), 2416916.
(393) Ren, K.; Quanji, X.; Du, X.; Cai, C.; Luo, J.; Yin, J. Hydrogen Bond and Hydrophobic Interaction Reinforced Tough and Anti-swelling Hydrogels via Polymerization-Induced Microphase Separation. *Biomacromolecules* **2025**, *26* (6), 3868−3878.
(394) Sha, Z.; Chen, X.; Song, H.; Zheng, Y.; Cui, W.; Ran, R. Toughening Hydrogels with Small Molecules: Tiny Matter, Big Impact. *Mater. Horiz.* **2025**, *12* (18), 7244−7276.
(395) Yang, Y.; Ru, Y.; Zhao, T.; Liu, M. Bioinspired Multiphase Composite Gel Materials: From Controlled Micro-Phase Separation to Multiple Functionalities. *Chem.* **2023**, *9* (11), 3113−3137.
(396) Baniasadi, M.; Minary-Jolandan, M. Alginate-Collagen Fibril Composite Hydrogel. *Materials* **2015**, *8* (2), 799−814.
(397) Fang, Y.-H.; Liang, C.; Liljeström, V.; Lv, Z.-P.; Ikkala, O.; Zhang, H. Toughening Hydrogels with Fibrillar Connected Double Networks. *Adv. Mater.* **2024**, *36* (27), 2402282.
(398) Geonzon, L. C.; Chan, J.; Kou, H.; Hou, L. X.; Oda, T.; Tuvikene, R.; Matsukawa, S.; Mayumi, K. Tough and Stiff Biobased Hydrogels Reinforced by Strain-Induced Ordering of Hierarchical Structure. *Chem. Mater.* **2025**, *37* (18), 6991−7001.
(399) Bertula, K.; Martikainen, L.; Munne, P.; Hietala, S.; Klefström, J.; Ikkala, O.; Nonappa. Strain-Stiffening of Agarose Gels. *ACS Macro Lett.* **2019**, *8* (6), 670−675.
(400) Xu, J.; Jiang, Y.; Gao, L. Synthetic Strain-Stiffening Hydrogels towards Mechanical Adaptability. *J. Mater. Chem. B* **2023**, *11* (2), 221−243.
(401) Prince, E. Designing Biomimetic Strain-Stiffening into Synthetic Hydrogels. *Biomacromolecules* **2024**, *25* (10), 6283−6295.
(402) Ollier, R. C.; Xiang, Y.; Yacovelli, A. M.; Webber, M. J. Biomimetic Strain-Stiffening in Fully Synthetic Dynamic-Covalent Hydrogel Networks. *Chem. Sci.* **2023**, *14*, 4796. .
(403) Ollier, R. C.; Bispat, A. S.; Xian, S.; Webber, B.; Webber, M. J. Dynamic-Covalent Origins of Strain-Stiffening in Synthetic Hydrogels. *ACS Materials Lett.* **2025**, *7* (7), 2516−2523.
(404) Yu, H.; Zhao, L.; Wang, L. Double-network PVA /Gelatin/Borax Hydrogels with Self-healing, Strength, Stretchable, Stable, and Transparent Properties. *J. Appl. Polym. Sci.* **2023**, *140* (20), e53852.
(405) Liu, W.; Yao, C.; Wang, D.; Du, G.; Ji, Y.; Li, Q. Dynamic Double-Networked Hydrogels by Hybridizing PVA and Herbal Polysaccharides: Improved Mechanical Properties and Selective Antibacterial Activity. *Gels* **2024**, *10* (12), 821.
(406) Rising, A.; Harrington, M. J. Biological Materials Processing: Time-Tested Tricks for Sustainable Fiber Fabrication. *Chem. Rev.* **2023**, *123* (5), 2155−2199.
(407) Harrington, M. J.; Masic, A.; Holten-Andersen, N.; Waite, J. H.; Fratzl, P. Iron-Clad Fibers: A Metal-Based Biological Strategy for Hard Flexible Coatings. *Science* **2010**, *328* (5975), 216−220.
(408) Holten-Andersen, N.; Harrington, M. J.; Birkedal, H.; Lee, B. P.; Messersmith, P. B.; Lee, K. Y. C.; Waite, J. H. pH-Induced Metal-Ligand Cross-Links Inspired by Mussel Yield Self-Healing Polymer Networks with near-Covalent Elastic Moduli. *Proc. Natl. Acad. Sci. U.S.A.* **2011**, *108* (7), 2651−2655.
(409) Yuan, T.; Cui, X.; Liu, X.; Qu, X.; Sun, J. Highly Tough, Stretchable, Self-Healing, and Recyclable Hydrogels Reinforced by in Situ-Formed Polyelectrolyte Complex Nanoparticles. *Macromolecules* **2019**, *52* (8), 3141−3149.
(410) Fu, J.; Fares, H. M.; Schlenoff, J. B. Ion-Pairing Strength in Polyelectrolyte Complexes. *Macromolecules* **2017**, *50* (3), 1066−1074.
(411) Yang, X.; Abe, K.; Biswas, S. K.; Yano, H. Extremely Stiff and Strong Nanocomposite Hydrogels with Stretchable Cellulose Nanofiber/Poly(Vinyl Alcohol) Networks. *Cellulose* **2018**, *25* (11), 6571−6580.
(412) Lin, S.; Cao, C.; Wang, Q.; Gonzalez, M.; Dolbow, J. E.; Zhao, X. Design of Stiff, Tough and Stretchy Hydrogel Composites via Nanoscale Hybrid Crosslinking and Macroscale Fiber Reinforcement. *Soft Matter* **2014**, *10* (38), 7519−7527.
(413) Harrington, M. J. Why and How to Investigate Biological Materials Processing: A Cross-Disciplinary Approach for Inspiring Sustainable Materials Fabrication. *Acc. Mater. Res.* **2025**, *6*, 294. .
(414) Harrington, M. J.; Mezzenga, R.; Miserez, A. Fluid Protein Condensates for Bio-Inspired Applications. *Nature Reviews Bioengineering* **2024**, *2* (3), 260−278.
(415) Cranford, S. W. *Biomateriomics/Steven W. Cranford, Markus J. Buehler*; Buehler, M. J., Series Ed.; Springer Series in Materials Science, 165; Springer: Dordrecht, 2012.
(416) Fratzl, P.; Weinkamer, R. Nature's Hierarchical Materials. *Prog. Mater. Sci.* **2007**, *52* (8), 1263−1334.
(417) Harrington, M. J.; Fratzl, P. Natural Load-Bearing Protein Materials. *Prog. Mater. Sci.* **2021**, *120*, 100767.
(418) Stockmayer, W. H. Theory of Molecular Size Distribution and Gel Formation in Branched-Chain Polymers. *J. Chem. Phys.* **1943**, *11* (2), 45−55.
(419) Stockmayer, W. H. Theory of Molecular Size Distribution and Gel Formation in Branched Polymers II. General Cross Linking. *J. Chem. Phys.* **1944**, *12* (4), 125−131.
(420) Flory, P. J. Molecular Size Distribution in Three Dimensional Polymers. I. Gelation1. *J. Am. Chem. Soc.* **1941**, *63* (11), 3083−3090.

https://doi.org/10.1021/acs.chemrev.5c00466
Chem. Rev. XXXX, XXX, XXX−XXX

(421) Semenov, A. N.; Rubinstein, M. Thermoreversible Gelation in Solutions of Associative Polymers. 1. Statics. *Macromolecules* **1998**, *31* (4), 1373−1385.
(422) Villegas, J. A.; Heidenreich, M.; Levy, E. D. Molecular and Environmental Determinants of Biomolecular Condensate Formation. *Nat. Chem. Biol.* **2022**, *18* (12), 1319−1329.
(423) Dignon, G. L.; Best, R. B.; Mittal, J. Biomolecular Phase Separation: From Molecular Driving Forces to Macroscopic Properties. *Annu. Rev. Phys. Chem.* **2020**, *71* (1), 53−75.
(424) Weinans, H.; Prendergast, P. J. Tissue Adaptation as a Dynamical Process Far from Equilibrium. *Bone* **1996**, *19* (2), 143−149.
(425) Merindol, R.; Walther, A. Materials Learning from Life: Concepts for Active, Adaptive and Autonomous Molecular Systems. *Chem. Soc. Rev.* **2017**, *46* (18), 5588−5619.
(426) Mikhailov, O. V. Gelatin as It Is: History and Modernity. *Int. J. Mol. Sci.* **2023**, *24* (4), 3583. .
(427) Calixto, S.; Ganzherli, N.; Gulyaev, S.; Figueroa-Gerstenmaier, S. Gelatin as a Photosensitive Material. *Molecules* **2018**, *23* (8), 2064.
(428) Mohanto, S.; Narayana, S.; Merai, K. P.; Kumar, J. A.; Bhunia, A.; Hani, U.; Al Fatease, A.; Gowda, B. H. J.; Nag, S.; Ahmed, M. G.; Paul, K.; Vora, L. K. Advancements in Gelatin-Based Hydrogel Systems for Biomedical Applications: A State-of-the-Art Review. *Int. J. Biol. Macromol.* **2023**, *253*, 127143.
(429) Monavari, M.; Homaeigohar, S.; Fuentes-Chandía, M.; Nawaz, Q.; Monavari, M.; Venkatraman, A.; Boccaccini, A. R. 3D Printing of Alginate Dialdehyde-Gelatin (ADA-GEL) Hydrogels Incorporating Phytotherapeutic Icariin Loaded Mesoporous SiO2-CaO Nanoparticles for Bone Tissue Engineering. *Materials Science and Engineering: C* **2021**, *131*, 112470.
(430) Ross-Murphy, S. B. Structure and Rheology of Gelatin Gels: Recent Progress. *Polymer* **1992**, *33* (12), 2622−2627.
(431) Gornall, J. L.; Terentjev, E. M. Helix−Coil Transition of Gelatin: Helical Morphology and Stability. *Soft Matter* **2008**, *4* (3), 544−549.
(432) Guo, L.; Colby, R. H.; Lusignan, C. P.; Whitesides, T. H. Kinetics of Triple Helix Formation in Semidilute Gelatin Solutions. *Macromolecules* **2003**, *36* (26), 9999−10008.
(433) Oh, J. W.; Chung, W. J.; Heo, K.; Jin, H. E.; Lee, B. Y.; Wang, E.; Zueger, C.; Wong, W.; Meyer, J.; Kim, C.; Lee, S. Y.; Kim, W. G.; Zemla, M.; Auer, M.; Hexemer, A.; Lee, S. W. Biomimetic Virus-Based Colourimetric Sensors. *Nat. Commun.* **2014**, *5*, 1−5.
(434) Seuring, J.; Agarwal, S. Polymers with Upper Critical Solution Temperature in Aqueous Solution. *Macromol. Rapid Commun.* **2012**, *33* (22), 1898−1920.
(435) Huggins, M. L. THERMODYNAMIC PROPERTIES OF SOLUTIONS OF LONG-CHAIN COMPOUNDS. *Ann. N.Y. Acad. Sci.* **1942**, *43* (1), 1−32.
(436) Flory, P. J. Thermodynamics of High Polymer Solutions. *J. Chem. Phys.* **1942**, *10* (1), 51−61.
(437) Flory, P. J.; Fox, T. G. Treatment of Intrinsic Viscosities. *J. Am. Chem. Soc.* **1951**, *73* (5), 1904−1908.
(438) Huggins, M. L. Solutions of Long Chain Compounds. *J. Chem. Phys.* **1941**, *9* (5), 440−440.
(439) Niskanen, J.; Tenhu, H. How to Manipulate the Upper Critical Solution Temperature (UCST)? *Polym. Chem.* **2017**, *8* (1), 220−232.
(440) Zhao, C.; Ma, Z.; Zhu, X. X. Rational Design of Thermoresponsive Polymers in Aqueous Solutions: A Thermodynamics Map. *Prog. Polym. Sci.* **2019**, *90*, 269−291.
(441) Dai, X.; Zhang, Y.; Gao, L.; Bai, T.; Wang, W.; Cui, Y.; Liu, W. A Mechanically Strong, Highly Stable, Thermoplastic, and Self-Healable Supramolecular Polymer Hydrogel. *Adv. Mater.* **2015**, *27* (23), 3566−3571.
(442) Shi, X.; Gao, H.; Dai, F.; Feng, X.; Liu, W. A Thermoresponsive Supramolecular Copolymer Hydrogel for the Embolization of Kidney Arteries. *Biomater. Sci.* **2016**, *4* (11), 1673−1681.
(443) Wu, Y.; Wang, H.; Gao, F.; Xu, Z.; Dai, F.; Liu, W. An Injectable Supramolecular Polymer Nanocomposite Hydrogel for Prevention of Breast Cancer Recurrence with Theranostic and Mammoplastic Functions. *Adv. Funct. Mater.* **2018**, *28* (21), 1801000.
(444) Liu, J.; Lin, S.; Liu, X.; Qin, Z.; Yang, Y.; Zang, J.; Zhao, X. Fatigue-Resistant Adhesion of Hydrogels. *Nat. Commun.* **2020**, *11* (1), 1071.
(445) Hassan, C. M.; Peppas, N. A. Structure and Morphology of Freeze/Thawed PVA Hydrogels. *Macromolecules* **2000**, *33* (7), 2472−2479.
(446) Peppas, N. A. Turbidimetric Studies of Aqueous Poly(Vinyl Alcohol) Solutions. *Makromol. Chem.* **1975**, *176* (11), 3433−3440.
(447) Lozinsky, V. I.; Galaev, I. Yu.; Plieva, F. M.; Savina, I. N.; Jungvid, H.; Mattiasson, B. Polymeric Cryogels as Promising Materials of Biotechnological Interest. *Trends Biotechnol.* **2003**, *21* (10), 445−451.
(448) Adelnia, H.; Ensandoost, R.; Shebbrin Moonshi, S.; Gavgani, J. N.; Vasafi, E. I.; Ta, H. T. Freeze/Thawed Polyvinyl Alcohol Hydrogels: Present. *Past and Future. European Polymer Journal* **2022**, *164*, 110974.
(449) Zhang, H.; Hussain, I.; Brust, M.; Butler, M. F.; Rannard, S. P.; Cooper, A. I. Aligned Two- and Three-Dimensional Structures by Directional Freezing of Polymers and Nanoparticles. *Nat. Mater.* **2005**, *4* (10), 787−793.
(450) Butler, M. F. Freeze Concentration of Solutes at the Ice/Solution Interface Studied by Optical Interferometry. *Cryst. Growth Des.* **2002**, *2* (6), 541−548.
(451) Butler, M. F. Instability Formation and Directional Dendritic Growth of Ice Studied by Optical Interferometry. *Cryst. Growth Des.* **2001**, *1* (3), 213−223.
(452) Hua, M.; Wu, S.; Ma, Y.; Zhao, Y.; Chen, Z.; Frenkel, I.; Strzalka, J.; Zhou, H.; Zhu, X.; He, X. Strong Tough Hydrogels via the Synergy of Freeze-Casting and Salting Out. *Nature* **2021**, *590* (7847), 594−599.
(453) Fan, C.; Liu, B.; Xu, Z.; Cui, C.; Wu, T.; Yang, Y.; Zhang, D.; Xiao, M.; Zhang, Z.; Liu, W. Polymerization of N -Acryloylsemicarbazide: A Facile and Versatile Strategy to Tailor-Make Highly Stiff and Tough Hydrogels. *MATERIALS HORIZONS* **2020**, *7* (4), 1160−1170.
(454) Xu, L.; Gao, S.; Guo, Q.; Wang, C.; Qiao, Y.; Qiu, D. A Solvent-Exchange Strategy to Regulate Noncovalent Interactions for Strong and Antiswelling Hydrogels. *Adv. Mater.* **2020**, *32* (52), 2004579.
(455) Bates, F. S.; Fredrickson, G. H. Block Copolymers—Designer Soft Materials. *Phys. Today* **1999**, *52* (2), 32−38.
(456) Lang, C.; LaNasa, J. A.; Utomo, N.; Xu, Y.; Nelson, M. J.; Song, W.; Hickner, M. A.; Colby, R. H.; Kumar, M.; Hickey, R. J. Solvent-Non-Solvent Rapid-Injection for Preparing Nanostructured Materials from Micelles to Hydrogels. *Nat. Commun.* **2019**, *10* (1), 3855.
(457) Lang, C.; LaNasa, J. A.; Utomo, N.; Xu, Y.; Nelson, M. J.; Song, W.; Hickner, M. A.; Colby, R. H.; Kumar, M.; Hickey, R. J. Solvent-Non-Solvent Rapid-Injection for Preparing Nanostructured Materials from Micelles to Hydrogels. *Nat. Commun.* **2019**, *10* (1), 3855.
(458) Semenov, A. N.; Joanny, J.-F.; Khokhlov, A. R. Associating Polymers: Equilibrium and Linear Viscoelasticity. *Macromolecules* **1995**, *28* (4), 1066−1075.
(459) Balsara, N. P.; Tirrell, M.; Lodge, T. P. Micelle Formation of BAB Triblock Copolymers in Solvents That Preferentially Dissolve the A Block. *Macromolecules* **1991**, *24* (8), 1975−1986.
(460) Imaizumi, S.; Kokubo, H.; Watanabe, M. Polymer Actuators Using Ion-Gel Electrolytes Prepared by Self-Assembly of ABA-Triblock Copolymers. *Macromolecules* **2012**, *45* (1), 401−409.
(461) Guvendiren, M.; Shull, K. R. Self-Assembly of Acrylic Triblock Hydrogels by Vapor-Phase Solvent Exchange. *Soft Matter* **2007**, *3* (5), 619−626.

https://doi.org/10.1021/acs.chemrev.5c00466
Chem. Rev. XXXX, XXX, XXX−XXX

(462) Guo, C.; Bailey, T. S. Highly Distensible Nanostructured Elastic Hydrogels from AB Diblock and ABA Triblock Copolymer Melt Blends. *Soft Matter* **2010**, *6* (19), 4807−4818.
(463) Zhang, Q.; Weber, C.; Schubert, U. S.; Hoogenboom, R. Thermoresponsive Polymers with Lower Critical Solution Temperature: From Fundamental Aspects and Measuring Techniques to Recommended Turbidimetry Conditions. *Mater. Horiz.* **2017**, *4* (2), 109−116.
(464) Cook, M. T.; Haddow, P.; Kirton, S. B.; McAuley, W. J. Polymers Exhibiting Lower Critical Solution Temperatures as a Route to Thermoreversible Gelators for Healthcare. *Adv. Funct. Mater.* **2021**, *31* (8), 2008123.
(465) de la Rosa, V. R.; Woisel, P.; Hoogenboom, R. Supramolecular Control over Thermoresponsive Polymers. *Mater. Today* **2016**, *19* (1), 44−55.
(466) Paricaud, P.; Galindo, A.; Jackson, G. Understanding Liquid-Liquid Immiscibility and LCST Behaviour in Polymer Solutions with a Wertheim TPT1 Description. *Mol. Phys.* **2003**, *101* (16), 2575−2600.
(467) Yuan, Y.; Raheja, K.; Milbrandt, N. B.; Beilharz, S.; Tene, S.; Oshabaheebwa, S.; Gurkan, U. A.; Samia, A. C. S.; Karayilan, M. Thermoresponsive Polymers with LCST Transition: Synthesis, Characterization, and Their Impact on Biomedical Frontiers. *RSC Appl. Polym.* **2023**, *1* (2), 158−189.
(468) Pasparakis, G.; Tsitsilianis, C. LCST Polymers: Thermoresponsive Nanostructured Assemblies towards Bioapplications. *Polymer* **2020**, *211*, 123146.
(469) Schild, H. G.; Tirrell, D. A. Microcalorimetric Detection of Lower Critical Solution Temperatures in Aqueous Polymer Solutions. *J. Phys. Chem.* **1990**, *94* (10), 4352−4356.
(470) Heskins, M.; Guillet, J. E. Solution Properties of Poly(N-Isopropylacrylamide). *J. Macromolecular Science: Part A - Chemistry* **1968**, *2* (8), 1441−1455.
(471) Jain, K.; Vedarajan, R.; Watanabe, M.; Ishikiriyama, M.; Matsumi, N. Tunable LCST Behavior of Poly(N-Isopropylacrylamide/Ionic Liquid) Copolymers. *Polym. Chem.* **2015**, *6* (38), 6819−6825.
(472) Ozsvar, J.; Yang, C.; Cain, S. A.; Baldock, C.; Tarakanova, A.; Weiss, A. S. Tropoelastin and Elastin Assembly. *Front. Bioeng. Biotechnol.* **2021**, *9*. DOI: 10.3389/fbioe.2021.643110.
(473) Clarke, A. W.; Arnspang, E. C.; Mithieux, S. M.; Korkmaz, E.; Braet, F.; Weiss, A. S. Tropoelastin Massively Associates during Coacervation To Form Quantized Protein Spheres. *Biochemistry* **2006**, *45* (33), 9989−9996.
(474) Kozel, B. A.; Rongish, B. J.; Czirok, A.; Zach, J.; Little, C. D.; Davis, E. C.; Knutsen, R. H.; Wagenseil, J. E.; Levy, M. A.; Mecham, R. P. Elastic Fiber Formation: A Dynamic View of Extracellular Matrix Assembly Using Timer Reporters. *J. Cellular Physiology* **2006**, *207* (1), 87−96.
(475) Urry, D. W. Entropic Elastic Processes in Protein Mechanisms. I. Elastic Structure Due to an Inverse Temperature Transition and Elasticity Due to Internal Chain Dynamics. *J. Protein Chem.* **1988**, *7* (1), 1−34.
(476) Aaron, B. B.; Gosline, J. M. Elastin as a Random-Network Elastomer: A Mechanical and Optical Analysis of Single Elastin Fibers. *Biopolymers* **1981**, *20* (6), 1247−1260.
(477) Tarakanova, A.; Yeo, G. C.; Baldock, C.; Weiss, A. S.; Buehler, M. J. Molecular Model of Human Tropoelastin and Implications of Associated Mutations. *Proc. Natl. Acad. Sci. U. S. A.* **2018**, *115* (28), 7338−7343.
(478) Yeo, G. C.; Baldock, C.; Wise, S. G.; Weiss, A. S. A Negatively Charged Residue Stabilizes the Tropoelastin N-Terminal Region for Elastic Fiber Assembly*. *J. Biol. Chem.* **2014**, *289* (50), 34815−34826.
(479) Varanko, A. K.; Su, J. C.; Chilkoti, A. Elastin-Like Polypeptides for Biomedical Applications. *Annu. Rev. Biomed. Eng.* **2020**, *22*, 343−369.
(480) Di Zio, K.; Tirrell, D. A. Mechanical Properties of Artificial Protein Matrices Engineered for Control of Cell and Tissue Behavior. *Macromolecules* **2003**, *36* (5), 1553−1558.
(481) McHale, M. K.; Setton, L. A.; Chilkoti, A. Synthesis and in Vitro Evaluation of Enzymatically Cross-Linked Elastin-Like Polypeptide Gels for Cartilaginous Tissue Repair. *Tissue Engineering* **2005**, *11* (11−12), 1768−1779.
(482) Nagapudi, K.; Brinkman, W. T.; Leisen, J. E.; Huang, L.; McMillan, R. A.; Apkarian, R. P.; Conticello, V. P.; Chaikof, E. L. Photomediated Solid-State Cross-Linking of an Elastin−Mimetic Recombinant Protein Polymer. *Macromolecules* **2002**, *35* (5), 1730−1737.
(483) Glassman, M. J.; Olsen, B. D. Arrested Phase Separation of Elastin-like Polypeptide Solutions Yields Stiff, Thermoresponsive Gels. *Biomacromolecules* **2015**, *16* (12), 3762−3773.
(484) Nagarsekar, A.; Crissman, J.; Crissman, M.; Ferrari, F.; Cappello, J.; Ghandehari, H. Genetic Engineering of Stimuli-Sensitive Silkelastin-like Protein Block Copolymers. *Biomacromolecules* **2003**, *4* (3), 602−607.
(485) Xia, X.-X.; Xu, Q.; Hu, X.; Qin, G.; Kaplan, D. L. Tunable Self-Assembly of Genetically Engineered Silk−Elastin-like Protein Polymers. *Biomacromolecules* **2011**, *12* (11), 3844−3850.
(486) Vancoillie, G.; Frank, D.; Hoogenboom, R. Thermoresponsive Poly(Oligo Ethylene Glycol Acrylates). *Prog. Polym. Sci.* **2014**, *39* (6), 1074−1095.
(487) Lutz, J.-F. Polymerization of Oligo(Ethylene Glycol) (Meth)-Acrylates: Toward New Generations of Smart Biocompatible Materials. *J. Polym. Sci., Part A: Polym. Chem.* **2008**, *46* (11), 3459−3470.
(488) Lutz, J.-F.; Akdemir, Ö.; Hoth, A. Point by Point Comparison of Two Thermosensitive Polymers Exhibiting a Similar LCST: Is the Age of Poly(NIPAM) Over? *J. Am. Chem. Soc.* **2006**, *128* (40), 13046−13047.
(489) Constantinou, A. P.; Wang, L.; Wang, S.; Georgiou, T. K. Thermoresponsive Block Copolymers of Increasing Architecture Complexity: A Review on Structure−Property Relationships. *Polym. Chem.* **2023**, *14* (3), 223−247.
(490) Du, H.; Wickramasinghe, R.; Qian, X. Effects of Salt on the Lower Critical Solution Temperature of Poly (N-Isopropylacrylamide). *J. Phys. Chem. B* **2010**, *114* (49), 16594−16604.
(491) Zhang, Y.; Furyk, S.; Sagle, L. B.; Cho, Y.; Bergbreiter, D. E.; Cremer, P. S. Effects of Hofmeister Anions on the LCST of PNIPAM as a Function of Molecular Weight. *J. Phys. Chem. C* **2007**, *111* (25), 8916−8924.
(492) Teodorescu, M.; Negru, I.; Stanescu, P. O.; Drăghici, C.; Lungu, A.; Sârbu, A. Thermogelation Properties of Poly(N-Isopropylacrylamide) − Block − Poly(Ethylene Glycol) − Block − Poly(N-Isopropylacrylamide) Triblock Copolymer Aqueous Solutions. *React. Funct. Polym.* **2010**, *70* (10), 790−797.
(493) Abou-Shamat, M. A.; Calvo-Castro, J.; Stair, J. L.; Cook, M. T. Modifying the Properties of Thermogelling Poloxamer 407 Solutions through Covalent Modification and the Use of Polymer Additives. *Macromol. Chem. Phys.* **2019**, *220* (16), 1900173.
(494) Huang, Y.; Yong, P.; Chen, Y.; Gao, Y.; Xu, W.; Lv, Y.; Yang, L.; Reis, R. L.; Pirraco, R. P.; Chen, J. Micellization and Gelatinization in Aqueous Media of pH- and Thermo-Responsive Amphiphilic ABC (PMMA82-b-PDMAEMA150-b-PNIPAM65) Triblock Copolymer Synthesized by Consecutive RAFT Polymerization. *RSC Adv.* **2017**, *7* (46), 28711−28722.
(495) O'Lenick, T. G.; Jiang, X.; Zhao, B. Thermosensitive Aqueous Gels with Tunable Sol−Gel Transition Temperatures from Thermo- and pH-Responsive Hydrophilic ABA Triblock Copolymer. *Langmuir* **2010**, *26* (11), 8787−8796.
(496) Zheng, H.; Liu, K.; Cui, Y.; Li, L.; Liu, Q.; Men, Y. Synthetic Reversible Fibrous Network Hydrogels Based on a Double-Helical Polyelectrolyte. *Angew. Chem., Int. Ed.* **2025**, *137*, No. e202503030.
(497) Wang, Y.; He, Y.; Yu, Z.; Gao, J.; ten Brinck, S.; Slebodnick, C.; Fahs, G. B.; Zanelotti, C. J.; Hegde, M.; Moore, R. B.; Ensing, B.; Dingemans, T. J.; Qiao, R.; Madsen, L. A. Double Helical Conformation and Extreme Rigidity in a Rodlike Polyelectrolyte. *Nat. Commun.* **2019**, *10* (1), 801.

https://doi.org/10.1021/acs.chemrev.5c00466
Chem. Rev. XXXX, XXX, XXX−XXX

(498) Deyerle, B. A.; Zhang, Y. Effects of Hofmeister Anions on the Aggregation Behavior of PEO−PPO−PEO Triblock Copolymers. *Langmuir* **2011**, *27* (15), 9203−9210.
(499) Zangi, R.; Hagen, M.; Berne, B. J. Effect of Ions on the Hydrophobic Interaction between Two Plates. *J. Am. Chem. Soc.* **2007**, *129* (15), 4678−4686.
(500) Wu, S.; Hua, M.; Alsaid, Y.; Du, Y.; Ma, Y.; Zhao, Y.; Lo, C.-Y.; Wang, C.; Wu, D.; Yao, B.; Strzalka, J.; Zhou, H.; Zhu, X.; He, X. Poly(Vinyl Alcohol) Hydrogels with Broad-Range Tunable Mechanical Properties via the Hofmeister Effect. *Adv. Mater.* **2021**, *33* (11), 2007829.
(501) Assaf, K. I.; Nau, W. M. The Chaotropic Effect as an Assembly Motif in Chemistry. *Angew. Chem., Int. Ed.* **2018**, *57* (43), 13968−13981.
(502) Assaf, K. I.; Ural, M. S.; Pan, F.; Georgiev, T.; Simova, S.; Rissanen, K.; Gabel, D.; Nau, W. M. Water Structure Recovery in Chaotropic Anion Recognition: High-Affinity Binding of Dodecaborate Clusters to γ-Cyclodextrin. *Angew. Chem., Int. Ed.* **2015**, *54* (23), 6852−6856.
(503) Hohenschutz, M.; Bauduin, P.; Lopez, C. G.; Förster, B.; Richtering, W. Superchaotropic Nano-Ion Binding as a Gelation Motif in Cellulose Ether Solutions. *Angew. Chem., Int. Ed.* **2023**, *62* (3), No. e202210208.
(504) Song, Y.-F.; Tsunashima, R. Recent Advances on Polyoxometalate-Based Molecular and Composite Materials. *Chem. Soc. Rev.* **2012**, *41* (22), 7384−7402.
(505) Mazzini, V.; Craig, V. S. J. Volcano Plots Emerge from a Sea of Nonaqueous Solvents: The Law of Matching Water Affinities Extends to All Solvents. *ACS Cent. Sci.* **2018**, *4* (8), 1056−1064.
(506) Oncsik, T.; Trefalt, G.; Borkovec, M.; Szilagyi, I. Specific Ion Effects on Particle Aggregation Induced by Monovalent Salts within the Hofmeister Series. *Langmuir* **2015**, *31* (13), 3799−3807.
(507) Kocak, G.; Tuncer, C.; Bütün, V. pH-Responsive Polymers. *Polym. Chem.* **2017**, *8* (1), 144−176.
(508) Abe, K.; Yano, H. Cellulose Nanofiber-Based Hydrogels with High Mechanical Strength. *Cellulose* **2012**, *19* (6), 1907−1912.
(509) Abe, K.; Yano, H. Formation of Hydrogels from Cellulose Nanofibers. *Carbohydr. Polym.* **2011**, *85* (4), 733−737.
(510) Solhi, L.; Guccini, V.; Heise, K.; Solala, I.; Niinivaara, E.; Xu, W.; Mihhels, K.; Kröger, M.; Meng, Z.; Wohlert, J.; Tao, H.; Cranston, E. D.; Kontturi, E. Understanding Nanocellulose−Water Interactions: Turning a Detriment into an Asset. *Chem. Rev.* **2023**, *123* (5), 1925−2015.
(511) Okano, T.; Sarko, A. Mercerization of Cellulose. II. Alkali−Cellulose Intermediates and a Possible Mercerization Mechanism. *J. Appl. Polym. Sci.* **1985**, *30* (1), 325−332.
(512) Dinand, E.; Vignon, M.; Chanzy, H.; Heux, L. Mercerization of Primary Wall Cellulose and Its Implication for the Conversion of Cellulose I→cellulose II. *Cellulose* **2002**, *9* (1), 7−18.
(513) Sun, Y.; Li, Y.; Nie, J.; Wang, Z.; Hu, Q. High-Strength Chitosan Hydrogels Prepared from LiOH/Urea Solvent System. *Chem. Lett.* **2013**, *42* (8), 838−840.
(514) Nie, J.; Lu, W.; Ma, J.; Yang, L.; Wang, Z.; Qin, A.; Hu, Q. Orientation in Multi-Layer Chitosan Hydrogel: Morphology, Mechanism and Design Principle. *Sci. Rep.* **2015**, *5* (1), 7635.
(515) Nabika, H.; Itatani, M.; Lagzi, I. Pattern Formation in Precipitation Reactions: The Liesegang Phenomenon. *Langmuir* **2020**, *36* (2), 481−497.
(516) Nie, J.; Wang, Z.; Hu, Q. Chitosan Hydrogel Structure Modulated by Metal Ions. *Sci. Rep.* **2016**, *6* (1), 36005.
(517) Huang, L.; Li, H.; Wen, S.; Xia, P.; Zeng, F.; Peng, C.; Yang, J.; Tan, Y.; Liu, J.; Jiang, L.; Wang, J. Control Nucleation for Strong and Tough Crystalline Hydrogels with High Water Content. *Nat. Commun.* **2024**, *15* (1), 7777.
(518) Zhao, Z.; Lei, S.; Zeng, M.; Huo, M. Recent Progress in Polymerization-Induced Self-Assembly: From the Perspective of Driving Forces. *Aggregate* **2024**, *5* (1), e418.
(519) Zeng, Z.; Li, Z.; Li, Q.; Song, G.; Huo, M. Strong and Tough Nanostructured Hydrogels and Organogels Prepared by Polymerization-Induced Self-Assembly. *Small Methods* **2023**, *7* (6), 2201592.
(520) Warren, N. J.; Armes, S. P. Polymerization-Induced Self-Assembly of Block Copolymer Nano-Objects via RAFT Aqueous Dispersion Polymerization. *J. Am. Chem. Soc.* **2014**, *136* (29), 10174−10185.
(521) Penfold, N. J. W.; Yeow, J.; Boyer, C.; Armes, S. P. Emerging Trends in Polymerization-Induced Self-Assembly. *ACS Macro Lett.* **2019**, *8* (8), 1029−1054.
(522) Charleux, B.; Delaittre, G.; Rieger, J.; D'Agosto, F. Polymerization-Induced Self-Assembly: From Soluble Macromolecules to Block Copolymer Nano-Objects in One Step. *Macromolecules* **2012**, *45* (17), 6753−6765.
(523) D'Agosto, F.; Rieger, J.; Lansalot, M. RAFT-Mediated Polymerization-Induced Self-Assembly. *Angew. Chem., Int. Ed.* **2020**, *59* (22), 8368−8392.
(524) Israelachvili, J. N. *Intermolecular and Surface Forces/Jacob N. Israelachvili.*, 2nd ed.; Academic Press: London, 1992.
(525) Halperin, A.; Tirrell, M.; Lodge, T. P. Tethered Chains in Polymer Microstructures. In *Macromolecules: Synthesis, Order and Advanced Properties*; Springer Berlin Heidelberg: Berlin, Heidelberg, 1992; pp 31−71.
(526) Jain, S.; Bates, F. S. Consequences of Nonergodicity in Aqueous Binary PEO−PB Micellar Dispersions. *Macromolecules* **2004**, *37* (4), 1511−1523.
(527) Israelachvili, J. N. *Intermolecular and Surface Forces*, 3rd ed.; Elsevier: London, 2011.
(528) Zhao, F.; Bae, J.; Zhou, X. Y.; Guo, Y. H.; Yu, G. H. Nanostructured Functional Hydrogels as an Emerging Platform for Advanced Energy Technologies. *Adv. Mater.* **2018**, *30* (48), 1801796.
(529) Motokawa, R.; Iida, Y.; Zhao, Y.; Hashimoto, T.; Koizumi, S. Living Polymerization Induced Macro- and Microdomain Investigated by Focusing Ultra-Small-Angle Neutron Scattering. *Polym. J.* **2007**, *39* (12), 1312−1318.
(530) Seo, M.; Hillmyer, M. A. Reticulated Nanoporous Polymers by Controlled Polymerization-Induced Microphase Separation. *Science* **2012**, *336* (6087), 1422−1425.
(531) Dudaryeva, O. Y.; Cousin, L.; Krajnovic, L.; Gröbli, G.; Sapkota, V.; Ritter, L.; Deshmukh, D.; Cui, Y.; Style, R. W.; Levato, R.; Labouesse, C.; Tibbitt, M. W. Tunable Bicontinuous Macroporous Cell Culture Scaffolds via Kinetically Controlled Phase Separation. *Adv. Mater.* **2025**, *37* (7), 2410452.
(532) Hoyle, C. E.; Lee, T. Y.; Roper, T. Thiol−Enes: Chemistry of the Past with Promise for the Future. *J. Polym. Sci., Part A: Polym. Chem.* **2004**, *42* (21), 5301−5338.
(533) Shi, X.; Zhang, J.; Corrigan, N.; Boyer, C. Controlling Mechanical Properties of 3D Printed Polymer Composites through Photoinduced Reversible Addition−Fragmentation Chain Transfer (RAFT) Polymerization. *Polym. Chem.* **2021**, *13* (1), 44−57.
(534) Priester, A.; Yeng, J.; Zhang, Y.; Wang, R.; Convertine, A. J. 3D Printing Soluble Solids via PISA. *Polym. Chem.* **2023**, *14* (20), 2452−2456.
(535) Priester, A.; Yeng, J.; Zhang, Y.; Wang, R.; Convertine, A. J. PISA Printing from CTA Functionalized Polymer Scaffolds. *RSC Appl. Polym.* **2024**, *2* (4), 612−623.
(536) Bobrin, V. A.; Yao, Y.; Shi, X.; Xiu, Y.; Zhang, J.; Corrigan, N.; Boyer, C. Nano- to Macro-Scale Control of 3D Printed Materials via Polymerization Induced Microphase Separation. *Nat. Commun.* **2022**, *13* (1), 3577.
(537) Grimm, L. M.; Setiadi, J.; Tkachenko, B.; Schreiner, P. R.; Gilson, M. K.; Biedermann, F. The Temperature-Dependence of Host−Guest Binding Thermodynamics: Experimental and Simulation Studies. *Chem. Sci.* **2023**, *14* (42), 11818−11829.
(538) Soto Tellini, V. H.; Jover, A.; García, J. C.; Galantini, L.; Meijide, F.; Tato, J. V. Thermodynamics of Formation of Host−Guest Supramolecular Polymers. *J. Am. Chem. Soc.* **2006**, *128* (17), 5728−5734.

https://doi.org/10.1021/acs.chemrev.5c00466
Chem. Rev. XXXX, XXX, XXX−XXX

(539) Ji, X.; Ahmed, M.; Long, L.; Khashab, N. M.; Huang, F.; Sessler, J. L. Adhesive Supramolecular Polymeric Materials Constructed from Macrocycle-Based Host−Guest Interactions. *Chem. Soc. Rev.* **2019**, *48* (10), 2682−2697.
(540) Hashidzume, A.; Zheng, Y.; Takashima, Y.; Yamaguchi, H.; Harada, A. Macroscopic Self-Assembly Based on Molecular Recognition: Effect of Linkage between Aromatics and the Polyacrylamide Gel Scaffold, Amide versus Ester. *Macromolecules* **2013**, *46* (5), 1939−1947.
(541) Yan, X.; Wang, F.; Zheng, B.; Huang, F. Stimuli-Responsive Supramolecular Polymeric Materials. *Chem. Soc. Rev.* **2012**, *41* (18), 6042−6065.
(542) Ma, X.; Zhao, Y. Biomedical Applications of Supramolecular Systems Based on Host−Guest Interactions. *Chem. Rev.* **2015**, *115* (15), 7794−7839.
(543) Gibb, C. L. D.; Gibb, B. C. The Thermodynamics of Molecular Recognition. *Supramol. Chem.* **2012**. DOI: 10.1002/9780470661345.smc005.
(544) Osaki, M.; Yonei, S.; Ueda, C.; Ikura, R.; Park, J.; Yamaguchi, H.; Harada, A.; Tanaka, M.; Takashima, Y. Mechanical Properties with Respect to Water Content of Host−Guest Hydrogels. *Macromolecules* **2021**, *54* (17), 8067−8076.
(545) Zhang, M.; Xu, D.; Yan, X.; Chen, J.; Dong, S.; Zheng, B.; Huang, F. Self-Healing Supramolecular Gels Formed by Crown Ether Based Host−Guest Interactions. *Angew. Chem., Int. Ed.* **2012**, *51* (28), 7011−7015.
(546) Kakuta, T.; Takashima, Y.; Sano, T.; Nakamura, T.; Kobayashi, Y.; Yamaguchi, H.; Harada, A. Adhesion between Semihard Polymer Materials Containing Cyclodextrin and Adamantane Based on Host−Guest Interactions. *Macromolecules* **2015**, *48* (3), 732−738.
(547) Appel, E. A.; Biedermann, F.; Rauwald, U.; Jones, S. T.; Zayed, J. M.; Scherman, O. A. Supramolecular Cross-Linked Networks via Host−Guest Complexation with Cucurbit[8]Uril. *J. Am. Chem. Soc.* **2010**, *132* (40), 14251−14260.
(548) Lee, J. H.; Park, J.; Park, J.-W.; Ahn, H.-J.; Jaworski, J.; Jung, J. H. Supramolecular Gels with High Strength by Tuning of Calix[4]-Arene-Derived Networks. *Nat. Commun.* **2015**, *6* (1), 6650.
(549) Li, S.; Lu, H.-Y.; Shen, Y.; Chen, C.-F. A Stimulus-Response and Self-Healing Supramolecular Polymer Gel Based on Host−Guest Interactions. *Macromol. Chem. Phys.* **2013**, *214* (14), 1596−1601.
(550) Xia, D.; Wang, P.; Ji, X.; Khashab, N. M.; Sessler, J. L.; Huang, F. Functional Supramolecular Polymeric Networks: The Marriage of Covalent Polymers and Macrocycle-Based Host−Guest Interactions. *Chem. Rev.* **2020**, *120* (13), 6070−6123.
(551) Wang, Q.; Mynar, J. L.; Yoshida, M.; Lee, E.; Lee, M.; Okuro, K.; Kinbara, K.; Aida, T. High-Water-Content Mouldable Hydrogels by Mixing Clay and a Dendritic Molecular Binder. *Nature* **2010**, *463* (7279), 339−343.
(552) Ito, K. Novel Cross-Linking Concept of Polymer Network: Synthesis, Structure, and Properties of Slide-Ring Gels with Freely Movable Junctions. *Polym. J.* **2007**, *39* (6), 489−499.
(553) Huang, X.; Li, R.; Duan, Z.; Xu, F.; Li, H. Supramolecular Polymer Gels: From Construction Methods to Functionality. *Soft Matter* **2022**, *18* (20), 3828−3844.
(554) Ohnsorg, M. L.; Mash, K. M.; Khang, A.; Rao, V. V.; Kirkpatrick, B. E.; Bera, K.; Anseth, K. S. Nonlinear Elastic Bottlebrush Polymer Hydrogels Modulate Actomyosin Mediated Protrusion Formation in Mesenchymal Stromal Cells. *Adv. Mater.* **2024**, *36*, 2403198.
(555) Pan, T.; Dutta, S.; Kamble, Y.; Patel, B. B.; Wade, M. A.; Rogers, S. A.; Diao, Y.; Guironnet, D.; Sing, C. E. Materials Design of Highly Branched Bottlebrush Polymers at the Intersection of Modeling, Synthesis, Processing, and Characterization. *Chem. Mater.* **2022**, *34*, 1990. .
(556) Müllner, M.; Müller, A. H. E. Cylindrical Polymer Brushes − Anisotropic Building Blocks, Unimolecular Templates and Particulate Nanocarriers. *Polymer* **2016**, *98*, 389−401.
(557) Li, Z.; Tang, M.; Liang, S.; Zhang, M.; Biesold, G. M.; He, Y.; Hao, S.-M.; Choi, W.; Liu, Y.; Peng, J.; Lin, Z. Bottlebrush Polymers: From Controlled Synthesis, Self-Assembly, Properties to Applications. *Prog. Polym. Sci.* **2021**, *116*, 101387.
(558) Verduzco, R.; Li, X. Y.; Pesek, S. L.; Stein, G. E. Structure, Function, Self-Assembly, and Applications of Bottlebrush Copolymers. *Chem. Soc. Rev.* **2015**, *44* (21), 7916−7916.
(559) Zhao, B. Shape-Changing Bottlebrush Polymers. *J. Phys. Chem. B* **2021**, *125* (24), 6373−6389.
(560) Abbasi, M.; Faust, L.; Wilhelm, M. Comb and Bottlebrush Polymers with Superior Rheological and Mechanical Properties. *Adv. Mater.* **2019**, *31* (26), 1806484.
(561) Li, X.; ShamsiJazeyi, H.; Pesek, S. L.; Agrawal, A.; Hammouda, B.; Verduzco, R. Thermoresponsive PNIPAAM Bottlebrush Polymers with Tailored Side-Chain Length and End-Group Structure. *Soft Matter* **2014**, *10* (12), 2008−2015.
(562) Kouwer, P. H. J.; Koepf, M.; Le Sage, V. A. A.; Jaspers, M.; van Buul, A. M.; Eksteen-Akeroyd, Z. H.; Woltinge, T.; Schwartz, E.; Kitto, H. J.; Hoogenboom, R.; Picken, S. J.; Nolte, R. J. M.; Mendes, E.; Rowan, A. E. Responsive Biomimetic Networks from Polyisocyanopeptide Hydrogels. *Nature* **2013**, *493* (7434), 651−655.
(563) Hughes, M. D. G.; Cussons, S.; Hanson, B. S.; Cook, K. R.; Feller, T.; Mahmoudi, N.; Baker, D. L.; Ariëns, R.; Head, D. A.; Brockwell, D. J.; Dougan, L. Building Block Aspect Ratio Controls Assembly, Architecture, and Mechanics of Synthetic and Natural Protein Networks. *Nat. Commun.* **2023**, *14* (1), 5593.
(564) Cook, M. T.; Haddow, P.; Kirton, S. B.; McAuley, W. J. Polymers Exhibiting Lower Critical Solution Temperatures as a Route to Thermoreversible Gelators for Healthcare. *Adv. Funct. Mater.* **2021**, *31* (8). DOI: 10.1002/adfm.202008123.
(565) Li, X. Y.; ShamsiJazeyi, H.; Pesek, S. L.; Agrawal, A.; Hammouda, B.; Verduzco, R. Thermoresponsive PNIPAAM Bottlebrush Polymers with Tailored Side-Chain Length and End-Group Structure. *Soft Matter* **2014**, *10* (12), 2008−2015.
(566) Vohidov, F.; Milling, L. E.; Chen, Q.; Zhang, W.; Bhagchandani, S.; Nguyen, H. V.-T.; Irvine, D. J.; Johnson, J. A. ABC Triblock Bottlebrush Copolymer-Based Injectable Hydrogels: Design, Synthesis, and Application to Expanding the Therapeutic Index of Cancer Immunochemotherapy. *Chem. Sci.* **2020**, *11* (23), 5974−5986.
(567) Saha, B.; Boykin, J.; Chung, H. Unveiling the Architectural Impact on the Salt-Tunable Adhesion Performance and Toughness of Polyzwitterions. *J. Am. Chem. Soc.* **2024**, *146* (33), 23467−23475.
(568) Zhang, J.; Yuan, X.; Wu, Z.; Ren, L. Synthesis and Self-Assembly of High Grafting Density Core-Shell Bottlebrush Polymer with Amphiphilic Side Chain. *React. Funct. Polym.* **2024**, *202*, 105997.
(569) Basak, S.; Chatterjee, R.; Bandyopadhyay, A. Beyond Traditional Stimuli: Exploring Salt-Responsive Bottlebrush Polymers—Trends, Applications, and Perspectives. *ACS Omega* **2024**, *9* (31), 33365−33385.
(570) Deng, Y.; Chen, B.; Zhu, K.; Ren, L.; Yuan, X. Activation of Upper Critical Solution Temperature Behaviors of Zwitterionic Poly(l-Methionine-g-Poly(Sulfobetaine Methacrylate)m) with a Bottlebrush Structure. *Macromolecules* **2024**, *57* (1), 191−200.
(571) Sheiko, S. S.; Dobrynin, A. V. Architectural Code for Rubber Elasticity: From Supersoft to Superfirm Materials. *Macromolecules* **2019**, *52* (20), 7531−7546.
(572) Keith, A. N.; Vatankhah-Varnosfaderani, M.; Clair, C.; Fahimipour, F.; Dashtimoghadam, E.; Lallam, A.; Sztucki, M.; Ivanov, D. A.; Liang, H.; Dobrynin, A. V.; Sheiko, S. S. Bottlebrush Bridge between Soft Gels and Firm Tissues. *ACS Cent. Sci.* **2020**, *6* (3), 413−419.
(573) Vashahi, F.; Martinez, M. R.; Dashtimoghadam, E.; Fahimipour, F.; Keith, A. N.; Bersenev, E. A.; Ivanov, D. A.; Zhulina, E. B.; Popryadukhin, P.; Matyjaszewski, K.; Vatankhah-Varnosfaderani, M.; Sheiko, S. S. Injectable Bottlebrush Hydrogels with Tissue-Mimetic Mechanical Properties. *Sci. Adv.* **2022**, *8* (3), eabm2469. .

(574) Beeren, I. A. O.; Morgan, F. L. C.; Rademakers, T.; Bauer, J.; Dijkstra, P. J.; Moroni, L.; Baker, M. B. Well-Defined Synthetic Copolymers with Pendant Aldehydes Form Biocompatible Strain-Stiffening Hydrogels and Enable Competitive Ligand Displacement. *J. Am. Chem. Soc.* **2024**, *146* (35), 24330−24347.
(575) Giraud-Guille, M.-M. Liquid Crystallinity in Condensed Type I Collagen Solutions: A Clue to the Packing of Collagen in Extracellular Matrices. *J. Mol. Biol.* **1992**, *224* (3), 861−873.
(576) Nyström, G.; Mezzenga, R. Liquid Crystalline Filamentous Biological Colloids: Analogies and Differences. *Curr. Opin. Colloid Interface Sci.* **2018**, *38*, 30−44.
(577) Jehle, F.; Priemel, T.; Strauss, M.; Fratzl, P.; Bertinetti, L.; Harrington, M. J. Collagen Pentablock Copolymers Form Smectic Liquid Crystals as Precursors for Mussel Byssus Fabrication. *ACS Nano* **2021**, *15* (4), 6829−6838.
(578) Onsager, L. The Effects of Shape on the Interaction of Colloidal Particles. *Ann. N.Y. Acad. Sci.* **1949**, *51* (4), 627−659.
(579) Dogic, Z.; Fraden, S. Ordered Phases of Filamentous Viruses. *Curr. Opin. Colloid Interface Sci.* **2006**, *11* (1), 47−55.
(580) Wegst, U. G. K.; Bai, H.; Saiz, E.; Tomsia, A. P.; Ritchie, R. O. Bioinspired Structural Materials. *Nat. Mater.* **2015**, *14* (1), 23−36.
(581) Tang, S.; Liu, K.; Chen, J.; Li, Y.; Liu, M.; Lu, L.; Zhou, C.; Luo, B. Dual-Cross-Linked Liquid Crystal Hydrogels with Controllable Viscoelasticity for Regulating Cell Behaviors. *ACS Appl. Mater. Interfaces* **2022**, *14* (19), 21966−21977.
(582) Chen, J.; Zhu, Z.; Chen, J.; Luo, Y.; Li, L.; Liu, K.; Ding, S.; Li, H.; Liu, M.; Zhou, C.; Luo, B. Photocurable Liquid Crystal Hydrogels with Different Chargeability and Tunable Viscoelasticity Based on Chitin Whiskers. *Carbohydr. Polym.* **2023**, *301*, 120299.
(583) Miyamoto, N.; Shintate, M.; Ikeda, S.; Hoshida, Y.; Yamauchi, Y.; Motokawa, R.; Annaka, M. Liquid Crystalline Inorganic Nanosheets for Facile Synthesis of Polymer Hydrogels with Anisotropies in Structure, Optical Property, Swelling/Deswelling, and Ion Transport/Fixation. *Chem. Commun.* **2013**, *49* (11), 1082−1084.
(584) Zhu, Z.; Song, G.; Liu, J.; Whitten, P. G.; Liu, L.; Wang, H. Liquid Crystalline Behavior of Graphene Oxide in the Formation and Deformation of Tough Nanocomposite Hydrogels. *Langmuir* **2014**, *30* (48), 14648−14657.
(585) Ma, J.; Lin, S.; Jiang, Y.; Li, P.; Zhang, H.; Xu, Z.; Wu, H.; Lin, P.; Breu, J.; Gao, W.; Gao, C. Digital Programming Graphene Oxide Liquid Crystalline Hybrid Hydrogel by Shearing Microlithography. *ACS Nano* **2020**, *14* (2), 2336−2344.
(586) Harrington, M. J.; Mezzenga, R.; Miserez, A. Fluid Protein Condensates for Bio-Inspired Applications. *Nature Reviews Bioengineering* **2024**, *2* (3), 260−278.
(587) Shen, Y.; Ruggeri, F. S.; Vigolo, D.; Kamada, A.; Qamar, S.; Levin, A.; Iserman, C.; Alberti, S.; George-Hyslop, P. S.; Knowles, T. P. J. Biomolecular Condensates Undergo a Generic Shear-Mediated Liquid-to-Solid Transition. *Nat. Nanotechnol.* **2020**, *15* (10), 841−847.
(588) He, W.; Wang, M.; Mei, G.; Liu, S.; Khan, A. Q.; Li, C.; Feng, D.; Su, Z.; Bao, L.; Wang, G.; Liu, E.; Zhu, Y.; Bai, J.; Zhu, M.; Zhou, X.; Liu, Z. Establishing Superfine Nanofibrils for Robust Polyelectrolyte Artificial Spider Silk and Powerful Artificial Muscles. *Nat. Commun.* **2024**, *15* (1), 3485.
(589) Hong, J.; Lin, Q.; Shao, Z. Bridging Biocondensation and Biomimetic Fibrillation by Regulating Intra- And Interchain Hydrogen Bonds in Artificial Biomacromolecular Condensates. *ACS Macro Lett.* **2023**, *12* (7), 888−893.
(590) Chen, J.; Tsuchida, A.; Malay, A. D.; Tsuchiya, K.; Masunaga, H.; Tsuji, Y.; Kuzumoto, M.; Urayama, K.; Shintaku, H.; Numata, K. Replicating Shear-Mediated Self-Assembly of Spider Silk through Microfluidics. *Nat. Commun.* **2024**, *15* (1), 527.
(591) Saric, M.; Eisoldt, L.; Döring, V.; Scheibel, T. Interplay of Different Major Ampullate Spidroins during Assembly and Implications for Fiber Mechanics. *Adv. Mater.* **2021**, *33* (9), 2006499.
(592) Giesa, T.; Perry, C. C.; Buehler, M. J. Secondary Structure Transition and Critical Stress for a Model of Spider Silk Assembly. *Biomacromolecules* **2016**, *17* (2), 427−436.
(593) Koeppel, A.; Laity, P. R.; Holland, C. Extensional Flow Behaviour and Spinnability of Native Silk. *Soft Matter* **2018**, *14* (43), 8838−8845.
(594) Mredha, Md. T. I.; Guo, Y. Z.; Nonoyama, T.; Nakajima, T.; Kurokawa, T.; Gong, J. P. A Facile Method to Fabricate Anisotropic Hydrogels with Perfectly Aligned Hierarchical Fibrous Structures. *Adv. Mater.* **2018**, *30* (9), 1704937.
(595) Zhang, X.; Wang, Y.; Wu, X.; Zhu, F.; Qin, Y.-X.; Chen, W.; Zheng, Q. A Universal Post-Treatment Strategy for Biomimetic Composite Hydrogel with Anisotropic Topological Structure and Wide Range of Adjustable Mechanical Properties. *Biomaterials Advances* **2022**, *133*, 112654.
(596) Qiao, P.; Li, B.; He, Y.; Shi, K.; Zhang, X.; Zhang, J.; Wang, Y.; Su, L.; Chen, Y.; Nishinari, K.; Yang, G. High-Performance Hydrogels via Alternate Compression−Decompression. *J. Phys. Chem. C* **2022**, *126* (51), 21825−21832.
(597) Xu, Z.; Chen, H.; Yang, H.-B.; Yao, X.; Qin, H.; Cong, H.-P.; Yu, S.-H. Hierarchically Aligned Heterogeneous Core-Sheath Hydrogels. *Nat. Commun.* **2025**, *16* (1), 400.
(598) Zhang, C.; Shen, S.; Wu, C.; Wang, L.; Lei, S.; Wang, Z. A Spatiotemporal Controllable Crosslinking Route for Preparing Tough Tissue-like Anisotropic PVA Hydrogel. *Chem. Eng. J.* **2023**, *465*, 142882.
(599) Zhang, S.; Liu, X.; Barreto-Ortiz, S. F.; Yu, Y.; Ginn, B. P.; DeSantis, N. A.; Hutton, D. L.; Grayson, W. L.; Cui, F.-Z.; Korgel, B. A.; Gerecht, S.; Mao, H.-Q. Creating Polymer Hydrogel Microfibres with Internal Alignment via Electrical and Mechanical Stretching. *Biomaterials* **2014**, *35* (10), 3243−3251.
(600) Dedroog, L. M.; Deschaume, O.; Abrego, C. J. G.; Koos, E.; de Coene, Y.; Vananroye, A.; Thielemans, W.; Bartic, C.; Lettinga, M. P. Stress-Controlled Shear Flow Alignment of Collagen Type I Hydrogel Systems. *Acta Biomaterialia* **2022**, *150*, 128−137.
(601) Zhu, S.; Wang, S.; Huang, Y.; Tang, Q.; Fu, T.; Su, R.; Fan, C.; Xia, S.; Lee, P. S.; Lin, Y. Bioinspired Structural Hydrogels with Highly Ordered Hierarchical Orientations by Flow-Induced Alignment of Nanofibrils. *Nat. Commun.* **2024**, *15* (1), 118.
(602) Ritchie, R. O. The Conflicts between Strength and Toughness. *Nat. Mater.* **2011**, *10* (11), 817−822.
(603) Huang, W.; Restrepo, D.; Jung, J.-Y.; Su, F. Y.; Liu, Z.; Ritchie, R. O.; McKittrick, J.; Zavattieri, P.; Kisailus, D. Multiscale Toughening Mechanisms in Biological Materials and Bioinspired Designs. *Adv. Mater.* **2019**, *31* (43), 1901561.
(604) Miserez, A.; Yu, J.; Mohammadi, P. Protein-Based Biological Materials: Molecular Design and Artificial Production. *Chem. Rev.* **2023**, *123* (5), 2049−2111.
(605) Sun, X.; Mao, Y.; Yu, Z.; Yang, P.; Jiang, F. A Biomimetic "Salting Out—Alignment—Locking" Tactic to Design Strong and Tough Hydrogel. *Adv. Mater.* **2024**, *36* (25), 2400084.
(606) Giesa, T.; Pugno, N. M.; Buehler, M. J. Natural Stiffening Increases Flaw Tolerance of Biological Fibers. *Phys. Rev. E* **2012**, *86* (4), No. 041902.
(607) Qiao, H.; Wu, B.; Sun, S.; Wu, P. Entropy-Driven Design of Highly Impact-Stiffening Supramolecular Polymer Networks with Salt-Bridge Hydrogen Bonds. *J. Am. Chem. Soc.* **2024**, *146* (11), 7533−7542.
(608) Yue, Y.; Yokota, Y.; Matsuba, G. Polyelectrolyte-Layered Hydrogels with Electrically Tunable Toughness, Viscoelasticity, Hysteresis, and Crack Resistance. *Macromolecules* **2022**, *55* (4), 1230−1238.
(609) Takahashi, R.; Wu, Z. L.; Arifuzzaman, M.; Nonoyama, T.; Nakajima, T.; Kurokawa, T.; Gong, J. P. Control Superstructure of Rigid Polyelectrolytes in Oppositely Charged Hydrogels via Programmed Internal Stress. *Nat. Commun.* **2014**, *5* (1), 4490.
(610) Zhang, Y.; Zhao, W.; Ma, S.; Liu, H.; Wang, X.; Zhao, X.; Yu, B.; Cai, M.; Zhou, F. Modulus Adaptive Lubricating Prototype Inspired by Instant Muscle Hardening Mechanism of Catfish Skin. *Nat. Commun.* **2022**, *13* (1), 377.
(611) Yang, Y.; Wang, X.; Yang, F.; Shen, H.; Wu, D. A Universal Soaking Strategy to Convert Composite Hydrogels into Extremely

https://doi.org/10.1021/acs.chemrev.5c00466
Chem. Rev. XXXX, XXX, XXX−XXX

Tough and Rapidly Recoverable Double-Network Hydrogels. *Adv. Mater.* **2016**, *28* (33), 7178−7184.
(612) Zhao, D.; Pang, B.; Zhu, Y.; Cheng, W.; Cao, K.; Ye, D.; Si, C.; Xu, G.; Chen, C.; Yu, H. A Stiffness-Switchable, Biomimetic Smart Material Enabled by Supramolecular Reconfiguration. *Adv. Mater.* **2022**, *34* (10), 2107857.
(613) Liu, C.; Morimoto, N.; Jiang, L.; Kawahara, S.; Noritomi, T.; Yokoyama, H.; Mayumi, K.; Ito, K. Tough Hydrogels with Rapid Self-Reinforcement. *Science* **2021**, *372* (6546), 1078−1081.
(614) Zhu, R.; Zhu, D.; Zheng, Z.; Wang, X. Tough Double Network Hydrogels with Rapid Self-Reinforcement and Low Hysteresis Based on Highly Entangled Networks. *Nat. Commun.* **2024**, *15* (1), 1344.
(615) Lin, X.; Wang, X.; Cui, H.; Rao, P.; Meng, Y.; Ouyang, G.; Guo, H. Hydrogels with Ultra-Highly Additive Adjustable Toughness under Quasi-Isochoric Conditions. *Mater. Horiz.* **2023**, *10* (3), 993−1004.
(616) Frick, J. M.; Ambrosi, A.; Pollo, L. D.; Tessaro, I. C. Influence of Glutaraldehyde Crosslinking and Alkaline Post-Treatment on the Properties of Chitosan-Based Films. *J. Polym. Environ* **2018**, *26* (7), 2748−2757.
(617) Jiang, L.-B.; Su, D.-H.; Ding, S.-L.; Zhang, Q.-C.; Li, Z.-F.; Chen, F.-C.; Ding, W.; Zhang, S.-T.; Dong, J. Salt-Assisted Toughening of Protein Hydrogel with Controlled Degradation for Bone Regeneration. *Adv. Funct. Mater.* **2019**, *29* (26), 1901314.
(618) Nonoyama, T.; Lee, Y. W.; Ota, K.; Fujioka, K.; Hong, W.; Gong, J. P. Instant Thermal Switching from Soft Hydrogel to Rigid Plastics Inspired by Thermophile Proteins. *Adv. Mater.* **2020**, *32* (4), 1905878.
(619) Lu, Y.; Chen, C.; Li, H.; Zhao, P.; Zhao, Y.; Li, B.; Zhou, W.; Fan, G.; Guan, D.; Zheng, Y. Visible Light-Responsive Hydrogels for Cellular Dynamics and Spatiotemporal Viscoelastic Regulation. *Nat. Commun.* **2025**, *16* (1), 1365.
(620) Matsuda, T.; Kawakami, R.; Namba, R.; Nakajima, T.; Gong, J. P. Mechanoresponsive Self-Growing Hydrogels Inspired by Muscle Training. *Science* **2019**, *363* (6426), 504−508.
(621) Seshimo, K.; Sakai, H.; Watabe, T.; Aoki, D.; Sugita, H.; Mikami, K.; Mao, Y.; Ishigami, A.; Nishitsuji, S.; Kurose, T.; Ito, H.; Otsuka, H. Segmented Polyurethane Elastomers with Mechanochromic and Self-Strengthening Functions. *Angew. Chem., Int. Ed.* **2021**, *60* (15), 8406−8409.
(622) Xu, X.; Eatmon, Y. L.; Christie, K. S. S.; McGaughey, A. L.; Guillomaitre, N.; Datta, S. S.; Ren, Z. J.; Arnold, C.; Priestley, R. D. Tough and Recyclable Phase-Separated Supramolecular Gels via a Dehydration−Hydration Cycle. *JACS Au* **2023**, *3* (10), 2772−2779.
(623) Lin, X. X.; Wang, X. L.; Zeng, L. P.; Wu, Z. L.; Guo, H.; Hourdet, D. Stimuli-Responsive Toughening of Hydrogels. *Chem. Mater.* **2021**, *33* (19), 7633−7656.
(624) Cui, W.; Zheng, Y.; Zhu, R.; Mu, Q.; Wang, X.; Wang, Z.; Liu, S.; Li, M.; Ran, R. Strong Tough Conductive Hydrogels via the Synergy of Ion-Induced Cross-Linking and Salting-Out. *Adv. Funct. Mater.* **2022**, *32* (39), 2204823.
(625) Hu, L.; Luo, H.; Xie, J.; Li, M.; Lu, H.; Shen, H.; Cui, W.; Ran, R. Mixed-Solvent-Induced Phase Separation Enables Anisotropy and Strengthening of Hydrogels Composed of Flexible Network Chains. *Small* **2025**, *21* (13), 2410734.
(626) Zhong, D.; Wang, Z.; Xu, J.; Liu, J.; Xiao, R.; Qu, S.; Yang, W. A Strategy for Tough and Fatigue-Resistant Hydrogels via Loose Cross-Linking and Dense Dehydration-Induced Entanglements. *Nat. Commun.* **2024**, *15* (1), 5896.
(627) Du, P.; Wang, J.; Hsu, Y.-I.; Uyama, H. Hydrophobic Association Hydrogel Enabled by Multiple Noncovalent Interactions for Wearable Bioelectronics in Amphibious Environments. *Chem. Mater.* **2024**, *36* (3), 1318−1332.
(628) Jia, L.; Li, Y.; Ren, A.; Xiang, T.; Zhou, S. Degradable and Recyclable Hydrogels for Sustainable Bioelectronics. *ACS Appl. Mater. Interfaces* **2024**, *16* (26), 32887−32905.
(629) Yang, J. W.; Bai, R. B.; Chen, B. H.; Suo, Z. G. Hydrogel Adhesion: A Supramolecular Synergy of Chemistry, Topology, and Mechanics. *Adv. Funct. Mater.* **2020**, *30* (2). DOI: 10.1002/adfm.201901693.
(630) Liu, Y.; Cui, H.; Wang, X.; Ouyang, G.; Guo, H. Hydrogels with Reversible Heat-Trained Toughness for Convenient Manufacture. *Adv. Mater. Technol.* **2023**, *8* (5), 2201346.
(631) Shi, X.; Li, J.; Sun, C.; Wu, S. The Aggregation and Phase Separation Behavior of a Hydrophobically Modified Poly(*N*-Isopropylacrylamide). *Colloids Surf., A* **2000**, *175* (1), 41−49.
(632) Halperin, A.; Kröger, M.; Winnik, F. M. Poly(N-Isopropylacrylamide) Phase Diagrams: Fifty Years of Research. *Angew. Chem., Int. Ed.* **2015**, *54* (51), 15342−15367.
(633) Mussault, C.; Guo, H.; Sanson, N.; Hourdet, D.; Marcellan, A. Effect of Responsive Graft Length on Mechanical Toughening and Transparency in Microphase-Separated Hydrogels. *Soft Matter* **2019**, *15* (43), 8653−8666.
(634) Van Durme, K.; Van Assche, G.; Van Mele, B. Kinetics of Demixing and Remixing in Poly(N-Isopropylacrylamide)/Water Studied by Modulated Temperature DSC. *Macromolecules* **2004**, *37* (25), 9596−9605.
(635) Kojima, H. Studies on the Phase Transition of Hydrogels and Aqueous Solutions of Thermosensitive Polymers. *Polym. J.* **2018**, *50* (6), 411−418.
(636) Motloung, B.; Pfukwa, R.; Klumperman, B. Ion-Mediated Gelation of Thermo-Responsive Cellulose Nanofibril/Poly(N-Isopropylacrylamide) Hybrid Hydrogels with Tunable De-Swelling Kinetics. *Macromol. Mater. Eng.* **2024**, *309* (8), 2300457.
(637) Lumsden, J. S. XXXIV.—Solubilities of the Calcium Salts of the Acids of the Acetic Series. *J. Chem. Soc., Trans.* **1902**, *81* (0), 350−362.
(638) Lin, X.; Wang, X.; Cui, H.; Ouyang, G.; Guo, H. A Universal Strategy for Preparing Tough and Smart Glassy Hydrogels. *Chem. Eng. J.* **2023**, *457*, 141280.
(639) Chen, L.; Zhao, C.; Huang, J.; Zhou, J.; Liu, M. Enormous-Stiffness-Changing Polymer Networks by Glass Transition Mediated Microphase Separation. *Nat. Commun.* **2022**, *13* (1), 6821.
(640) Huang, W.; Yang, J.; Long, C.; Yuan, J.; Lin, L.; Lv, Y.; Li, L.; Chen, Y. Dynamic Regulation Properties of Carrageenan Hydrogels Based on the Hofmeister Effect. *Int. J. Biol. Macromol.* **2025**, *315*, 144228.
(641) LeHoux, J.-G.; Dupuis, G. Recovery of Chitosan from Aqueous Acidic Solutions by Salting-out: Part 1. Use of Inorganic Salts. *Carbohydr. Polym.* **2007**, *68* (2), 295−304.
(642) Cai, H.; Tepermeister, M.; Yuan, C.; Silberstein, M. N. Regulating Hydrogel Mechanical Properties with an Electric Field. *Mater. Horiz.* **2025**, *12*, 5388.
(643) Es Sayed, J.; Mukherjee, A.; El Aani, S.; Vengallur, N.; Koch, M.; Giuntoli, A.; Kamperman, M. Structure−Property Relationships of Granular Hybrid Hydrogels Formed through Polyelectrolyte Complexation. *Macromolecules* **2024**, *57* (7), 3190−3201.
(644) Li, J.; Chee, H. L.; Chong, Y. T.; Chan, B. Q. Y.; Xue, K.; Lim, P. C.; Loh, X. J.; Wang, F. Hofmeister Effect Mediated Strong PHEMA-Gelatin Hydrogel Actuator. *ACS Appl. Mater. Interfaces* **2022**, *14* (20), 23826−23838.
(645) Ren, J.; Chen, G.; Yang, H.; Zheng, J.; Li, S.; Zhu, C.; Yang, H.; Fu, J. Super-Tough, Non-Swelling Zwitterionic Hydrogel Sensor Based on the Hofmeister Effect for Potential Motion Monitoring of Marine Animals. *Adv. Mater.* **2024**, *36* (48), 2412162.
(646) Pandian, M.; Reshma, G.; Arthi, C.; Másson, M.; Rangasamy, J. Biodegradable Polymeric Scaffolds and Hydrogels in the Treatment of Chronic and Infectious Wound Healing. *Eur. Polym. J.* **2023**, *198*, 112390.
(647) Yang, S.; Yu, Y.; Jo, S.; Lee, Y.; Son, S.; Lee, K. H. Calcium Ion-Triggered Liquid-Liquid Phase Separation of Silk Fibroin and Spinning through Acidification and Shear Stress. *Nat. Commun.* **2024**, *15* (1), 10394.
(648) Li, J.; Wang, H.; Liu, B.; Chen, J.; Gu, J.; Lin, S. Photoinduced Contraction Fibers and Photoswitchable Adhesives Generated by Stretchable Supramolecular Gel. *Adv. Funct. Mater.* **2022**, *32* (30), 2201851.

https://doi.org/10.1021/acs.chemrev.5c00466
Chem. Rev. XXXX, XXX, XXX−XXX

(649) Ohzono, T.; Minamikawa, H.; Koyama, E.; Norikane, Y. Unlocking Entropic Elasticity of Nematic Elastomers Through Light and Dynamic Adhesion. *Adv. Mater. Interf.* **2021**, *8* (14), 2100672.
(650) Chau, M.; De France, K. J.; Kopera, B.; Machado, V. R.; Rosenfeldt, S.; Reyes, L.; Chan, K. J. W.; Förster, S.; Cranston, E. D.; Hoare, T.; Kumacheva, E. Composite Hydrogels with Tunable Anisotropic Morphologies and Mechanical Properties. *Chem. Mater.* **2016**, *28* (10), 3406−3415.
(651) Yuk, H.; Zhang, T.; Parada, G. A.; Liu, X.; Zhao, X. Skin-Inspired Hydrogel−Elastomer Hybrids with Robust Interfaces and Functional Microstructures. *Nat. Commun.* **2016**, *7* (1), 12028.
(652) Hou, J.-B.; Jiang, Z.-C.; Xiao, Y.-Y.; Cheng, R.-D.; Zhao, Y. Room Temperature Shape Self-Adjustable Tough Hydrogel Based on Multi-Physical Crosslinking. *Chem. Eng. J.* **2024**, *499*, 156144.
(653) Nixon, R. M.; ten Hove, J. B.; Orozco, A.; Jenkins, Z. M.; Baenen, P. C.; Wiatt, M. K.; Zuluaga, J.; Sawyer, W. G.; Angelini, T. E. Mechanical Properties Derived from Phase Separation in Co-Polymer Hydrogels. *J. Mechanical Behavior of Biomedical Materials* **2016**, *55*, 286−294.

https://doi.org/10.1021/acs.chemrev.5c00466
Chem. Rev. XXXX, XXX, XXX−XXX